



National Library  
of Canada

Bibliothèque nationale  
du Canada

Canadian Theses Service

Service des thèses canadiennes

Ottawa, Canada  
K1A 0N4

## NOTICE

The quality of this microform is heavily dependent upon the quality of the original thesis submitted for microfilming. Every effort has been made to ensure the highest quality of reproduction possible.

If pages are missing, contact the university which granted the degree.

Some pages may have indistinct print especially if the original pages were typed with a poor typewriter ribbon or if the university sent us an inferior photocopy.

Reproduction in full or in part of this microform is governed by the Canadian Copyright Act, R.S.C. 1970, c. C-30, and subsequent amendments.

## AVIS

La qualité de cette microforme dépend grandement de la qualité de la thèse soumise au microfilmage. Nous avons tout fait pour assurer une qualité supérieure de reproduction.

S'il manque des pages, veuillez communiquer avec l'université qui a conféré le grade.

La qualité d'impression de certaines pages peut laisser à désirer, surtout si les pages originales ont été dactylographiées à l'aide d'un ruban usé ou si l'université nous a fait parvenir une photocopie de qualité inférieure.

La reproduction, même partielle, de cette microforme est soumise à la Loi canadienne sur le droit d'auteur, SRC 1970, c. C-30, et ses amendements subséquents.

UNIVERSITY OF ALBERTA

CONCRETE CONTRIBUTION TO SHEAR STRENGTH  
IN SLENDER BEAMS

by

WAYNE ALLAN KASSIAN



A THESIS

SUBMITTED TO THE FACULTY OF GRADUATE STUDIES AND RESEARCH  
IN PARTIAL FULFILLMENT OF THE REQUIREMENTS FOR THE DEGREE  
OF

MASTER OF SCIENCE IN CIVIL ENGINEERING

DEPARTMENT OF CIVIL ENGINEERING

EDMONTON, ALBERTA

SPRING, 1990



National Library  
of Canada

Bibliothèque nationale  
du Canada

Canadian Theses Service    Service des thèses canadiennes

Ottawa, Canada  
K1A 0N4

## NOTICE

The quality of this microform is heavily dependent upon the quality of the original thesis submitted for microfilming. Every effort has been made to ensure the highest quality of reproduction possible.

If pages are missing, contact the university which granted the degree.

Some pages may have indistinct print especially if the original pages were typed with a poor typewriter ribbon or if the university sent us an inferior photocopy.

Reproduction in full or in part of this microform is governed by the Canadian Copyright Act, R.S.C. 1970, c. C-30, and subsequent amendments.

## AVIS

La qualité de cette microforme dépend grandement de la qualité de la thèse soumise au microfilmage. Nous avons tout fait pour assurer une qualité supérieure de reproduction.

S'il manque des pages, veuillez communiquer avec l'université qui a conféré le grade.

La qualité d'impression de certaines pages peut laisser à désirer, surtout si les pages originales ont été dactylographiées à l'aide d'un ruban usé ou si l'université nous a fait parvenir une photocopie de qualité inférieure.

La reproduction, même partielle, de cette microforme est soumise à la Loi canadienne sur le droit d'auteur, SRC 1970, c. C-30, et ses amendements subséquents.

ISBN 0-315-60312-7

UNIVERSITY OF ALBERTA

RELEASE FORM

NAME OF AUTHOR: . . . Wayne Allan Kassian

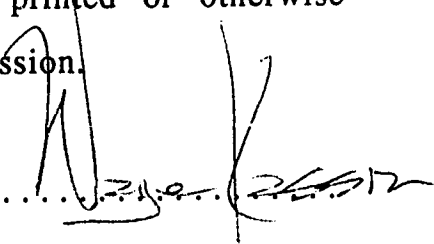
TITLE OF THESIS: . . . . Concrete Contribution to Shear Strength  
in Slender Beams

DEGREE: . . . . . Master of Science in Civil Engineering

YEAR THIS DEGREE GRANTED: 1990

Permission is hereby granted to the UNIVERSITY OF ALBERTA LIBRARY to reproduce single copies of this thesis and to lend or sell such copies for private, scholarly or scientific research purposes only.

The author reserves other publication rights, and neither the thesis nor extensive extracts from it may be printed or otherwise reproduced without the author's written permission.

(Signed) . . . . . 

PERMANENT ADDRESS:

3916 - 120 St.

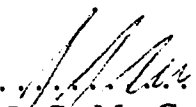
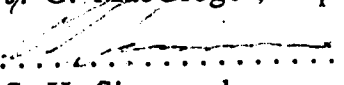
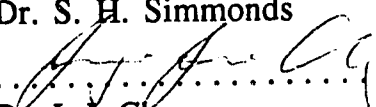
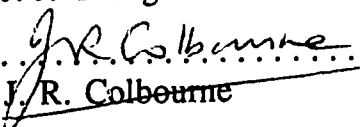
Edmonton, Alberta

Canada, T6J 1X6

DATE: *Mar* .26 1990

UNIVERSITY OF ALBERTA  
FACULTY OF GRADUATE STUDIES AND RESEARCH

The undersigned certify that they have read, and recommend to the Faculty of Graduate Studies and Research for acceptance, a thesis entitled CONCRETE CONTRIBUTION TO SHEAR STRENGTH IN SLENDER BEAMS submitted by WAYNE ALLAN KASSIAN in partial fulfillment of the requirements for the degree of Master of Science in Civil Engineering.

  
.....  
Dr. J. G. MacGregor, Supervisor  
  
.....  
Dr. S. H. Simmonds  
  
.....  
Dr. J. J. Cheng  
  
.....  
Dr. J. R. Colbourne

DATE . Feb. 27 . 1990

## ABSTRACT

Traditional design procedures for determining the shear strength of slender concrete beams are based primarily on empirical relationships using an average nominal shear stress. The variable angle truss model approach introduces a conceptual model which provides a better understanding of the flow of internal forces and failure mechanisms in cracked concrete beams. In 1987, a variable angle truss model was proposed for use in the 1989 ACI Code. Since the traditional concrete contribution shear transfer mechanisms were not directly included in the proposed design procedure, the variable angle model appeared to be unnecessarily conservative and was not accepted. This study was carried out to develop a new concrete contribution term which can be applied to the truss model design procedure proposed in the ACI 1987 draft.

The basic behavior of concrete beams subjected to shear is discussed and the ACI 318-83 procedure is briefly summarized. A concrete contribution term for shear is derived from the Modified Compression Field Theory. Expressions suitable for design equations are developed for both reinforced and prestressed concrete beams. Predictions of the proposed design procedure are compared to the results of various experimental investigations and to predictions of the ACI 318-83 Code. A concrete contribution expression is recommended and suggestions for further research are given.

## **ACKNOWLEDGEMENTS**

I wish to thank Dr. James G. MacGregor for his supervision and guidance throughout this work. I would also like to acknowledge the financial support provided by the Natural Science and Engineering Research Council of Canada.

I deeply appreciate the encouragement of my wife, Shelley, whose support, patience and understanding greatly contributed to the completion of this study.

# TABLE OF CONTENTS

<b>Chapter</b>	<b>Page</b>
List of Tables	
List of Figures	
Notation	
1. Introduction . . . . .	1
1.1 General . . . . .	1
1.2 Objectives and Scope . . . . .	2
1.3 Organization of the Thesis . . . . .	2
2. Modelling Slender Beams Failing in Shear . . . . .	4
2.1 Basic Considerations . . . . .	4
2.1.1 Shear Stresses in Elastic Beams . . . . .	4
2.1.2 Principles of B and D Regions . . . . .	11
2.1.3 Shear Cracking . . . . .	12
2.1.4 Function of Shear Reinforcement . . . . .	17
2.1.5 Modes of Shear Failure . . . . .	18
2.1.6 Basic Mechanisms of Shear Transfer . . . . .	24
2.2 Traditional Truss Models for Reinforced Concrete Beams . . . . .	26
2.3 ACI 318-83 Shear Design Procedure . . . . .	30
2.3.1 Reinforced Concrete . . . . .	30



2.3.1.1	Shear Strength Provided by the Reinforcement . . . . .	31
2.3.1.2	Shear Strength Provided by the Concrete . . . . .	35
2.3.2	Prestressed Concrete . . . . .	39
2.4	CAN3-A23.3-M84 Simplified Method . . . . .	42
2.5	Variable Angle Truss Models . . . . .	45
2.6	Staggering Concept for Shear Design . . . . .	51
2.7	Modified Compression Field Theory . . . . .	54
3.	Review of Available Concrete Contribution Expressions . . . . .	61
3.1	General . . . . .	61
3.2	Swiss Design Code S.I.A. 162 . . . . .	62
3.3	C.E.B.-F.I.P Model Code 1978 -Refined Method. . . . .	67
3.4	Ramirez and Breen . . . . .	74
4.	Derivation of a New Concrete Contribution Term Using the Modified Compression Field Theory . . . . .	80
4.1	Concrete Contribution Model . . . . .	80
4.2	Capacity of Crack Interface . . . . .	84
4.2.1	Effect of Longitudinal Strain . . . . .	92
4.2.2	Effect of Vertical Spacing of Longitudinal Bars . . . . .	95
4.2.3	Effect of Prestressing . . . . .	98
4.2.4	Expression for Capacity of Crack Interface . . . . .	104
4.3	Capacity of Cracked Concrete in Tension . . . . .	108
4.3.1	Effect of Longitudinal Strain . . . . .	115
4.3.2	Effect of Concrete Cracking Strength . . . . .	115

4.3.3	Effect of Prestressing . . . . .	117
4.3.4	Expression for Capacity of Cracked Concrete in Tension . . . . .	120
4.4	Development of Concrete Contribution Equations for Use in Design . . . . .	123
4.5	Proposed Design Equations . . . . .	126
4.6	Special Considerations . . . . .	135
5.	Comparison of Predictions with Experimental Results Reported in Literature . . . . .	137
5.1	General . . . . .	137
5.2	Reinforced Concrete . . . . .	141
5.2.1	Selection of Test Beams . . . . .	141
5.2.2	Comparison to A.C.I. Code Procedure . . . . .	141
5.2.3	Comparison to General Concrete Contribution Expressions . . . . .	144
5.2.4	Comparison to Proposed Design Equations . . . . .	148
5.2.5	Influence of Cross Section on Shear Strength . . . . .	150
5.2.6	Influence of Reinforcement on Shear Strength . . . . .	153
5.2.7	Other Factors Influencing Predicted Shear Strength . . . . .	158
5.3	Prestressed Concrete . . . . .	165
5.3.1	Selection of Test Beams . . . . .	165
5.3.2	Comparison to A.C.I. Code Procedure . . . . .	165
5.3.3	Comparison to Concrete Contribution Expressions . . . . .	167
5.3.4	Influence of Amount of Shear Reinforcement on Shear Strength . . . . .	170

5.3.5	Other Factors Influencing Predicted Shear Strength . . . . .	178
6.	Design and Analysis Examples . . . . .	184
7.	Summary, Conclusions and Recommendations . . . . .	193
7.1	Summary and Conclusions . . . . .	193
7.2	Recommendations . . . . .	195
7.3	Future Research . . . . .	197
	References . . . . .	198
	Appendix A Reinforced Concrete Results. . . . .	204
	Appendix B Prestressed Concrete Results. . . . .	223

## LIST OF TABLES

<b>Table</b>		<b>Page</b>
Table 3.1	Values of $\tau_{rd}$ in the CEB-FIP 1978 Model Code . . . . .	70
Table 3.2	Values of $\kappa_v$ determined from the Model Code . . . . .	72
Table 4.1	Mid-depth strain $\epsilon_x$ , for $\rho=0.0075$ and $\rho=0.75\rho_b$ . . . . .	94
Table 4.2	Maximum average crack spacing if $s_x=8$ in and $s=24$ in . . . . .	96
Table 5.1	Summary of reinforced concrete test beam properties . . . . .	142
Table 5.2	Details of reinforced concrete test beams . . . . .	143
Table 5.3	Summary of predicted shear capacity results for the reinforced concrete beams examined . . . . .	151
Table 5.4	Summary of predicted shear capacity results for reinforced concrete beams . . . . .	155
Table 5.5	Summary of prestressed concrete test beam properties . . . . .	166
Table 5.6	Details of prestressed concrete test beams . . . . .	166
Table 5.7	Summary of predicted shear capacity results for the prestressed concrete beams examined . . . . .	172

## LIST OF FIGURES

Figure		Page
Figure 2.1	Shear in an elastic rectangular beam . . . . .	5
Figure 2.2	Stress conditions of an elemental block . . . . .	8
Figure 2.3	Stresses in an idealized cracked concrete beam . .	10
Figure 2.4	Examples of B-regions and D-regions . . . . .	13
Figure 2.5	Stress distribution in beams: a) without axial load b) effect of prestress . . . . .	15
Figure 2.6	Variation in moment and shear capacity with a/d ratio for rectangular beams . . . . .	19
Figure 2.7	Failure modes in deep beams . . . . .	21
Figure 2.8	Typical shear failure modes of short beams $1.5 < a/d < 2.5$ . . . . .	21
Figure 2.9	Internal forces resisting shear at inclined crack . .	25
Figure 2.10	Forces developed by aggregate interlock . . . . .	25
Figure 2.11	Redistribution of internal shear forces in a beam with shear reinforcement . . . . .	25
Figure 2.12	Truss analogy of a concrete beam . . . . .	28
Figure 2.13	Pin-jointed truss analogy . . . . .	28
Figure 2.14	Internal forces in a traditional truss model . . . . .	28
Figure 2.15	Shear strength provided by vertical web reinforcement . . . . .	32
Figure 2.16	Comparison of Eqn. 2.21 with experimental results . . . . .	38
Figure 2.17	Variable angle truss model of a beam . . . . .	47
Figure 2.18	Variable angle truss - equilibrium conditions . . . .	47
Figure 2.19	Forces in tension and compression chords of truss . . . . .	50

Figure 2.20	Design of stirrups using the staggering concept for a top-loaded beam . . . . .	52
Figure 2.21	Stress fields resisting shear in the web of a reinforced concrete beam . . . . .	56
Figure 2.22	Principal stresses and longitudinal equilibrium . .	56
Figure 2.23	Average strain conditions in cracked concrete . . .	58
Figure 2.24	Stress-strain relationships for cracked concrete . .	58
Figure 2.25	Suitable solution technique for shear using the Modified Compression Field Theory . . . . .	60
Figure 3.1	The Swiss Code concrete contribution for reinforced concrete beams . . . . .	63
Figure 3.2	Effect of prestress on shear strength . . . . .	63
Figure 3.3	The Swiss Code concrete contribution for prestressed concrete beams . . . . .	65
Figure 3.4	Idealized representation of shear failure . . . . .	65
Figure 3.5	1978 CEB-FIP concrete contribution for reinforced concrete beams . . . . .	71
Figure 3.6	Concrete contribution proposed by Ramirez and Breen for concrete beams . . . . .	75
Figure 3.7	Ramirez and Breen evaluation of the concrete contribution in prestressed concrete beams . . . . .	77
Figure 3.8	Replot of data in Figure 3.7 for prestressed concrete beams without web reinforcement . . . . .	77
Figure 4.1	Force transmission models . . . . .	81
Figure 4.2	Transformation of interface shear stress to vertical shear stress . . . . .	85
Figure 4.3	Crack shear stress based on Collins and Mitchell . .	86
Figure 4.4	Mohr's circle of average strains . . . . .	91
Figure 4.5	Compatibility of strains . . . . .	91
Figure 4.6	Crack shear stress vs. longitudinal strain, $s=2$ inches . . . . .	93

Figure 4.7	Crack shear stress vs. longitudinal strain, s=24 inches . . . . .	93
Figure 4.8	Influence of vertical spacing of longitudinal bars on crack shear . . . . .	97
Figure 4.9	Concrete contribution for prestressed beams . . . . .	101
Figure 4.10	Increase in concrete contribution due to prestressing . . . . .	103
Figure 4.11	Proposed increase in concrete contribution . . . . .	105
Figure 4.12	Crack shear stress vs. crack inclination (Eqn. 4.17b) . . . . .	107
Figure 4.13	Crack shear stress vs. stirrup spacing (Eqn. 4.17b) . . . . .	107
Figure 4.14	Post cracking tensile stress-strain curves . . . . .	109
Figure 4.15	Variation of stress in web reinforcement . . . . .	112
Figure 4.16	Influence of longitudinal strain on concrete tensile capacity . . . . .	116
Figure 4.17	Shear capacity provided by concrete tension . . . . .	118
Figure 4.18	Cracking stress vs. cylinder strength . . . . .	119
Figure 4.19	Concrete contribution due to tensile stresses in the concrete . . . . .	122
Figure 4.20	Concrete contribution expressions . . . . .	124
Figure 4.21	Proposed concrete contribution equation . . . . .	127
Figure 4.22	Total concrete contribution for prestressed members . . . . .	130
Figure 4.23	Effect of prestress on concrete contribution . . . . .	130
Figure 4.24	Maximum concrete contribution from Eqns. 4.37 and 4.38 . . . . .	132
Figure 5.1	Frequency distribution of resistance R . . . . .	138
Figure 5.2	Comparison of measured and predicted failure moments of 112 reinforced concrete beams . . . . .	139

Figure 5.3	Comparison of measured and computed failure shears for 106 reinforced concrete beams . . . . .	145
Figure 5.4	Comparison of measured and computed failure shears for 106 reinforced concrete beams . . . . .	149
Figure 5.5	Influence of beam cross-sectional shape on predicted shear capacity, reinforced concrete beams . . . . .	152
Figure 5.6	Influence of shear reinforcement on proposed design equations, reinforced concrete beams . . . . .	156
Figure 5.7	Influence of stirrup spacing on proposed design equations, reinforced concrete beams . . . . .	157
Figure 5.8	Influence of longitudinal reinforcement on predictions of shear strength, reinforced concrete beams . . . . .	159
Figure 5.9	Influence of longitudinal reinforcement on proposed shear design procedure, reinforced concrete beams . . . . .	160
Figure 5.10	Influence of concrete strength on shear strength predictions, reinforced concrete beams . . . . .	162
Figure 5.11	Influence of nominal shear stress on the proposed design equations, reinforced concrete beams . . . . .	163
Figure 5.12	Effect of shear span to depth ratio on the proposed design equations, reinforced concrete beams . . . . .	164
Figure 5.13	Comparison of measured and computed failure shears for 77 prestressed concrete beams . . . . .	168
Figure 5.14	Comparison of measured and computed failure shears for 77 prestressed concrete beams . . . . .	171
Figure 5.15	Effect of amount of shear reinforcement on the predicted shear capacities, prestressed concrete beams . . . . .	174
Figure 5.16	Effect of shear reinforcement on the predicted shear capacities, prestressed concrete beams . . . . .	175



Figure 5.17	Effect of stirrup spacing on predicted capacity using the proposed design method, prestressed concrete beams . . . . .	176
Figure 5.18	Effect of amount of prestressed reinforcement on predicted shear capacities, prestressed concrete beams . . . . .	177
Figure 5.19	Effect of concrete strength on predicted shear capacities, prestressed concrete beams . . . . .	179
Figure 5.20	Effect of amount of prestress on predicted shear capacities, prestressed concrete beams . . . . .	180
Figure 5.21	Influence of prestress stresses on predicted shear capacities, prestressed concrete beams . . . . .	182
Figure 5.22	Effect of shear span to depth ratio on predicted shear capacities, prestressed concrete beams . . . . .	183
Figure 6.1	Simply supported beam - Example 1 . . . . .	187
Figure 6.2	Details of T-Beam for Example 2 . . . . .	189
Figure 6.3	Prestressed concrete beam - Example 3 . . . . .	192

## NOTATION

$a$	shear span, distance between concentrated load and face of support, or maximum aggregate size
$A_b$	area of an individual bar
$A_g$	gross area of section
$A_{ps}$	cross-sectional area of prestressed reinforcement
$A_{sw}$	cross-sectional area of web reinforcement
$A_v$	area of web reinforcement within a distance $s$
$b$	width of compression face of member
$b_w$	web width
$C$	compressive force in concrete
$d$	effective depth, the distance from extreme compression fiber to centroid of tension reinforcement
$d_p$	distance from extreme compression fiber to centroid of prestressed reinforcement
$D$	diagonal compressive force due to shear, or constant relating the tensile strength of concrete to $\sqrt{f'_c}$
$E_c$	modulus of elasticity of concrete
$f'_c$	specified compressive strength of concrete
$f_{ci}$	compressive stress perpendicular to the crack surface
$f_{ck}$	characteristic concrete strength
$f_{cr}$	stress in the concrete at cracking

$f_{cu}$  allowable compressive stress in an inclined concrete strut

$f_{cube}$  compressive strength of concrete cube

$f_d$  stress due to unfactored dead load at extreme fiber of section where tensile stress is caused by externally applied loads

$f_{pc}$  compressive stress in concrete at the level of the centroid due to effective prestress force

$f_{pe}$  compressive stress at the tension face due to the tensile force alone

$f_{ps}$  stress in the prestressed reinforcement at nominal strength

$f_{pu}$  specified tensile strength of the prestressing steel

$f_{py}$  specified yield stress of the prestressed reinforcement

$f_s$  stress in the reinforcement

$f_{se}$  effective prestress in the prestressing tendons after all losses

$f_{sl}$  stress in the longitudinal reinforcement

$f_t$  principal tensile stress

$f_x$  normal stress caused by flexure

$f_y$  specified yield strength of reinforcement

$f_{yv}$  specified yield strength of stirrups

$f_{ywd}$  design stress of the web reinforcement

$f_1$  average principal tensile stress

$f_2$  principal compressive stress in the concrete

$F_1$  tensile force in the compression chord reinforcement due to shear at an average location between two cracks

- $F_2$  tensile force in the compression chord reinforcement due to shear at a crack
- $h$  overall thickness of member
- $I$  moment of inertia of section
- $jd$  distance between the resultants of the internal compressive and tensile forces on a cross section
- $K$  factor indicating increase in cracking shear stress due to prestressing
- $l_b$  length available for stirrup to develop bond between crack and midway between cracks
- $M$  bending moment
- $M_{cr}$  moment causing flexural cracking due to externally applied loads
- $M_{max}$  maximum factored moment at section due to externally applied loads
- $M_n$  predicted failure moment
- $M_o$  decompression moment at transfer related to the tensile fiber
- $M_{sdu}$  maximum design moment in the span
- $M_{test}$  measured failure moment
- N.A. neutral axis
- $N_u$  axial load normal to the cross section
- $N_v$  axial tension force due to shear
- $Q$  first moment of area around the neutral axis
- $R$  resistance or strength

$\bar{R}$	mean resistance
s	stirrup spacing measured along the longitudinal axis of the beam or sample standard deviation
$s_{m\theta}$	average crack spacing perpendicular to the crack
$s_x$	vertical spacing of longitudinal bars
T	tensile force in reinforcement
V	shear force
$V_{ai}$	component of aggregate interlock in the same plane as the crack interface
$V_{an}$	component of aggregate interlock normal to the inclined crack
$V_{ay}$	component of aggregate interlock in vertical direction
$V_c$	shear force carried by the concrete
$V_{calc}$	predicted failure shear
$V_{cd}$	shear force carried by the concrete contribution
$V_{ci}$	shear strength provided by concrete when diagonal cracking results from combined shear and moment
$V_{cw}$	shear force causing web shear cracking
$V_{cz}$	shear strength provided by uncracked concrete compression zone
$V_d$	shear force at section due to unfactored dead load, or shear carried by dowel action
$V_f$	factored shear force at section
$V_n$	nominal shear strength

- $V_p$  vertical component of effective prestress force
- $V_r$  factored shear resistance
- $V_{rdz}$  shear limit to prevent web crushing failures
- $V_s$  component of shear resisted by the web reinforcement
- $V_{sd}$  design shear force
- $V_{test}$  measured failure shear from beam test
- $V_u$  factored shear force at section
- $V_v$  vertical shear force
- $V_{wd}$  shear force carried by the truss action in the web
- $V_1$  factored shear force at section due to externally applied loads occurring simultaneously with  $M_{max}$
- $w$  crack width
- $w_f$  factored uniform load applied to beam
- $\bar{X}$  mean value of  $V_{test} / V_{calc}$ .
- $y$  distance from neutral axis to point on cross section under consideration
- $y_t$  distance from the centroidal axis of cross section to extreme fiber in tension
- $z$  lever arm between top and bottom chords of truss model
- $\alpha$  inclination of principal tensile stress to the longitudinal axis of a beam or angle of compression struts in a beam web, or inclination of a haunched beam.
- $\alpha_1$  factor to account for the effects of bond

$\alpha_2$	factor to account for the type of loading condition
$\beta_1$	ratio of depth of rectangular stress block to depth of neutral axis, or factor including the effect of prestressing on $\tau_{rd}$
$\gamma_p$	factor to account for type of prestressing tendon
$\gamma_{xy}$	shear strain in the web
$\Delta f_s$	specified yield stress subtract stirrup stress, $f_y - f_s$
$\epsilon_x$	longitudinal strain at mid-depth of web, tension positive
$\epsilon_y$	transverse strain, tension positive
$\epsilon_1$	principal tensile strain in the web
$\epsilon_2$	principal compressive strain, negative quantity
$\epsilon'_c$	strain corresponding to peak stress of $f'_c$ , negative quantity
$\lambda$	correction factor to account for unit weight of concrete
$v$	shear stress
$v_{ci}$	concrete contribution shear stress at the crack interface which is equivalent to a vertical shear stress acting at the section
$v_{cp}$	increase in concrete contribution shear stress due prestressing
$v_{cr}$	shear stress causing diagonal cracking
$v_{cw}$	shear stress causing web shear cracking
$v_n$	nominal shear stress
$v_{max}$	maximum value of shear stress

- $\rho$  ratio of nonprestressed tension reinforcement =  $A_s/bd$
- $\rho_b$  reinforcement ratio corresponding to balanced strain conditions
- $\rho_p$  ratio of prestressed reinforcement
- $\rho_v = A_v / b_w s$
- $\rho_w = A_s / b_w d$
- $\phi$  strength reduction factor
- $\phi_c$  material resistance factor for concrete
- $\phi_p$  material resistance factor for prestressing tendons
- $\phi_s$  material resistance factor for reinforcement
- $\sigma$  normal stress on face of element
- $\sigma_{cp}$  axial prestress
- $\theta$  angle of compression struts in web of a beam or inclination of principal compressive stress to the longitudinal axis of a beam
- $\theta_{st}$  angle between the steel member and the compression strut
- $\tau$  shear stress on face of element
- $\tau_{rd}$  function relating to the concrete quality
- $\kappa = \kappa_v + \kappa_{vp}$
- $\kappa_v = v_{ci} / \sqrt{f'_c}$
- $\kappa_{vp} = v_{cp} / \sqrt{f'_c}$



# 1. INTRODUCTION

## 1.1 General

Traditional design procedures for shear in concrete are based primarily on empirical relationships using an average nominal shear stress. This average stress is used as a measure of the shear stresses resulting from an applied shear force. However, the shear failure mechanisms are more complex and change as the type of beam changes. Thus, an allowable shear stress procedure is not a very convincing model regarding the internal mechanism of shear failure. The variable angle truss model introduces a conceptual model which provides a better understanding of the flow of internal forces and the failure mechanism in a cracked concrete beam.

In the simplest truss model, the beam stirrups act as vertical tension members resisting the entire vertical shear. The General Method in the Canadian design code CAN3-A23.3-M84<sup>1</sup> uses this procedure, and the nominal shear resistance is entirely provided by the truss action supplied by the vertical web reinforcement and inclined concrete struts. However, other mechanisms also provide resistance to shear, including shear in the uncracked concrete compression zone, shear transfer by aggregate interlock across the crack, and dowel action of the longitudinal reinforcement. If this additional shear capacity, traditionally called the "concrete contribution" is neglected, the truss model can be unnecessarily conservative. The Modified Compression Field Theory developed by

Collins and Vecchio<sup>2</sup> considers the contribution of concrete and aggregate interlock to shear resistance, and can be used to predict the shear strength of reinforced and prestressed concrete beams.

## 1.2 Objectives and Scope

The objective of this work is to derive a new concrete contribution " $V_c$ " term for use in the General Method proposed for the ACI Code Clause 11.4, 1987 draft<sup>3</sup> for both reinforced concrete and prestressed concrete in shear. The derivation will be based on the modified compression field theory and will be chosen to be applicable to relatively slender beams with a shear span ratio greater than 2.5.

A major goal is to develop a final design equation that is simple and easy to use. The total shear capacity obtained when the new concrete contribution is added to the truss shear component should provide strengths comparable to the existing ACI 318 Building Code<sup>4</sup> unless there is experimental evidence to warrant a change. As a result, the new method should not require more web reinforcement than the existing simplified method which has proven to perform satisfactorily in practice.

## 1.3 Organization of the Thesis

In Chapter 2 of this thesis, the basic behavior of concrete beams subjected to shear is discussed. In addition, various models are

presented which describe the behavior of web-reinforced beams subjected to shear. The ACI 318-83 design procedure is briefly summarized. Chapter 3 discusses several concrete contribution expressions that have been developed by other researchers or are used by other design codes. In Chapter 4, a new concrete contribution term is derived using the Modified Compression Field Theory for both reinforced and prestressed concrete beams. A simplified design equation is also presented. Chapter 5 compares the predictions of shear strength using the derived concrete contribution expression, the proposed design equation, and the existing ACI method to examine the reliability of each method. Chapter 6 presents design examples comparing the proposed design procedure to the existing ACI Code procedure. The conclusions, recommendations, and discussion of future research are presented in Chapter 7.

Because this thesis proposes revisions to the ACI Code, U.S. Customary units have been used throughout.

## **2. MODELLING SLENDER BEAMS FAILING IN SHEAR**

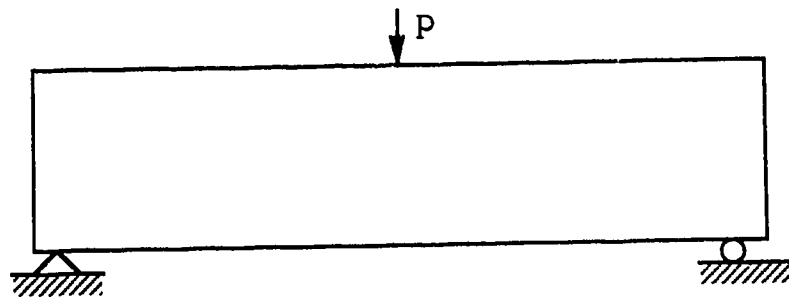
### **2.1 Basic Considerations**

The behavior of reinforced concrete in shear is complex. Several factors contribute to this complexity, including the formation of cracks in concrete, biaxial stress effects, and the influence of beam and load geometry on beam behavior. Consequently, the post cracking behavior of reinforced concrete beams is not identical for all types of members, and there are various independent parameters involved in determining the shear strength of a beam.

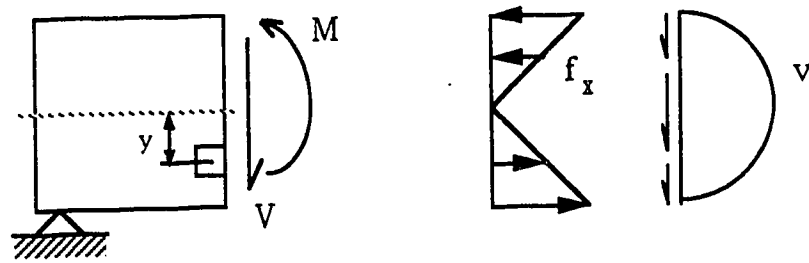
Since no universally-applicable or universally-accepted theory exists for beams failing in shear, several rational models for evaluating the shear strength of concrete beams have been proposed in recent years. Prior to developing a new expression for the concrete contribution to the shear strength of concrete beams, the lack of a generally accepted theory necessitates a discussion of the basic shear carrying actions and their simulation in models. The general behavior of concrete beams subjected to shear and various shear design models are briefly presented in the following sections.

#### **2.1.1 Shear Stresses in Elastic Beams**

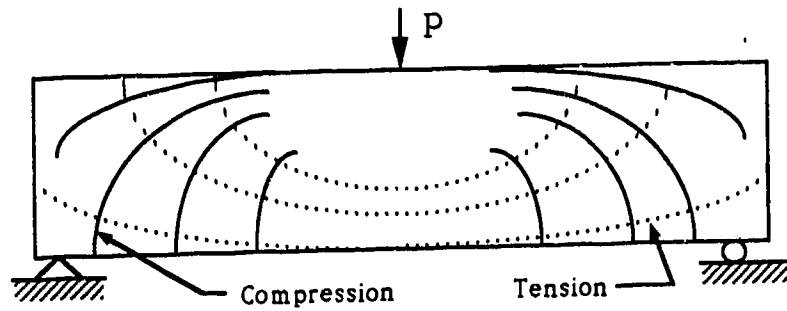
Examination of an elastic rectangular beam subjected to shear provides a useful background to examining shear behavior in cracked concrete beams. Figure 2.1 shows a typical rectangular



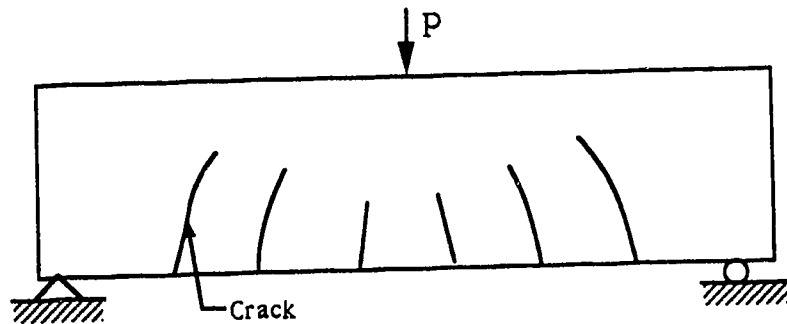
a) Loading



b) Flexural and shear stresses



c) Principal stress trajectories in a homogeneous rectangular beam



d) Potential crack locations

Figure 2.1 Shear in an elastic rectangular beam.

beam subjected to a single point load at midspan. Internal moments and shears are developed to resist the applied load and maintain equilibrium of every segment in the beam. From elementary mechanics of materials, where stresses are proportional to strains, the shear stress  $v$  is given by

$$v = \frac{VQ}{Ib} \quad (2.1)$$

where  $V$  is the total shearing force at the section investigated,  $Q$  equals the first moment of the section above the point where shear stresses are being calculated,  $I$  is the moment of inertia of the entire section about the neutral axis, and  $b$  is the beam width.

The flexural stress  $f_x$  in a beam at any point located a distance ' $y$ ' from the neutral axis can be determined from the flexure formula as

$$f_x = \frac{My}{I} \quad (2.2)$$

where  $M$  is the bending moment, with a magnitude less than or equal to the cracking moment of the section. The flexural stresses are distributed as shown in Figure 2.1b.

Except at the extreme fibers of the beam, elements located away from the neutral axis are subject to both shear and bending stresses. The state of stress at each point can be resolved into equivalent tensile and compressive principal stresses. The principal tensile

stress  $f_t$  can be determined from Mohr's circle of stress, which is widely used for stress transformations as shown in Figure 2.2. The two principal stresses act on orthogonal or mutually perpendicular planes, and no shear stresses exist simultaneously with either one of these stresses. The principal tensile stress acting on a plane inclined at an angle  $\theta$  to the longitudinal axis of the beam can be expressed as

$$f_t = \sqrt{\left(\frac{f_x}{2}\right)^2 + v^2} - \frac{f_x}{2} \quad (2.3)$$

$$\tan 2\theta = \frac{2v}{f_x} \quad (2.4)$$

where  $f_x$  is expressed as a positive quantity in compression. From these equations it is evident the magnitude and inclination of principal stresses are affected by flexural stresses. Curves can be drawn parallel to the direction of principal stresses. These curves, known as stress trajectories, indicate the directions of principal stress, and form a set of orthogonal curves since the principal stresses are mutually perpendicular at any point. A typical example is illustrated in Figure 2.1c.

Prior to the formation of cracks, the distribution of shear stress in a plain rectangular concrete beam without reinforcement will be similar to that derived for a homogeneous elastic beam as shown in Figure 2.1b. The shearing stresses will have a parabolic distribution, and when integrated over the cross section will equal the total

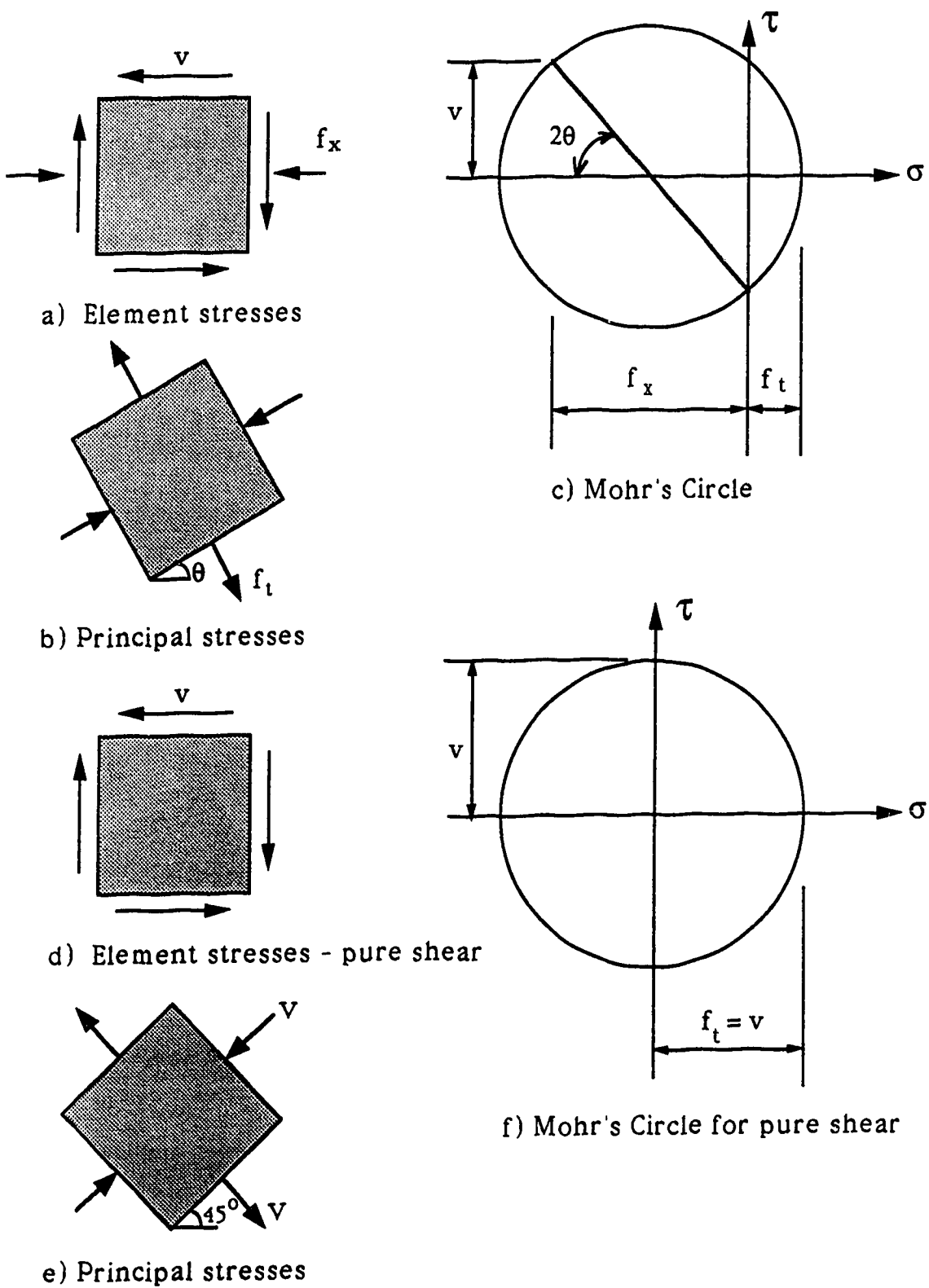


Figure 2.2 Stress conditions of an elemental block.



vertical shear. For a rectangular beam, the maximum shear stress is given by

$$v_{\max} = \frac{1.5 V}{bh} \quad (2.5)$$

The average shear stress is equal to:

$$v = \frac{V}{bh} \quad (2.6)$$

Materials that are weak in tension, such as concrete, tend to form inclined cracks at right angles to the principal tensile stresses as illustrated in Figure 2.1d. After the first crack forms, internal stresses must redistribute, thus altering the original assumed stress distribution. The formation of a crack in a plain concrete beam will immediately cause failure. Cracking is usually initiated at the extreme fiber in the flexural tension zone, where large tensile stresses exist. If a beam has tension reinforcement, further loading is possible beyond the initiation of flexural cracking. In a cracked concrete beam, the concrete below the neutral axis is assumed to carry no tensile stresses, and the longitudinal reinforcement supplies the entire tensile force required for equilibrium. Providing shear stresses are transmitted across the crack, the average shear stresses between two cracks will be distributed as shown in Figure 2.3. Since there is no variation in horizontal shear throughout the tensile zone, the average shear stresses remain constant in this region and no shear stresses exist below the longitudinal reinforcement. From

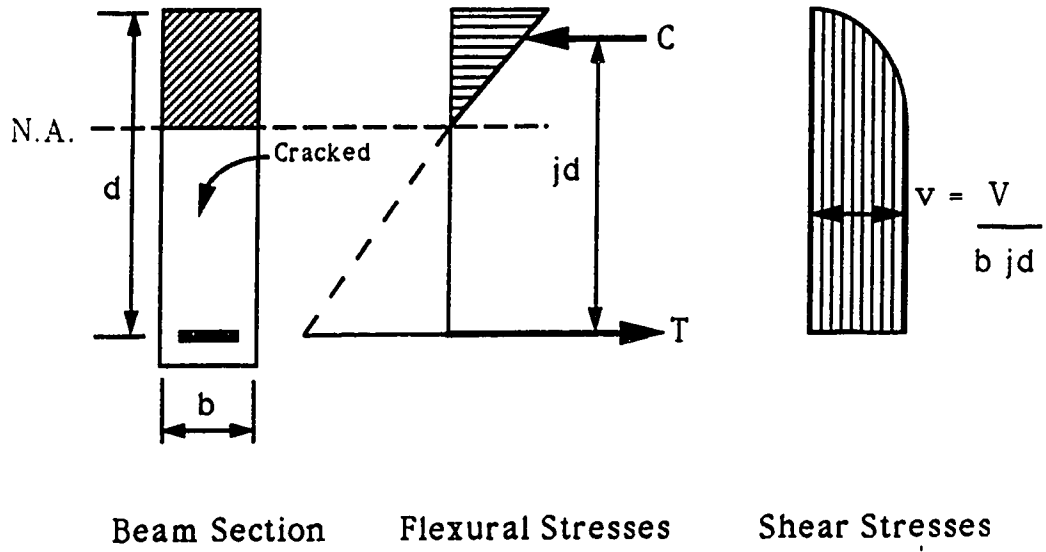


Figure 2.3 Stresses in an idealized cracked concrete beam.

Figure 2.3, equating internal moments on each side of a beam segment between two cracks and examining the horizontal shear flow gives the average shear stress in the tension zone as

$$v = \frac{V}{b j d} \quad (2.7)$$

A shear stress expressed in this manner gives a general measure of the average shear stresses resulting from a shear force. However, the elastic analysis considered in this section provides only a basic understanding of shear stresses. Reinforced concrete is not an elastic, homogeneous material, and in its ultimate state the actual behavior and shear resistance mechanisms in a concrete beam are more complex, and will be discussed in subsequent sections.

### 2.1.2 Principles of B and D Regions

The principal stress trajectories for the rectangular beam in Figure 2.1d are not specifically shown at the supports or at the point of load application because the stress trajectory pattern is severely disturbed in these regions. A relatively new concept in the design of concrete structures is the division of a structure into separate design regions based on the type of load path and strain distribution, as presented by Schlaich et al<sup>5</sup>. Those portions of a beam in which plane sections remain plane are referred to as B-regions, where B denotes beam or Bernoulli. At discontinuous or disturbed regions of a beam such as corners, openings, or concentrated loads, plane

sections do not remain plane and the behavior is very different than in B-regions. These discontinuous portions of a beam are designated D-regions. Figure 2.4 shows beams with both D and B regions.

D regions, which extend about one member depth on each side of a discontinuity, transfer load by in-plane forces such as arch action. As a result, D-regions tend to be stronger than B-regions. Slender concrete beams generally maintain linear strains over most of their length and are governed by beam theory or B-region behavior. Stresses in uncracked B regions are easily determined from cross-sectional forces and member properties. The post-cracking behavior of these regions can be determined from truss models, as will be discussed in later sections. The traditional Pratt truss beam model is generally not applicable to D-regions, or in members in which this behavior dominates, such as corbels, brackets and deep beams. These relatively short and deep members can have different failure modes as compared to slender beams, and require special attention to anchorage, bond, bearing and serviceability details. Strut and tie or truss models developed for the load carrying mechanisms in D-regions are very dependent on the beam geometry and location of loads, and members in which this behavior dominates will not be further considered.

### **2.1.3 Shear Cracking**

As noted previously, inclined cracks will form in a concrete beam when the principal tensile stress reaches the cracking stress. These

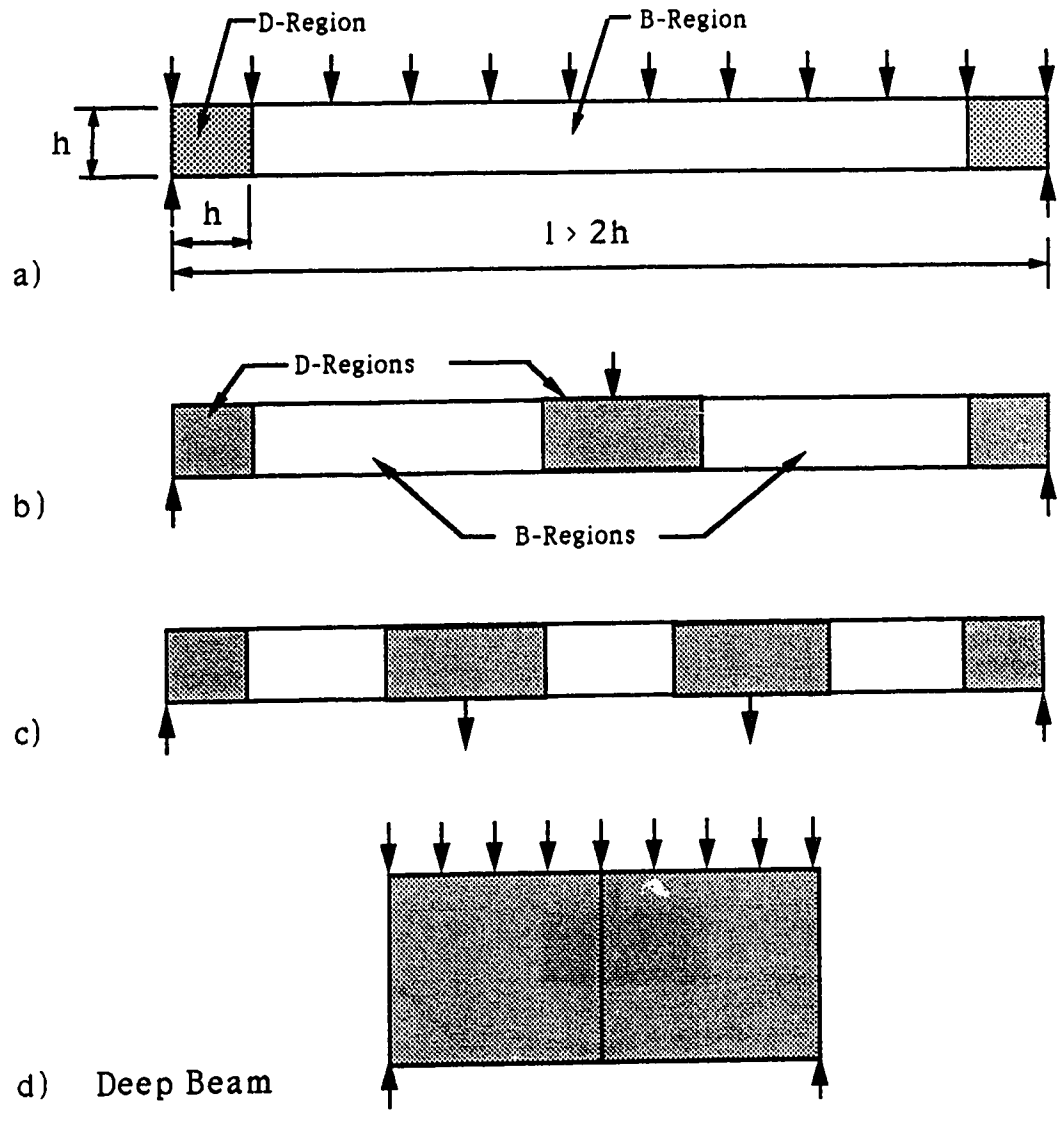


Figure 2.4 Examples of B-regions and D-regions.

cracks may develop in the webs of reinforced or prestressed concrete beams as flexure-shear cracks or web-shear cracks. Flexure-shear cracks form as extensions of or are affected by existing flexural cracks, and are the most common type of inclined cracking exhibited by concrete beams. In contrast, web-shear cracks form independently of any flexural cracks and originate near the centroid of a member. Web-shear cracks generally occur only in prestressed thin webbed concrete I beams, and are observed relatively rarely.

The principal tensile stress causing web shear cracking is easily determined by examining the state of stress at the centroid of a member, as shown in Figure 2.5. If the concrete cracks when the principal tensile stress  $f_t$  reaches the cracking stress  $f_{cr}$ , Eqn. (2.3) becomes

$$f_{cr} = \sqrt{\left(\frac{f_{pc}}{2}\right)^2 + v^2} - \frac{f_{pc}}{2} \quad (2.8)$$

or

$$v_{cr} = f_{cr} \sqrt{1 + \frac{f_{pc}}{f_{cr}}} \quad (2.9)$$

where  $f_{pc}$  is the compressive stress at the level of the centroid and is expressed as a positive quantity and  $v_{cr}$  is the shear stress that will cause diagonal cracking. From correlations with several test results, the ACI Code suggests the principal tensile stress at web shear cracking be taken as  $4\sqrt{f'_c}$  psi ( $0.33\sqrt{f'_c}$  MPa). Therefore, the shear stress to cause web shear cracking  $v_{cw}$  can be found from Eqn. (2.9)

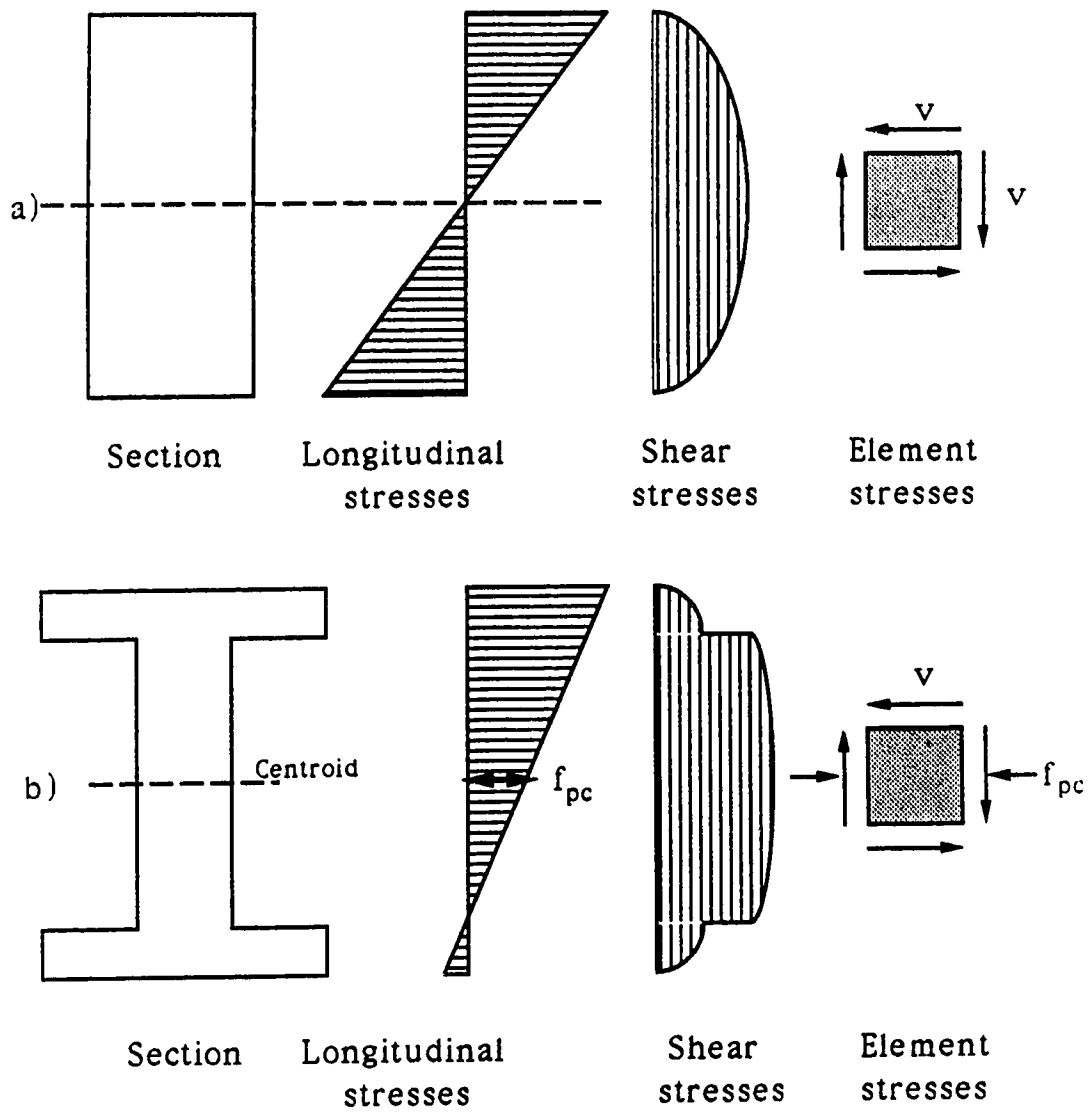


Figure 2.5 Stress distribution in beams: a) without axial load  
b) effect of prestress.

as

$$v_{cw} = 4\sqrt{f'_c} \sqrt{1 + \frac{f_{pc}}{4\sqrt{f'_c}}} \text{ psi} \quad (2.10)$$

Eqn. 2.10 can be approximated by a linear expression as given by Eqn. 2.11 which is utilized in ACI-318-83.

$$v_{cw} = 3.5\sqrt{f'_c} + 0.3f_{pc} \text{ (psi)} \quad (2.11)$$

or

$$V_{cw} = (3.5\sqrt{f'_c} + 0.3f_{pc}) b_w d \text{ (lbs)} \quad (2.11b)$$

Predicting the onset of flexure-shear cracking is a complex problem due to the effects of previously formed flexural cracks. The stress distribution and stress trajectories for an uncracked beam cannot be applied, and the principal stresses near the flexural crack tips initiate diagonal shear cracking. As a result, empirical equations are generally derived to estimate the flexure-shear cracking stress. The ACI Code presents the following expression for the shear at flexure-shear cracking in prestressed concrete beams:

$$V_{ci} = 0.6 \sqrt{f'_c} b_w d + V_d + \frac{V_1 M_{cr}}{M_{max}} \quad (2.12)$$

ACI Eqn. 11-11

where  $M_{cr}$  is the flexural cracking moment,  $V_1/M_{max}$  is the shear to moment ratio, and  $V_d$  is the shear force due to the unfactored dead



load. Tests indicate  $V_{ci}$  obtained using Eqn. 2.12 need not be taken less than  $1.7 \sqrt{f'_c} b_w d$ . Flexure-shear cracking is most often observed in beam tests adjacent to point load locations, where both the bending moment and shear force are at their maximum values. On the other hand, the bending moment and shear force distribution for a beam with distributed loads would cause the location of crack initiation to shift towards the support, where web-shear cracking may predominate.

#### **2.1.4 Function of Shear Reinforcement**

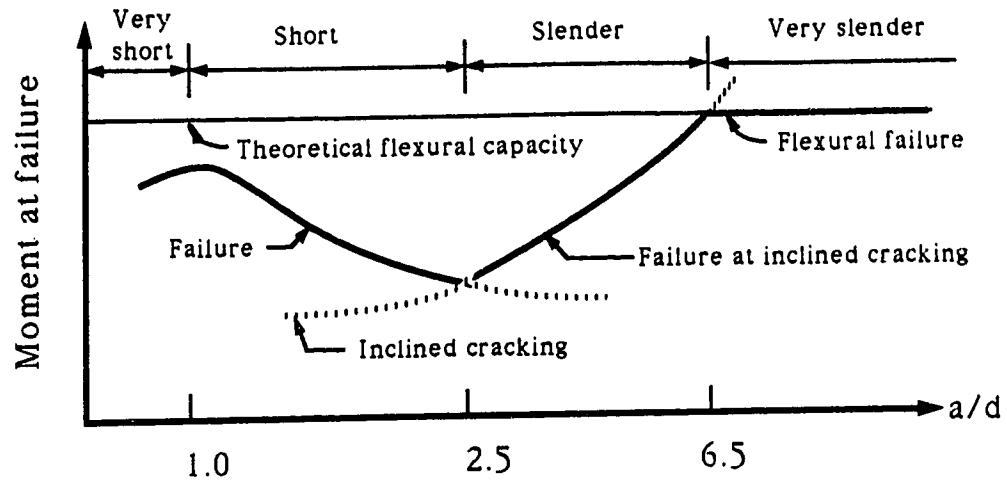
Inclined cracks occur along the principal stress trajectories as shown in Figure 2.1d. The behavior and opening of the cracks is influenced by several factors, including the amount and location of both web reinforcement and longitudinal reinforcement. The horizontal component of crack opening is resisted by the longitudinal flexural reinforcement. Vertical web reinforcement must be provided to restrain the vertical component of the crack opening and assist in maintaining aggregate interlock. In addition to restricting the growth of inclined cracks, the vertical web reinforcement transfers vertical shear forces across the cracks. Although the main purpose of web reinforcement is to provide additional shear strength, it also improves serviceability and provides additional ductility to reinforced concrete beams. Also, stirrups can increase the shear resistance provided by dowel action, since the longitudinal bars are supported and tied in place. Shear reinforcement is usually provided by either stirrups or bent bars, in combination with the

longitudinal reinforcement in the beam. In North America, vertical stirrups are used predominantly and bent bars or inclined stirrups are used only rarely.

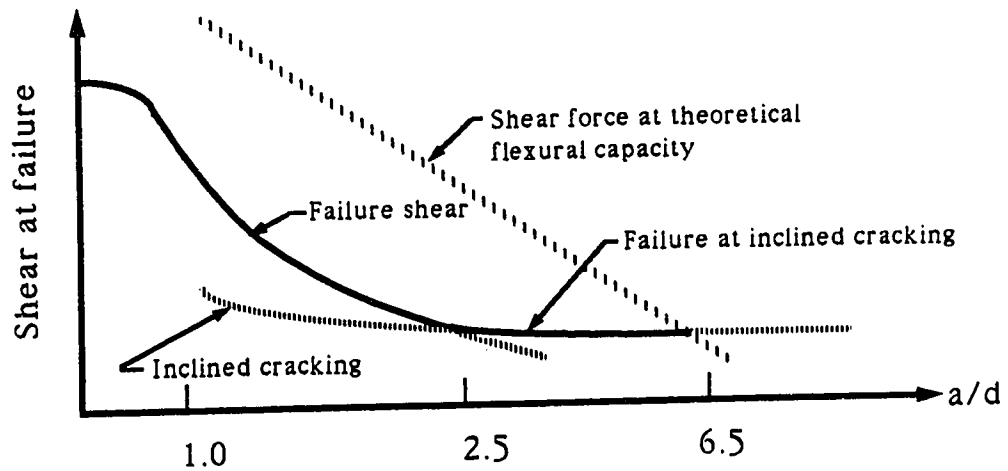
### 2.1.5 Modes of Shear Failure

Shear strength is often investigated by testing simply supported rectangular beams subjected to symmetrical two point loading. The advantage of this testing arrangement is that it provides an almost constant shear force in the end portions of the beam. Tests performed on beams without web reinforcement having constant cross-section have indicated the mode of failure is highly dependent on the shear span ratio  $a/d$ . The dependence of shear strength on the  $a/d$  ratio is clearly shown in Figure 2.6. The shear stress causing diagonal cracking is not influenced strongly by the  $a/d$  ratio, but at small  $a/d$  ratios the ultimate shear capacity increases substantially beyond the initial cracking shear. The difference in behavior shown in Figure 2.6 suggests beams be divided into four categories, typically referred to as very short, short, slender, or very slender beams.

Beams with short or very short shear spans are commonly referred to as deep beams, and their behavior is dominated by D-region behavior. Very short shear spans, having  $a/d < 1$ , develop diagonal cracks connecting the support to the load point, and resist load by arch action. The tied arch system provides considerable reserve strength after inclined cracks form. Failure can occur by



a) Failure moments



b) Ultimate shear forces

Figure 2.6 Variation in moment and shear capacity with  $a/d$  ratio for rectangular beams without web reinforcement (adapted from Ref.13).

crushing of the concrete compression strut, or more commonly by yielding or loss of anchorage in the longitudinal reinforcement tension chord as shown in Figure 2.7.

Relatively short shear spans, with  $a/d$  from 1 to 2.5, also exhibit some reserve strength after inclined cracking. Internal forces redistribute after cracking, permitting further increases in load. Failure may occur either by loss of bond in the tension reinforcement described as a "shear-tension" failure, or by concrete crushing above the crack, commonly referred to as a "shear-compression" failure, as shown in Figure 2.8. Failure of short shear span beams usually occurs prior to the attainment of the flexural capacity, because inclined cracks generally extend higher into the compression zone than flexural cracks.

Most practical beams are slender beams having  $a/d$  ratios from approximately 2.5 to 6, which transmit shear primarily by beam action or B-region behavior. In slender beams without web reinforcement, flexural cracks form prior to any diagonal cracks, however when inclined flexure-shear cracks develop, equilibrium cannot be maintained and failure occurs suddenly without warning. This type of failure is referred to as diagonal-tension failure. Failure of slender beams without web reinforcement occurs at the onset of inclined cracking, and only for small shear spans is the ultimate load greater than the flexure-shear cracking load. Very slender beams, with  $a/d$  greater than approximately 6, are characterized by flexural failures prior to inclined cracking, and are able to attain their full

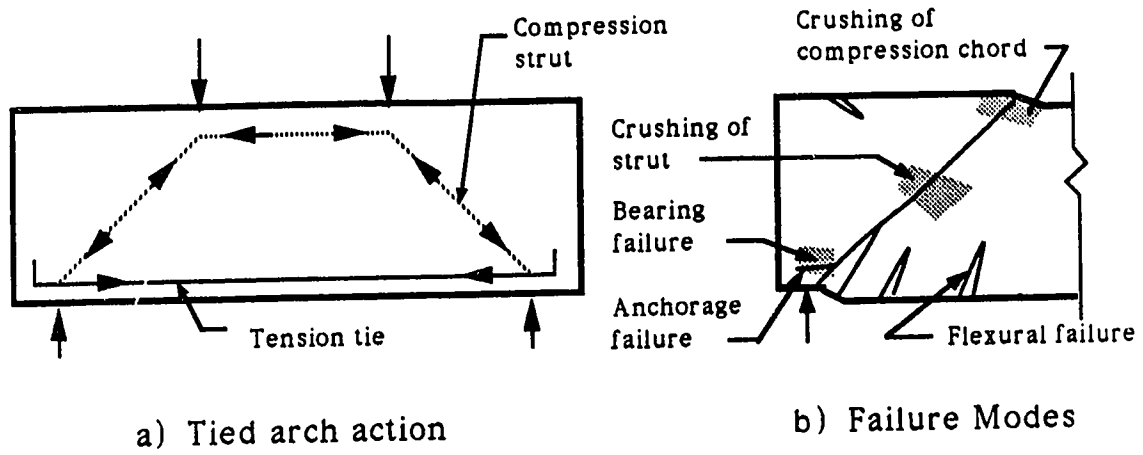


Figure 2.7 Failure modes in deep beams.

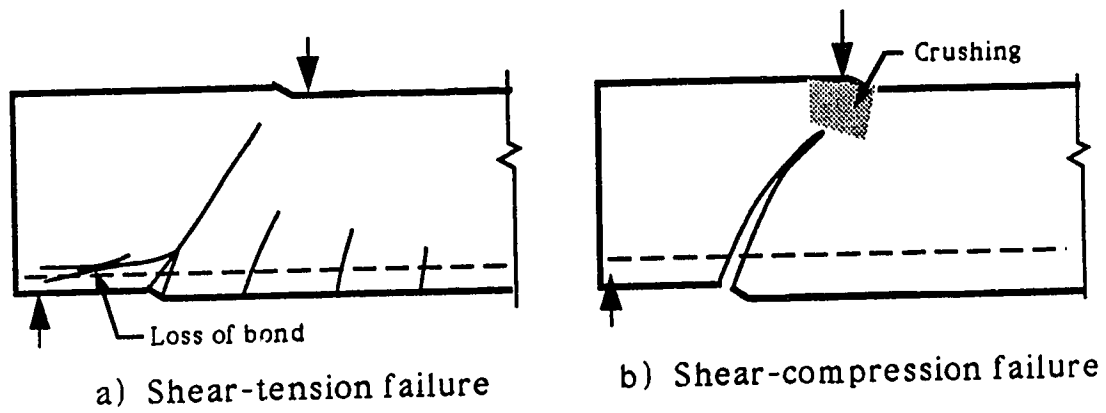


Figure 2.8 Typical shear failure modes of short beams,  
 $1.5 < a/d < 2.5$ .

flexural capacity. As a result, the ultimate strength of very slender beams is not affected by shear.

In prestressed concrete beams without web reinforcement, flexural cracking is delayed due to the effects of longitudinal compressive stresses increasing the flexural stress necessary to cause cracking. Prior to failure, a considerable portion of a prestressed beam may remain uncracked in flexure. Slender prestressed members without web reinforcement fail primarily by two modes, either flexure-shear cracking, where an inclined crack grows from or is influenced by a flexural crack, or by web-shear cracking where the principal tensile stress in an uncracked web reaches the tensile capacity of the concrete. Either type of cracking is followed by failure due to crushing of the concrete above the crack, shearing of the compression zone, loss of anchorage of the tensile reinforcement or possibly crushing of the concrete web. Since prestressed concrete members often have cross sectional shapes with compression flanges, the propagation of inclined cracks into the compression zone may be postponed, thus delaying shear-compression type failures. Anchorage failures can occur in prestressed concrete beams, particularly when pretensioned strands are used and a crack forms in the vicinity of the support.

Since the shear failure modes of concrete beams without web reinforcement are very sudden and without warning, web reinforcement is provided in beams to eliminate the "trough" shown in Figure 2.6, such that a beam will fail in flexure prior to failing in

shear. This design philosophy is particularly important in slender beams, where the formation of an inclined crack can cause immediate failure if no web reinforcement is provided. Shear reinforcement is designed to yield prior to reaching the ultimate shear capacity in order to provide some ductility as compared to the other shear failure modes. Another possible failure mode for concrete beams with web reinforcement is crushing of the web between two cracks. This is known as a web crushing failure, and only occurs in thin-webbed I beams. In members without web reinforcement and large compression flanges, an inclined crack may extend along the web flange junction until local flange instability causes failure. The presence of web reinforcement across this junction tends to stabilize the flange.

Provided the web reinforcement yields, failure of a beam with shear reinforcement will generally be more gradual than a beam without, due to the ductile load-deflection response of the reinforcement. If an insufficient amount of shear reinforcement is provided, formation of an inclined crack may cause immediate yielding of the reinforcement resulting in a sudden failure, although this mode of failure is not well documented. If an excess of web reinforcement is provided, the beam may fail due to web crushing prior to yielding of the web reinforcement. Due to its brittle nature, this is an undesirable failure mode.

### 2.1.6 Basic Mechanisms of Shear Transfer

Figure 2.9 shows the free body diagram of a reinforced concrete beam at an inclined crack location, and identifies several shear transfer mechanisms. The uncracked concrete in the compression zone provides a shear resistance  $V_{cz}$ . The longitudinal reinforcement resists vertical shear transverse to its axis by dowel action  $V_d$ .  $V_s$ , the component of shear resisted by the web reinforcement, if any, is provided by tension in the stirrups. Aggregate interlock,  $V_a$ , is the result of relative movement or slip between the rough and interlocked crack surfaces. As shown in Figure 2.10, aggregate interlock includes two components,  $V_{an}$  normal to the inclined crack and  $V_{ai}$  in the same plane as the crack interface.

In a beam with web reinforcement, all of the shear transfer mechanisms participate in the redistribution of internal forces after the formation of a crack as shown in Figure 2.11. As a crack widens upon increasing load, the aggregate interlock component of shear decreases, and dowel action will become ineffective as splitting cracks form along the longitudinal reinforcement. Consequently, the proportion of shear transferred by the various shear mechanisms varies for different stages of loading.

In providing shear strength, the dominance of particular shear transfer mechanisms changes for different types of beams. For slender concrete beams without shear reinforcement, the aggregate interlock and dowel force substantially diminish with increased crack



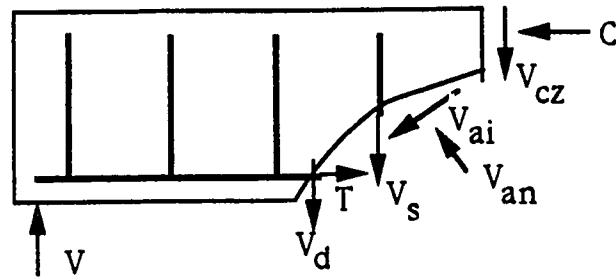


Figure 2.9 Internal forces resisting shear at inclined crack.

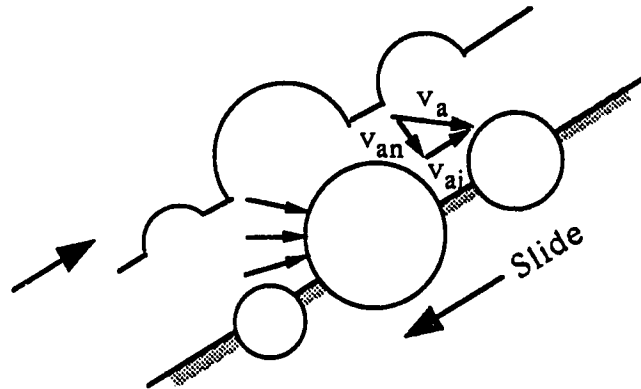


Figure 2.10 Forces developed by aggregate interlock.

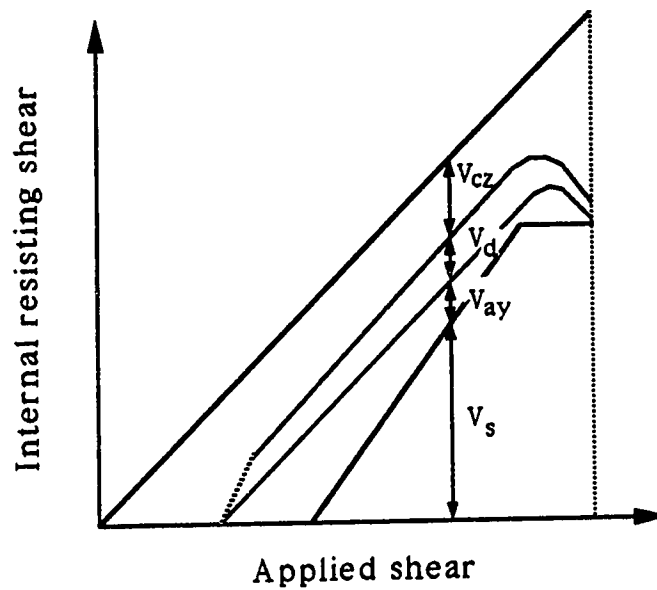


Figure 2.11 Redistribution of internal shear forces in a beam with shear reinforcement.

width until the entire vertical shear is resisted by the concrete compression zone above the crack. Failure of this region under increased load may be very sudden and brittle. Therefore, as noted previously the shear strength of slender beams without shear reinforcement is generally assumed to be reached when the first crack forms. In contrast, deep beams without web reinforcement develop arch action after inclined cracking, and can have substantial post-cracking shear strength.

Concrete members with shear reinforcement continue to carry shear forces after the formation of a diagonal crack. Following inclined cracking, the proportion of shear carried by web reinforcement will continuously increase until the shear reinforcement yields, as shown in Figure 2.11. After it yields, other shear transfer mechanisms must provide the additional shear resistance required under increasing applied loads. Final failure will generally occur due to splitting along the longitudinal reinforcement or crushing of the compression zone above the crack. Generally failure occurs soon after the stirrups yield.

## **2.2 Traditional Truss Models for Concrete Beams**

As noted previously, an element at the neutral axis of a concrete beam is subjected to shear stresses. Pure shear stresses produce tensile and compressive stresses in the element acting at  $45^\circ$  to the neutral axis as shown in Figure 2.2. Since concrete is weak and cracks in tension, reinforcement is provided to equilibrate the tensile

forces, while the concrete is capable of resisting the compressive stresses. This development of tension and compression fields suggests a reinforced concrete beam could be modelled as a truss, with web reinforcement acting as tension members and portions of concrete between the cracks acting as diagonal compression members. The flexural compression zone provides the required compression chord while the longitudinal tensile reinforcement acts as a bottom tension chord as illustrated in Figure 2.12.

At the beginning of the century, Ritter<sup>6</sup> and Morsch<sup>7</sup> independently developed truss analogies for cracked reinforced concrete beams. Ritter visualized diagonal concrete struts acting from the top of one stirrup to the bottom of the next. Morsch introduced the concept that inclined compression fields, not discrete diagonal compressive struts, can be used to model the flow of forces in a cracked concrete beam. In its simplest form, several stirrups are collected into one vertical tension member, and various inclined concrete struts are combined into one diagonal member as shown in Figure 2.13b. This model assumes that after cracking the diagonal compression stresses remain at  $45^{\circ}$ . Although Morsch recognized the possible reorientation of the principal compressive stress and the flatter inclination of crack angle that occurs as loading progresses, he recommended use of the  $45^{\circ}$  truss model as a conservative approach in design.

The traditional truss model is used to investigate equilibrium of the applied loads, reactions, and internal forces in a beam. In order

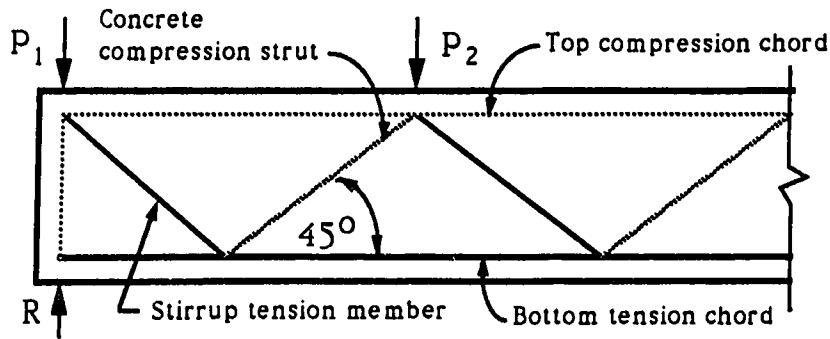
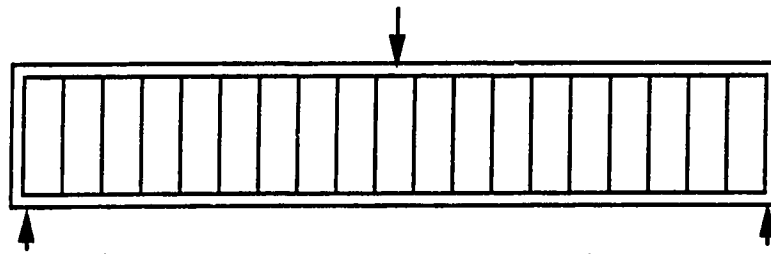
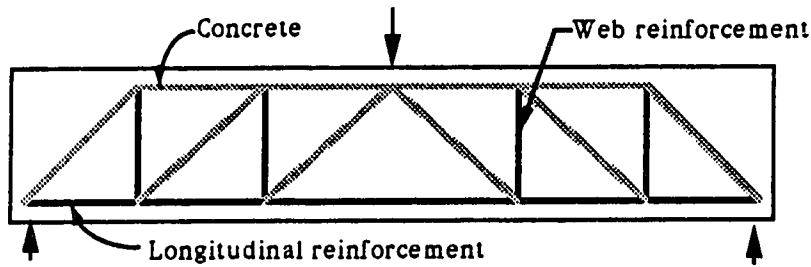


Figure 2.12 Truss analogy of a concrete beam.

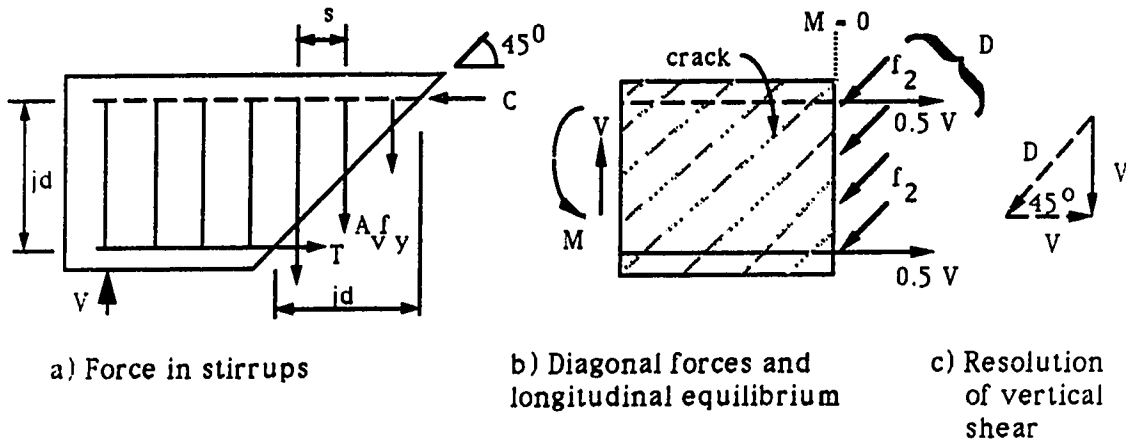


a) Beam subjected to single point load



b) Truss model of a reinforced concrete beam

Figure 2.13 Pin-jointed truss analogy.



a) Force in stirrups

b) Diagonal forces and longitudinal equilibrium

c) Resolution of vertical shear

Figure 2.14 Internal forces in a traditional truss model.

to ensure the truss is capable of resisting the applied loads, the stresses in the reinforcement, the uniaxially stressed concrete struts, and the pinned connections must be examined. The truss shown in Figure 2.13 is statically determinate. Alternatively, if a truss with closely spaced stirrups is considered it will be statically determinate if all the stirrups are assumed to yield. From the free body diagram shown in Figure 2.14 the force in one stirrup is calculated as

$$A_v f_y = \frac{V s}{jd} \quad (2.13)$$

or

$$V = \frac{A_v f_y jd}{s} \quad (2.13b)$$

where  $V$  is the vertical force acting on the section,  $A_v$  is the total cross sectional area of web reinforcement within the distance  $s$ , and  $jd$  is the internal lever arm.

From Figures 2.14b and 2.14c, the shear force  $V$  can be resolved into a diagonal compression force  $D$  and a horizontal force. For a  $45^\circ$  truss the horizontal force will be equal to  $V$ . In other words, the horizontal component of the diagonal force must be resisted by an equal tensile force in the longitudinal reinforcement. If the shear stresses are uniformly distributed over an area  $b_w jd$ , then a tensile force of  $V/2$  acts on both the top and bottom chords of the truss, as shown in Figure 2.14b.

Although analysis of the traditional pin-jointed truss is very simple, it neglects the effects of the uncracked concrete in the compression zone, dowel action, tensile stresses in the concrete between and cracks, and aggregate interlock on the crack surfaces. Since these mechanisms can provide a significant portion of the total shear resistance, the traditional truss model can be modified to include their effects and account for the flatter inclined cracks that form in actual concrete beams. In the ACI Code, the conservatism of the traditional  $45^\circ$  truss model is accounted for by adding an empirical correction term, commonly referred to as the concrete contribution. The ACI shear design procedure will be discussed in the following section.

## **2.3 ACI 318-83 Shear Design Procedure**

### **2.3.1 Reinforced Concrete**

The ACI Code is based on the  $45^\circ$  truss model, with an empirical correction to account for the conservatism of the model. The ACI Code does not consider a whole member approach where an entire beam is visualized as a truss, but instead derives a sectional approach from the basic truss concepts, where any section of a beam can be examined independently of other portions. In the ACI Code, the nominal ultimate capacity of a concrete beam  $V_n$  must be greater than or equal to the factored shear force  $V_u$  such that the following relation is satisfied:

$$V_u \leq \phi V_n \quad (2.14)$$

ACI Eqn 11-1

where  $\phi$  is a strength reduction factor equal to 0.85 for shear. The nominal shear resistance  $V_n$  is equal to the sum of two components, namely

$$V_n = V_c + V_s \quad (2.15)$$

ACI Eqn 11-2

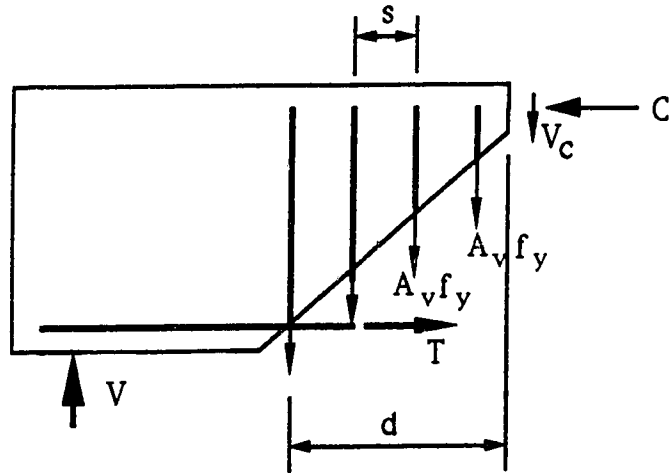
where  $V_c$  is the shear carried by the concrete and  $V_s$  is the strength contributed by the web reinforcement.

### 2.3.1.1 Shear Strength Provided by the Reinforcement

The ACI Code expression for  $V_s$ , the shear strength provided by the web reinforcement, is obtained by examining a segment of a concrete beam isolated by an idealized straight diagonal crack. See Figure 2.15. The horizontal projection of the crack is assumed equal to the effective depth  $d$ , suggesting the crack angle is slightly less than  $45^\circ$ . If web reinforcement is assumed to yield as the ultimate shear strength is reached, the shear resisted by vertical stirrups is

$$V_s = \frac{A_v f_y d}{s} \quad (2.16)$$

ACI Eqn 11-17



Number of stirrups,  $N = d/s$

Then 
$$V = \frac{A_v f_y d}{s} \quad \text{or} \quad s = \frac{A_v f_y d}{V}$$

**Figure 2.15** Shear strength provided by vertical web reinforcement.



Eqn. 2.16 is similar to Eqn 2.13 obtained from the simple truss model, except that the ACI Code assumes the lever arm is equal to the effective depth.

Shear reinforcement is required whenever the effect of the factored loads exceeds the resistance provided by the concrete. In the 1950's, Elstner and Hognestad<sup>8</sup> illustrated the hazards of using concrete beams without shear reinforcement. Since many members experience brittle shear failures after the formation of the first diagonal crack, ACI Sec. 11.5.5.1 requires a minimum amount of shear reinforcement wherever

$$V_u \geq \phi V_c/2 \quad (2.17)$$

except for slabs, footings, concrete joists, and certain categories of wide and shallow beams. These members are assumed to be able to redistribute internal forces before a diagonal tension failure occurs, and are therefore excluded from the minimum web reinforcement requirement.

ACI Sec. 11.5.5.3 specifies the minimum area of shear reinforcement for nonprestressed members as

$$A_v = 50 \frac{b_w s}{f_y} \quad (2.18)$$

ACI Eqn 11-14

Satisfying this minimum web steel requirement is equivalent to the reinforcement providing a nominal shear stress of 50 psi ( 0.34 MPa) acting on the beam web.

In order to ensure that the web reinforcement yields prior to a shear compression failure or brittle web crushing failure, ACI Sec. 11.5.6.8. places an upper limit on the amount of shear reinforcement as

$$V_{s(\max)} = 8\sqrt{f'c} b_w d \quad (2.19)$$

This equation also guards against excessive crack widths at service loads.

Prior to inclined cracking, web reinforcement is subjected to only minimal strains, and does not become effective until after diagonal cracking has taken place. Stirrups are therefore ineffective if not crossed by a crack. As a result, ACI Sec. 11.5.4.1 places a limit on the maximum spacing of vertical shear reinforcement as the smaller of  $d/2$  or 24 inches (600 mm) for vertical stirrups. This Code limitation is based on the assumption of a  $45^\circ$  inclined crack, thus ensuring at least one stirrup will intercept the crack. Although Eqn. 2.19 provides a general serviceability check on crack widths, cracks that widen under high stresses are best restrained by closely spaced and properly detailed reinforcement. Therefore, when the factored shear resistance provided by the web reinforcement  $V_s$  exceeds  $4\sqrt{f'c}b_w d$ , ACI Sec. 11.5.4.3 requires the maximum spacing for vertical stirrups

be reduced to  $d/4$  or 12 inches (300mm).

As noted previously, it is desirable to ensure the web reinforcement yields prior to reaching the ultimate capacity in shear so as to provide some ductility in the failure mode. Consequently, shear failures as a result of poor detailing or anchorage failure must be avoided. As shown in Figure 2.15, both end portions of a stirrup must be able to anchor or develop the yield strength of the reinforcement  $f_y$ . Since the crack may extend very close to the extreme compression or tension face of a beam, a vertical stirrup must be able to develop its yield strength even at the extreme end of its length. In order to ensure adequate anchorage, ACI Sec. 12.13.1 specifies web reinforcement be extended as close to the compression and tension surfaces as practical, and several types of permissible anchorage details are given.

### **2.3.1.2 Shear Strength Provided by the Concrete**

In beams with web reinforcement, the ACI Code assumes the shear resisted by the concrete is equal to the strength of a concrete beam without any shear reinforcement. As a result, the shear transfer mechanisms denoted in Figure 2.9 are combined into one  $V_c$  term, which has been assumed to be equal to the shear causing inclined cracking in a beam without stirrups, that is

$$V_c = V_{cz} + V_d + V_{ay} = \text{Cracking Shear} \quad (2.20)$$

Therefore, although the actual contribution to the total shear capacity of  $V_{cz}$ ,  $V_d$ , and  $V_a$  varies, the total contribution of these components is assumed to be constant throughout all loading stages. For members subjected to shear and flexure, ACI 318-83 recommends two equations for the concrete contribution to shear as

$$V_c = 2\sqrt{f'_c} b_w d \quad (2.21)$$

ACI Eqn 11-3

$$V_c = (1.9\sqrt{f'_c} + 2500\rho \frac{V_u d}{M_u}) b_w d \quad (2.22)$$

ACI Eqn 11-6

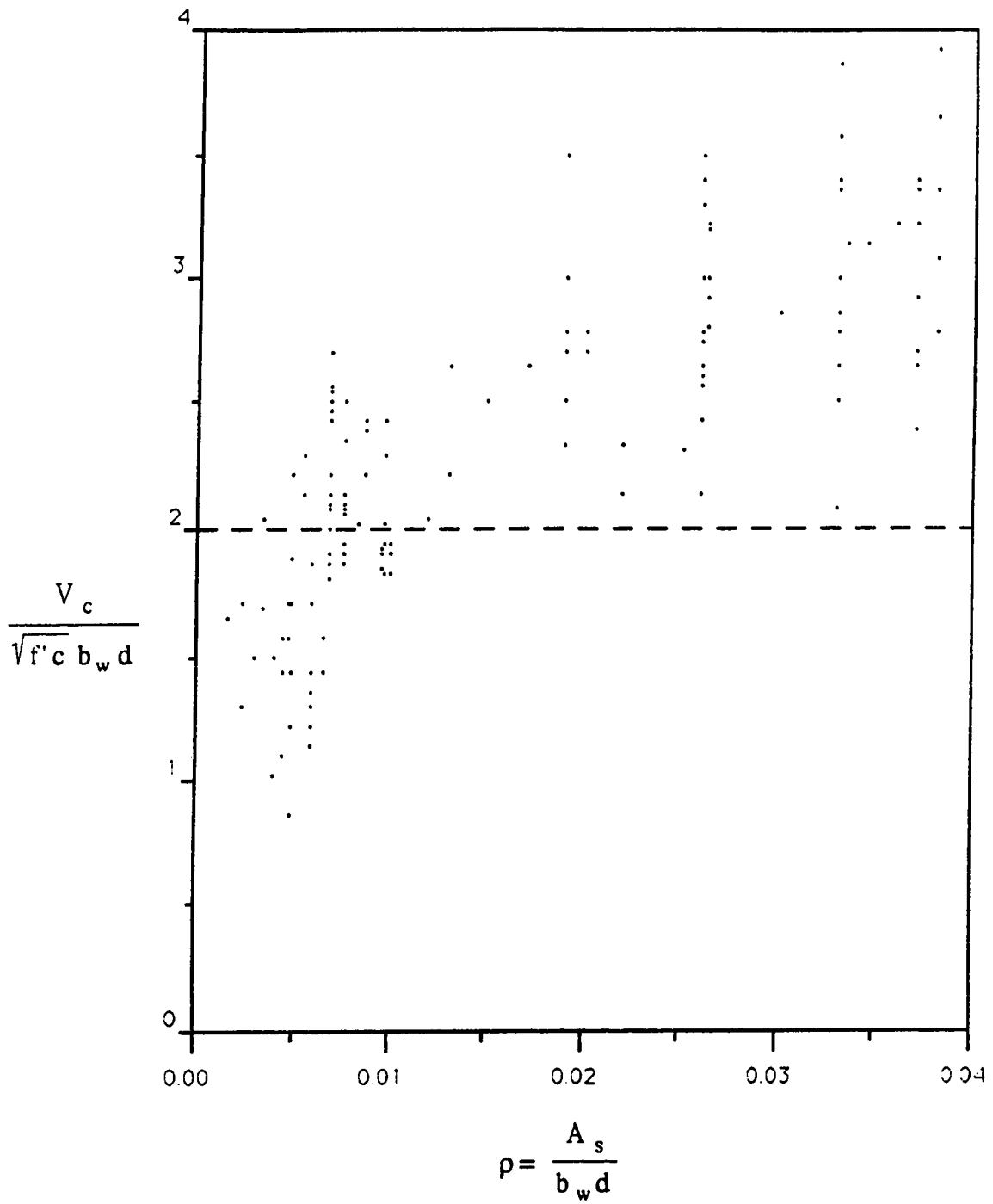
where Eqn. 2.22 is that originally presented by the 1962 ACI-ASCE Committee on Shear and Diagonal Tension<sup>9</sup>. Eqn. 2.22 is very tedious to use because the shear, moment and longitudinal reinforcement ratio  $\rho$  typically change throughout a beam span, requiring  $V_c$  to be computed at numerous locations. Test results of both short and slender beams were used to develop Eqn. 2.22, which therefore combined the results of beams in which D-region and B-region behavior dominates respectively. A single equation which attempts to predict the shear strength of two completely different types of beam behavior will have shortcomings. Recent studies suggest the effect of  $\rho$  is underestimated in Eqn. 2.22, and it does not treat the shear span ratio, expressed as  $Vd/M$ , adequately. As noted by the ACI-ASCE Committee 426 in 1977<sup>10</sup>, the applicability of Eqn. 2.22 is suspect and not recommended. Therefore Eqn. 2.22 will not be

considered further. Figure 2.16 compares Eqn. 2.21 with the test results of several simply supported beams without web reinforcement. Referring to Figure 2.16, Eqn. 2.21 generally underestimates the shear capacity for beams with large reinforcement ratios and overestimates the shear strength for small steel percentages. Although this equation can be very conservative in some situations, it is very simple to use and the nominal shear capacity of a reinforced concrete beam with vertical stirrups can be expressed as

$$V_n = 2\sqrt{f_c} + \frac{A_v f_y d}{s} \quad (2.23)$$

which must be multiplied by the strength reduction factor  $\phi = 0.85$  to calculate the factored shear resistance of the section.

From Figure 2.14c, it is evident the truss model predicts that both vertical and longitudinal reinforcement is required to resist shear. A longitudinal tension force is required to equilibrate the horizontal component of the inclined compressive force and the effect of inclined cracking is to increase the tension force in the flexural reinforcement. This will be discussed in more detail in a later section. The ACI Code does not explicitly specify the amount of longitudinal reinforcement necessary for shear, but indirectly considers the increase in tension force through its bar detailing requirements in ACI Sec. 12.10.3. To include the effects of shear on longitudinal bar forces, as well as to consider other contingencies, the



**Figure 2.16** Comparison of Eqn. 2.21 with experimental results (adapted from Ref. 13).

ACI Code specifies bars be extended a minimum of the effective depth  $d$  or 12 bar diameters past the theoretical cut-off location.

As is evident from Eqn. 2.9, axial compression increases the inclined cracking stress while axial tension tends to decrease it. For axial compression and tension, ACI Code Sections 11.3.1.2 and 11.3.2.3 permit the use of simplified expressions as

$$\text{Axial Compression: } V_c = 2 \left( 1 + \frac{N_u}{2000 A_g} \right) \sqrt{f'_c} b_w d \quad (2.24)$$

ACI Eqn 11-4

$$\text{Axial Tension: } V_c = 2 \left( 1 - \frac{N_u}{500 A_g} \right) \sqrt{f'_c} b_w d \quad (2.25)$$

ACI Eqn 11-9

where  $N_u$  is positive in compression and negative in tension. For members subjected to significant axial tension, ACI Sec. 11.3.1.3 suggests a simplified alternate to Eqn. 2.25 where the concrete is assumed to carry no shear and the shear reinforcement is designed to transfer the total shear force.

### 2.3.2 Prestressed Concrete

For prestressed concrete beams with web reinforcement perpendicular to their longitudinal axis, the ACI Code gives the nominal shear strength as

$$V_n = \frac{A_v f_y d}{s} + V_c \quad (2.26)$$

which is identical to the expression used for reinforced concrete members. As in nonprestressed beams, the shear force  $V_c$  resisted by the cracked concrete in a prestressed beam is assumed equivalent to the shear causing inclined cracking. As mentioned in previous sections, prestressed concrete beams form diagonal cracks either as flexure-shear cracks or web-shear cracks. For flexure-shear cracking, the ACI Code expression is given by

$$V_{ci} = 0.6\sqrt{f'_c} b_w d + V_d + \frac{V_l M_{cr}}{M_{max}} \quad (2.12)'$$

ACI Eqn 11-11

$$V_{ci} \geq 1.7\sqrt{f'_c} b_w d \quad (2.12b)$$

where the terms are as previously defined. The flexure cracking moment is determined by

$$M_{cr} = \frac{I}{y_t} (6\sqrt{f'_c} + f_{pe} - f_d) \quad (2.27)$$

ACI Eqn 11-12

where  $y_t$  is the distance from the tension face to the concrete centroid,  $f_{pe}$  is the compressive stress at the tension face due to the tensile force alone, and  $f_d$  is the extreme fiber stress due to unfactored dead load. According to ACI Sec. 11.4.2.3, the effective



depth  $d$  need not be taken less than 80% of the overall depth of the member. As mentioned in Section 2.1.3, the ACI expression for the shear force causing web-shear cracking is

$$V_{cw} = (3.5\sqrt{f'_c} + 0.3f_{pc}) b_w d + V_p \quad (2.28)$$

ACI Eqn 11-13

where  $V_p$  is the vertical component of the effective prestress force. Eqn. 2.28 is a linear approximation to Eqn. 2.10. In the ACI Code, the shear resistance provided by the concrete is equal to the lesser of  $V_{ci}$  or  $V_{cw}$ . Since calculation of  $V_{ci}$  and  $V_{cw}$  can be very tedious, ACI Sec. 11.4.1 provides an alternate expression for members with a prestress force at least equal to 40% of the flexural reinforcement strength as

$$V_c = (0.6\sqrt{f'_c} + 700 \frac{V_u d}{M_u}) b_w d \quad (2.29)$$

ACI Eqn 11-10

where  $V_u d / M_u$  is not to be taken greater than 1.0. Where Eqn 2.29 is used,  $V_c$  need not be less than  $2\sqrt{f'_c} b_w d$  and must not exceed  $5\sqrt{f'_c} b_w d$ . Although this equation is easier to use than Eqns. 2.12 and 2.28, it can be very conservative in some situations, particularly for composite beams or slender I beams<sup>11</sup>.

The ACI Code requirements for minimum shear reinforcement in prestressed concrete beams are similar to those for reinforced

concrete beams, except that in addition to Eqn. 2.18, prestressed beams must also satisfy a minimum area requirement of

$$A_v = \frac{A_{ps} f_{pu} s}{80 f_y d} \sqrt{\frac{d}{b_w}} \quad (2.30)$$

ACI Eqn 11-15

where  $f_{pu}$  is the specified tensile strength of the prestressing steel and  $A_{ps}$  is the cross-sectional area of the prestressed reinforcement. In prestressed concrete members, the maximum spacing of shear reinforcement is limited to the smaller of  $0.75h$  or 24 inches (600 mm). As with reinforced concrete members, when  $V_s$  exceeds  $4\sqrt{f'_c}b_w d$  the maximum spacing limits are reduced by half, resulting in a maximum spacing of  $0.375h$  or 12 inches (300 mm). The minimum practical spacing of stirrups is 3 or 4 inches.

## 2.4 CAN3-A23.3-M84 Simplified Method

The Canadian Standards Association design code, CAN3-A23.3-M84<sup>1</sup> presents two shear design procedures, the Simplified Method and the General Method. The Simplified Method is similar to the ACI shear design procedure, because it is based on the same sectional approach, whereby an empirical correction term is added to the  $45^\circ$  truss model equations. The basic design expression for shear is given as

$$V_r \geq V_f \quad (2.31)$$

CSA Eqn 11-5

where  $V_r$  is the factored shear resistance and  $V_f$  is the factored shear force. The factored shear resistance is given by

$$V_r = V_c + V_s \quad (2.32)$$

CSA Eqn 11-6

where  $V_c$  is the concrete contribution and  $V_s$  is the shear resistance provided by the web reinforcement. In the Simplified Method, the concrete contribution for reinforced concrete members is expressed in S.I. units as

$$V_c = 0.2\lambda\phi_c\sqrt{f_c} b_w d \quad (2.33)$$

CSA Eqn 11-7

where  $\phi_c$  is the material resistance factor for concrete and  $\lambda$  is a factor that accounts for the effects of low density concrete. The design equations in the Canadian Code are different than the ACI Code because different load factors are used and the CSA Code considers specific resistance factors for different materials. In the 1984 Canadian Code, there is no expression similar to Eqn. 2.22, although a similar expression was used in the 1977 edition.

For prestressed concrete beams, the concrete contribution is the lesser of

$$V_c = (0.06\lambda\sqrt{f'_c} + 6\frac{V_f d_p}{M_f})\phi_c b_w d \quad (2.34)$$

CSA Eqn 11-10

or

$$V_c = 0.4\lambda\phi_c\sqrt{f'_c} \left( \sqrt{1 + \frac{f_{pc}}{0.4\lambda\phi_c\sqrt{f'_c}}} \right) b_w d_p + \phi_p V_p \quad (2.35)$$

CSA Eqn 11-11

but  $V_c$  need not be taken less than  $0.2\lambda\phi_c\sqrt{f'_c}b_w d$ . When shear reinforcement is perpendicular to the axis of a member, the contribution of shear reinforcement is given by

$$V_s = \phi_s \frac{A_v f_y d}{s} \quad (2.36)$$

CSA Eqn 11-12

where  $\phi_s$  is the material resistance factor for the reinforcement and all other terms are as previously defined. If the load factors and material resistance factors are considered as unity, it is apparent the shear design provisions in the simplified method of the Canadian Code are similar to the ACI Code procedures for both reinforced and prestressed concrete members.

The General Method in the Canadian Code is a new addition based on the Compression Field Theory developed by Collins and Mitchell<sup>12</sup>. The basic design approach is to model a cracked reinforced concrete beam as a truss with a continuous field of diagonal compression struts, vertical tension ties, and parallel top

and bottom chords. The concrete is assumed to be ineffective in resisting tensile stresses. In addition to examining equilibrium relations from the truss model, stress strain relationships and compatibility requirements are also considered. Within specified limits, a designer is free to choose the angle of inclination of the compression field provided it satisfies all of the specified design requirements. Since the compressive stress in the diagonal struts increases as the inclination decreases, the compressive stresses for a given angle must be checked against a maximum allowable stress to prevent concrete from crushing. Although the General Method provides a rational model for shear design, it does not consider the contributions of tension in the concrete or aggregate interlock, and it is a more complex design procedure than the Simplified Method.

## 2.5 Variable Angle Truss Models

To account for the conservatism of a  $45^\circ$  truss model, both the ACI Code and the Canadian Code Simplified Method add a concrete contribution to the capacity of the truss action in the web. The  $45^\circ$  truss model can also be adjusted and made more accurate by taking into consideration that  $\theta$  is typically less than  $45^\circ$ , and this modification is referred to as a variable angle truss model. A variable angle analogy departs from the traditional assumption that the inclination of the diagonal compression struts is steadfast at  $45^\circ$ , and provides a more realistic model of a beam's behavior in shear.

Variable angle truss models can incorporate the different types of

behavior in a beam's B and D-regions. In B-regions, it is suitable to model the internal flow of forces as a continuous field of parallel diagonal struts, having a constant angle of inclination  $\theta$ . In D-regions, a uniform compression field does not accurately model the internal flow of forces, and a better representation is provided by a fan shaped stress field or compression fan, as illustrated in Figure 2.17.

In its original form, the variable angle truss model neglects the tensile stresses in the concrete. A free body diagram of the internal forces acting at a section parallel to a uniform compression field is shown in Figure 2.18. The truss model does not include the shear components  $V_{cz}$ ,  $V_{ay}$ , and  $V_d$  in Figure 2.9, hence the vertical component of the shear force is resisted entirely by the stirrups in combination with the inclined compression struts. Vertical equilibrium of the free body shown in Figure 2.18a gives

$$V = \frac{A_v f_s j d}{s \tan \theta} \quad (2.37)$$

where  $f_s$  is the tensile stress in the stirrups, and all other variables are as previously defined. Figure 2.18b summarizes additional equilibrium conditions for a variable angle truss model. Figure 2.18b shows a length of beam over which the shear force remains constant, and considers a vertical section at a location of zero moment. The vertical shear can be resolved into an inclined compression force  $D$  and a horizontal tension force  $N_v$ . The total diagonal compressive force can be expressed as

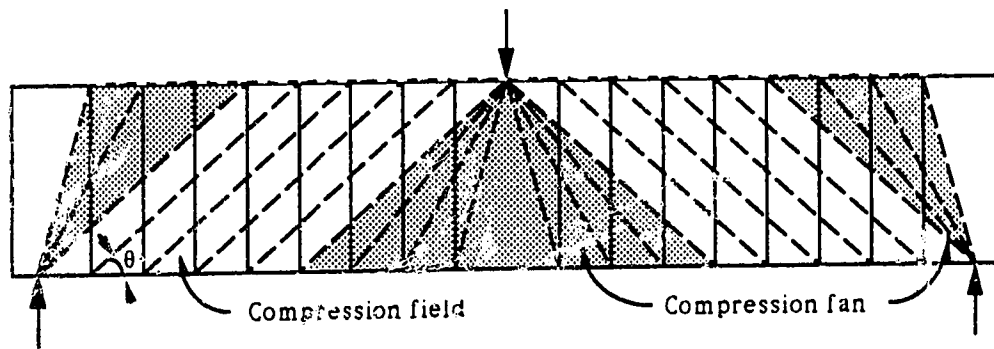
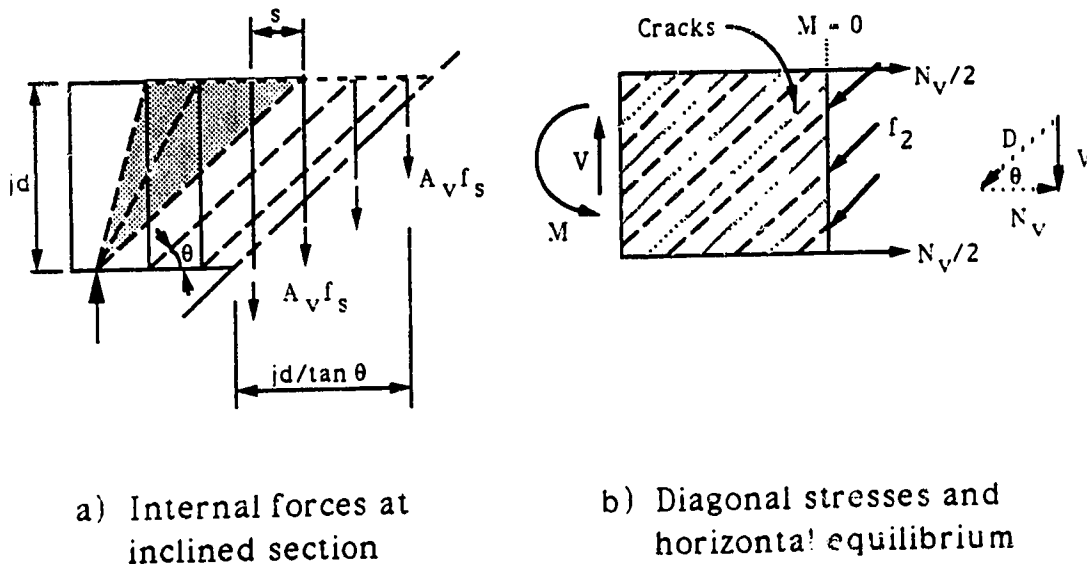


Figure 2.17 Variable angle truss model of a beam.



a) Internal forces at inclined section

b) Diagonal stresses and horizontal equilibrium

Figure 2.18 Variable angle truss - equilibrium conditions.

$$D = \frac{V}{\sin \theta} \quad (2.38)$$

The compressive stress  $f_2$  in the diagonals acts on a web area of ( $b_w jd \cos\theta$ ), and Eqn. 2.38 can be rewritten as

$$f_2 b_w jd \cos\theta = \frac{V}{\sin\theta} \quad (2.39)$$

or

$$f_2 = \frac{V}{b_w jd \cos\theta \sin\theta} \quad (2.39b)$$

or

$$f_2 = \frac{V}{b_w jd} \left( \tan\theta + \frac{1}{\tan\theta} \right) \quad (2.39c)$$

From Figure 2.18b, the longitudinal component of the inclined compressive force  $D$  is resisted by an axial tension force  $N_v$ , where

$$N_v = \frac{V}{\tan\theta} \quad (2.40)$$

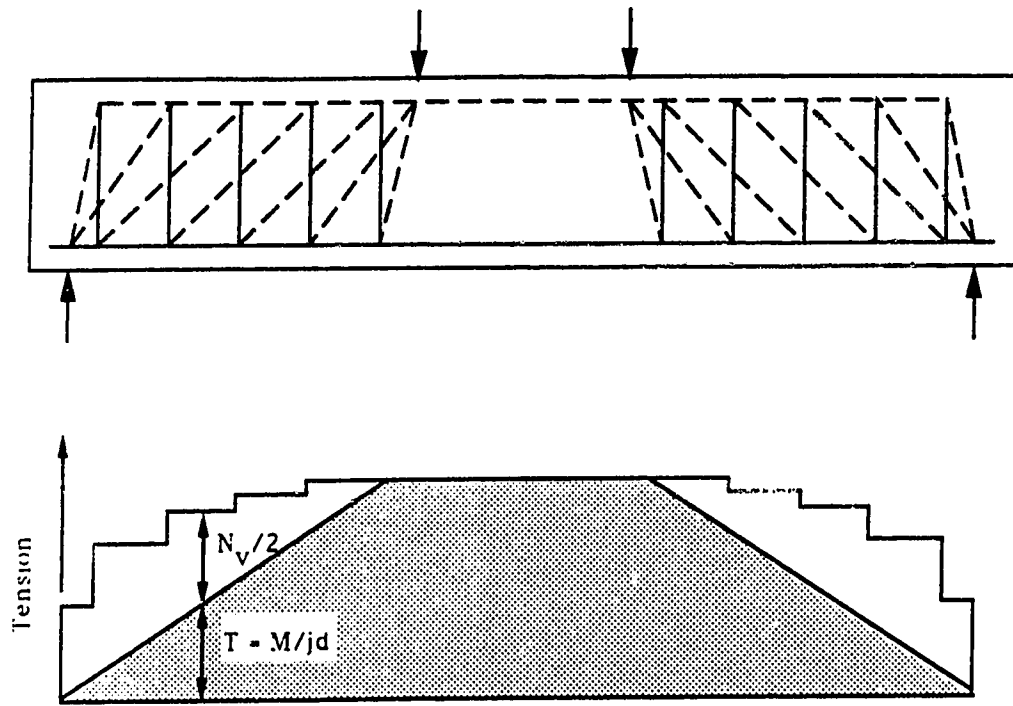
If the shear stresses are assumed to be uniformly distributed over the effective depth of the beam, the resultants  $D$  and  $N_v$  act at mid-depth of the beam. Consequently,  $N_v/2$  will act on both the top and bottom chords of the truss, and these forces will add to those caused by flexure and axial load. The variable angle truss model therefore directly indicates that shear causes tension in both the vertical stirrups and the longitudinal reinforcement, reducing the force in the truss compression chord and increasing the force in the tension chord. As noted in Section 2.3.1.2, the ACI Code indirectly includes the increase in longitudinal tension force caused by shear through its



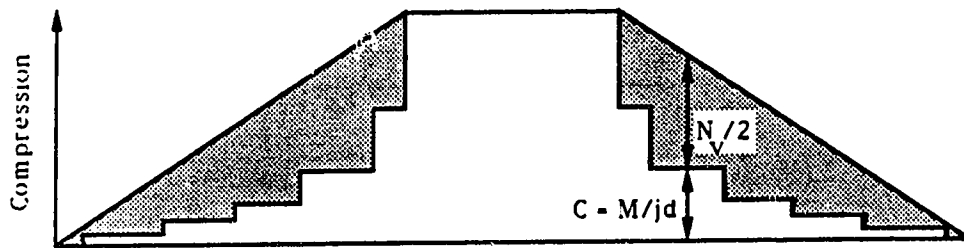
bar detailing requirements.

At concentrated load locations, the flow of forces in a concrete beam can be modelled by compression fans, where the inclination of the compression struts varies and increases to  $90^\circ$  directly below the load location. From Eqn. 2.40, as  $\theta$  approaches  $90^\circ$ ,  $N_v$  decreases to zero and therefore the tension force in the reinforcement at this location is not influenced by shear. Consequently, the amount of flexural reinforcement required at the location of maximum moment is not influenced by shear. At locations away from the point of maximum moment, the net effect of shear on the longitudinal bar forces is to shift the moment diagram by an amount  $jd/2\tan\theta$ , as shown in Figure 2.19.

Compared to the ACI Code, a variable angle truss model more accurately represents the internal flow of forces in a cracked concrete beam, but the system of forces is indeterminate, as only three equilibrium equations are available to solve for the four unknowns  $f_2$ ,  $f_s$ ,  $N_v$  and  $\theta$ . The truss can be made statically determinate by assuming the stirrups have yielded at failure, hence  $f_s = f_y$ . To ensure the stirrups will yield prior to the diagonal concrete struts crushing in compression, the maximum compressive stress in the web must be examined. The allowable compressive stress in an inclined compression strut is less than the concrete cylinder strength due to several factors, including the effects of tensile stresses in the concrete caused by the stirrups. Values of permissible effective concrete strengths in the order of  $0.25f_c$  to



a) Variation of tension in bottom chord



b) Variation of compression in top chord

Figure 2.19 Forces in tension and compression chords of truss.

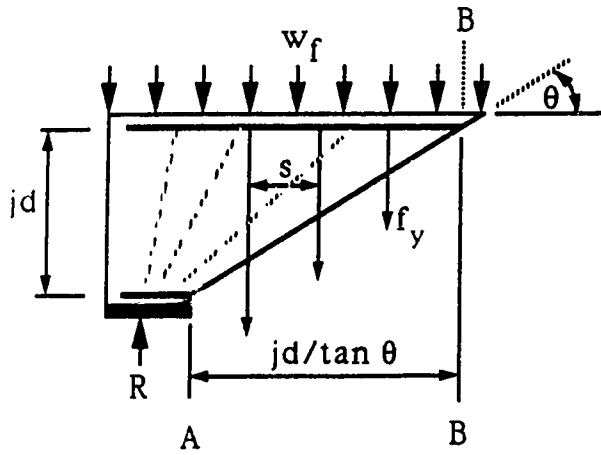
$0.45f_c$  have been proposed<sup>13</sup>. The General Method of the Canadian Code relates the effective concrete strength to the average strain perpendicular to the compression diagonals.

## 2.6 Staggering Concept for Shear Design

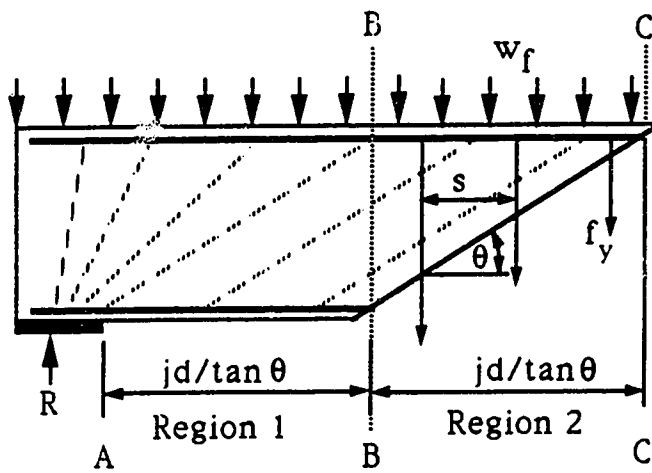
Equilibrium equations for a variable angle truss model are derived by examining regions of constant shear, where the required spacing of transverse reinforcement can be readily determined. In order to determine the distribution of stirrups in a beam with a varying shear force along its length, additional considerations must be examined.

A simply supported slender beam subject to a uniformly distributed load on the top face can be modeled by a variable angle truss. A uniform compression field with the concrete struts at a constant angle of inclination can be used throughout the member except at the supports and at midspan where compression fans occur. A freebody diagram of the end portion of a beam is shown in Figure 2.20a. Section A-B is the closest inclined section to the support. Vertical equilibrium requires stirrups crossing section A-B equal the upward reaction minus the applied load within the length  $jd/\tan\theta$ . Consequently, the stirrups can be designed to resist the shear at B, or the lowest value of shear within this region. This procedure is known as the "staggering concept" for shear design.

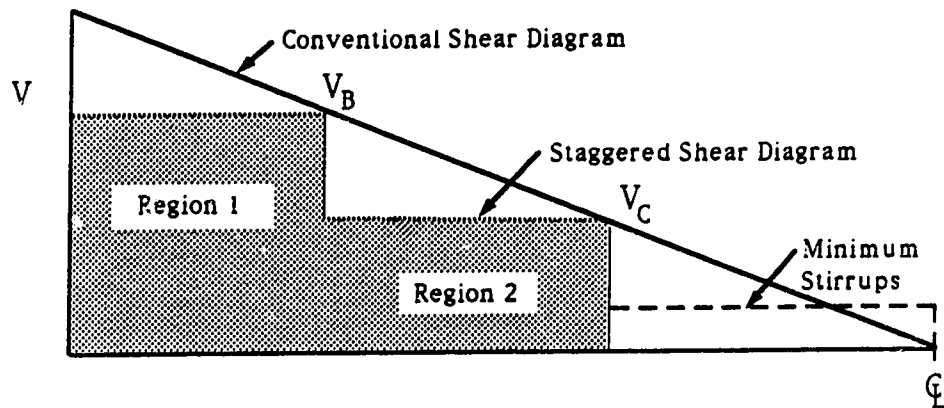
As shown in Figure 2.20b, the staggering rule can also be applied



a) Region 1 - stirrup design



b) Region 2 - stirrup design



c) Staggered shear force diagram

**Figure 2.20** Design of stirrups using the staggering concept for a top-loaded beam.

to adjacent regions, resulting in uniformly spaced bands of stirrups throughout the beam length. Figure 2.20c illustrates the shears for which the stirrups can be designed under the given loading condition and compares the staggered shear force diagram to the conventional shear diagram.

The use of a staggered shear diagram for uniformly loaded beams that differs in shape from the traditional linear shear force diagram has been the topic of much discussion in recent years. Hsu<sup>14</sup> examined beams subjected to uniformly distributed load assuming failure when the first stirrup yielded and assuming no redistribution of stirrup forces occurs. Hsu concluded the staggering concept is an upper bound solution and is unsafe. In the discussion of Hsu's paper, Marti<sup>15</sup>, Regan<sup>16</sup>, Rogowsky<sup>17</sup> and Mueller<sup>18</sup> indicate that according to the theory of plasticity, a safe lower bound solution can be achieved even with limited plasticity of a concrete beam.

In order to check the validity of the staggering concept, Mailhot<sup>19</sup> tested three full scale uniformly loaded concrete beams. Stirrups were designed according to the staggering concept and all beams had continuous longitudinal reinforcement. The experimental results indicate the staggered shear design is safe, and that a sufficient degree of plasticity is obtained by a redistribution of stirrup forces in the members. Cerruti and Marti<sup>20</sup> tested two large scale I-beams designed by the staggering rule and curtailed the longitudinal reinforcement as is common in practice. These test beams also demonstrate the redistribution of internal forces in a beam web and

confirm the validity of the staggering concept for shear design.

The General Method in the Canadian Code CSA A23.3 M84 permits staggered shear design for beams uniformly loaded at the top. For beams with load applied near the bottom face, stirrup design based on the lowest shear according to the staggering rule underestimates the amount of web reinforcement required. Consequently, the staggering rule must not be applied to beams with loads applied near the bottom of the member. From Figure 2.20a, if the beam self weight is substantial and is included in the uniform load  $w_f$ , the overestimation of the downward load in the freebody will underestimate the shear at section B-B, and an insufficient amount of web reinforcement may be provided. As a result, use of the staggering rule should be carefully examined for a particular beam and loading condition.

## 2.7 Modified Compression Field Theory

While the ACI Code shear design method generally leads to satisfactory designs, it is highly empirical and does not provide designers with a rational model for shear design. A variable angle truss model provides a better representation of the forces in a cracked beam by accounting for the possible deviation of the compressive stress field from  $45^\circ$ , but it does not directly consider any contribution of the concrete shear transfer mechanisms to shear strength. The Modified Compression Field Theory developed by Collins and Vecchio<sup>2</sup> is an extension of the Compression Field

Theory<sup>12</sup> originally developed for concrete membrane elements. This design approach is based on a rational physical model, in which the behavior and flow of forces in a cracked concrete beam are easily visualized, and it refines the variable angle truss approach by considering the contributions of aggregate interlock and tension in the concrete to shear strength.

Prior to cracking, a portion of a concrete beam subjected to pure shear develops equal principal tensile and compressive stresses at  $45^\circ$ , as shown in Figure 2.21a. After the concrete diagonally cracks, the tensile stresses in the concrete are reduced, but the tension in the cracked concrete still contributes to the shear resistance of the beam. The Modified Compression Field Theory models a cracked concrete beam as a truss with a continuous field of diagonal compression in combination with the tensile stresses in the concrete between the cracks, as illustrated in Figure 2.21b. The inclination of the compression field is permitted to vary from  $45^\circ$ .

Figure 2.22 shows the stresses resisting the applied shear at a location of zero moment. At a crack, there is no tensile stress in the concrete. Due to bond between the concrete and the stirrups, tension in the stirrups causes tensile stresses in the concrete strut that reach a maximum value midway between the cracks. Bond also effects the tensile stress in the web reinforcement  $f_s$ , such that the stirrup stress at the centreline of a strut will be lower than at a crack location. In developing its equilibrium and compatibility relationships, the Modified Compression Field Theory considers

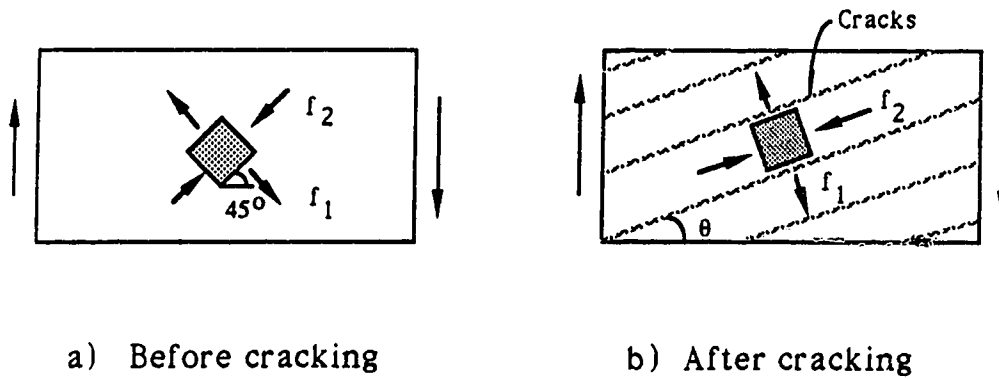


Figure 2.21 Stress fields resisting shear in the web of a reinforced concrete beam.

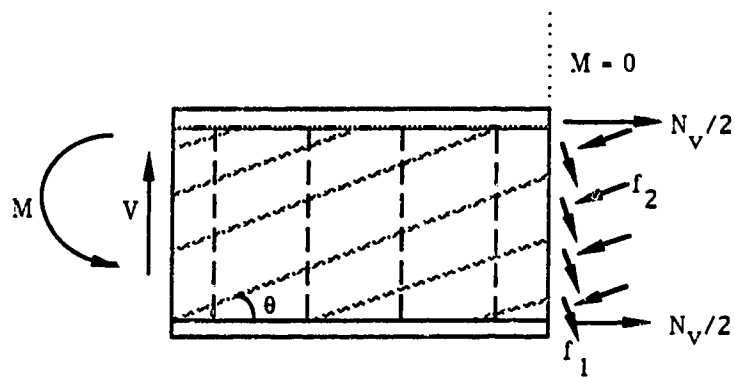


Figure 2.22 Principal stresses and longitudinal equilibrium.



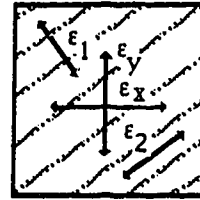
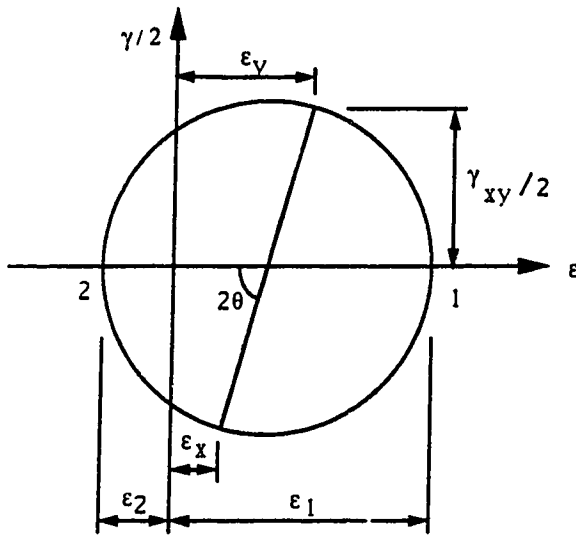
average stresses in a cracked concrete beam. The average principal tensile stress  $f_1$  is at an average location in a concrete strut, and is less than the maximum tensile stress at the centreline of the strut. The stresses at an inclined crack and in the concrete between two cracks are considered more fully in Chapter 4 (See Figure 4.1). Collins and Vecchio assume the principal stress axes coincide with the principal strain axes. In order to minimize the effects of local cracking, the strains in a concrete element are expressed as average strains, which are measured over lengths long enough to include the effects of several cracks. From Mohr's circle of strains, the following relationships can be derived

$$\tan^2 \theta = \frac{\epsilon_x - \epsilon_2}{\epsilon_y - \epsilon_2} \quad (2.41)$$

$$\epsilon_1 = \epsilon_x + \epsilon_y - \epsilon_2 \quad (2.42)$$

where  $\epsilon_x$  is the longitudinal strain,  $\epsilon_y$  is the transverse strain, and  $\epsilon_1$  and  $\epsilon_2$  are the principal tensile and compressive strains respectively, as shown in Figure 2.23. The longitudinal strain is taken at mid-depth, and compressive strains are expressed as negative quantities.

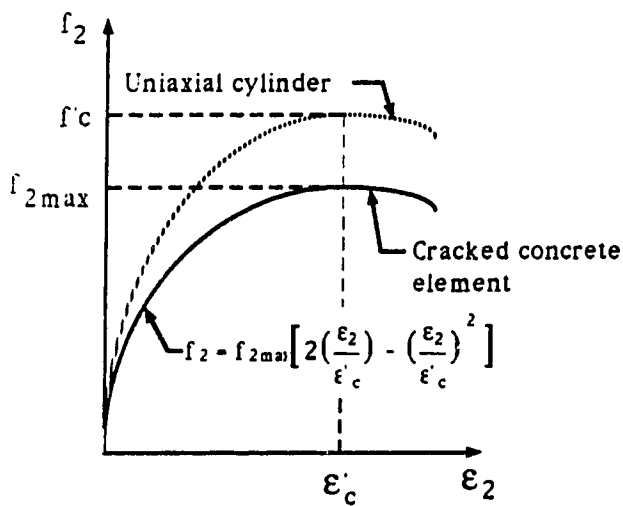
Collins and Vecchio develop constitutive relationships relating the average stresses in the concrete to average strains, as shown in Figure 2.24. The average stress-strain relationships differ from those of standard concrete cylinder tests, due in part to the effects of tensile stresses which reduce the compressive strength as compared



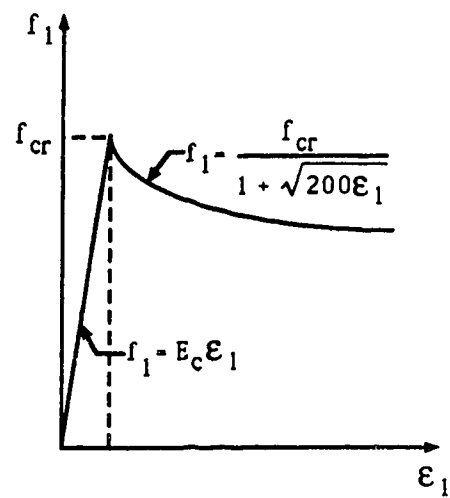
a) Mohr's circle of strains

b) Average strains in cracked concrete

Figure 2.23 Average strain conditions in cracked concrete.



a) Compression



b) Tension

Figure 2.24 Stress-strain relationships for cracked concrete.

to uniaxial compression tests. In addition to considering the contribution to shear provided by the average tensile stresses in cracked concrete, the ability of a crack interface to transmit shear by aggregate interlock is also examined. This local variation of stress at crack locations will be more thoroughly discussed in Chapter 4.

The equilibrium, compatibility, and constitutive relationships developed by the Modified Compression Field Theory can be used to determine the shear strength and the complete load-deformation response of a member subjected to shear. The general design approach is based on a sectional design format, and the same procedure can be used for both nonprestressed and prestressed concrete beams. A typical solution algorithm is summarized in Figure 2.25. The complete response of a beam subjected to shear can be obtained by following the solution procedure using a range of  $\epsilon_1$  values. Although the Modified Compression Field Theory is a very involved procedure and it is quite complex as a regular design method, it may be useful in circumstances where a detailed shear analysis is required.

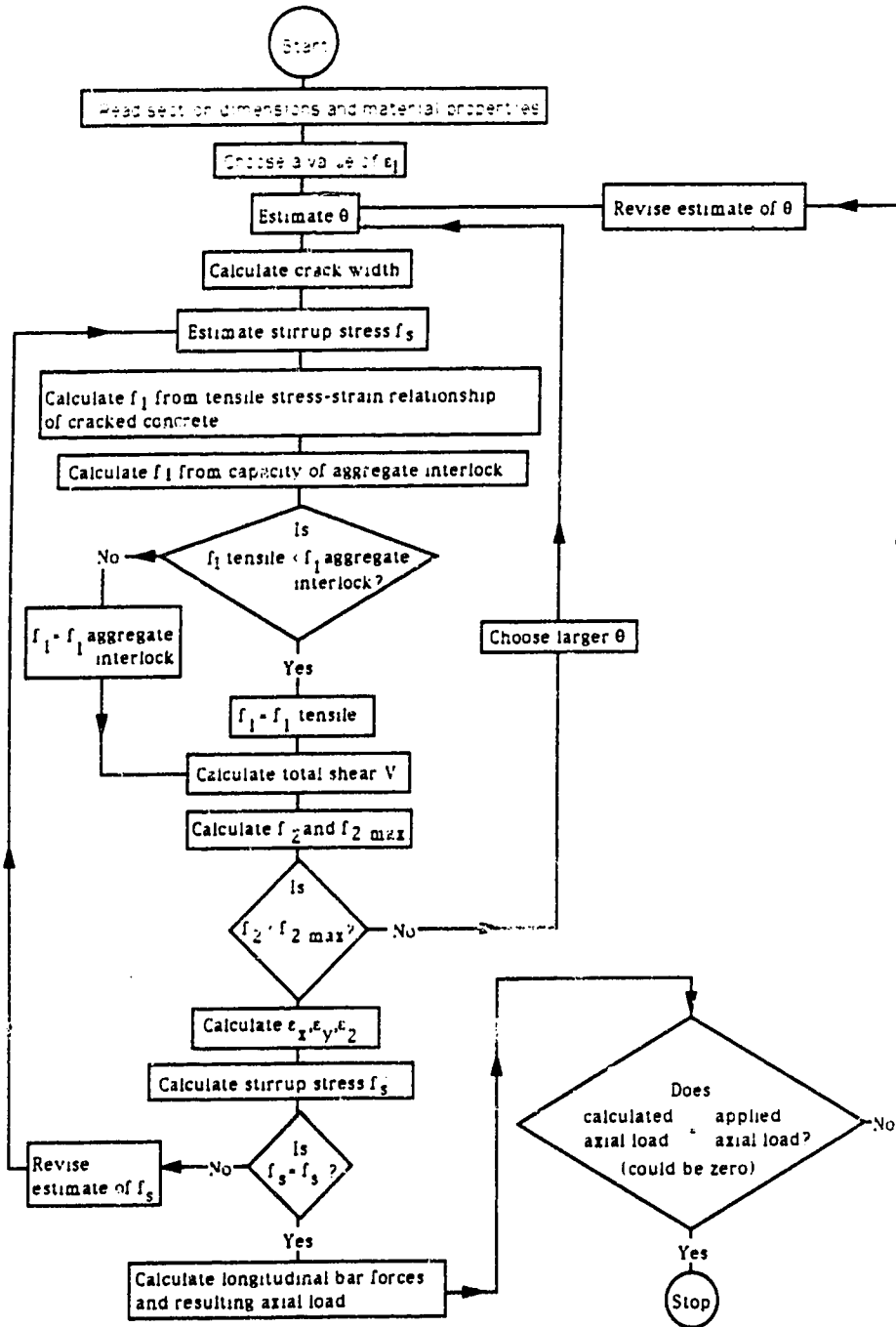


Figure 2.25 Suitable solution technique for shear using the Modified Compression Field Theory (adapted from Ref. 27)

### 3. REVIEW OF AVAILABLE CONCRETE CONTRIBUTION EXPRESSIONS

#### 3.1 General

The ACI Code procedure for shear design is based on the classical  $45^\circ$  truss model equations accompanied by an empirical correction term to account for the so called concrete contribution. Consistent with many codes of practice, the concrete contribution has been established by examining numerous beam test results. Since the inclination of diagonal cracks is typically less than  $45^\circ$  as the ultimate load is approached, the variable angle truss model provides a more accurate representation of the actual flow of forces in a cracked concrete beam. However, the beam web in a variable angle model is typically represented by uniaxial compression struts and tension ties, where the contributions of shear transfer mechanisms such as dowel action, aggregate interlock, and the shear carried by the compression zone are not explicitly considered. These mechanisms are implicitly included in the variable angle model by allowing the inclination of the compression struts to vary from  $45^\circ$ , which is the approach adopted in the Canadian Code<sup>1</sup>. However, in order to ensure the variable angle truss model is not unduly conservative, an allowance for the other shear transfer mechanisms is often included directly in the design model. Several available expressions for the additional concrete contribution in variable angle truss models will be discussed in the following sections.

### 3.2 Swiss Design Code SIA 162

As a slender reinforced concrete beam is subjected to load, the concrete is effectively able to resist the applied shear up to the formation of the first diagonal crack. After diagonal cracking occurs, the shear reinforcement begins to carry load and assists in providing the required shear resistance. Referring to Figure 2.11, the aggregate interlock component of shear resistance decreases as the cracks widen under increasing load. The proportion of shear carried by the stirrups continuously increases until yielding of the web reinforcement occurs. The Swiss Code, Structural Design Code SIA 162<sup>21</sup> is based on a variable angle truss approach, and suggests that prior to diagonal cracking the concrete contribution equals the shear stress necessary to produce diagonal cracking in the web. After the formation of cracks, the concrete contribution in a beam with web reinforcement is considered to continuously diminish and approach zero as the applied shear stress increases. Figure 2.1 shows the concrete contribution suggested by SIA 162 for a reinforced concrete beam.

As indicated by Eqn. 2.9, the effect of prestressing is to increase the diagonal cracking stress. In the Swiss Code, the concrete contribution for prestressed members is similar to that of reinforced concrete beams, except the cracking shear is increased by a factor  $K$ . The value of  $K$  is dependent on the prestress force, and is determined by examining the state of stress at the neutral axis of a prestressed

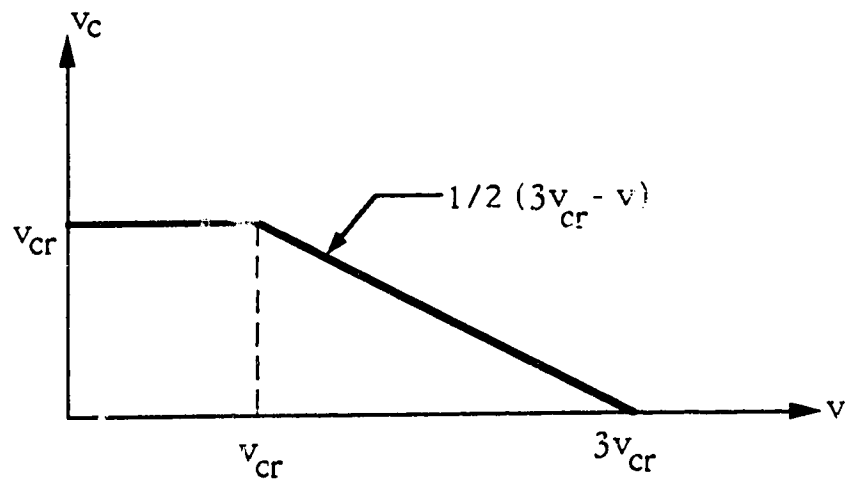


Figure 3.1 The Swiss Code concrete contribution for reinforced concrete beams.

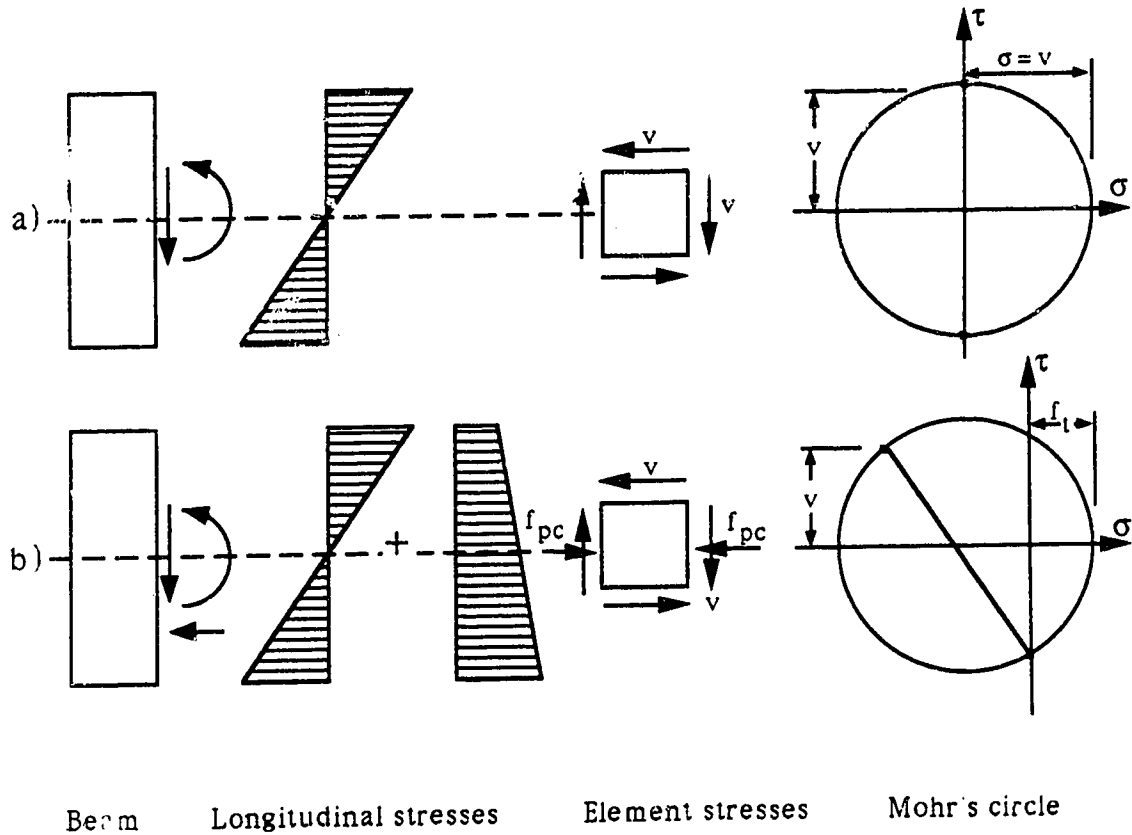


Figure 3.2 Effect of prestress on shear strength:  
a) without axial load b) with prestress.

concrete beam. From Figure 3.2, the effect of prestress on an uncracked beam is to shift the Mohr's circle, reducing the principal tension stress for a given shear stress. The principal tensile stress at the neutral axis of a prestressed member is smaller than the applied shear stress, but in a reinforced concrete beam the tensile stress equals the applied shear stress. Prior to diagonal cracking, the concrete contribution in the Swiss Code is expressed as  $KV_{CR}$ . The expression for  $K$  is determined from the Mohr's circle as

$$K = \sqrt{1 + \frac{f_{pc}}{f_t}} \quad (3.1)$$

where  $f_t$  is the principal tension stress and  $f_{pc}$  is the compressive stress at the neutral axis. This is the same expression used in deriving Eqn. 2.10, which is the basis of the ACI Code equation for the web shear cracking strength of a beam. In the same way as for reinforced concrete beams, the Swiss Code assumes a continuously diminishing concrete contribution for prestressed concrete beams, as shown in Figure 3.3. An upper limit of  $K = 1.0$  is used in those portions of a beam where the extreme fiber stresses are tensile. This in effect reduces  $V_c$  to the value for reinforced concrete if flexure-shear cracking can occur.

Once the concrete contribution is determined, the nominal resistance provided by the truss action and any inclined prestressing tendons can be combined to determine the total shear resistance of



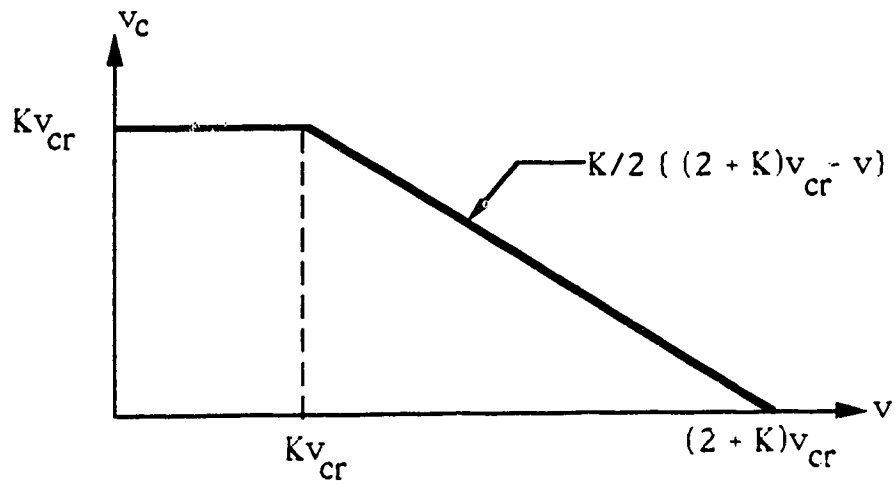


Figure 3.3 The Swiss Code concrete contribution for prestressed concrete beams.

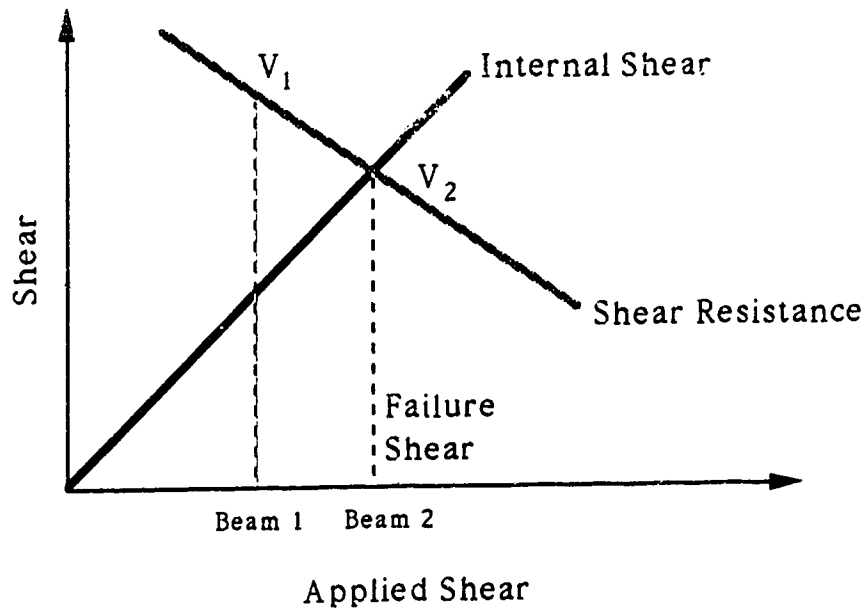


Figure 3.4 Idealized representation of shear failure.

the beam. The shear carried by the truss action is given by

$$V_s = \frac{A_v f_y z \cot \alpha}{s} \quad (3.2)$$

where  $z$  is the lever arm between the top and bottom chords, and  $\alpha$  is the inclination of the compression diagonal. The Swiss Code suggests the angle of inclination must be within the specified limits of  $27^\circ \leq \alpha \leq 63^\circ$ .

The concrete contribution in the Swiss Code is obtained from an expression that is easy to use. It is advantageous that the same general approach can be used for both reinforced and prestressed concrete beams. In SIA 162 the shear strength provided by the concrete in a prestressed member is expressed in a simple manner as a function of the cracking stress for a reinforced concrete beam. The resulting design procedure is simple to use, particularly when compared to the ACI design equations for prestressed concrete beams.

Although the Swiss Code approach is reasonable, the way in which the expression for the concrete contribution is presented does have some disadvantages. For beams that are designed to fail in flexure prior to failing in shear, the shear stress at the flexural failure load can be calculated and the corresponding concrete contribution at this stress can be determined from the suggested relationships. For two beams that are identical except for different amounts of flexural

reinforcement, the Swiss Code suggests each beam will have a different shear resistance. Referring to Figure 3.4, Beam 1 has a smaller flexural capacity than Beam 2, and at flexural failure its shear resistance is determined to be  $V_1$ . The shear capacity of Beam 2, which has a larger flexural capacity than Beam 1, is calculated at a higher applied shear stress corresponding to the larger failure moment, and the shear resistance is determined to be  $V_2$ . Since the applied shear for Beam 2 equals the shear resistance,  $V_2$  corresponds to the actual failure shear of the beam, which is less than the shear capacity predicted for Beam 1. Examining the shear capacity proposed by the Swiss Code reveals it does not represent the ultimate failure shear of a beam, but is a measure of whether or not a beam has previously failed in shear at a specified shear stress. Consequently, the procedure provides a theoretical shear capacity and not the actual failure shear of a beam. The actual shear failure load is reached when the applied shear equals the total shear resistance provided by the truss action and the concrete contribution, as shown schematically in Figure 3.4.

### **3.3 CEB-FIP Model Code 1978 - Refined Method**

The European CEB-FIP Model Code 1978<sup>22</sup> presents two shear design procedures, the Standard Method and the Refined or Accurate Method. The Refined Method is based on a variable angle truss model with an additional concrete contribution resembling the Swiss Code approach. The concrete contribution continuously diminishes

after inclined cracking, and is combined with the shear resistance provided by the truss action of inclined struts and shear reinforcement. In the CEB-FIP Code, the design shear  $V_{sd}$ , which is the shear force multiplied by a load safety factor, must satisfy the relations

$$V_{sd} \leq V_{Rd2} \quad (3.3)$$

CEB 11-6

and

$$V_{sd} \leq V_{wd} + V_{cd} \quad (3.4)$$

CEB 11-7  
and 11-8

where  $V_{Rd2}$  is a shear limit to prevent web crushing failures, and  $V_{wd}$  and  $V_{cd}$  are the shear force carried by the truss action in the web and the concrete contribution respectively. The shear carried by the truss action is given by

$$V_{wd} = \frac{A_{sw}}{s} 0.9d f_{ywd} (\cot\theta + \cot\alpha) \sin\alpha \quad (3.5)$$

CEB 11-19

where  $A_{sw}$  and  $f_{ywd}$  are the area and design stress of the web reinforcement respectively,  $\theta$  is the angle of inclination of the compression struts, and  $\alpha$  is the inclination of the web reinforcement to the beam axis. The angle  $\theta$  is chosen such that  $3/5 \leq \cot\theta \leq 5/3$ , or  $31^\circ \leq \theta \leq 59^\circ$ . These limits are chosen to provide control of cracking under working load conditions, and the most economical value of  $\theta$  is

at  $\theta = 31^\circ$ . The design stress of the web reinforcement  $f_{ywd}$  is the yield stress divided by a resistance safety factor. For stirrups perpendicular to the beam axis, the truss contribution is expressed as

$$V_{wd} = \frac{A_{sw} f_{ywd} (0.9d)}{s \tan \theta} \quad (3.6)$$

which is similar to the traditional truss contribution commonly used in North America if  $\theta = 45^\circ$ .

The concrete contribution  $V_{cd}$  in reinforced concrete members is a function of  $\tau_{rd}$ , and is given by the following expressions

$$\text{If } V_{sd} \leq 2.5 \tau_{rd} b_{wd} : V_{cd} = 2.5 \tau_{rd} b_{wd} \quad (3.7)$$

$$\text{If } V_{sd} \geq 7.5 \tau_{rd} b_{wd} : V_{cd} = 0 \quad (3.8)$$

and for intermediate values,  $V_{cd}$  is obtained by linear interpolation between the above values.  $\tau_{rd}$  is a function of the concrete quality, particularly the tensile strength, and values are given in Table 3.1 for different characteristic concrete compressive strengths  $f_{ck}$ . The characteristic value of compressive strength corresponds to the lower 5% fractile, and can be related to the mean cylinder compressive strength by adopting the Model Code expression

$$f_{c \text{ mean}} = f_{ck} + 8 \text{ MPa} \quad (3.9)$$

or

$$f_{c \text{ mean}} = f_{ck} + 1160 \text{ psi} \quad (3.9b)$$

The CEB-FIP concrete contribution for nonprestressed beams is shown graphically in Figure 3.5 as a function of the factored design shear stress  $v_{sd}$ .

$f_{ck}$		$\tau_{rd}$	
(MPa)	(psi)	(MPa)	(psi)
12	1740	0.18	26.1
16	2320	0.22	31.9
20	2900	0.26	37.7
25	3625	0.30	43.5
30	4350	0.34	49.3
35	5075	0.38	55.1
40	5800	0.42	60.9
45	6575	0.46	66.7
50	7250	0.50	72.5

**Table 3.1** Values of  $\tau_{rd}$  in the CEB-FIP 1978 Model Code.

For design, the Model Code applies a material safety factor of 1.5 to the concrete strength. If the material safety factors are removed, the maximum concrete contribution can be determined from

$$V_{cd} = 3.75 \tau_{rd} b_w d \quad (3.10)$$

To convert this expression to the form  $\kappa_v \sqrt{f_c} b_w d$ , the characteristic concrete strength must be related to the specified compressive strength  $f_c$ . The specified strength is less than the average strength,

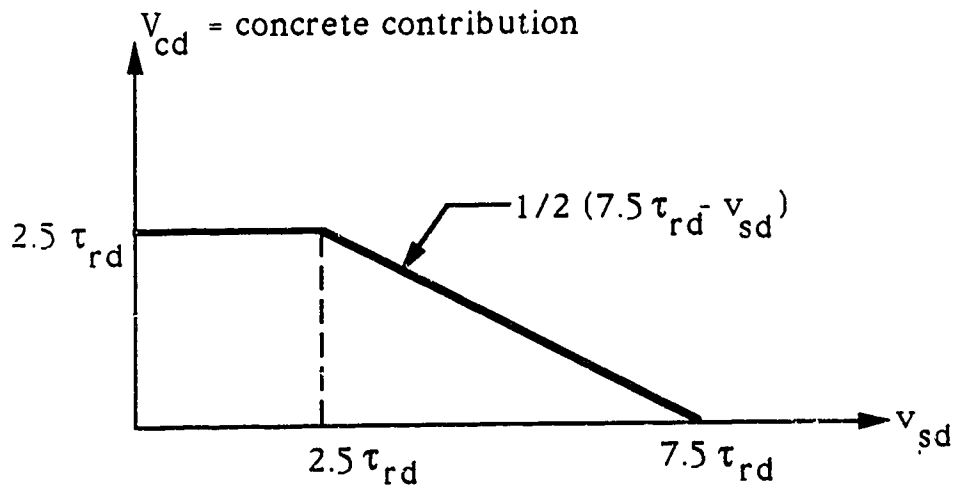


Figure 3.5 1978 CEB-FIP concrete contribution for reinforced concrete beams.

and can be related to the mean strength of the concrete by the approximate expression

$$f_{c \text{ mean}} = 1.15 f_c \quad (3.11)$$

or by an equation similar to Eqn. 3.9b. Using Eqn. 3.9b and Eqn. 3.11, values of  $\kappa_v$  from 1.95 to 3.18 are obtained for various values of  $f_c$  as shown in Table 3.2. This range is within the limits suggested in ACI Section 11.3 for nonprestressed members, where  $2.0 \leq \kappa_v \leq 3.5$ .

$f_c$ (psi)	$\kappa_v$
-----	-----
1930	1.95
3030	2.17
3530	2.38
4160	2.53
4790	2.67
5420	2.81
6050	2.94
6730	3.05
7310	3.18

Table 3.2 Values of  $\kappa_v$  determined from the Model Code.

For prestressed concrete beams, the CEB Refined Method neglects the beneficial effect of a prestressing force on shear strength. The simplified or Standard Method attributes a favorable effect of prestressing by increasing values of  $\tau_{Rd}$  by



$$\beta_1 = 1 + \frac{M_o}{M_{sdu}} \leq 2 \quad (3.12)$$

CEB 11-3

where  $M_{sdu}$  is the maximum design moment in the span and  $M_o$  is the decompression moment at transfer related to the tensile fiber for the section where  $M_{sdu}$  is acting. The manner in which prestressing is considered has been questioned<sup>23</sup>, particularly since its effect is considered in relation to the maximum moment in the span and not to the moments at the section under consideration. Equation. 3.11 was derived solely on test results of beams failing by flexure-shear cracking, and web-shear failures were not considered. The 1978 CEB-FIP shear design procedure for prestressed concrete beams has been shown to be relatively conservative<sup>24</sup>, and it contains inconsistencies such that the more "accurate" Refined Method can require more shear reinforcement than the Standard Method.

Walraven<sup>23</sup> has criticized the manner in which the values of  $\tau_{rd}$  were determined in the 1978 Model Code, and has proposed considerably lower values, particularly for higher strength concretes. Walraven suggests that a concrete contribution which is constant during all stages of loading and is independent of the nominal shear stress provides better agreement with test results. Walraven recommends a concrete contribution expression in the form

$$V_{cd} = (2.5 \tau_{rd} + 0.2 \sigma_{cp}) b_w d \quad (3.13)$$

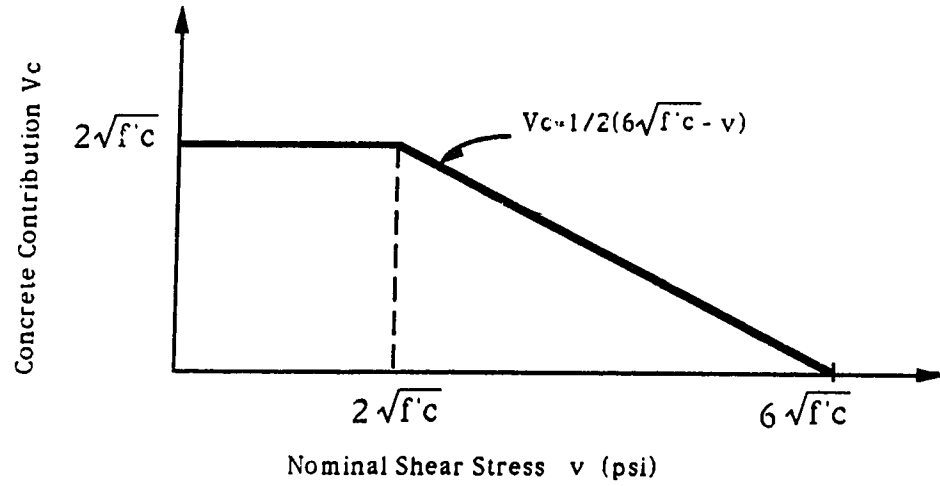
$$\tau_{rd} = 0.0875 (f'c)^{2/3} \quad (3.14)$$

where  $\sigma_{cp}$  is the axial prestress. He suggests the angle of the compression struts be limited to  $35^\circ \leq \theta \leq 55^\circ$ .

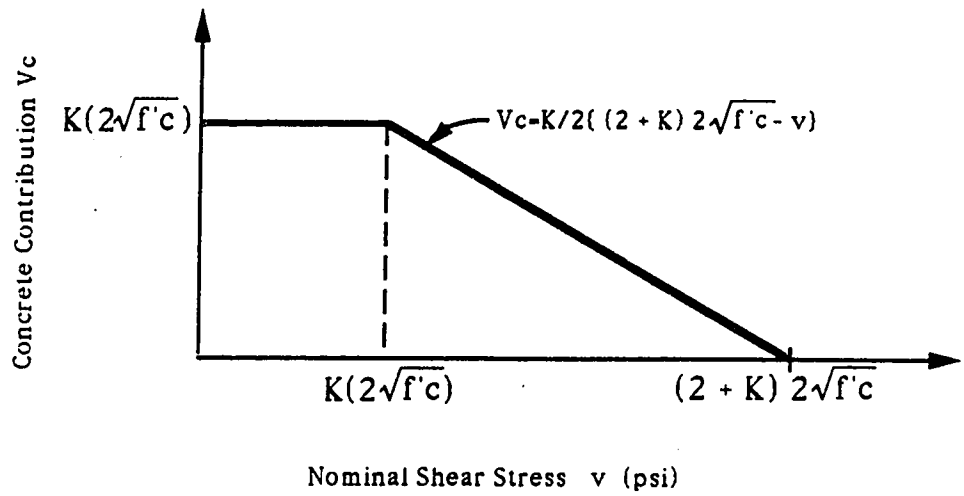
The 1988 first predraft of the CEB-FIP Model Code 1990<sup>25</sup> has discontinued the approach of using of two different methods as in the 1978 Code, and provides a simple truss analogy design procedure for both reinforced and prestressed concrete beams. The forces in the truss members are examined at ultimate limit states, and the additional concrete contribution term shown in Figure 3.5 is no longer used. The June 1989 draft of MC90 suggests the angle of inclination of the compression struts in the web may be freely chosen between  $18.4^\circ$  and  $45^\circ$ .

### 3.4 Ramirez and Breen

Ramirez and Breen<sup>26</sup> proposed a concrete contribution term similar to that recommended by past Swiss and CEB-FIP codes. This approach considers a diminishing concrete contribution which approaches zero as the nominal shear stress increases, as shown in Figure 3.6(a). To correspond with the ACI Code, Ramirez and Breen suggest the shear stress necessary to produce diagonal cracking be taken as  $2\sqrt{f'_c}$ . When the applied shear stress exceeds three times the uncracked shear strength, it is suggested there is no concrete contribution to the total shear capacity of the beam at failure. For prestressed concrete beams, a similar approach is used in which the



a) Reinforced concrete



b) Prestressed concrete beams

Figure 3.6 Concrete contribution proposed by Ramirez and Breen<sup>26</sup> for concrete beams.

concrete contribution is equal to  $Kv_{cr}$ , as shown in Figure 3.6(b). Ramirez and Breen recommend  $K$  be calculated according to Eqn. 3.1, but  $1.0 \leq K \leq 2.0$ . At locations of a member where the stress in the extreme tension fiber at ultimate exceeds  $6\sqrt{f'_c}$ , they suggest  $K$  shall be taken equal to 1.0.

As noted in the discussion of the Swiss Code, the concrete contribution determined in this manner is a theoretical shear capacity at a specified nominal shear stress, which would typically be determined at the load causing flexural failure. As a result, it provides a measure to ensure shear failure has not occurred prior to the flexural failure, but it does not give the actual failure shear capacity of the beam.

The benefits of using a variable angle truss model as a conceptual model for shear in reinforced and prestressed concrete beams are clearly shown by Ramirez and Breen. Several test results were examined which generally indicate the proposed concrete contribution is a safe lower bound solution. In order to experimentally verify the truss model concrete contribution, Ramirez and Breen considered tests of beams both with and without web reinforcement. When examining the capacity of members with little or very small amounts of web reinforcement, Ramirez and Breen used graphs similar to Figure 3.7 to suggest that their proposed concrete contribution is a safe lower bound. Presumably, values falling outside or above the proposed equation indicate the actual

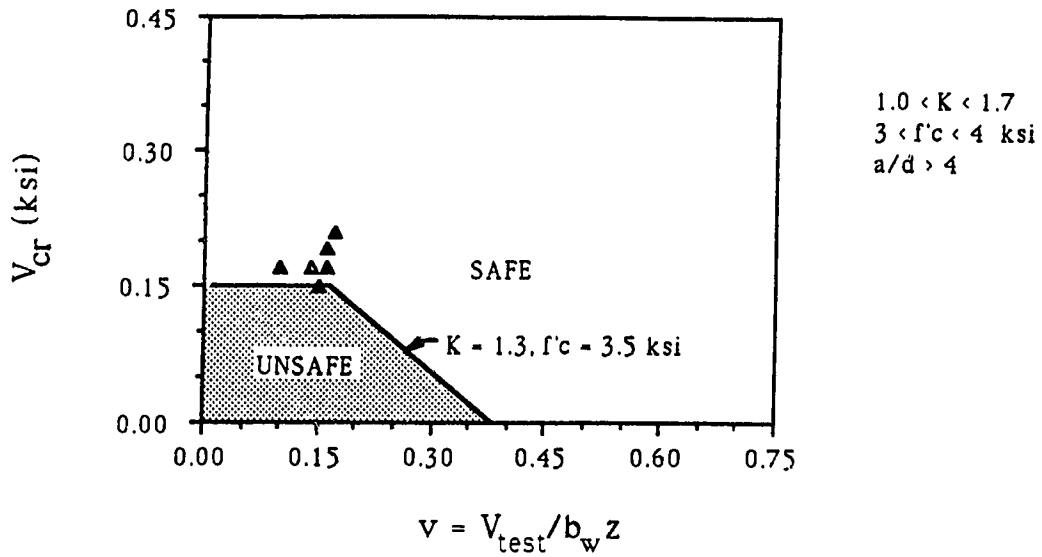


Figure 3.7 Ramirez and Breen evaluation of the concrete contribution in prestressed concrete beams (adapted from Ref. 26).

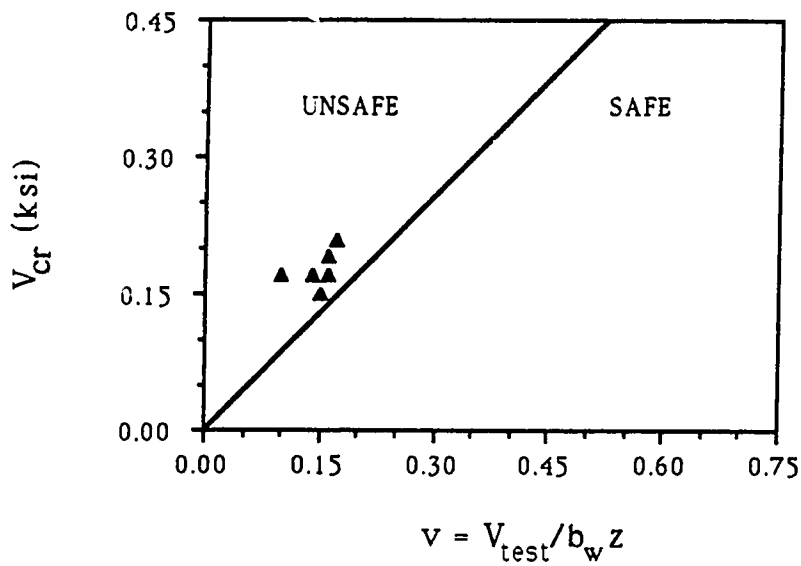


Figure 3.8 Replot of data in Figure 3.7 for prestressed concrete beams without web reinforcement.

concrete contribution is greater than estimated, hence a safe condition. Values located inside or enclosed by the equation boundary are unsafe, as the actual concrete contribution is smaller than estimated.

However, examining data plotted in this manner will not ensure the concrete contribution from a test beam will always be a safe lower bound solution. In Figure 3.7 the furthest left data point is shown to be located above the proposed equation, presumably indicating the actual concrete contribution is higher than predicted. Consequently, the proposed concrete contribution is considered a safe estimation of the actual capacity. If the test data for this particular beam without web reinforcement is examined, the beam is noted to have failed at a shear stress of 0.1 ksi. Therefore, the actual concrete contribution should be at most 0.1 ksi. Using the proposed concrete contribution expression, the theoretical concrete capacity is calculated to be 0.17 ksi. This value exceeds the maximum load the beam could withstand, and is hence an unsafe estimate of the actual concrete contribution.

A better way of examining this data, would be to determine the actual, not the theoretical concrete contribution, subtracting the nominal truss contribution provided by the web reinforcement from the total shear capacity. This would involve assumptions regarding the angle of inclination of the compression struts  $\theta$ . Alternatively, the data could be examined by observing whether the actual

concrete contribution minus the proposed concrete contribution is always a positive quantity. For beams without web reinforcement, if the predicted concrete capacity falls above a  $45^\circ$  line on a graph similar to Figure 3.7, the capacity is overestimated and an unsafe prediction of shear strength results. The test data in Figure 3.7 is replotted in Figure 3.8. It is evident the concrete contribution proposed by Ramirez and Breen is not always a safe lower bound solution. A re-evaluation of the test results summarized by Ramirez and Breen for beams without web reinforcement indicates the proposed concrete contribution expression provides a safe estimate of the concrete contribution for all 141 reinforced concrete beams investigated. For the 90 prestressed concrete beams without web reinforcement, 17 had unsafe predictions of the concrete capacity, with the poorest estimate providing a test/predicted ratio of 0.59. The mean ratio of all 90 prestressed concrete beams is 1.55 with a standard deviation of 0.63.

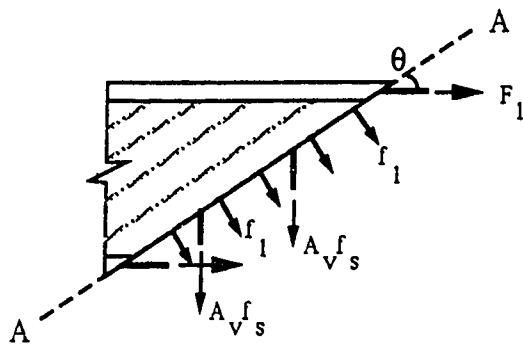
## 4. DERIVATION OF A NEW CONCRETE CONTRIBUTION TERM USING THE MODIFIED COMPRESSION FIELD THEORY

### 4.1 Concrete Contribution Model

Figure 4.1 shows two sections through the web of a beam. For clarity, the vertical component of an inclined prestressing tendon, if any, is not shown. In Figure 4.1b the section is cut along an idealized inclined crack. In Figure 4.1a, the section is at an average location in the concrete beam between two inclined cracks, corresponding to Section A-A in Figure 4.1b. The Modified Compression Field Theory assumes a tensile stress  $f_1$  acts on section A-A along with the stirrup forces  $A_v f_s$ . A shear stress  $v_{c1}$  is assumed to act along the crack accompanied by stirrup forces  $A_v f_y$ , where  $f_s < f_y$ . Consequently, the concrete contribution in a variable angle truss model can be expressed in two ways, either in terms of tensile stresses in the concrete between the cracks or as an aggregate interlock mechanism. Since the truss model assumes the cracks extend through the compression zone, the shear carrying capacity of the concrete compression zone is neglected. Also, the dowel action of the longitudinal reinforcement is not considered.

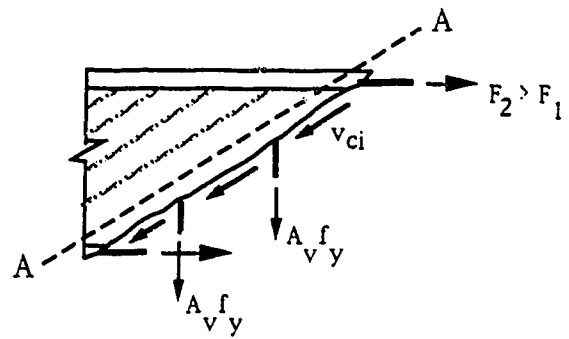
As shown in Figure 4.1, vertical equilibrium of each force transmission model provides two equations for the total shear  $V$ , Eqns. 4.1 and 4.1b.  $A_v$  is the cross-sectional area of web reinforcement,  $s$  represents the spacing of web reinforcement,  $\theta$  is





a) **Model 1: Stresses at an average location between two cracks**

$$V = \frac{A_v f_s j d}{s \tan \theta} + \frac{f_1}{\tan \theta} b_w j d + V_p \quad (4.1)$$



b) **Model 2: Stresses at a crack**

$$V = \frac{A_v f_y j d}{s \tan \theta} + v_{ci} b_w j d + V_p \quad (4.1b)$$

**Figure 4.1 Force transmission models.**

the angle of inclination at ultimate of the cracks or compression struts,  $V_p$  is the vertical component of prestressing force, and  $jd$  is the distance between the centroids of the top and bottom chords of the truss. Eqn. 4.1 uses the tensile concrete stress  $f_1$  between the cracks in conjunction with the stirrup stress  $f_s$  at an average location in the compression strut, while Eqn. 4.1b considers the shear stress at the crack  $v_{ci}$  and the stirrup yield stress  $f_y$ . Vecchio and Collins<sup>2</sup> assume  $f_1$  to be the average principal tensile stress in the cracked concrete. The tensile stress changes from  $f_s$  to  $f_y$  along the length of the web reinforcement because at the crack there is no tensile stress in the concrete and the reinforcement stress will be higher than average. Inside the strut, the concrete tension goes from zero at the crack locations to a maximum at the centreline of the strut. At this location, midway between the cracks, the reinforcement stress is less than at the cracks. These local variations in tensile stress of the reinforcement must be considered when examining equilibrium of each model. The longitudinal reinforcement also has variations in stress along its length with the maximum stress at the crack locations, because a portion of the force is transferred to the concrete by bond between cracks.

Since the current ACI Code equation for the nominal strength provided by shear reinforcement uses the specified yield stress  $f_y$  which occurs at the cracks, and because it is easier to visualize vertical shear being resisted by a "friction" on a crack interface rather than by tension in concrete between the cracks, Model 2 in

Figure 4.1 will be used for development of the concrete contribution term.

The two sets of stresses shown in Figure 4.1 are statically equivalent. The concrete tension and aggregate interlock are related by

$$f_1 = v_{ci} \tan \theta + \frac{A_v}{s b_w} (f_y - f_s) \quad (4.2)$$

or

$$v_{ci} = \frac{f_1}{\tan \theta} - \frac{A_v}{s b_w \tan \theta} (f_y - f_s) \quad (4.2b)$$

In determining the concrete contribution to shear, two possible failure modes must be considered, namely the capacity of the cracked concrete in tension and the capacity of the crack interface. The smaller or limiting value of these two quantities will provide a lower bound for the concrete contribution to the truss model. In order to develop the capacity of a rough and interlocked crack surface to transmit shear, the cracked concrete member must be capable of resisting the effects of this force, or the member will fail before breakdown of the aggregate interlock mechanism. As a result, either the crack interface will reach its capacity prior to the cracked concrete failing in tension, or vice versa. The capacity of each mechanism will now be examined separately.

## 4.2 Capacity of Crack Interface

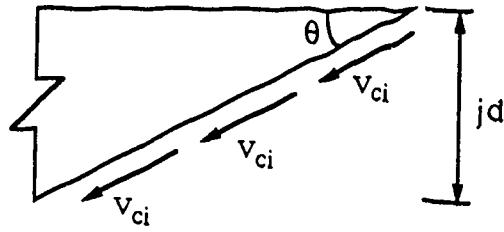
As shown in Figure 4.2, the interface shear stress  $v_{ci}$  acting on an inclined crack is equivalent to a shear stress  $v_{ci}$  acting on a vertical section. As a result, an expression for the stress along a crack interface corresponds to a vertical shear stress, and can be applied over a beam's web area to determine the shear resistance provided by aggregate interlock. From Walraven's test data, neglecting the beneficial effects of axial compression on a crack, Vecchio and Collins<sup>2</sup> derived the following relationship for the shear stress across a crack

$$v_{ci} = \frac{0.18\sqrt{f_c}}{0.31 + \frac{24w}{a + 16}} \quad (\text{MPa}) \quad (4.3)$$

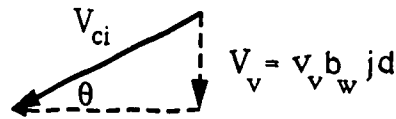
$$v_{ci} = \frac{2.16\sqrt{f_c}}{0.31 + \frac{24w}{a + 0.63}} \quad (\text{psi}) \quad (4.3b)$$

where  $w$  is the crack width (mm or in.) and  $a$  is the maximum aggregate size (mm or in.). Collins and Mitchell<sup>27</sup> proposed Eqn. 4.4 for the relationship between shear stress on the crack surface and crack width, which is shown graphically in Figure 4.3.

$$v_{ci} = \frac{0.17\sqrt{f_c}}{0.3 + 0.6w} \quad (\text{MPa}) \quad (4.4)$$



Total force on crack  $V_{ci} = v_{ci} b_w \frac{jd}{\sin\theta}$



Vertical shear  $V_v = V_{ci} \sin\theta = v_{ci} b_w jd$

or  $v_v = v_{ci}$

Figure 4.2 Transformation of interface shear stress to vertical shear stress.

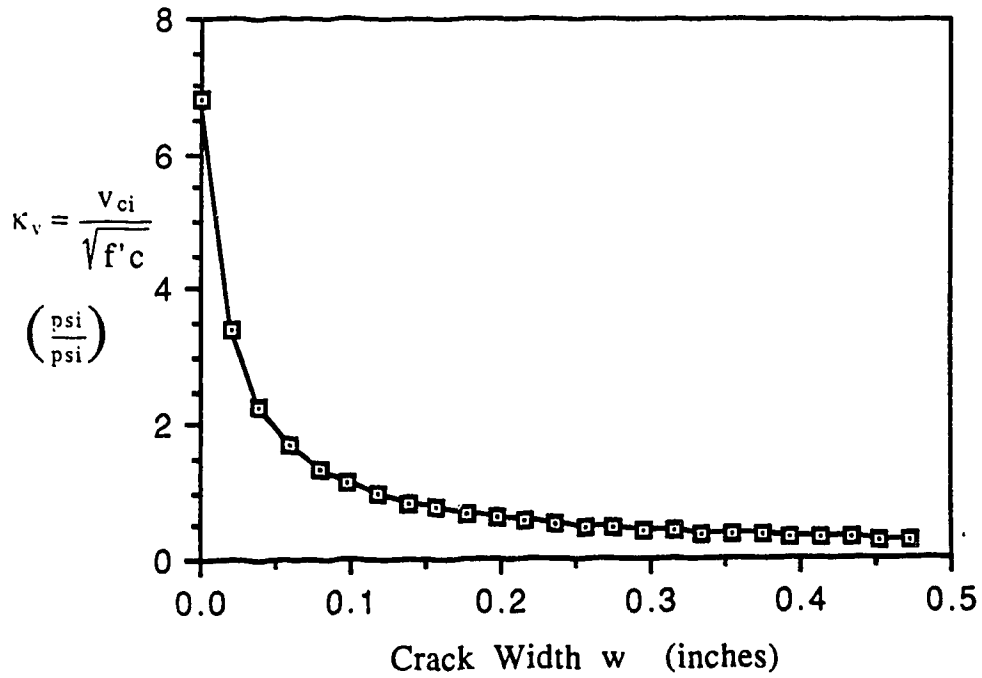


Figure 4.3 Crack shear stress based on Collins and Mitchell.

$$v_{ci} = \frac{2.0\sqrt{f'_c}}{0.3 + 15.2w} \quad (\text{psi}) \quad (4.4b)$$

This is a simple and straightforward relationship which applies to typical maximum aggregate sizes greater than or equal to 3/4 inch (20 mm). If the maximum aggregate size is less than 3/4 inch, Eqn. 4.4 overestimates the shear across the crack compared to Eqn. 4.3. Considering an uncracked beam with zero crack width and 2900 psi (20 MPa) concrete, the maximum capacity of the crack interface obtained using Eqn. 4.4 is 360 psi (2.5 MPa), corresponding to  $\kappa_v=6.69$ . Although the shear friction concept in ACI Section 11.7 permits stresses up to 0.2  $f'_c$ , or 580 psi for 2900 psi concrete, a shear stress of 360 psi is greater than the ACI Code expression  $2\sqrt{f'_c}$ , where  $\kappa_v=2.0$ . In order to ensure Eqn. 4.4 provides strengths comparable to the existing ACI shear design procedure, an upper limit is required on the maximum shear stress. As will be shown in a later section, a limit on shear stress is provided by the maximum allowable concrete capacity in tension. The concrete tension failure mechanism will be derived using the tensile capacity of cracked concrete suggested in the Modified Compression Field Theory.

If the Collins and Mitchell expression for shear stress at a crack interface is to be used as a design equation, the crack width  $w$  must be easily calculated or determined in terms of other known variables. A typical crack varies in width along its length, but the average crack width  $w$  can be related to the principal tensile strain  $\epsilon_1$  and the average crack spacing  $s_{m\theta}$  measured perpendicular to the

cracks by

$$W = \epsilon_1 S_{m\theta} \quad (4.5)$$

Consequently, using Eqn. 4.4 the shear capacity at the crack interface can be expressed as

$$v_{ci} = \frac{0.17 \sqrt{f'_c}}{0.3 + 0.6 (\epsilon_1 S_{m\theta})} \quad (\text{MPa}) \quad (4.6)$$

$$v_{ci} = \frac{2.0 \sqrt{f'_c}}{0.3 + 15.2 (\epsilon_1 S_{m\theta})} \quad (\text{psi}) \quad (4.6b)$$

The July 1988 draft copy of OHBDC-III 28 contains a similar expression for shear in members with transverse reinforcement perpendicular to the member axis. Clause 8.9.2.12 gives the concrete contribution equal to

$$v_{ci} = \frac{0.17 \phi_c \sqrt{f'_c}}{0.3 + 180\epsilon_1} \quad (\text{MPa}) \quad (4.7)$$

where  $\phi_c$  is a material strength resistance factor. In order to be conservative and underestimate the crack shear stress, the largest practical denominator in Eqn. 4.6 should be obtained for a design equation. It is apparent that the OHBDC-III assumes the maximum average crack spacing will be 12 in. (300 mm). Eqn. 4.7 is the only expression given for the concrete contribution in the OHBDC-III and assumes the failure mechanism in shear is based solely on the crack



interface.

The actual mean crack spacing  $s_{m\theta}$  in Eqn. 4.6 will depend, among other things, on the amount and location of both transverse and longitudinal reinforcement in the beam web. Expressions are available which can be used to estimate the mean crack spacing, however they are generally too complex for general use. For simplicity, Collins and Mitchell <sup>27</sup> recommend the mean crack spacing be approximated by Eqn. 4.8, where  $s_x$  equals the vertical spacing of longitudinal bars distributed in the web and  $s$  is the stirrup spacing. Collins and Mitchell recommend that both  $s$  and  $s_x$  be taken greater or equal to 4 inches (100 mm).

$$s_{m\theta} = \frac{1}{\frac{\sin \theta}{s} + \frac{\cos \theta}{s_x}} \quad (4.8)$$

It must be recognized that there can be a wide variation in crack spacings, particularly due to the nonisotropic properties of cracked concrete. Expressions for the crack spacing can only provide a guide to estimate the large range of actual crack spacings that can exist in an actual member. Since the Modified Compression Field Theory is based on average behavior, however, local variations are not believed to be critical.

Vecchio and Collins suggest the principal compressive strain  $\epsilon_2$  in the concrete be taken as -0.002. From Mohr's circle of strains a

compatibility condition is obtained relating the longitudinal strain  $\epsilon_x$  at mid-depth of the web and the principal tensile strain  $\epsilon_1$  at mid-depth, as shown by Figure 4.4 and Eqn 4.9.

$$\epsilon_1 = \epsilon_x + \frac{\epsilon_x + 0.002}{\tan^2 \theta} \quad (4.9)$$

Substituting Eqns. 4.8 and 4.9 into Eqn. 4.6 gives

$$v_{ci} = \frac{0.17\sqrt{f'c}}{0.3 + 0.6 \left( \epsilon_x + \frac{\epsilon_x + 0.002}{\tan^2 \theta} \right) \left( \frac{1}{\frac{\sin \theta}{s} + \frac{\cos \theta}{s_x}} \right)} \quad (\text{MPa}) \quad (4.10)$$

$$v_{ci} = \frac{2.0\sqrt{f'c}}{0.3 + 15.2 \left( \epsilon_x + \frac{\epsilon_x + 0.002}{\tan^2 \theta} \right) \left( \frac{1}{\frac{\sin \theta}{s} + \frac{\cos \theta}{s_x}} \right)} \quad (\text{psi}) \quad (4.10b)$$

where  $v_{ci}$  is the interface shear along the crack, which is equivalent to a shear stress  $v_{ci}$  acting on a vertical section. Eqn. 4.10 is too complex for general use. The expression can be simplified by selecting a value of  $\epsilon_x$ , and also by reducing the last term in the denominator as will be discussed in subsequent sections.

In order to examine the effects of the crack inclination on shear capacity, the angle  $\theta$  will be taken as  $20^\circ \leq \theta \leq 70^\circ$ . A lower limit is placed on the angle to control excessive cracking under service loads.

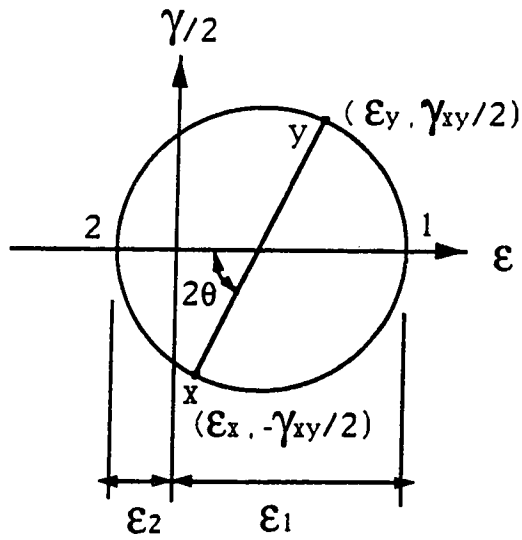


Figure 4.4 Mohr's circle of average strains.

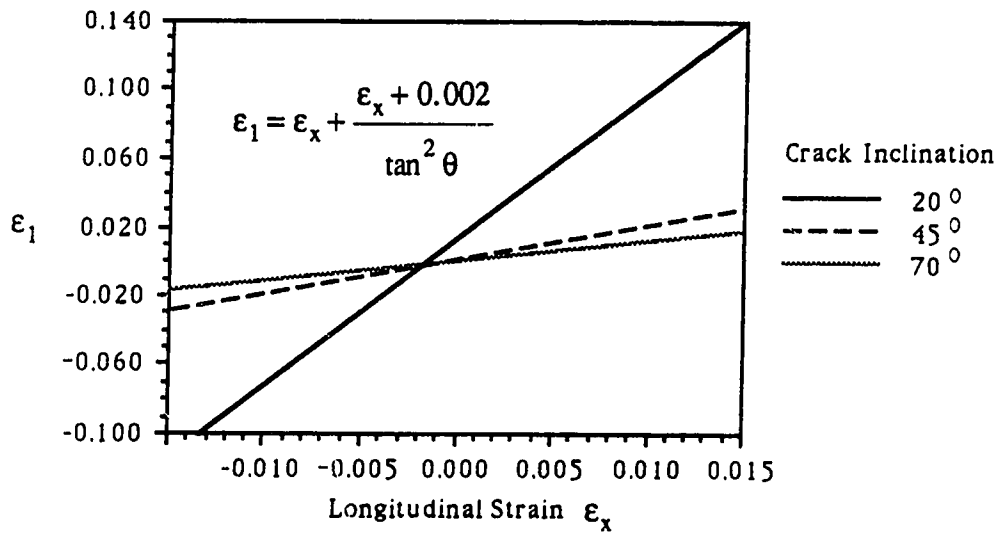


Figure 4.5 Compatibility of strains.

A limit is also required on  $\theta$  to control excessive strains in the beam reinforcement.

#### 4.2.1 Effect of Longitudinal Strain

The compatibility condition for strains, Eqn. 4.9, is shown graphically in Figure 4.5. It is apparent that for crack inclinations between 45 and 70 degrees, the principal tensile strain  $\epsilon_1$  is not as sensitive to changes in  $\epsilon_x$  as it is for inclinations less than 45 degrees. The sensitivity of Eqn 4.10 to various values of  $\epsilon_x$  is shown in Figures 4.6 and 4.7. Several general trends can be observed from the figures. As the longitudinal strain  $\epsilon_x$  increases, the rate of change of crack shear stress  $v_{ci}$  decreases. Also, the larger the crack inclination  $\theta$ , the more sensitive Eqn. 4.10 is to a particular value of  $\epsilon_x$ . For small crack inclinations, an increase in the stirrup spacing  $s$  or the vertical spacing of longitudinal bars  $s_x$  results in a smaller rate of change of shear stress or value of  $\kappa_v$ .

In typical design situations  $\theta$  would be less than or equal to  $45^\circ$ . The General Method in the Canadian Code CAN3-A23.3-M84<sup>1</sup> suggests  $\epsilon_x$  be taken as 0.002. If the actual longitudinal strain is less than this value, the capacity of the crack interface will be underestimated. If  $\epsilon_x$  is larger than 0.002, an unsafe prediction of the capacity results because the crack shear stress is overestimated. MacGregor<sup>13</sup> suggests the practical range of longitudinal reinforcement ratios,  $\rho$ , for beams developing shear failures is about

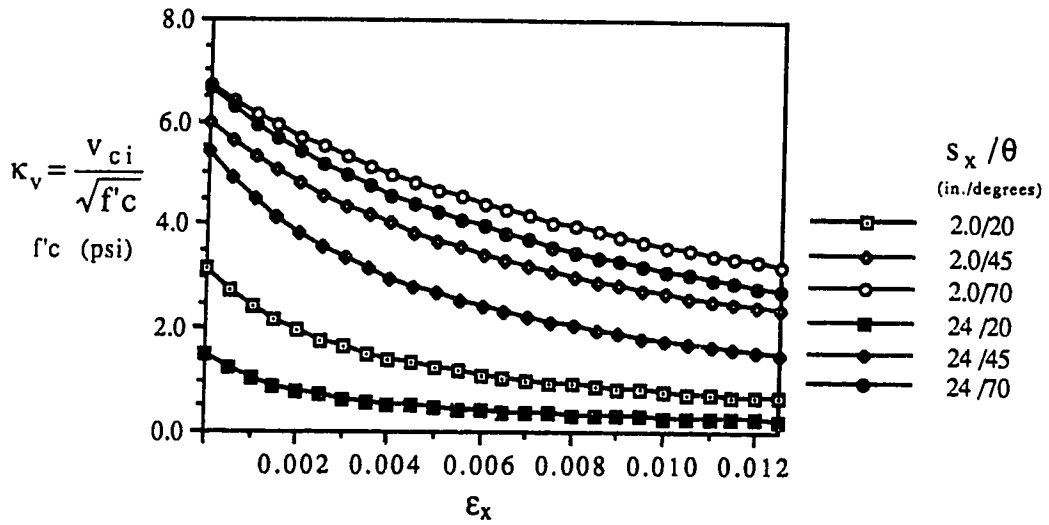


Figure 4.6 Crack shear stress vs. longitudinal strain,  $s = 2$  inches.

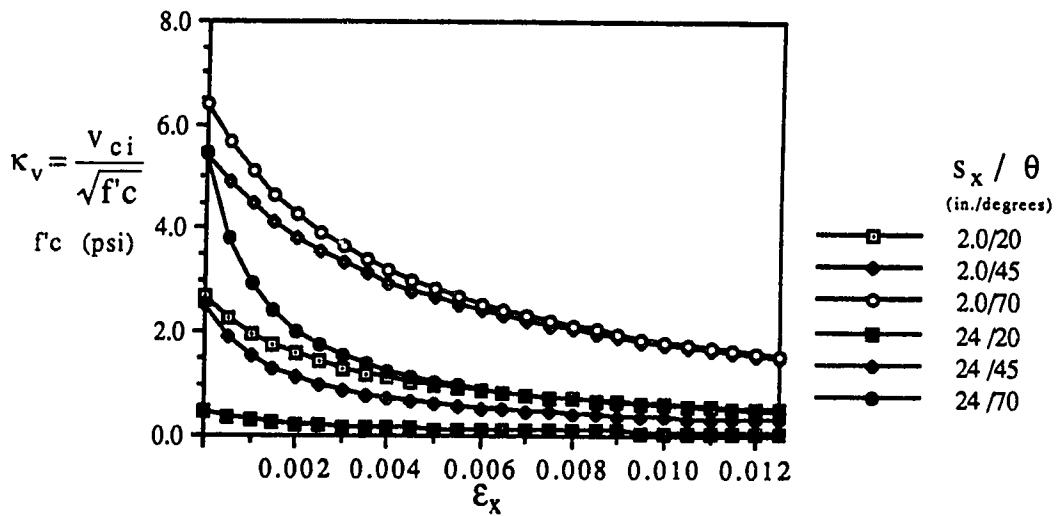


Figure 4.7 Crack shear stress vs. longitudinal strain,  $s = 24$  inches.

0.0075 to 0.025. In flexure, the smaller reinforcement ratio will give the largest longitudinal strain at failure. For beams with  $\rho=0.0075$ , strains larger than  $\epsilon_x=0.002$  are obtained at mid-depth of the section as shown in Table 4.1. As a result, it is possible that in negative moment regions where maximum moment and maximum shear coincide, a beam could be designed to fail in shear at a strain  $\epsilon_x=0.002$ , and in flexure at a strain greater than 0.002. This is opposite to the shear strength design philosophy which assumes that shear failure occurs at the same time or after flexural failure.

	$f'_c$		$f_y$ (longitudinal bars)		$\epsilon_x$	
	(psi)	(MPa)	(ksi)	(MPa)	$\rho=0.0075$	$\rho=0.75\rho_b$
2500		17.2	40	276	0.0060	$-8.0 \times 10^{-5}$
			60	413	0.0030	0.0038
3000		20.7	40	276	0.0078	$-8.0 \times 10^{-5}$
			60	413	0.0042	0.0038
4000		27.6	40	276	0.0114	$-8.0 \times 10^{-5}$
			60	413	0.0066	0.0038
5000		34.5	40	276	0.0140	$-8.0 \times 10^{-5}$
			60	413	0.0083	0.0038

**Table 4.1.** Mid-depth strain  $\epsilon_x$ , for  $\rho=0.0075$  and  $\rho=0.75\rho_b$ .

To ensure the crack capacity equation will always be conservative, it seems reasonable to select a value of strain larger than 0.002. However, if values of allowable shear stress are

evaluated using a conservative estimate of longitudinal strain such as 0.006 , the stress  $v_{ci}$  at the crack interface computed using Eqn 4.10 with a 45 degree crack inclination corresponds to transverse shear stresses considerably less than permitted by the currently used ACI Code or Simplified Method in the Canadian Code.

Consistent with CAN3-A23.3-M84, a value of  $\epsilon_x=0.002$  will be selected to simplify Eqn 4.10 for reinforced concrete beams, unless test data indicates a change is warranted. Tests of continuous beams must be examined in addition to simply supported beams in order to examine the effects at locations where maximum moment and shear coincide. For prestressed concrete beams, the same value of  $\epsilon_x=0.002$  is recommended, since, although prestressed members have smaller strains prior to cracking, the ultimate strains are comparable to reinforced concrete beams. Consequently, for the purpose of this derivation the strain distribution at shear failure has been defined as that producing a mid-depth strain of 0.002 for both reinforced concrete members and prestressed concrete members.

#### **4.2.2 Effect of Vertical Spacing of Longitudinal Bars**

The vertical spacing of longitudinal steel  $s_x$  complicates the concrete contribution equation, and selecting a value of  $s_x$  will simplify the final design equation. The choice of a large value for  $s_x$  leads to a low or safe estimate of  $v_{ci}$ , but the beneficial effects of longitudinal reinforcement distributed in a beam web which

restrains cracks from opening is not considered.

The influence of various values of  $s_x$  on the crack shear stress is shown in Figure 4.8, assuming a longitudinal strain  $\epsilon_x$  of 0.002. A value of  $s_x$  will be chosen to provide a value of  $\kappa_v=2$  at  $\theta=45^\circ$  with a stirrup spacing of 24 in. (600mm) to agree with the well established current practice. This corresponds to a value of  $s_x=8$  inches (200mm). Referring to Figure 4.8, the graph is generally flat for longitudinal bar spacings greater than about 8 inches. Selecting this particular value of  $s_x$  places an upper limit on crack spacings calculated using Eqn. 4.8, as shown in Table 4.2.

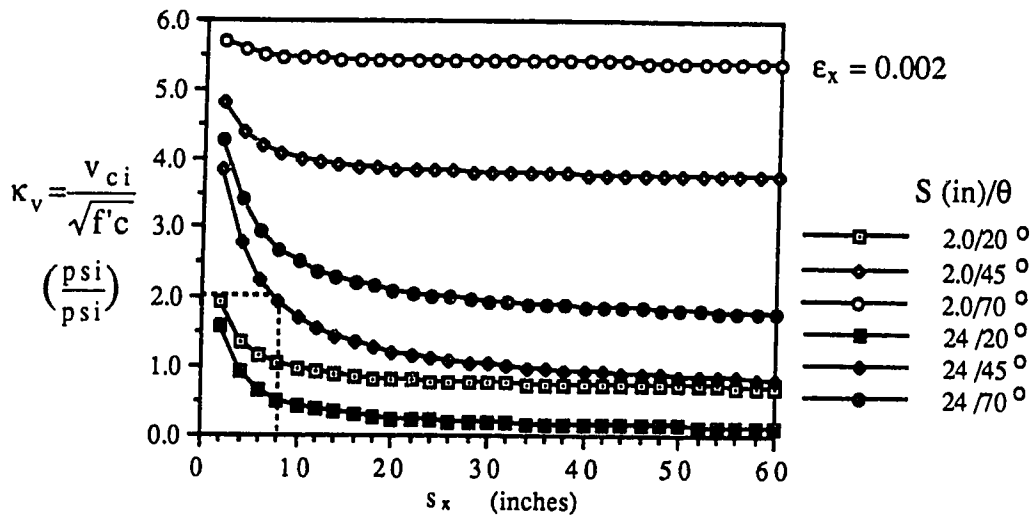
Crack Inclination $\theta$	Maximum Average $s_{m\theta}$ (Eqn. 4.8)	
	inches	(mm)
20	7.6	(190)
45	8.5	(215)
70	12.2	(310)

**Table 4.2.** Maximum average crack spacing if  $s_x=8$  in. and  $s=24$  in.

The crack spacings given in Table 4.2 represent the largest average values obtained for a given crack inclination. Actual crack spacings would fluctuate above and below these average values. As noted previously, the 1988 draft of OHBDC-III<sup>28</sup> assumes a maximum average crack spacing of 12 in. (300 mm), regardless of the crack inclination or stirrup spacing.

In order to verify the selection of  $s_x=8$  inches for use in simplifying





**Figure 4.8** Influence of vertical spacing of longitudinal bars on crack shear.

the crack spacing term in Eqn. 4.10, average crack spacings were calculated using Eqn. 4.8 and compared to 39 of the test beams summarized by Ramirez<sup>29</sup>. Beams were generally of rectangular cross section with overall depths ranging from 12 to 35.4 inches and had web reinforcement with stirrup spacings ranging from 3.5 to 12 inches. All beams failed in shear under a single or double point load. Average crack spacings and inclinations were estimated from photographs of the actual specimens. Comparing the estimated average crack spacing to that calculated using Eqn. 4.8 with  $s_x=8$  inches and the approximate crack angle  $\theta$ , the ratio of actual to predicted  $s_{m\theta}$  had a mean value of 1.12. In general, good agreement was obtained using a value of  $s_x$  equal to 8 inches in the crack spacing equation.

#### 4.2.3 Effect of Prestressing

Eqn. 4.4, which is the basis for the general concrete contribution expression given by Eqn. 4.10, neglects the beneficial effects of axial compression on aggregate interlock. In order to include the effect of axial compression due to prestressing on the concrete contribution, the difference in shear behavior as compared to a reinforced concrete beam must be examined. Generally, prestressing delays the formation of flexural cracks, and has a favorable influence on shear strength. It is advantageous to distinguish between regions of a beam that are cracked and uncracked in flexure. The ACI and CSA Codes accomplish this by distinguishing between web-shear and flexure-shear cracking. In an uncracked beam, axial compression tends to increase the shear required

to produce diagonal cracks as a result of principal tensile stresses in the concrete. In those portions of a prestressed concrete beam not previously cracked in flexure, Ramirez and Breen<sup>26</sup> suggest the increase in concrete contribution as compared to a reinforced concrete beam be given by

$$K = \sqrt{1 + \frac{f_{pc}}{2\sqrt{f'_c}}} \quad (4.11)$$

$$\text{but } 1.0 \leq K \leq 2.0$$

where  $f'_c$  is in psi. This expression is similar to Eqn. 3.1, with the principal tension stress at inclined cracking taken as  $2\sqrt{f'_c}$ . As shown in Figure 3.6, the concrete contribution varies for different levels of nominal shear stress.

In flexurally cracked regions of a beam, a portion of the cross-section is subjected to tension. Ramirez and Breen suggest the beneficial effects of prestressing not be considered in these zones. They suggest flexural cracking occurs when the extreme fiber tensile stress due to effective prestress and factored loads exceeds the tensile strength of concrete, taken as  $6\sqrt{f'_c}$ .  $K$  is taken equal to 1.0 in the flexurally cracked regions. The Swiss Code follows a similar procedure.

One disadvantage of this procedure is that the concrete contribution abruptly changes at a section where the tensile stress exceeds  $6\sqrt{f'_c}$ , but the simplicity of the method is well suited to design applications, particularly when compared to the complexity of the existing ACI shear

design procedure for prestressed concrete beams. Figure 4.9 compares Ramirez and Breen's maximum concrete contribution for prestressed concrete beams to the ACI equation for web shear cracking and to Eqn. 4.10b increased by Eqn. 4.11 with  $\epsilon_x = 0.002$ ,  $s_x = 8$  in. and  $s = 24$  in. Increasing Eqn 4.10b by the factor K results in concrete contribution shear stresses less than permitted by the current ACI Code for prestressed concrete beams. Since it is expected the inclination of an axial force with respect to a crack interface should affect the friction or aggregate interlock along the crack surface, Ramirez and Breen's assumption that the increase in concrete contribution due to prestress is independent of the crack inclination  $\theta$  may not be appropriate.

Eqn. 4.4, which relates the shear stress on a crack surface to the crack width, is obtained from a more general expression developed by Collins and Vecchio<sup>2</sup> given in inch and psi units as

$$v_{ci} = 0.18 v_{ci \max} + 1.64 f_{ci} - 0.82 \frac{f_{ci}^2}{v_{ci \max}} \quad (4.12)$$

$$v_{ci \max} = \frac{12\sqrt{f_c}}{0.31 + \frac{24 w}{a + 0.63}} \quad (4.13)$$

which includes the effect of a compressive stress  $f_{ci}$  perpendicular to the crack surface. Eqn 4.4 neglects the influence of  $f_{ci}$  on aggregate interlock and is derived from the first term of Eqn. 4.12. An increase in the concrete contribution shear stress due to a compressive force

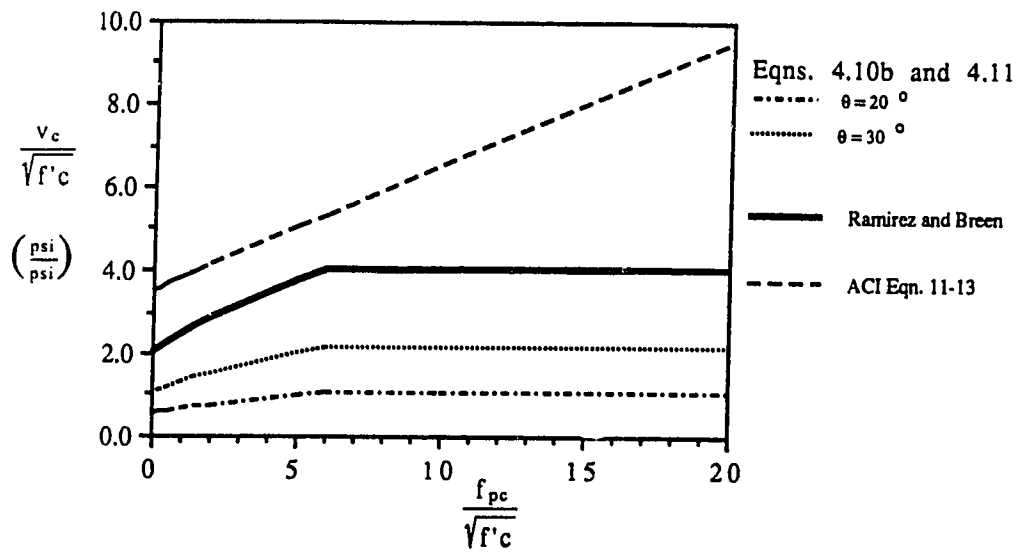


Figure 4.9 Concrete contribution for prestressed beams.

perpendicular to a crack, denoted  $v_{cp}$ , can therefore be expressed as

$$v_{cp} = 1.64 f_{ci} - 0.82 \frac{f_{ci}^2}{v_{ci \max}} \quad (4.14)$$

where  $f_{ci}/v_{ci \max} \leq 1.0$ . Since the Modified Compression Field Theory is based on average behavior, it is suggested the prestressing conditions at the centroid of the section be considered. The component of  $f_{pc}$  perpendicular to the crack surface can be obtained from  $f_{ci} = f_{pc} \sin \theta$  and substituting  $v_{ci \max} = \kappa_v \sqrt{f'_c}/0.18$  into Eqn 4.14 gives

$$\frac{v_{cp}}{\sqrt{f'_c}} = 1.64 \frac{f_{pc}}{\sqrt{f'_c}} \sin \theta - \frac{0.148}{\kappa_v} \left( \frac{f_{pc}}{\sqrt{f'_c}} \right)^2 \sin^2 \theta \quad (4.15)$$

The increase in shear due to an axial stress  $f_{pc}$  in the direction of the beam axis is therefore dependent on the level of prestress and the crack inclination. The increase in shear stress given by Eqn. 4.15 is shown graphically in Figure. 4.10 and is compared to the maximum increase in shear due to prestressing proposed by Ramirez and Breen. Eqn. 4.15 permits larger increases in shear stress due to prestressing, particularly for increasing values of  $f_{pc}$ .

In order to simplify Eqn. 4.15, the following approximate equations are proposed:

$$\kappa_{vp} = \frac{v_{cp}}{\sqrt{f'_c}} = (0.06 + 0.01\theta) \frac{f_{pc}}{\sqrt{f'_c}} \quad (4.16)$$

$$\kappa_{vp} \leq 0.2\theta - 0.9 \quad (4.16b)$$

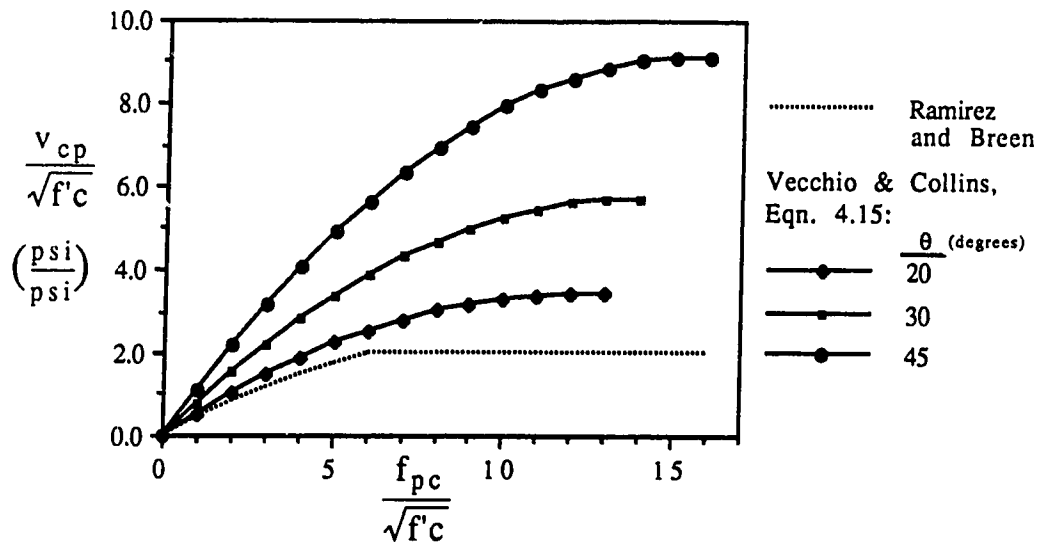


Figure 4.10 Increase in concrete contribution due to prestressing

As shown in Figure 4.11, Eqn. 4.16 underestimates the increase in shear as compared to the more complex equations and is a safe approximation. In order to determine the total concrete contribution for a prestressed concrete beam, the additional shear stress  $v_{cp}$  obtained from Eqn. 4.16 is added to that given by Eqn. 4.10. In flexurally cracked regions, it is suggested the effects of prestressing not be considered and  $v_{cp}$  will be taken equal to zero. Consequently, in regions of a prestressed concrete beam subjected to flexural tension stresses, the total concrete contribution is equivalent to a nonprestressed beam.

#### 4.2.4 Expression for Capacity of Crack Interface

In the preceding sections, a basic equation for aggregate interlock as a function of crack width was expressed in terms of other variables,  $\epsilon_x$ ,  $s_x$ ,  $s_x$  and  $\theta$ . In order to reduce the number of variables and simplify the expression for use as a design equation, the effect of several parameters on the capacity of the crack interface was examined. It was suggested particular values of  $\epsilon_x$  and  $s_x$  could be chosen as constants in the final equation. Using the selected values of  $s_x=8$  in. (200 mm) and  $\epsilon_x=0.002$ , Eqn. 4.10 can be expressed as

$$v_{ci} = \frac{2.0\sqrt{f'_c}}{0.3 + \left(0.0304 + \frac{.0608}{\tan^2 \theta}\right) \left(\frac{1}{\frac{s}{\sin \theta} + \frac{\cos \theta}{8}}\right)} \quad (\text{psi}) \quad (4.17)$$



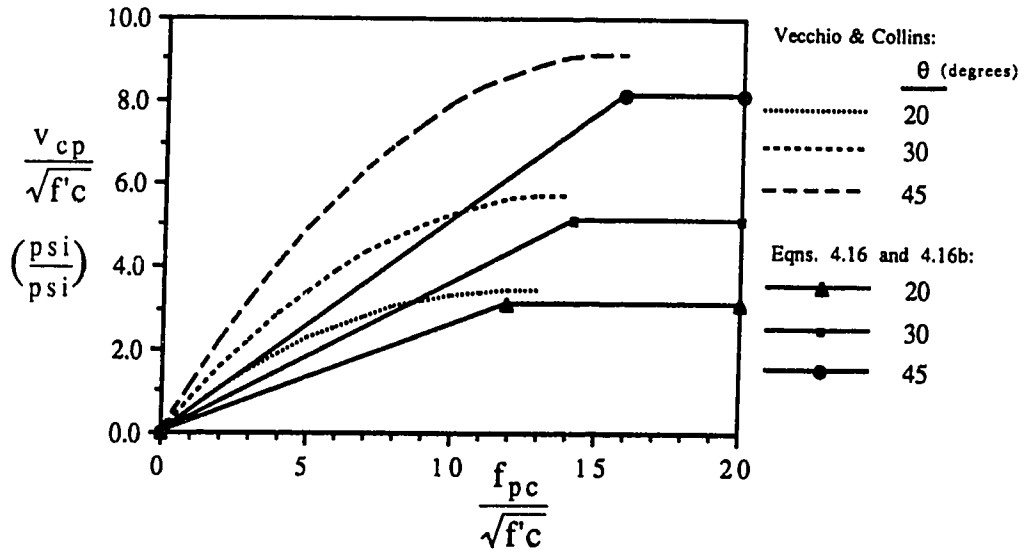


Figure 4.11 Proposed increase in concrete contribution.

$$v_{ci} = \frac{0.17\sqrt{f_c}}{0.3 + \left(0.0012 + \frac{.0024}{\tan^2 \theta}\right) \left(\frac{1}{\frac{\sin \theta}{s} + \frac{\cos \theta}{200}}\right)} \quad (\text{MPa}) \quad (4.17b)$$

and for prestressed concrete beams, the concrete contribution obtained from Eqn. 4.17 is added to that given by

$$v_{cp} = (0.06 + 0.01\theta) f_{pc} \quad (4.16)$$

$$\leq (0.2\theta - 0.9)\sqrt{f_c} \quad (4.16b)$$

where  $v_{cp}=0$  in those portions of a beam where the extreme fiber tensile stress due to factored loads and effective prestress exceeds  $6\sqrt{f_c}$ .

Since the aggregate interlock expression is based on Eqn. 4.4b, which assumes an maximum aggregate size of at least 3/4 inch, for smaller maximum aggregate sizes Eqn. 4.17 may overestimate the interface shear stress. However, it is suggested Eqn. 4.17 be applied to beams with maximum aggregate sizes as small as 3/8 inch unless test data indicates a change is warranted.

Eqn. 4.17 is shown graphically in Figures 4.12 and 4.13. Although from these graphs it is easy to determine the shear stress for a particular beam's stirrup spacing and crack angle, Eqn 4.17 is still too complex for general use. This equation will be simplified for design

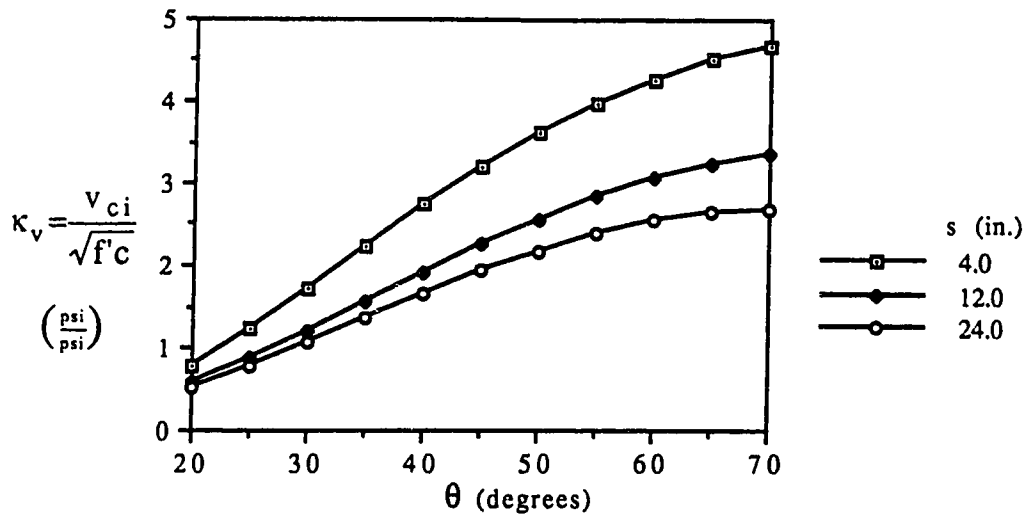


Figure 4.12 Crack shear stress vs. crack inclination (Eqn. 4.17b).

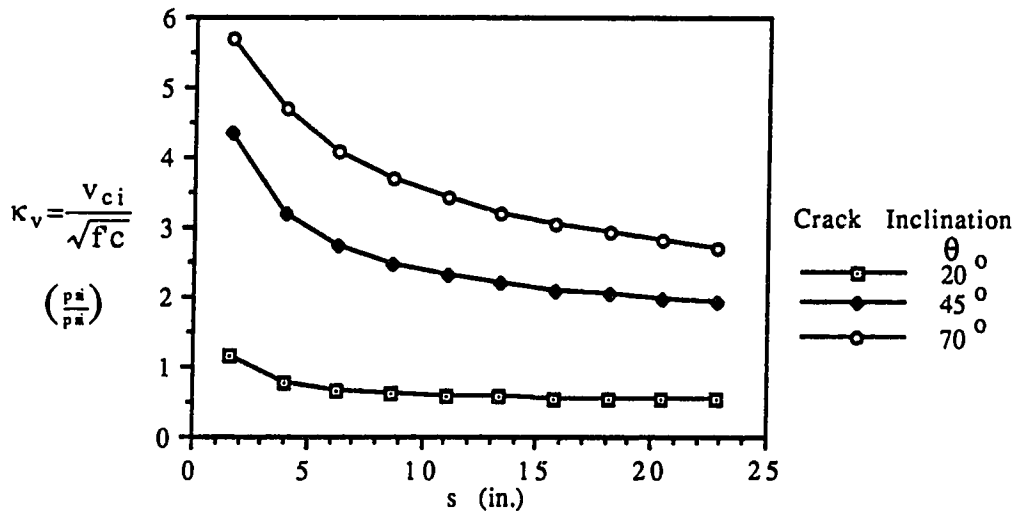


Figure 4.13 Crack shear stress vs. stirrup spacing (Eqn. 4.17b).

applications by developing easy to use approximate expressions, which will be presented and discussed in subsequent sections.

### 4.3 Capacity of Cracked Concrete in Tension

As shown in Figure 4.1, the concrete contribution to shear can be expressed in terms of tensile stresses in the concrete. In addition to the aggregate interlock mechanism examined in Sec. 4.2, another possible failure mode is governed by the capacity of the cracked concrete web in tension. Since the inclined compression struts are subjected to biaxial compression-tension, their tensile strength will be less than the uniaxial tension strength. For a cracked concrete element, Vecchio and Collins suggest the post cracking tensile stress-strain relationship given by

$$f_1 = \frac{f_{cr}}{1 + \sqrt{200\varepsilon_1}} \quad (4.18)$$

where  $f_{cr}$  is defined as the stress in the concrete at cracking. For diagonally cracked concrete beams, Collins and Mitchell<sup>27</sup> recommend Eqn. 4.19. As shown in Figure 4.14, Collins and Mitchell's equation provides a lower bound to values obtained using Eqn 4.18.

$$f_1 = \frac{\alpha_1 \alpha_2 f_{cr}}{1 + \sqrt{500\varepsilon_1}} \quad (4.19)$$

where  $\alpha_1$  and  $\alpha_2$  are factors originally developed in the CEB-FIP Model Code to account for the effects of bond and type of loading respectively.

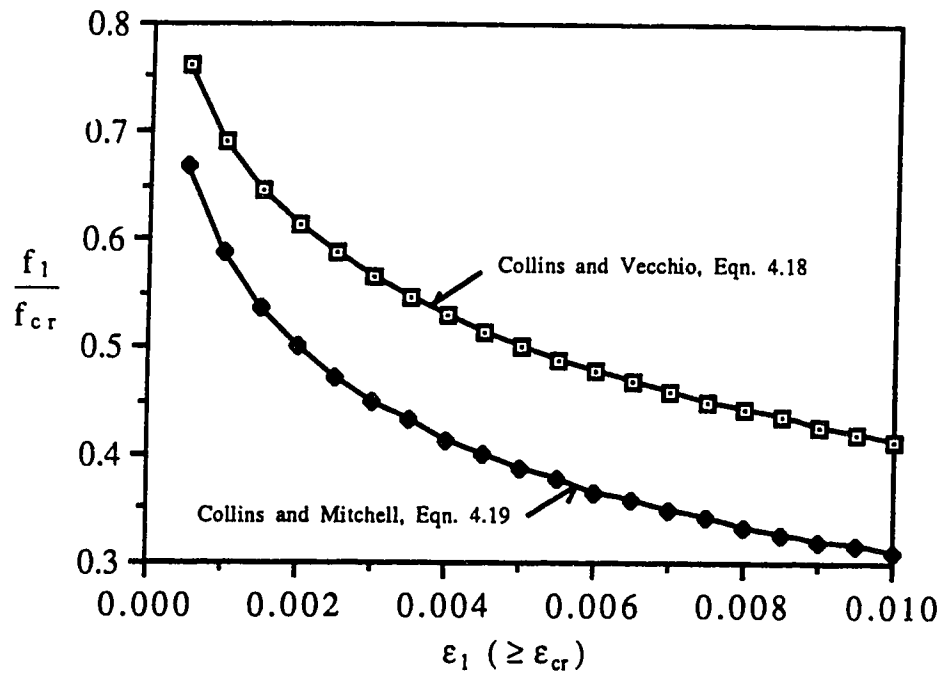


Figure 4.14 Post cracking tensile stress-strain curves.

For deformed bars and monotonically applied loads the Model Code suggests  $\alpha_1=\alpha_2=1.0$ . For undeformed bars and sustained loads, it suggests  $\alpha_1=\alpha_2=0.7$ . The lower estimate of tensile stress obtained from Eqn. 4.19 will be used in deriving the shear capacity provided by the concrete web in tension. Since most web reinforcement in the United States is #3 or #4 deformed bars,  $\alpha_1$  will be taken as 1.0. In addition, since the final design equation will be compared to test results of generally short term loading conditions,  $\alpha_2$  will also be taken equal to unity.

As in the derivation of the crack interface expression, Eqn. 4.19 must be expressed in terms of easily calculated variables if it is to be used for design purposes. One simplification is to make use of Eqn. 4.9, which relates the principal tensile strain  $\epsilon_1$  to the longitudinal strain  $\epsilon_x$ . Also, since the tensile strength of concrete is approximately proportional to  $\sqrt{f'_c}$ , the stress in the concrete at cracking can be expressed in the form  $D\sqrt{f'_c}$  where D is a constant. Consequently, Eqn. 4.19 can be rewritten as

$$f_1 = \frac{D\sqrt{f'_c}}{1 + \sqrt{500 \left( \epsilon_x + \frac{\epsilon_x + 0.002}{\tan^2 \theta} \right)}} \quad (4.20)$$

Because it is conceptually easier to visualize shear resistance resulting from shear stress along the crack than from concrete in tension, Model 2 in Figure 4.1 was selected as the basis for deriving the concrete contribution term. Consequently, the principal tensile stress  $f_1$

in the cracked concrete must be expressed as an equivalent stress along the crack interface, which can be accomplished using Eqn. 4.2b. In order to calculate  $v_{ci}$  from this equation, the stress in the reinforcement  $f_s$  at an average location in the compression strut must be determined. Denoting the change in reinforcement stress ( $f_y - f_s$ ) as  $\Delta f_s$ , Eqn. 4.2b becomes

$$v_d = \frac{f_1}{\tan \theta} - \frac{A_v(\Delta f_s)}{s b_w \tan \theta} \quad (4.21)$$

If a vertical stirrup has only minimal bond to the concrete strut,  $\Delta f_s$  is approximately zero. This may be a reasonable approximation if undeformed web reinforcement is used, because as it contracts in diameter due to axial tension only minimal bond is expected between the reinforcement and the concrete. However, if deformed bars are used the change in stress  $\Delta f_s$  will not be negligible. To develop a design expression that will be conservative and underestimate  $v_{ci}$ , it is beneficial to use the largest practical  $\Delta f_s$ . If web reinforcement is considered to have bond characteristics similar to deformed bars, ACI Clause 12.2.2 can be used to determine the maximum  $\Delta f_s$  due to bond as

$$\Delta f_{s \max} = \frac{l_b \sqrt{f'_c}}{0.04 A_b} \quad (4.22)$$

As shown in Figure 4.15, the stress in a stirrup midway between two cracks can be determined by considering the bond between the bar and the concrete within half a crack width. For typical maximum crack

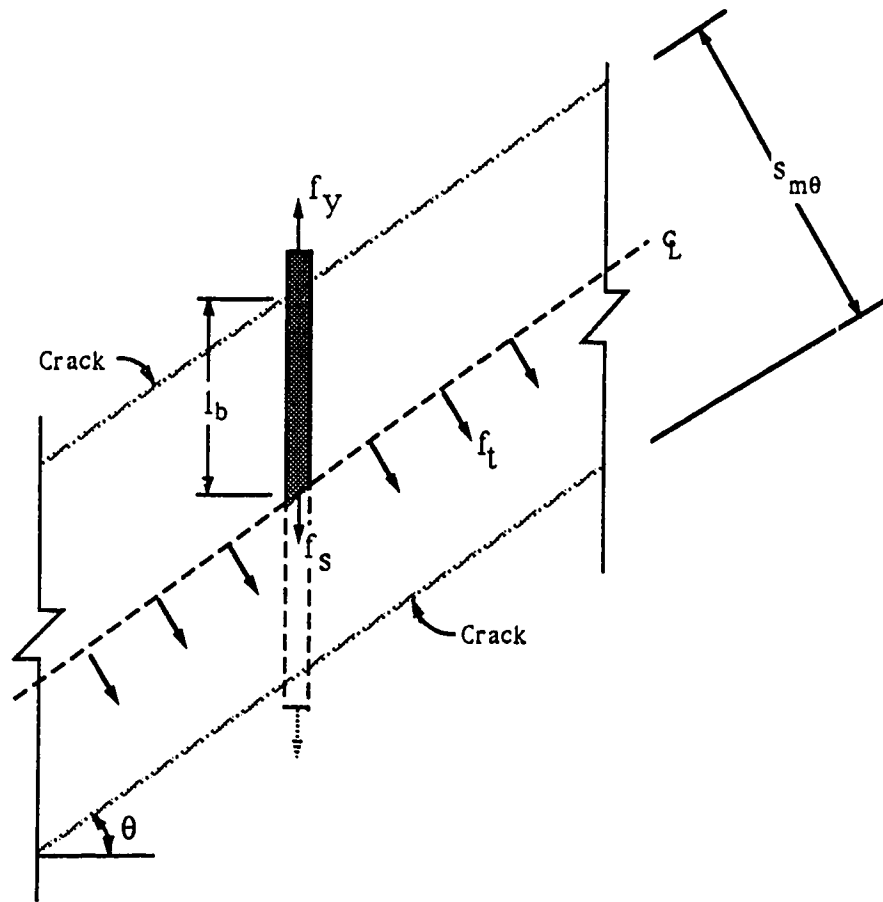


Figure 4.15 Variation of stress in web reinforcement.



spacings, it can be shown that  $\Delta f_s \text{ max}$  at the centreline of a strut can equal  $f_y$ . That is, if a stirrup is considered to have bond similar to a deformed bar, it is possible to develop the bar's full yield strength within half of a typical crack spacing. From Figure 4.15, the ultimate value of tension the concrete can withstand prior to failure is another condition limiting the maximum  $\Delta f_s$  at the centreline of a strut. Consequently, the maximum value of change in stirrup stress that the concrete is capable of equilibrating in tension can be determined. However, if the maximum tensile stress at the centreline of a concrete strut is reached, a new crack forms in the concrete strut but the cracked concrete beam web still provides resistance to shear. The Modified Compression Field Theory considers the tensile behavior of a concrete element as cracking proceeds under increasing loads, and examines the bar stress at an average location in the concrete, not at the centreline of a concrete strut. The stress in the reinforcement  $f_s$  at an average location in a strut, which is at the inclined section where  $f_1$  acts, can be determined by examining the average strains in a cracked concrete element. The average transverse strain  $\epsilon_y$  can be determined from Mohr's circle as

$$\epsilon_y = \frac{\epsilon_x + 0.002}{\tan^2 \theta} - 0.002 \quad (4.23)$$

where the principal compressive strain is equal to -0.002, as suggested by Vecchio and Collins.

If the longitudinal strain  $\epsilon_x$  is taken equal to 0.002, as in the aggregate interlock expression developed in Section 4.2,  $\epsilon_y$  calculated using Eqn. 4.18 will be greater than a tensile strain of 0.002 for crack inclinations less than or equal to 45 degrees. Consequently, the transverse strain equals or exceeds the yield strains of 0.0013 and 0.002 for Grade 40 and Grade 60 reinforcing bars respectively. For crack inclinations greater than 45° the average transverse strain  $\epsilon_y$  calculated using Eqn. 4.23 is less than 0.002, and average yielding of the web reinforcement may not occur. Therefore, if  $\theta$  is limited to less than or equal to 45°,  $f_s (= E_s \epsilon_y)$  at an average location in a strut equals  $f_y$  in tension, and  $\Delta f_s$  in Eqn. 4.21 equals 0. As a result, Eqn 4.21 can be expressed as

$$v_{ci} = \frac{f_1}{\tan \theta} \quad (4.24)$$

Substituting this expression into Eqn 4.20 gives

$$v_{ci} = \frac{D \sqrt{f'_c}}{\left\{ 1 + \sqrt{500 \left( \epsilon_x + \frac{\epsilon_x + 0.002}{\tan^2 \theta} \right)} \right\} \tan \theta} \quad (4.25)$$

which is a general expression for the equivalent interface shear of the concrete contribution provided by cracked concrete in tension, provided  $\Delta f_s = 0$ . To ensure this condition is satisfied,  $\theta$  should be limited to less than or equal to 45° for a longitudinal strain  $\epsilon_x = 0.002$ . Limiting  $\theta$  to a value of 45° is reasonable for typical design situations, and is consistent

with the maximum inclination of  $45^\circ$  permitted in the June 1989 draft of the CEB-FIP Model Code 1990<sup>25</sup>.

#### 4.3.1 Effect of Longitudinal Strain

The influence of  $\epsilon_x$  on the magnitude of shear is shown in Figure 4.16. It is apparent that the larger the crack inclination, the less sensitive Eqn. 4.25 is to different values of  $\epsilon_x$ . As in the derivation of the crack interface expression,  $\epsilon_x$  is selected as 0.002 which gives

$$v_{ci} = \frac{D\sqrt{f_c}}{\left\{ 1 + \sqrt{1 + \frac{2}{\tan^2 \theta}} \right\} \tan \theta} \quad (4.26)$$

Consequently, the strain distribution at shear failure is defined as that producing a mid-depth strain of 0.002. If the actual  $\epsilon_x$  is larger than this value, the shear stress calculated using Eqn. 4.26 corresponding to the concrete capacity will be overestimated. However, as shown in Figure 4.16, for longitudinal strains greater than 0.002 the curves flatten out and the variation in concrete contribution is not substantial.

#### 4.3.2 Effect of Concrete Cracking Strength

Eqn. 4.26 is equally valid for either psi or MPa units, provided D is specified in the corresponding units. The tensile strength of concrete is approximately proportional to the square root of the compressive strength, and ACI Sec. 11.4.2.1. suggests a value of  $6\sqrt{f_c}$  for strength

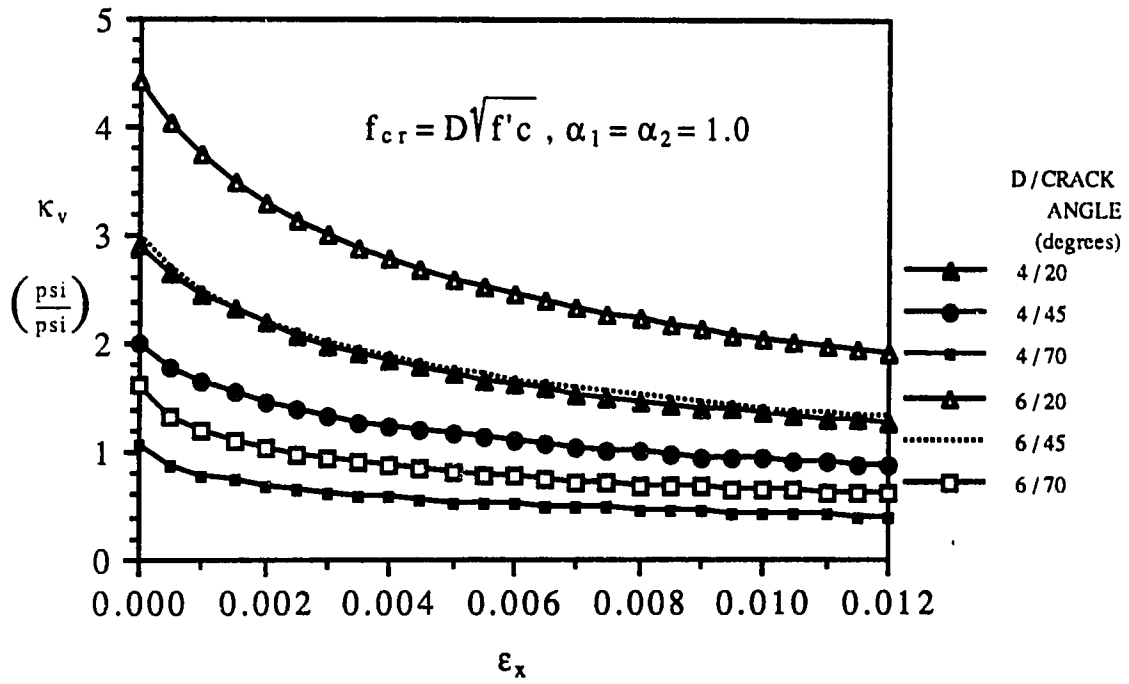


Figure 4.16 Influence of longitudinal strain on concrete tensile capacity.

calculations. The Modified Compression Field Theory suggests the tensile stress in the concrete at cracking  $f_{cr} = D\sqrt{f'_c}$  be taken as  $4\sqrt{f'_c}$  psi ( $0.33\sqrt{f'_c}$  MPa), which is the same expression used in the ACI Code for predicting the principal tensile stress at web-shear cracking. Eqn. 4.26 is shown in Figure 4.17 with  $D$  ranging from 4 to 6. The value of  $D=4$  suggested in the Modified Compression Field Theory was not rigorously established by Vecchio and Collins, but since it provided reasonable agreement with their test results it was used. In order to provide shear strengths comparable to the existing ACI Code equation of  $2\sqrt{f'_c}$ , a value of  $\kappa_v=2.0$  should be obtained using the proposed concrete tension capacity at  $\theta = 45^\circ$ . This requirement suggests a value of  $f_{cr}=5.5\sqrt{f'_c}$  be used in developing the general expression for the shear capacity provided by cracked concrete in tension. Figure 4.18, which compares the proposed value of  $f_{cr}$  with the test results given by Collins and Vecchio<sup>30</sup>, indicates a choice of  $D=5.5$  is reasonable as a design simplification, although the number of factors that influence the cracking strength create a wide scatter of test results.

### 4.3.3 Effect of Prestressing

Prestressing tends to increase the load at which cracks develop. The value of  $f_{cr} = 4\sqrt{f'_c}$  suggested in the Modified Compression Field Theory is based on the results of reinforced concrete panels subjected almost exclusively to pure shear. For a given shear stress, the effect of axial compression in an uncracked beam is to shift the Mohr's circle of stress and reduce the the principal tensile stress compared to that

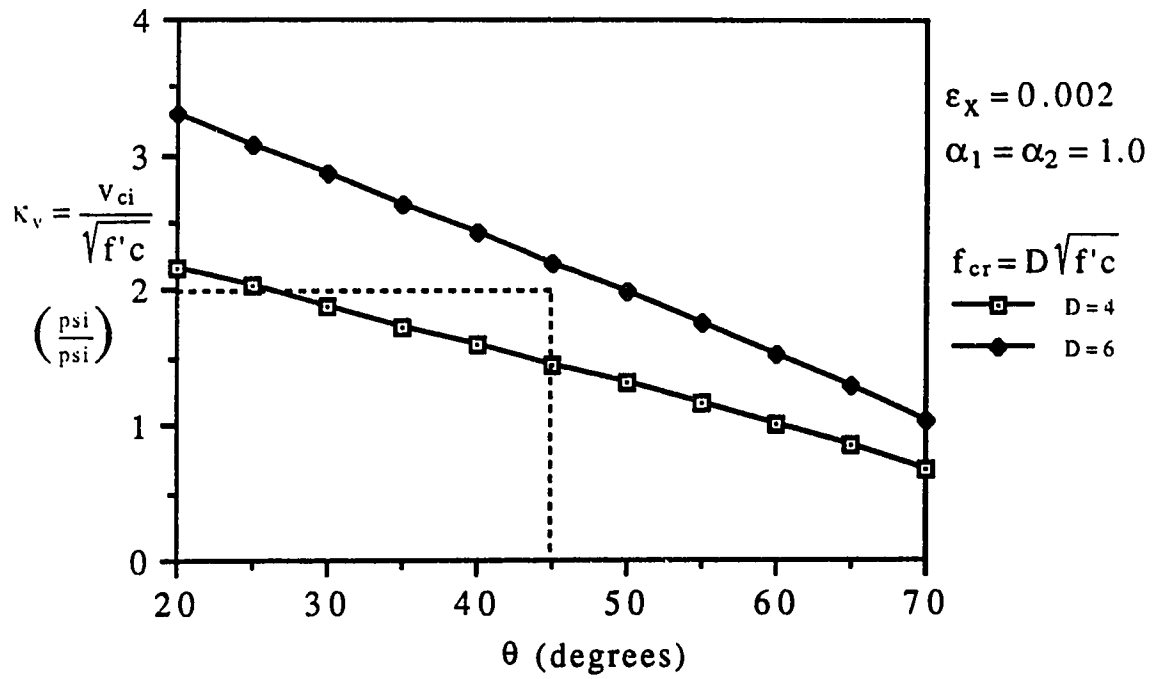


Figure 4.17 Shear capacity provided by concrete tension.

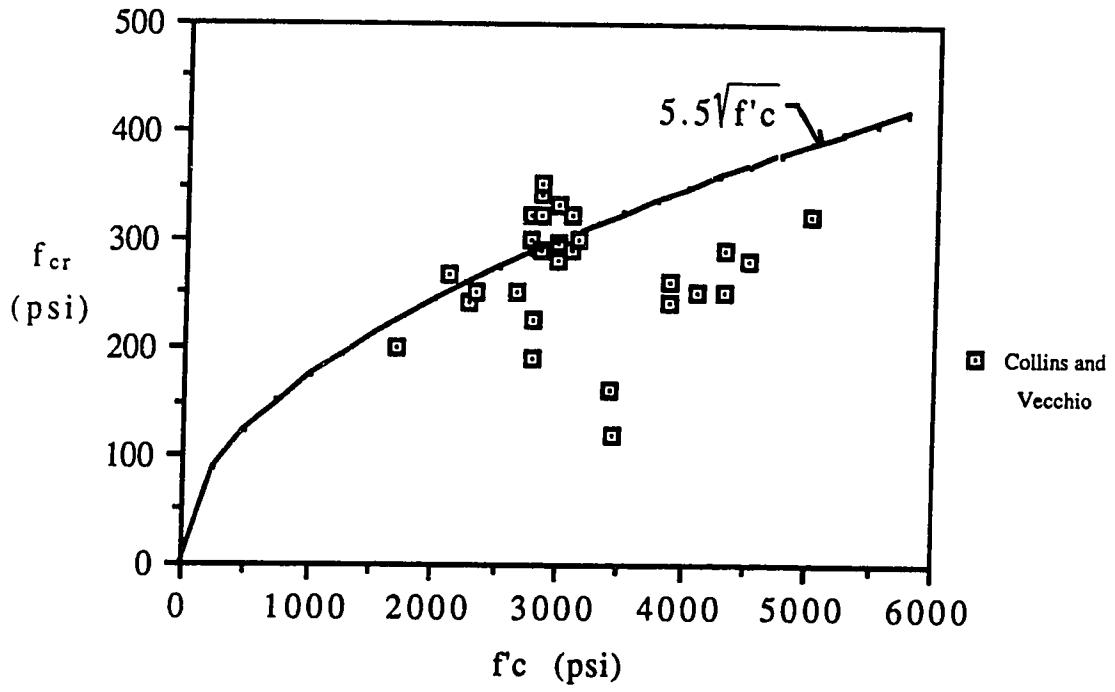


Figure 4.18 Cracking stress vs. cylinder strength.

produced by pure shear. The increase in cracking stress due to prestressing is given by Eqn. 4.11 as

$$K = \sqrt{1 + \frac{f_{pc}}{2\sqrt{f'_c}}} \quad (4.11)$$

where all terms are as previously defined. Consequently, for prestressed concrete beams the concrete contribution due to tension in the concrete can be expressed using Eqn. 4.26 with the numerator in the form  $KD\sqrt{f'_c}$ .

In the regions of a beam where flexural cracking has occurred, the shear capacity of a prestressed beam is similar to that of reinforced concrete beam, suggesting  $K=1.0$  in this case. Ramirez and Breen recommend a limit of  $K=1.0$  be imposed to those regions of a beam where the extreme tensile stress due to the factored load and the effective prestress exceeds  $6\sqrt{f'_c}$ . Ramirez and Breen suggest  $K \leq 2.0$ . Based on their evaluation, it is suggested the increase in cracking stress due to prestressing be calculated according to Eqn 4.11, but  $1.0 \leq K \leq 2.0$ , and  $K=1.0$  in flexurally cracked regions.

#### 4.3.4 Expression for Capacity of Cracked Concrete in Tension

Using the tensile stress-strain relationship for cracked concrete recommended by Collins and Mitchell, the contribution to shear provided by tension in the concrete has been converted into an equivalent stress  $v_{ci}$  acting along a crack interface. The interface shear



stress is analogous to a vertical shear stress acting on the beam section. The resulting expression gives an upper limit to the concrete contribution to shear provided by tensile stresses in a slender reinforced concrete beam as

$$v_{ci} = \frac{5.5\sqrt{f_c}}{\left\{ 1 + \sqrt{1 + \frac{2}{\tan^2 \theta}} \right\} \tan \theta} \quad (\text{psi}) \quad (4.27)$$

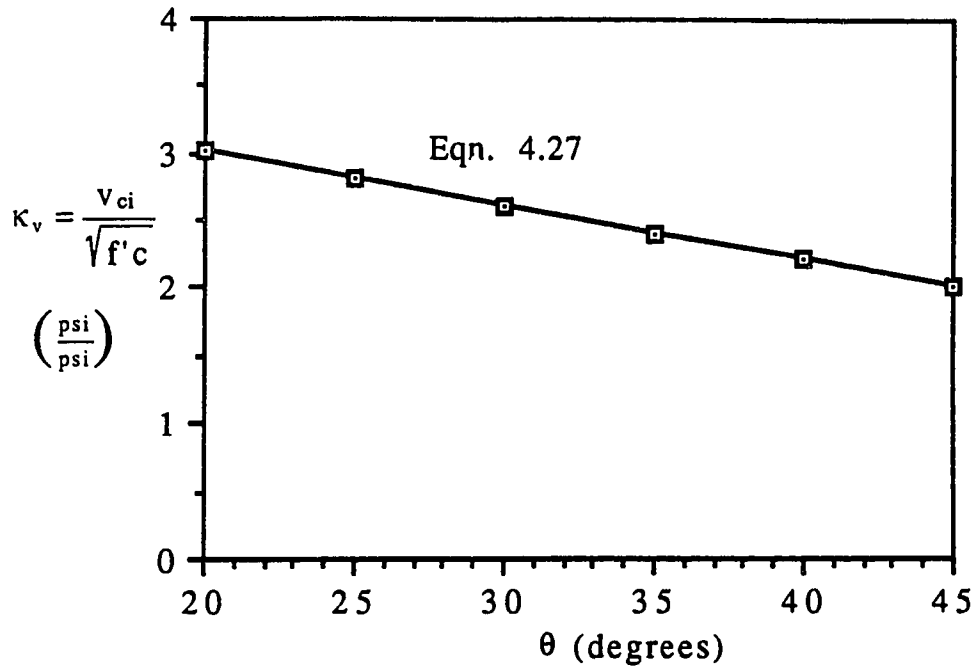
$$v_{ci} = \frac{0.46\sqrt{f_c}}{\left\{ 1 + \sqrt{1 + \frac{2}{\tan^2 \theta}} \right\} \tan \theta} \quad (\text{MPa}) \quad (4.27b)$$

Eqn. 4.27 is shown graphically in Figure 4.19. Although the general expression involves only two variables  $f_c$  and  $\theta$ , the equation is complex and may not be appropriate as a design expression. Simplified relationships can be derived to approximate Eqn 4.27, as will be discussed in Section 4.4.

For prestressed concrete beams, the concrete contribution predicted by Eqn. 4.27 is multiplied by

$$K = \sqrt{1 + \frac{f_{pc}}{2\sqrt{f_c}}} \quad (4.11)$$

with  $1.0 \leq K \leq 2.0$ . and  $K=1.0$  in flexurally cracked regions.



**Figure 4.19** Concrete contribution due to tensile stresses in the concrete.

#### 4.4 Development of Concrete Contribution Equations for Use in Design

For slender reinforced concrete beams, the concrete contribution can be expressed as

$$V_c = v_{ci} b_w j d \quad (4.28)$$

The shear carried by the concrete, which is equivalent to the interface shear, is limited by both the aggregate interlock capacity and the tensile stress-strain response of cracked concrete, as given by Eqns. 4.17 and 4.27 respectively. These expressions are shown in Figure 4.20. It is apparent that for small crack inclinations, the aggregate interlock along the crack governs the shear capacity. For large crack inclinations and small stirrup spacings, the tensile capacity of the concrete controls the shear strength. In most situations, typical beam designs would use inclinations less than  $45^\circ$ , and for typical stirrup spacings the aggregate interlock expression would govern the allowable concrete contribution. As noted in Section 4.2, OHBDC-III assumes the crack interface controls the shear strength in all circumstances. As shown in Figure 4.20, this assumption may not be appropriate for large crack inclinations and small stirrup spacings.

For prestressed concrete beams, the concrete contribution due to aggregate interlock is determined by adding the allowable shear stress from Eqn. 4.16 to Eqn. 4.17. The contribution due to tension in the concrete is obtained by multiplying Eqn. 4.27 by Eqn. 4.11. The lower

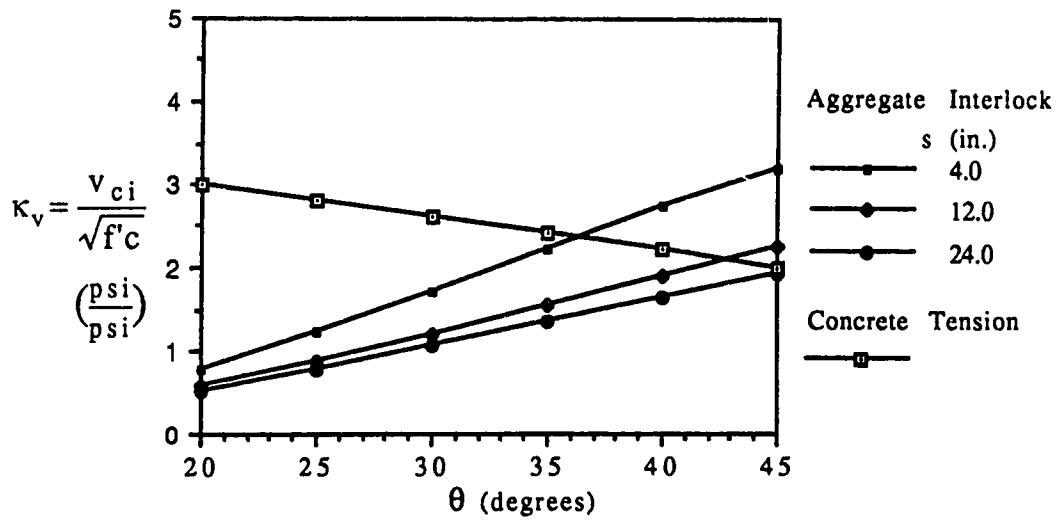


Figure 4.20 Concrete contribution expressions.

or limiting value of the two expressions determines the concrete contribution to shear.

The total shear resistance is calculated by adding the shear carried by the concrete to the shear resisted by the stirrups plus the vertical component of any inclined prestressing tendons. Assuming the vertical stirrups have yielded at failure and the internal lever arm is equal to the 90% of the effective depth, the shear contributed by the web reinforcement given by Eqn. 2.37 can be expressed as

$$V_s = \frac{A_v f_y 0.9d}{s \tan \theta} \quad (4.29)$$

which is the expression suggested in the 1987 draft of Chapter 11 in the ACI Code.

For a given angle  $\theta$ , it is difficult to have the stirrup spacing as a variable in both the concrete contribution as in Eqn. 4.17 and in the web reinforcement equations, since a trial and error procedure must be used to solve for the required stirrup spacing. As a result, the expressions derived earlier in this chapter are considered too complex as Code equations. Approximate and simple to use equations will be developed to simplify the concrete contribution expressions, and reduce the likelihood of calculation errors.

## 4.5 Proposed Design Equations

In order to simplify the general expressions derived for the concrete contribution to shear in B-regions of slender reinforced concrete beams, the following approximate equations are proposed:

$$\text{Interface shear capacity: } \kappa_v = 0.05\theta - 0.25 \quad (4.30)$$

$$\text{Capacity of cracked concrete in tension: } \kappa_v = 4.25 - 0.05\theta \quad (4.31)$$

where  $\theta$  is in degrees and is limited to a maximum value of  $45^\circ$ . A lower limit on  $\theta$  is required to prevent web crushing, which is discussed in Chapter 5. Eqns. 4.30 and 4.31 are compared to values obtained from Eqns. 4.17 and 4.27 in Figure 4.21. Eqn. 4.30 provides the smaller or limiting value of the concrete contribution and governs for all compression strut inclinations less than  $45^\circ$ , and gives  $\kappa_v=1.0$  at  $\theta=25^\circ$ , and  $\kappa_v=2.0$  at  $45^\circ$ . Consequently, for reinforced concrete beams Eqn. 4.30 determines the allowable concrete contribution in a variable angle model. At an inclination of  $45^\circ$  the concrete contribution is  $2\sqrt{f'_c}$ , which is the same as given by the ACI expression in Eqn. 2.21. Although the beneficial effects of tightly spaced stirrups ( $s=4$  in.) in restraining crack growth and maintaining aggregate interlock are not included in Eqn. 4.30, the proposed design equation is much easier to use than Eqns. 4.17 and 4.27. As shown in Figure 4.21 it is conservative for both the aggregate interlock and concrete tension limit states.

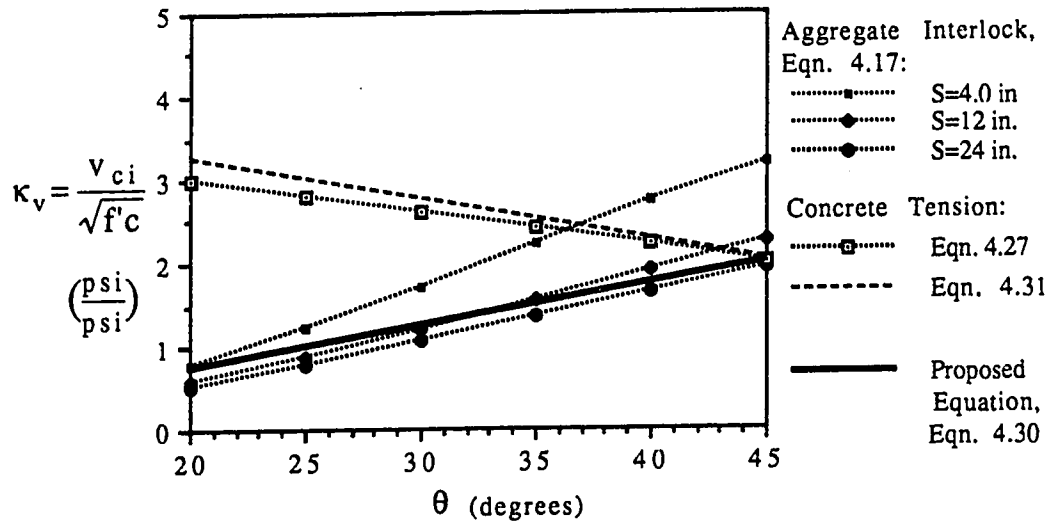


Figure 4.21 Proposed concrete contribution equation.

The proposed concrete contribution can be expressed in the traditional ACI form of

$$V_c = v_{ci} b_w d \quad (4.32)$$

which can be written as  $V_c = \kappa_v \sqrt{f'_c} b_w d \quad (4.32b)$

where  $\kappa_v = 0.05\theta - 0.25, \theta \leq 45^\circ$

In Eqn. 4.32 it is assumed the interface shear acts over the effective depth  $d$ . In many instances the distance between top and bottom chords in a concrete truss model is approximately equal to the effective depth, and this assumption in the concrete contribution expression is not believed to be critical, particularly when the dowel action and the shear carried by the uncracked concrete compression zone have been neglected in the derivation.

Similarly, the effective depth can replace the internal lever arm in the web reinforcement contribution, such that the shear provided by stirrups can be expressed as

$$V_s = \frac{A_v f_y d}{s \tan \theta} \quad (4.33)$$

The total shear capacity of a reinforced concrete beam is obtained by adding  $V_s$  to  $V_c$ .



For prestressed concrete beams, the concrete contribution is given by

$$\text{Crack Interface: } \kappa = (0.05\theta - 0.25) + \kappa_{vp} \quad (4.34)$$

$$\text{where } \kappa_{vp} = (0.06 + 0.01\theta) f_{pc}/\sqrt{f_c} \\ \leq 0.2\theta - 0.9$$

$$\text{Tension Capacity: } \kappa = (4.25 - 0.05\theta) K \quad (4.35)$$

$$\text{where } K = \sqrt{1 + \frac{f_{pc}}{2\sqrt{f_c}}} \\ 1.0 \leq K \leq 2.0$$

The concrete contribution proposed by these equations is shown in Figures 4.22 and 4.23. For small crack inclinations Eqn. 4.34 governs the concrete contribution, and as  $\theta$  approaches 45 degrees Eqn. 4.35 limits the shear strength. In addition, as the compressive stress  $f_{pc}$  increases, the inclination corresponding to the maximum concrete contribution decreases. In order to further simplify these expressions, Eqn. 4.35 can be rearranged in a form similar to the crack interface capacity such that

$$\kappa = \kappa_v + \kappa_{vp} \quad (4.36)$$

By examining the additional concrete contribution due to prestressing as limited by the smaller value determined from Eqns. 4.34 and 4.35, the following values of  $\kappa_{vp}$  are suggested as design expressions:

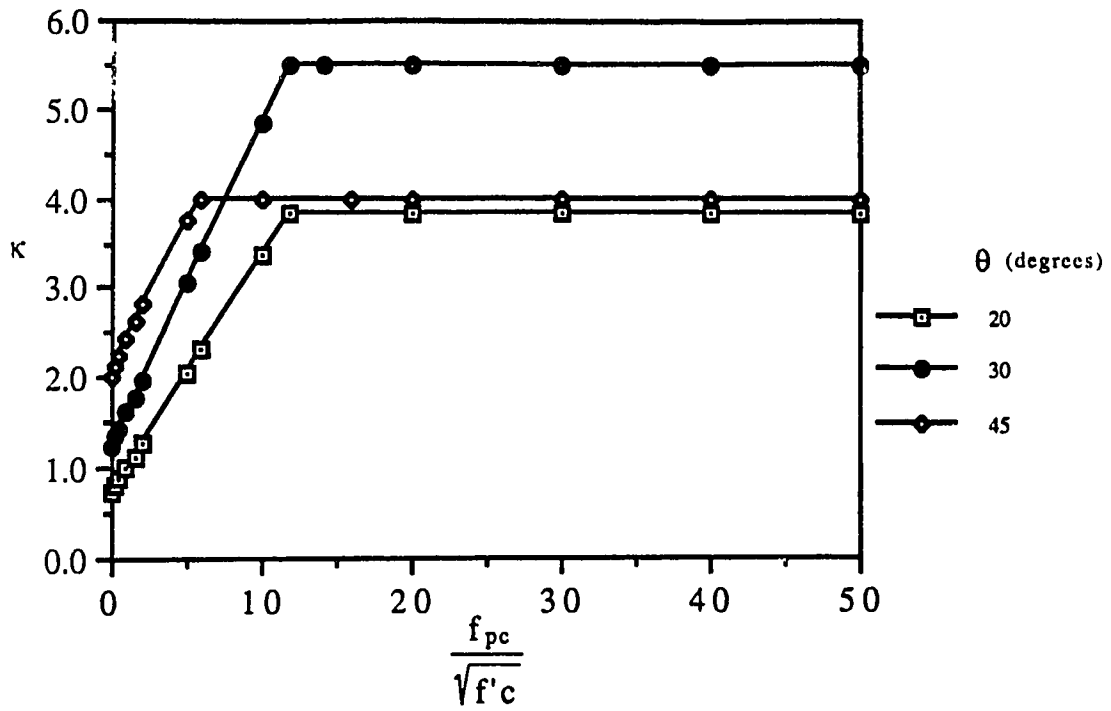


Figure 4.22 Total concrete contribution for prestressed members.

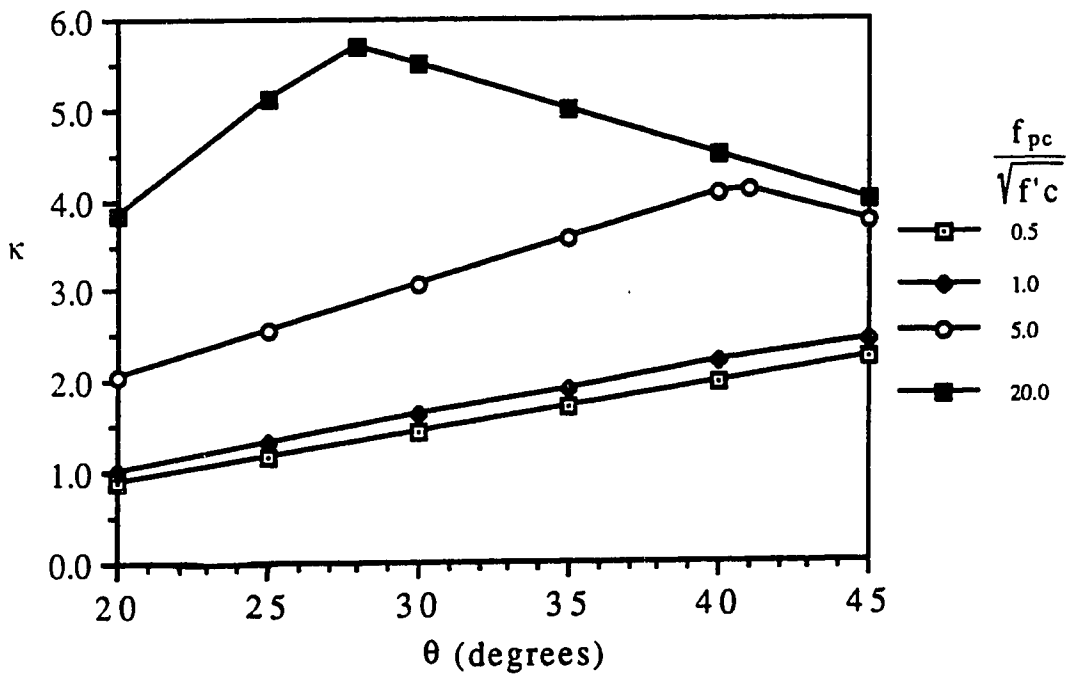


Figure 4.23 Effect of prestress on concrete contribution.

$$\begin{aligned} \kappa_{vp} &= (0.01\theta + 0.06) f_{pc}/\sqrt{f'_c} & (4.37) \\ &\leq 0.2\theta - 1.0 \end{aligned}$$

$$\text{and} \quad \kappa_{vp} \leq 8.75 - 0.15\theta \quad (4.38)$$

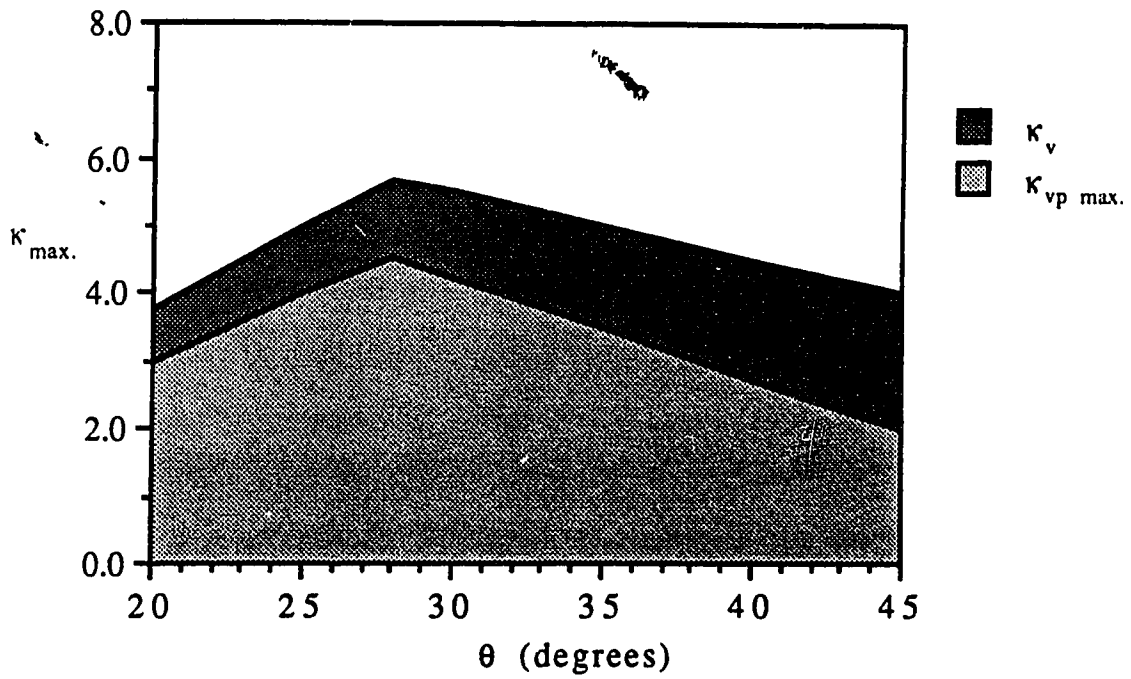
The smaller value of  $\kappa_{vp}$  governs. These expressions provide a maximum concrete contribution of  $\kappa=5.7$  at  $\theta=28^\circ$ , with  $\kappa=3.75$  at  $\theta=20^\circ$  and  $\kappa=4.0$  at  $\theta=45^\circ$ . The concrete contribution obtained from Eqns. 4.37 and 4.38 is shown in Figure 4.24. Values given by the proposed design equations are comparable to those given by Eqn. 2.28 (ACI 11-13). Since the upper limit of Eqn. 2.12 (ACI 11-11) is provided by Eqn. 2.28, the maximum concrete contribution using the  $V_{ci}$  and  $V_{cw}$  expressions is similar to those given by the proposed equations. The maximum value of  $5.7\sqrt{f'_c}$  obtained from the proposed design expressions is larger than the limit of  $5\sqrt{f'_c}$  suggested in the ACI Code Eqn 11-10 (Eqn. 2.29) for beams with an effective prestress equal to at least 40% of the flexural reinforcement tensile strength.

For prestressed concrete beams, the concrete contribution is given by

$$V_c = v_{ci} b_w d + v_{cp} b_w d \quad (4.39)$$

$$\text{which can be written as} \quad V_c = (\kappa_v + \kappa_{vp}) \sqrt{f'_c} b_w d \quad (4.39b)$$

where  $\kappa_v$  is calculated according to Eqn. 4.30, and  $\kappa_{vp}$  is the smaller of Eqns. 4.37 or 4.38. In flexurally cracked regions,  $\kappa_{vp}$  is taken equal to zero such that the concrete contribution is equivalent to a



**Figure 4.24** Maximum concrete contribution from Eqns. 4.37 and 4.38.

nonprestressed concrete beam.

The lower concrete contribution limit of  $1.7\sqrt{f'_c}$  suggested in the ACI Code includes the vertical component of an inclined tendon  $V_p$ . In the proposed method, the lower limit is taken as  $2\sqrt{f'_c}$  at  $45^\circ$  decreasing to  $1.0\sqrt{f'_c}$  at  $25^\circ$ , and the shear carried by an inclined tendon is not considered as part of the concrete contribution. The total shear resistance is given by

$$V = V_s + V_c + V_p \quad (4.40)$$

The following procedure is recommended to account for the concrete contribution to shear in the General Method proposed for the ACI Code Clause 11.4, 1987 draft:

- 1) For nonprestressed members subject to shear and flexure only,

$$V_c = \kappa_v \sqrt{f'_c} b_w d \quad (4.32b)$$

$$\kappa_v = 0.05\theta - 0.25 \quad (4.30)$$

where  $\theta$  is in degrees and shall not exceed 45.

- 2) For the case of shear in prestressed concrete members

$$V_c = (\kappa_v + \kappa_{vp})\sqrt{f'_c} b_w d \quad (4.39b)$$

where  $\kappa_v$  is calculated according to Eqn. 4.30 and  $\kappa_{vp}$  is given by

$$\kappa_{vp} = (0.01\theta + 0.06) \frac{f_{pc}}{\sqrt{f'c}} \quad (4.37)$$

but shall not be taken greater than 0.20 - 1.0 nor 8.75 - 0.15 $\theta$ . In members where the stress in the extreme tension fiber due to the ultimate load and the applied effective prestress force exceeds  $6\sqrt{f'c}$ ,  $\kappa_{vp}$  shall be taken equal to zero.

In determining the minimum permissible angle  $\theta$  to avoid diagonal crushing, the ACI 1987 draft suggests

$$\theta > 15^\circ + (75,000 + f_{sl}) \frac{v_n}{1000 f'c} \quad (4.41)$$

where  $v_n$  is the nominal shear stress and  $f_{sl}$  is the stress in the longitudinal reinforcement in psi. The ACI draft indicates the reinforcement stress  $f_{sl}$  may be taken as the yield strength,  $f_y$ , of the longitudinal bars for reinforced concrete beams, or as  $(f_{ps} - f_{se})$  for members in which the longitudinal reinforcement consists of only prestressing tendons, where  $f_{ps}$  is the stress in the prestressed reinforcement at nominal strength and  $f_{se}$  is the effective stress in the prestressing tendons after losses. For members with tensile reinforcement consisting of a combination of reinforcing bars and prestressing tendons, the ACI draft suggests  $f_{sl}$  be taken as the larger of  $f_y$  or  $(f_{ps} - f_{se})$ . As will be shown in Chapter 5, a suitable

simplification to the proposed ACI procedure in determining a lower limit on  $\theta$  for prestressed concrete beams is to assume  $f_{ps}$  equals the tensile stress of the prestressed reinforcement  $f_{py}$ .

#### 4.6 Special Considerations

The concrete contribution expressions developed in the previous sections are based on a variable angle truss model with a continuous field of diagonal compression. Although several simplifying assumptions were required to develop the final design equations, the derivation is based on a rational model in which the internal forces and failure mechanisms are easily visualized. It is inherent in the development of the concrete contribution equations that premature failures due to poor detailing or crushing of the concrete web are avoided. These failure modes can be avoided by incorporating adequate code provisions. Although the design expressions were developed and generalized to suit a basic design procedure, for simplicity several factors which may influence the actual concrete contribution were not considered. Aggregate interlock is a major component of the concrete contribution model. Vibrations, load reversals, moving loads and sustained loads may effect the aggregate interlock mechanism. In addition, water rise during concrete placement in deeper beams may weaken the upper portion of concrete, reducing the effectiveness of aggregate interlock in this zone. Fatigue, creep, and temperature effects may also influence the shear behavior as predicted by the proposed design equations.

In order to rationally consider the factors influencing shear strength, it is important a design model provide clear concise concepts of shear failure. Therefore, although it is desirable to have design equations accurately verified by test results, it is also important they provide rational models of shear failure. Test specimens are normally statically determinate, and are usually monotonically loaded up to failure by concentrated loads. In contrast, actual structures will generally not be limited to the same conditions, and the accuracy of a shear design equation to practical structures is unclear. The existing ACI shear design method has generally been substantiated by test specimens, but it is not based on a clear conceptual design model. The proposed design equations developed in Chapter 4 have been derived from a rational shear design model in which the shear failure mechanisms are easily visualized. As a result, the proposed procedure is better suited to examine the factors affecting shear strength in actual structures. Predictions of shear strength using the proposed equations will be examined with actual test results in the following Chapter.

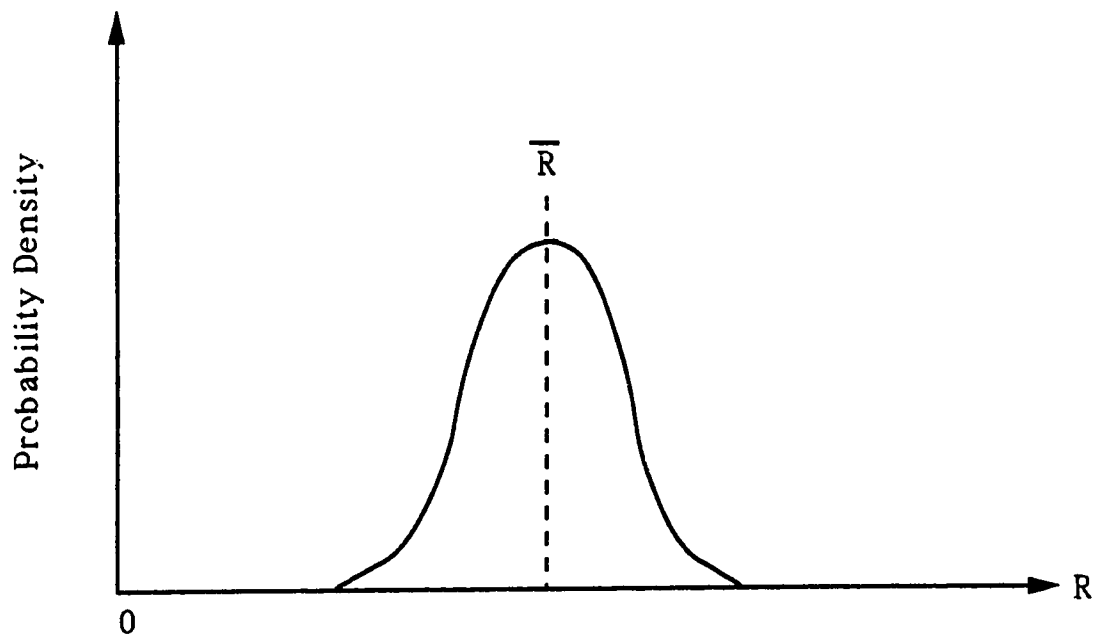


## **5. COMPARISON OF PREDICTIONS WITH EXPERIMENTAL RESULTS REPORTED IN LITERATURE**

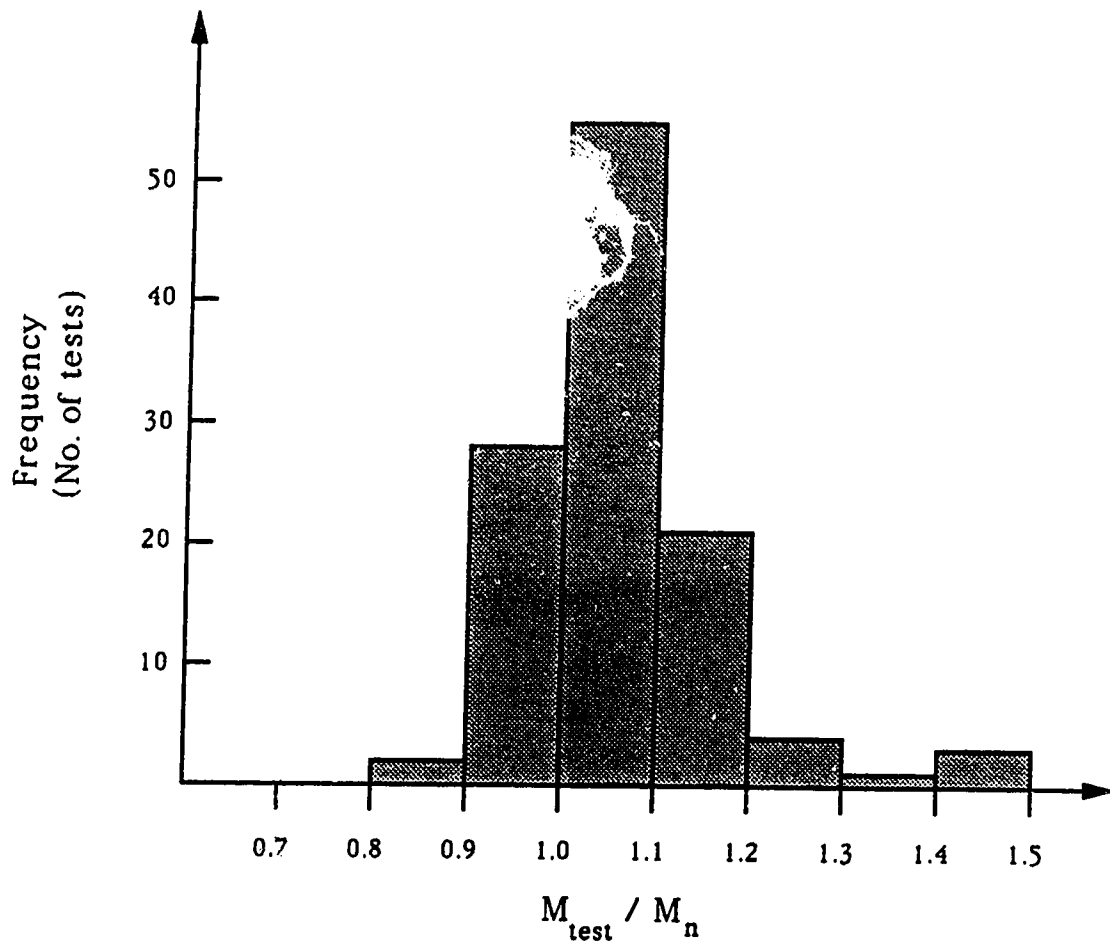
### **5.1 General**

When a beam fails in shear, the internal forces equilibrating the applied loads have reached their shear capacity or shear resistance. A theoretically derived shear capacity will not exactly predict the actual failure load of a test specimen. This variability is due in part to simplifying assumptions, uncertainty and randomness of material properties, workmanship, construction methods, and deviations between actual and specified dimensions. The actual resistance of a beam, whether it is the shear, moment or axial load resistance, can be schematically represented by a probability distribution curve as shown in Figure 5.1.

From an economic and safety standpoint, it is preferable to have a small dispersion or standard deviation of the actual resistance and the ratio of the predicted to actual resistances. Since the actual resistance of a particular type of member is variable, a beam with below average strength may have a lower capacity than predicted by theory. Consequently, when comparing a design equation to test results, the actual strength of some beams may be lower than the calculated nominal strength. This concept is illustrated in Figure 5.2 where the flexural capacity of 112 beams is compared to the nominal flexural capacity using the assumption of a rectangular stress block. It is apparent that the actual flexural strength of some beams is



**Figure 5.1** Frequency distribution of resistance  $R$ .



**Figure 5.2** Comparison of measured and predicted failure moments of 112 reinforced concrete beams (adapted from Ref. 13).

overestimated by the design expression. Similarly, the shear strength calculated from the proposed design equations may overestimate the actual failure shears for some test beams. Resistance factors and the traditional factors of safety attempt to consider the variability of the resistance of a member.

In order to verify the proposed expressions for the concrete contribution, predictions of shear strength will be compared to test results reported in literature for both reinforced and prestressed concrete beams. Slender beams with a shear span to depth ratio  $a/d > 2.5$  will be examined. In order to select suitable test results, several conditions assumed in the development of the proposed equations must be satisfied. Since the variable angle truss model inherently assumes web reinforcement has yielded, test results should indicate that yielding of the transverse reinforcement occurred at or before failure. In addition, no premature web crushing, loss of bond or other indications of untimely failure should be evident in the test specimens.

As noted by Ramirez and Breen<sup>26</sup>, the majority of shear failure tests undertaken in North America have been performed on beams containing no or very small amounts of web reinforcement. Researchers generally design shear tests to avoid bending failures, and consequently unrealistically low amounts of shear reinforcement or unrealistically high amounts of flexural reinforcement are frequently used. Since beams without stirrups cannot be modelled as a variable angle truss with vertical web reinforcement acting as

tension ties, test results on such beams cannot be utilized. This considerably reduces the number of suitable shear test specimens reported in the literature.



















## **5.2 Reinforced Concrete**

### **5.2.1 Selection of Test Beams**

Ramirez<sup>29</sup> summarizes shear test results of several investigators where slender reinforced concrete beams with vertical stirrups were tested and yielding of the stirrups was reported at or before failure. The majority of the members examined were simply supported rectangular beams or T-beams, subjected to a symmetrical single or two point load. A few beams had shear span to depth ratios less than 2.5, and these specimens are not included in this investigation. In addition to the test beams considered by Ramirez, several other tests series available in the literature are examined to verify the proposed concrete contribution expressions, including a few beams subjected to negative bending and to continuous loading. A general summary of the test information is provided in Tables 5.1 and 5.2. Stirrup spacings in the test beams varied from 2.0 to 11.8 inches (50 to 300 mm), and concrete strengths ranged from 1060 to 12000 psi (7.3 to 83 MPa).

### **5.2.2 Comparison to A.C.I. Code Procedure**

The test results of 106 reinforced concrete beams are compared to the failure shears predicted by the existing ACI method with  $\phi=1.0$  using Eqns. 2.16 and 2.21. The results are shown schematically in













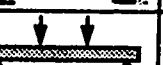


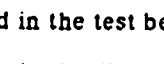

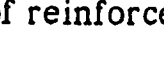
TEST SERIES	$f'_c$ (ksi)	s (in)	a/d	SECTION
Anderson & Ramirez <sup>31</sup>	4.23 - 4.69	3.5 - 7.0	2.65	
Johnson & Ramirez <sup>32</sup>	5.28 - 10.49	5.25 - 10.5	3.1	
Elzanaty, Nilson & Slate <sup>33</sup>	3.00 - 9.10	7.5	4.0	
Bresler & Scordelis <sup>34</sup>	3.36 - 4.29	7.5 - 8.25	3.9 - 4.9	
Mattock et al (N-0) <sup>35</sup>	1.98 - 6.52	4.0 - 7.5	2.5 - 6.0	
Mphonde & Frantz <sup>36</sup>	3.20 - 12.0	3.5	3.6	
Cerruti & Marti <sup>20</sup>	6.48	4.1	Uniform load	
Hsiung & Frantz <sup>37</sup>	6.00 - 6.54	4.2 - 4.5	3.0	
Taylor <sup>38</sup>	3.00 - 3.14*	3.5 - 4.5	3.6 - 4.5	
Sorensen <sup>39</sup>	4.51 - 4.97	5.9 - 8.3	3.5	
Rodriguez et al <sup>40</sup>	2.72 - 3.59**	6.0 - 10.0	2.8 - 4.1	
Bach, Nielsen & Braestrup <sup>41</sup>	1.06 - 5.28	3.5 - 8.27	3.0	
Debaiky et al ( $\alpha = 0$ ) <sup>42</sup>	2.93 - 4.56	3.94 - 7.87	3.5	
Clark <sup>43</sup>	3.20 - 4.28	6.0 - 10.0	2.4	
Olesen, Sozen & Seiss (Fps-0) <sup>44</sup>	6.15 - 6.88***	2.0 - 3.5	2.8 - 4.2	
Lyngberg (Fps-0) <sup>45</sup>	3.73 - 3.86	6.18	2.8	
Rodrigues & Darwin <sup>46</sup>	4.01 - 5.38	7.0	3.9 - 4.0	
Mailhot <sup>19</sup>	5.67	4.72 - 11.8	Uniform Load	

\*  $f'_c$  taken as  $0.8 \times f'_{\text{cube}}$

\*\* Concrete strength from batch in middle third of beam

\*\*\* Average of two batches used in each beam

Table 5.1 Summary of reinforced concrete test beam properties.

TEST SERIES	TYPE	COMMENTS
Anderson & Ramirez		Cracks indicating possible anchorage failure are evident
Johnson & Ramirez		Roller supports used may have provided some restraint against lateral movement of test beams
Elzanaty, Nilson & Slate		—————
Bresler & Scordelis		Yielding of stirrups inferred from vertical displacement measurements.
Mattock et al (N-0) *		Stub axle supports at centroid of test specimens
Mphonde & Frantz		—————
Cerruti & Marti		$V_{test}$ calculated at edge of support plate
Hsiung & Frantz		—————
Taylor		—————
Sorensen		—————
Rodriguez et al **		—————
Bach, Nielsen & Braestrup		Longitudinal steel yield strength taken as ultimate tensile strength. Generally two wires used per leg of stirrup
Debaiky et al ( $\alpha = 0$ )		Haunched beams not considered.
Clark		Steel plate supports may restrain lateral beam movement
Olesen, Sozen & Seiss (Fps-0)		Yielding of stirrups inferred from measurements of crack openings.
Lynberg (Fps-0)		—————
Rodrigues & Darwin		Lightly reinforced T-beams in negative bending
Mailhot		$V_{test}$ taken at support face. Evidence of a flexural failure after yielding of stirrups adjacent to support.

\* One restrained beam also included in the test beams examined.

\*\* One continuous beam with third point loading also included in the test series.

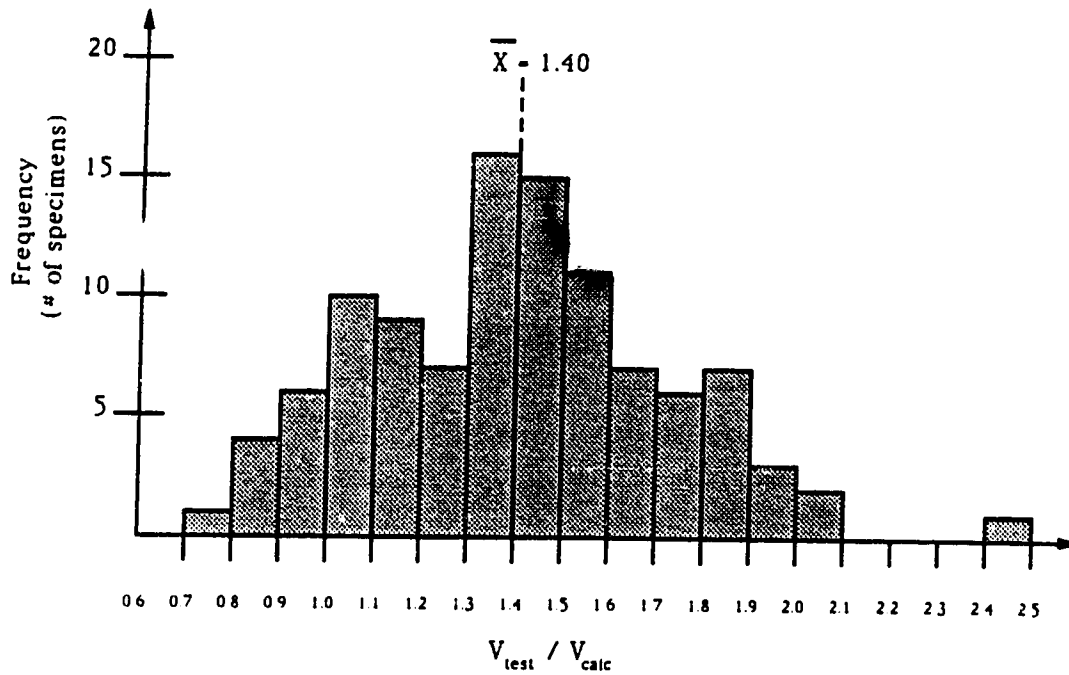
Table 5.2 Details of reinforced concrete test beams.

Figure 5.3a. For the beams examined, the ACI shear design procedure safely estimates the failure shear of all but eleven beams. The mean  $V_{test}/V_{calc}$  ratio is 1.40 with a standard deviation of 0.32 (coefficient of variation of 0.23). The  $V_{test}/V_{calc}$  ratio ranges from 0.76 to 2.43. This relatively large spread of predicted capacities is expected because, as shown in Figure 2.16, Eqn. 2.21 is a lower bound to the concrete contribution with a relatively large scatter of test results. Three of the test beams have  $V_{test}/V_{calc}$  ratios less than 0.85, which suggests the strength of these beams is overestimated when a strength reduction factor of  $\phi=0.85$  is applied to the calculated shear capacities. The lowest  $V_{test}/V_{calc}$  ratio of 0.76 is obtained from a lightly reinforced T-beam in negative bending tested by Rodrigues and Darwin<sup>46</sup> (Beam E-80,  $\rho_v f_{yv}=73.5$  psi,  $\rho_w=0.48\%$ ). As shown in Figure 2.16, for low values of  $\rho_w$  the shear capacity is less than predicted by the ACI Code. Detailed results for each of the 106 beams examined are provided in Appendix A.

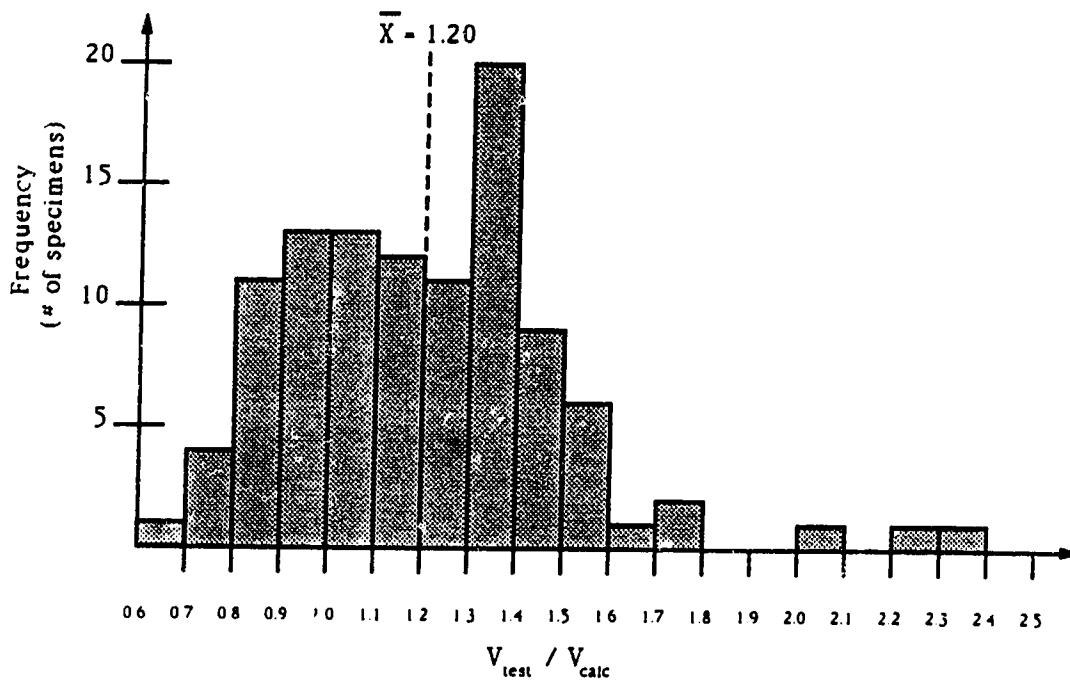
### 5.2.3 Comparison to General Concrete Contribution Expressions

The failure load of the reinforced concrete test beams can also be predicted using the general concrete contribution expressions given by Eqns. 4.17 and 4.27. For each beam, several possible angles of inclination of the diagonal compressive stresses can be chosen. A designer is free to choose the angle of inclination  $\theta$  provided the concrete web does not crush in compression and yielding of the stirrups is ensured. These requirements can be satisfied by placing





a) ACI shear design procedure



b) Proposed general concrete contribution equations

**Figure 5.3** Comparison of measured and computed failure shears for 106 reinforced concrete beams.

lower and upper limits on  $\theta$ . From the derivation of the proposed concrete contribution equations, limiting  $\theta$  to less than or equal to  $45^\circ$  is sufficient to ensure the stirrups yield. Consistent with the 1987 draft of Chapter 11 in the ACI Code, the following lower limit was imposed:

To avoid diagonal crushing,

$$\theta > 15^\circ + (75,000 + f_{sl}) \frac{v_n}{1000 f'_c} \quad (4.41)$$

where  $v_n$  is the nominal shear stress, and  $f_{sl}$  is the stress in the longitudinal reinforcement, which may be taken as the yield strength,  $f_y$ , all in psi. The lower limit on  $\theta$  was also checked in a more rigorous manner in which the diagonal compressive stress  $f_2$  is computed from Mohr's stress circle as

$$f_2 = v_n \left( \tan\theta + \frac{1}{\tan\theta} \right) - f_1 \quad (5.1)$$

or

$$f_2 = v_n \left( \tan\theta + \frac{1}{\tan\theta} \right) - v_{ci} \tan\theta \quad (5.2)$$

and compared to the allowable compressive stresses in an inclined strut given by the ACI draft as

$$f_{cu} = \frac{f'_c (\theta_{st} - 10)}{(50 + f_y/2,000)} \quad (5.3)$$

but  $\leq 0.85 f'_c$

where  $\theta_{st}$  is the angle between the steel tension member and the compressive strut, in degrees. In Eqn. 5.3, both the transverse and longitudinal reinforcement are considered as tension ties and must be checked separately to determine the lower limiting value.

For each particular test specimen,  $\theta$  was varied between  $15^\circ$  and  $45^\circ$  in one degree increments, and the allowable lower limit was determined in each case. The lower limit on  $\theta$  given by Eqn. 4.41 provides very good agreement with the value obtained by checking the compressive stress  $f_2$  in the inclined strut. For design applications, the choice of a small  $\theta$  decreases the allowable concrete contribution but increases the number of stirrups crossed by an inclined crack. Consequently, for each particular test specimen, an optimum capacity providing the largest shear resistance for the given member is obtained. The stirrup capacity is calculated from

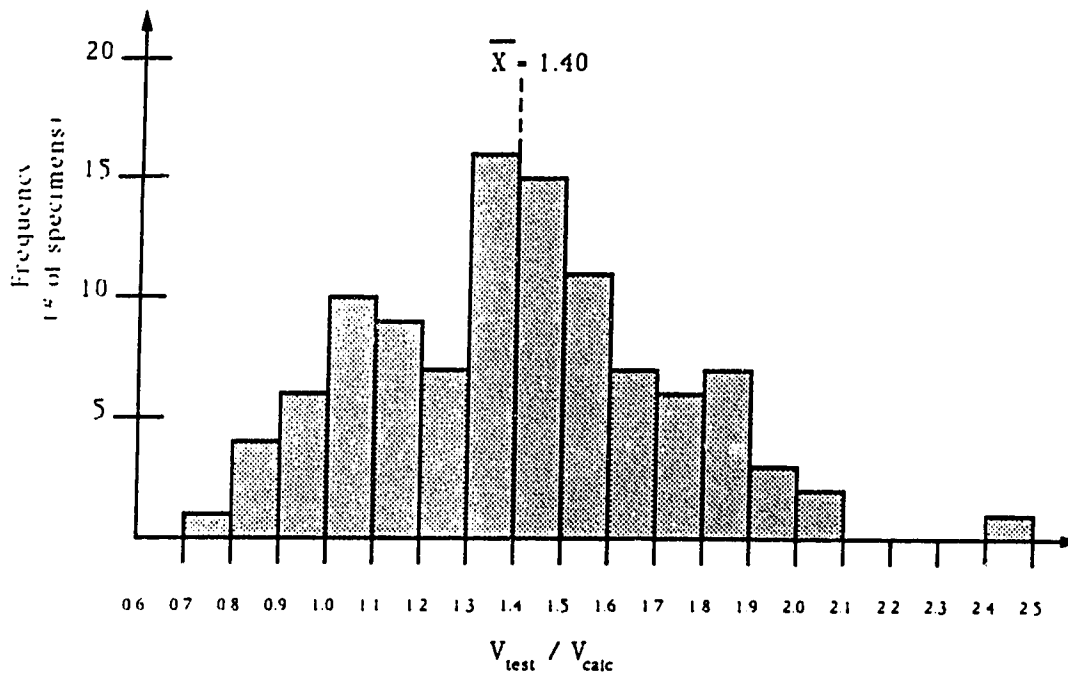
$$V_s = \frac{A_v f_y d}{s \tan \theta} \quad (4.33)$$

Using this web reinforcement contribution and the general concrete contribution expressions derived in Chapter 4, the mean  $V_{test}/V_{calc}$  ratio for the 106 beams considered is 1.20 with a standard deviation of 0.29 (coefficient of variation of 0.24). The results are shown schematically in Figure 5.3b. Twenty-nine beams have a  $V_{test}/V_{calc}$  ratio less than 1.0 with the lowest ratio equal to 0.68, as compared to only eleven beams below 1.0 in the ACI shear

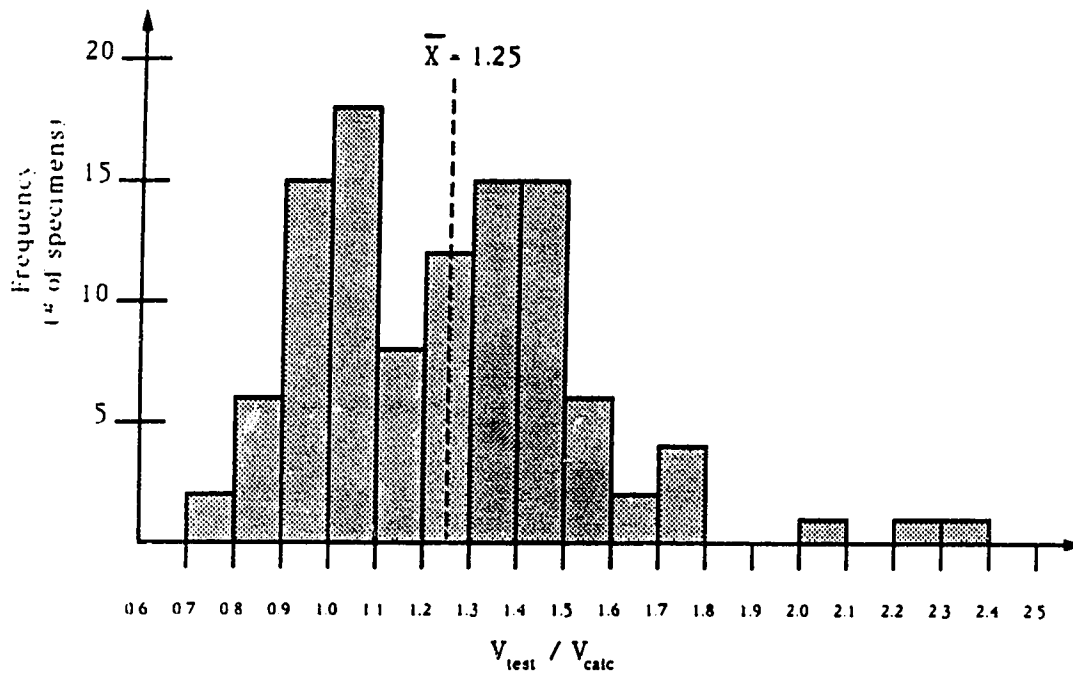
design method with the lowest ratio of 0.76. Using the general concrete contribution expressions, seven beams have a  $V_{\text{test}}/V_{\text{calc}}$  ratio less than 0.85 as compared to three beams when using the ACI procedure. The low value of 0.68 is obtained from the lightly reinforced T-beam tested by Rodrigues and Darwin<sup>46</sup> (Beam E-80), which is also the most unconservative prediction obtained from the ACI Code procedure. The two beams with  $V_{\text{test}}/V_{\text{calc}}$  ratios equal to 2.09 and 2.31 shown in Figure 5.3 are T-beams tested by Nielsen et al<sup>41</sup> with concrete strengths of 1400 psi and 1360 psi respectively. Due to the low concrete strengths, a strut inclination  $\theta$  chosen to be less than  $45^\circ$  but large enough to prevent web crushing according to Eqn. 4.41 could not be obtained. In order to calculate a shear capacity such that the web concrete does not crush prior to yielding of the stirrups, the web reinforcement area was incrementally reduced until a solution was obtained at  $\theta=45^\circ$ . As shown in Figure 5.3 and indicated by the coefficient of variation, the dispersion of predictions for all the test beams is about the same as in the ACI procedure, but predicted capacities are closer to the actual failure shears.

#### 5.2.4 Comparison to Proposed Design Equations

Using the proposed concrete contribution design equations given in Section 4.5 and the stirrup capacity from Eqn. 4.33, the mean  $V_{\text{test}}/V_{\text{calc}}$  ratio for all 106 beams is 1.25 with a standard deviation of 0.29 (coefficient of variation of 0.23), and extreme values of 0.74 and 2.31. Results of the proposed design equations are shown in Figure 5.4. Twenty three beams fall below a  $V_{\text{test}}/V_{\text{calc}}$  ratio of 1.0



a) ACI shear design procedure



b) Proposed design equations

Figure 5.4 Comparison of measured and computed failure shears for 106 reinforced concrete beams.

and three beams fall below 0.85. A summary of results using all three shear design procedures is shown in Table 5.3. The proposed design equations provide similar results to the more general concrete contribution expressions, and have a mean test to predicted ratio closer to 1.0 than the ACI method. The sample standard deviation of the proposed design equations is a little less than the ACI procedure. Both shear design methods have a coefficient of variation of 0.23.

If the web reinforcement contribution is calculated according to the ACI draft expression given by Eqn. 4.29 which is similar to Eqn. 4.33 with  $d$  replaced by  $0.9d$ , the mean  $V_{\text{test}}/V_{\text{calc}}$  ratio is 1.31 with a standard deviation of 0.30 (coefficient of variation equal to 0.23), and a low test to predicted ratio of 0.78. Consequently, replacing the effective depth by an approximate lever arm of  $0.9d$  in the stirrup contribution slightly decreases the predicted strengths toward conservative values, but the change is not substantial.

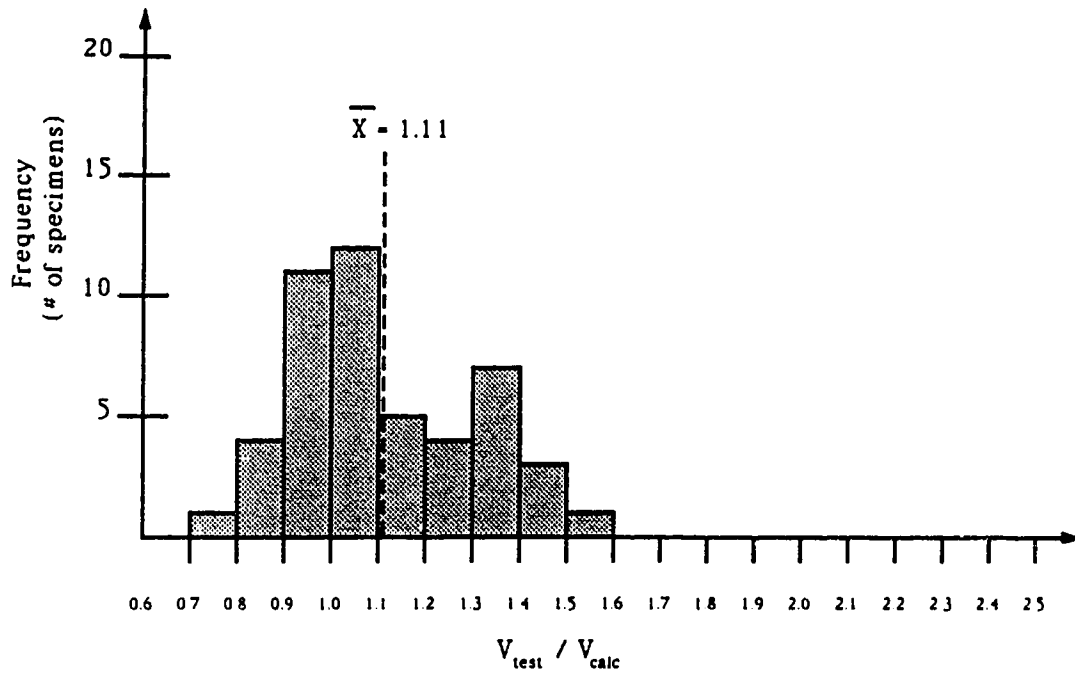
### 5.2.5 Influence of Cross-Section on Shear Strength

As shown in Figure 5.4b there appears to be two peaks in the frequency distribution curve, one at a  $V_{\text{test}}/V_{\text{calc}}$  ratio of about 1.0 and the other at ratio of approximately 1.4. Although there are many factors that can influence shear strength, the presence of two peaks in the proposed design equations may be attributed to the difference between predictions for rectangular beams as compared to T or I-beams. As shown in Figure 5.5, the 58 T-beams examined have a mean  $V_{\text{test}}/V_{\text{calc}}$  ratio of 1.36 while the 48 rectangular beams

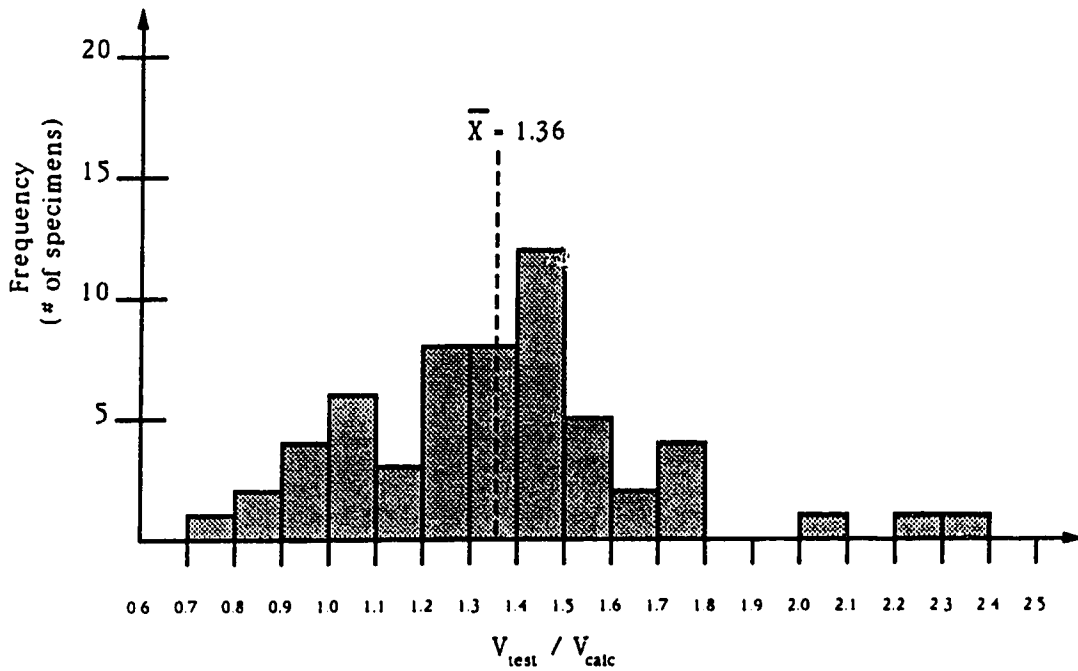
TEST SERIES	# TESTS	ACI METHOD		GENERAL EXPRESSIONS		PROPOSED DESIGN EQNS.	
		$\bar{X}$	S	$\bar{X}$	S	$\bar{X}$	S
Anderson & Ramirez	3	1.17	0.095	0.90	0.073	0.94	0.069
Johnson & Ramirez	4	1.08	0.075	0.99	0.047	1.03	0.064
Elzanaty, Nilson & Slate	3	1.32	0.212	1.12	0.216	1.10	0.191
Bresler & Scordelis	6	1.50	0.077	1.34	0.081	1.37	0.120
Mattock et al (N=0)	15	1.70	0.188	1.37	0.132	1.38	0.123
Mphonde & Frantz	8	1.39	0.137	1.11	0.109	1.27	0.154
Cerruti & Marti	1	1.75	—	1.36	—	1.40	—
Hsiung & Frantz	4	1.01	0.073	0.83	0.054	0.86	0.056
Taylor	2	1.40	0.002	1.03	0.008	1.09	0.008
Sorensen	3	1.75	0.184	1.32	0.125	1.33	0.130
Rodriguez et al	5	1.27	0.035	0.99	0.031	0.99	0.034
Bach, Nielsen & Braestrup	17	1.44	0.443	1.57	0.348	1.59	0.346
Debaiky et al (a=0)	6	1.40	0.135	1.16	0.159	1.17	0.148
Clark	9	1.36	0.159	1.02	0.126	1.03	0.116
Olesen Sozen & Seiss (Fps=0)	8	1.31	0.327	1.08	0.228	1.22	0.320
Lyngerberg (Fps=0)	2	1.53	0.033	1.51	0.002	1.52	0.008
Rodrigues & Darwin	7	0.93	0.111	0.84	0.099	0.92	0.110
Mailhot	3	1.73	0.268	1.37	0.005	1.41	0.023
TOTAL	106	1.40	0.315	1.20	0.293	1.25	0.290

$\bar{X}$  - mean  $V_{test} / V_{calc}$   
 S - sample standard deviation

Table 5.3 Summary of predicted shear capacity results for the reinforced concrete beams examined.



a) Rectangular beams



b) T or I-beams

Figure 5.5 Influence of beam cross-sectional shape on predicted shear capacity, reinforced concrete beams.



have a mean ratio of 1.11. Using the ACI method, the T-beams have a mean test to predicted shear strength ratio of 1.47 and the rectangular beams have a ratio of 1.31. The difference in predicted behavior between the two types of members suggests T-beams may be better capable of redistributing internal forces after stirrups yield and may have more reserve strength as compared to rectangular beams. In beam tests, I-beams typically fail by web crushing, whereas rectangular beams usually fail in diagonal tension or shear compression. T-beams also fail in these two later failure modes, but the presence of large flanges generally tends to provide better support reactions for the inclined compression struts. The presence of flanges may reduce the likelihood of the concrete cover on the beam web from spalling. It appears from the test specimens examined that after yielding of the stirrups, the shear strength predictions of the ACI Code and the proposed design equations are more conservative for T or I-beams than rectangular beams.

#### **5.2.6 Influence of Reinforcement on Shear Strength**

In order to examine the effect of both longitudinal and transverse reinforcement on the shear capacity predicted by the proposed equations, several different parameters were investigated. Many different types of stirrups were used in the various test series examined. In each case, anchorage was sufficient to ensure yielding of the stirrups at or before failure. Provided stirrups are properly detailed to provide the required anchorage, the effect of stirrup configuration or differences between detailing will not be considered.

Table 5.4 indicates the difference in predicted shear capacities between test beams with deformed stirrups and smooth stirrups for both the ACI method and the proposed design equations. Although more test results are required to substantiate any difference between the two types of stirrups, in both shear design methods beams with smooth stirrups had a lower  $V_{\text{test}}/V_{\text{calc}}$  ratio than beams with deformed stirrups.

The influence of the web reinforcement ratio  $\rho_v (=A_v/b_w s)$  and  $\rho_v f_{yv}$  is shown in Figure 5.6. The majority of the test beams with a  $V_{\text{test}}/V_{\text{calc}}$  ratio less than 1.0 are lightly reinforced with  $\rho_v f_{yv}$  less than about 100 psi. From Eqn. 2.18 (ACI Eqn. 11-14) the minimum value suggested in the ACI Code is 50 psi. As shown in Figure 5.6, as the amount of web reinforcement decreases, the proposed design equations generally tend to overestimate the shear capacity. As previously noted, for beams without web reinforcement the variable angle truss model is not a suitable design procedure since no reinforcement is available to act as vertical tension ties. Consequently, as the amount of web reinforcement decreases, the shear strength predictions based on the truss model become less conservative.

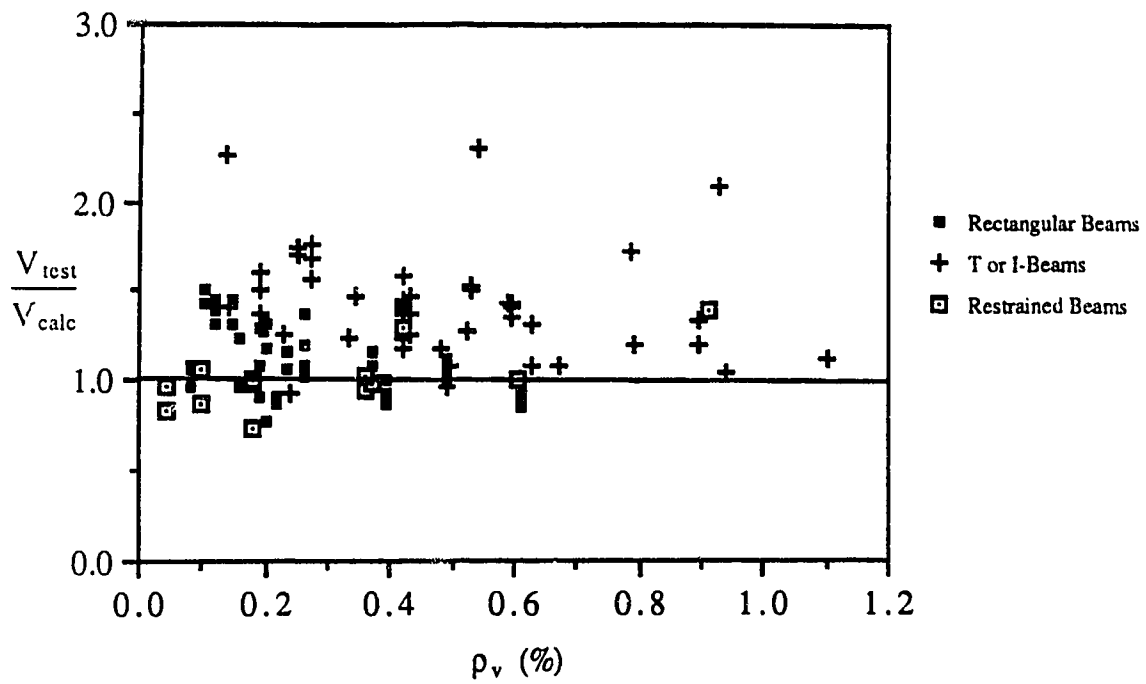
The effect of stirrup spacing on the shear strength predicted by the proposed design equations is shown in Figure 5.7a as a function of the maximum spacing of  $d/2$  suggested in the ACI Code. Although several test beams had stirrup spacings exceeding this limit, generally safe estimates of shear strength were obtained for these

BEAM DESCRIPTION	# TESTS	ACI METHOD	PROPOSED EQNS.
		$\bar{X}$	$\bar{X}$
T or I-Beams	58 <sup>a</sup>	1.47	1.36
- deformed stirrups	3	1.60	1.48
- smooth stirrups	35	1.34	1.35
Rectangular Beams	48 <sup>b</sup>	1.31	1.11
- deformed stirrups	24	1.33	1.11
- smooth stirrups	7	1.14	0.96

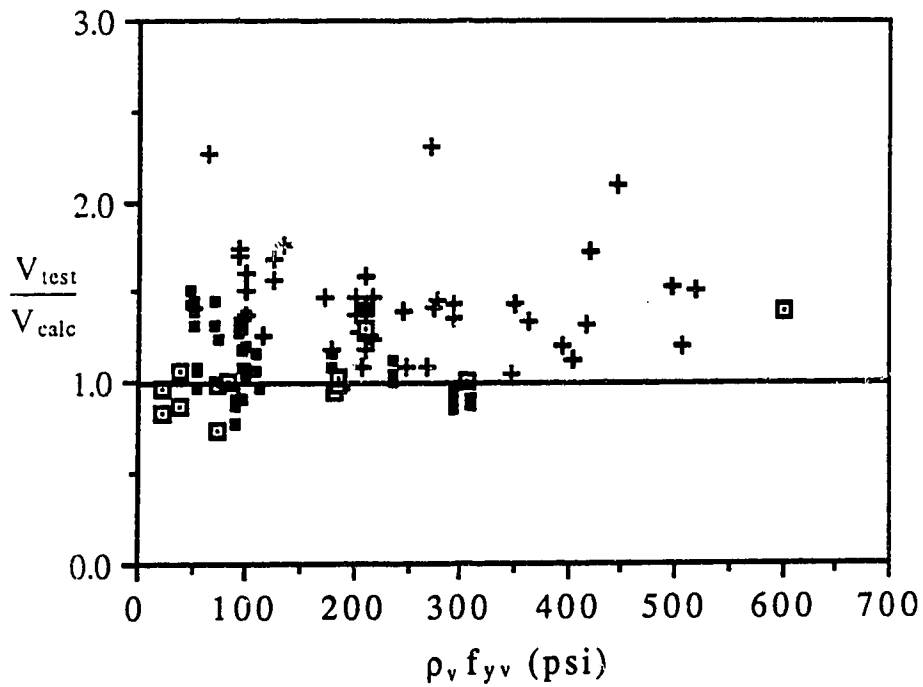
$\bar{X}$  = mean  $V_{test} / V_{calc}$

- a) Type of stirrup not reported for 20 T or I-beams.  
b) Type of stirrup not reported for 17 rectangular beams.

Table 5.4 Summary of predicted shear capacity results for reinforced concrete beams.

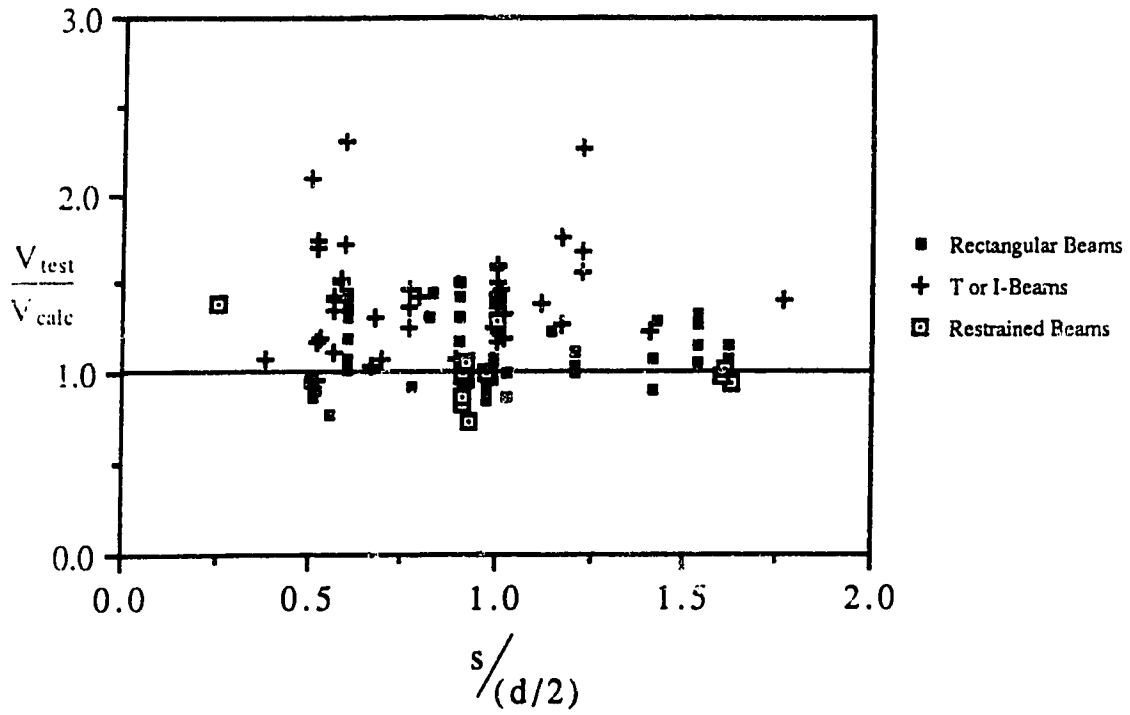


a) Effect of web reinforcement ratio

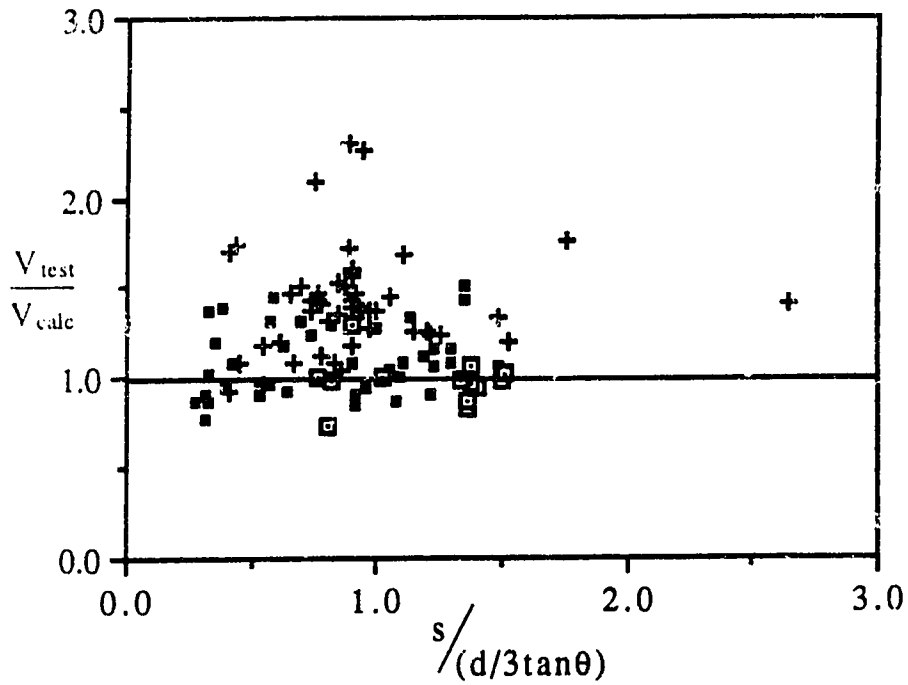


b) Effect of web reinforcement

**Figure 5.6** Influence of shear reinforcement on proposed design equations, reinforced concrete beams.



a) Effect of stirrup spacing



b) Effect of stirrup spacing

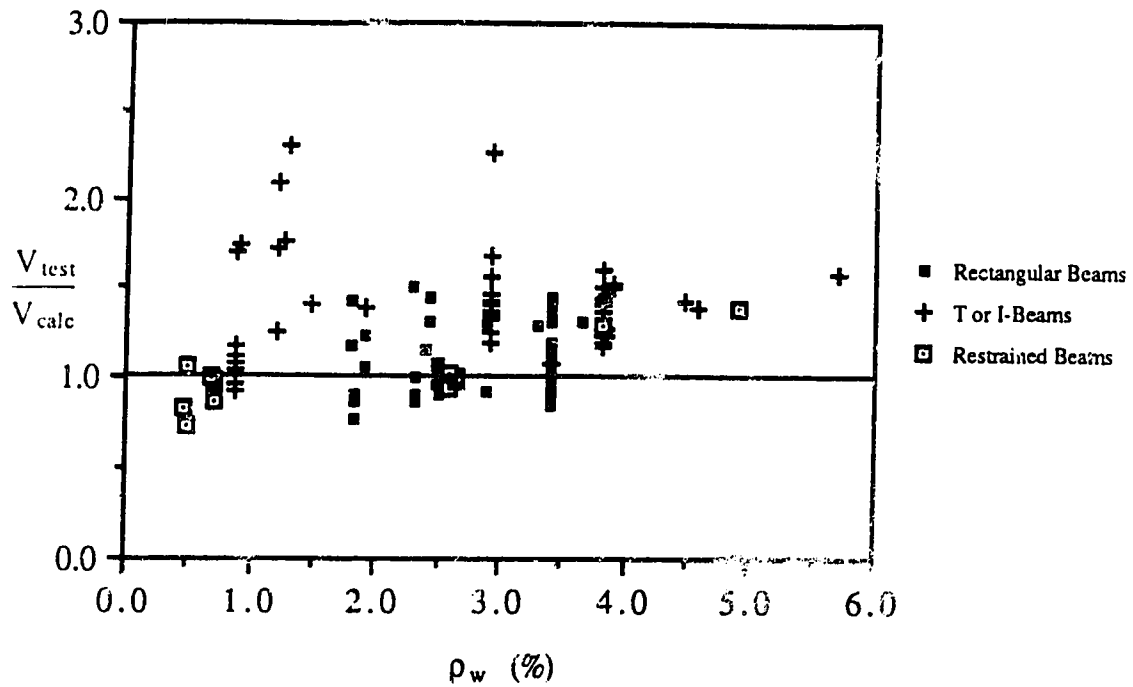
**Figure 5.7** Influence of stirrup spacing on proposed design equations, reinforced concrete beams.

beams. For a variable angle truss model, the Canadian Code suggests the spacing of transverse reinforcement be limited to the smaller of  $d_v/3\tan\theta$ ,  $d_v$  or 600 mm (24 in.). In order to maintain maximum spacing requirements in the traditional ACI format, it is suggested the internal lever arm  $a$  be replaced by the effective depth  $d$ . As shown in Figure 5.7b, several beams that exceed a suggested maximum stirrup spacing of  $d/3\tan\theta$  have unconservative predictions of shear strength using the proposed design equations.

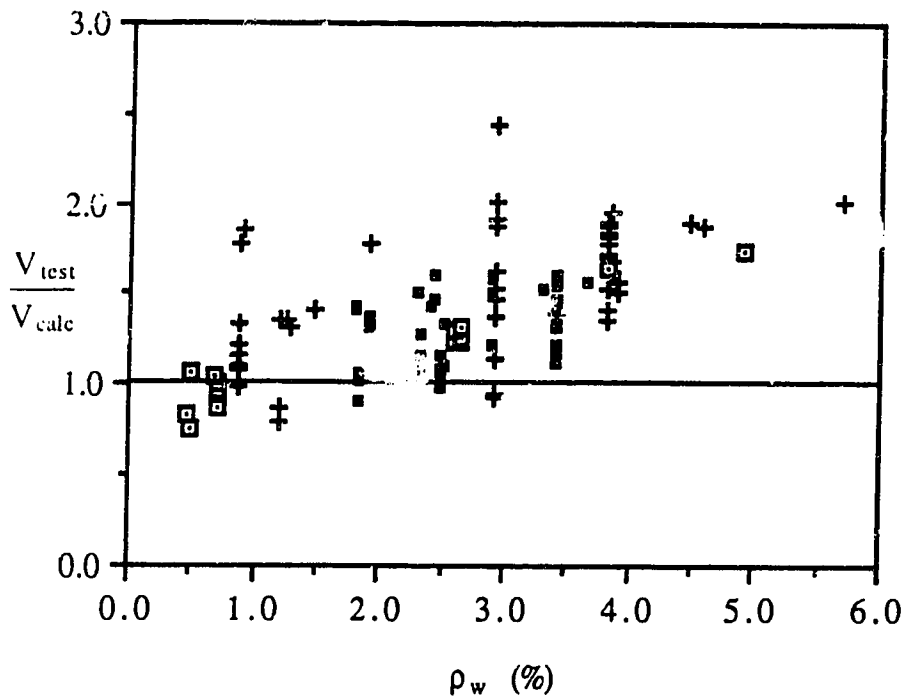
Shear resistance due to dowel action is dependent, among other things, on the amount of longitudinal reinforcement in a beam. Figure 5.8 indicates the influence of the longitudinal reinforcement ratio  $\rho_w$  ( $=A_s/b_w d$ ) on the shear strength predictions for both the proposed method and the ACI shear design procedure. As the amount of longitudinal reinforcement increases, the  $V_{test}/V_{calc}$  ratio increases for both methods. As shown in Figure 2.16, The ACI expression is known to underestimate the shear capacity for beams with large reinforcement ratios. Since the effect of dowel action is neglected in the truss model, it is expected that for increasing amounts of longitudinal reinforcement the shear strength calculated from the proposed design equations will be underestimated. A similar trend is shown in Figure 5.9, which indicates the influence of  $\rho_w f_y$  on predicted shear strength.

### 5.2.7 Other Factors Influencing Predicted Shear Strength

High strength concretes tend to have smooth crack surfaces as

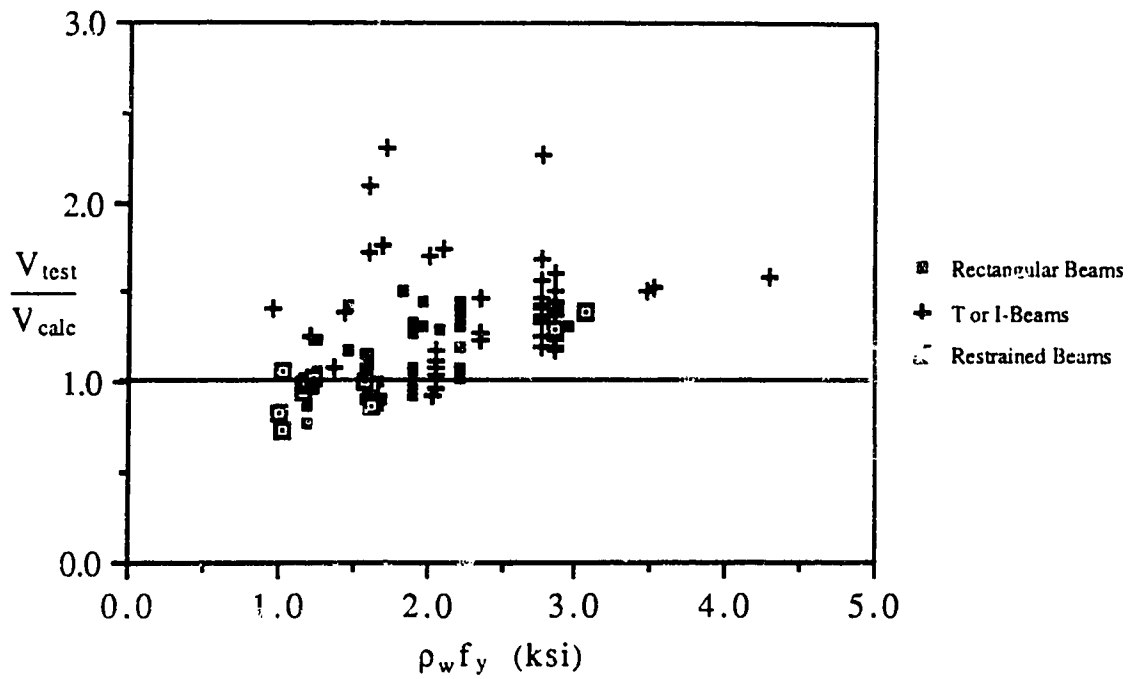


a) Proposed design procedure



b) ACI shear design procedure

**Figure 5.8** Influence of longitudinal reinforcement on predictions of shear strength, reinforced concrete beams.



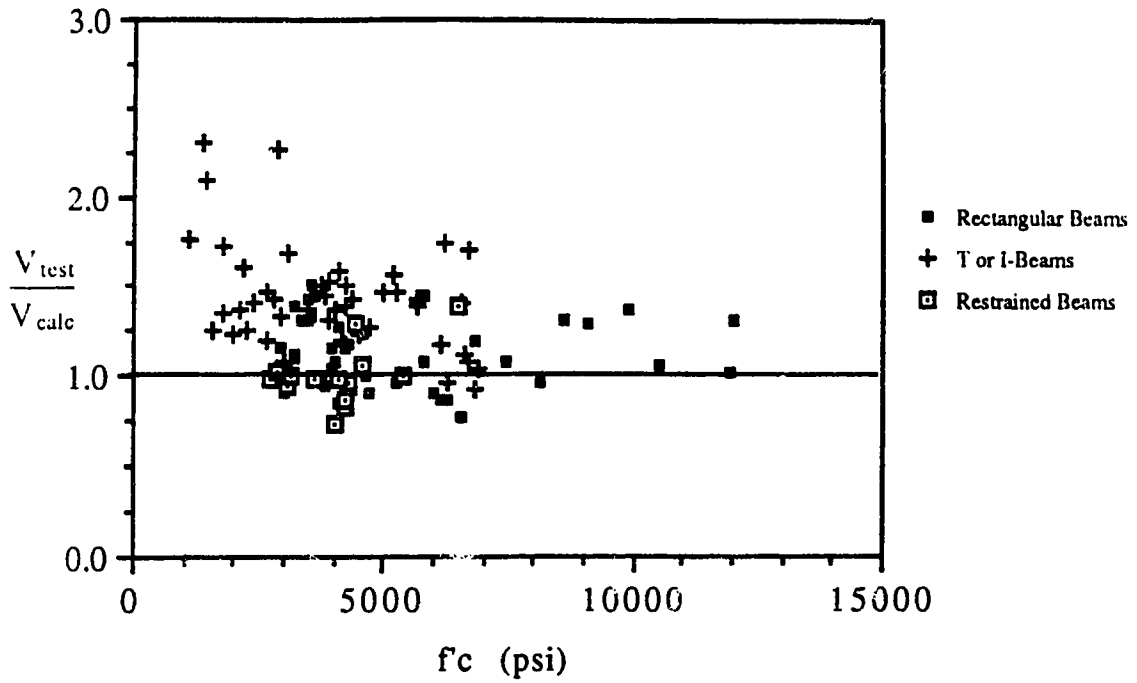
**Figure 5.9** Influence of longitudinal reinforcement on proposed shear design procedure, reinforced concrete beams.



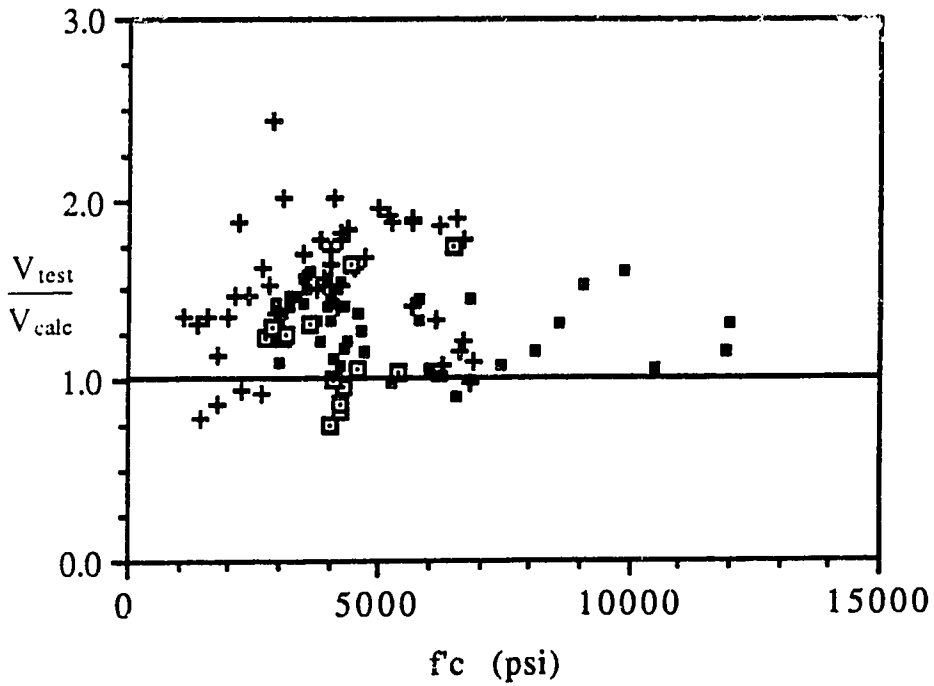
compared to rough crack surfaces typical of lower strength concretes. The smoothness of a crack surface for high strength concretes may tend to decrease aggregate interlock, thereby reducing shear carried by the concrete. Although the interface shear expression derived from Eqn. 4.4 does not consider changes in crack surface roughness for varying concrete strengths, the proposed design equations safely predicted the failure shears for the very high strength beams examined, as shown in Figure 5.10.

The influence of shear stress magnitude on the proposed design equations, expressed as  $v_n/\sqrt{f'_c}$ , is shown in Figure 5.11. Generally, as the magnitude of shear stress increases, the  $V_{test}/V_{calc}$  ratio decreases for both rectangular and T-beam.

In the test beams examined, only slender members with a shear span to depth ratio greater than 2.5 were considered. The majority of the beams had shear span to depth ratios between 2.5 and 4.0. The influence of  $a/d$  on the predicted shear strength is shown in Figure 5.12. Although more test data is required, it does not appear the proposed design equations for slender beams are influenced by the  $a/d$  ratio. As shown in Figure 2.6, the failure modes of beams with  $a/d$  ranging from about 2.5 to 6.5 are similar. Consequently, the effect of the  $a/d$  ratio on the predicted shear strength of these beams is not believed to be critical.

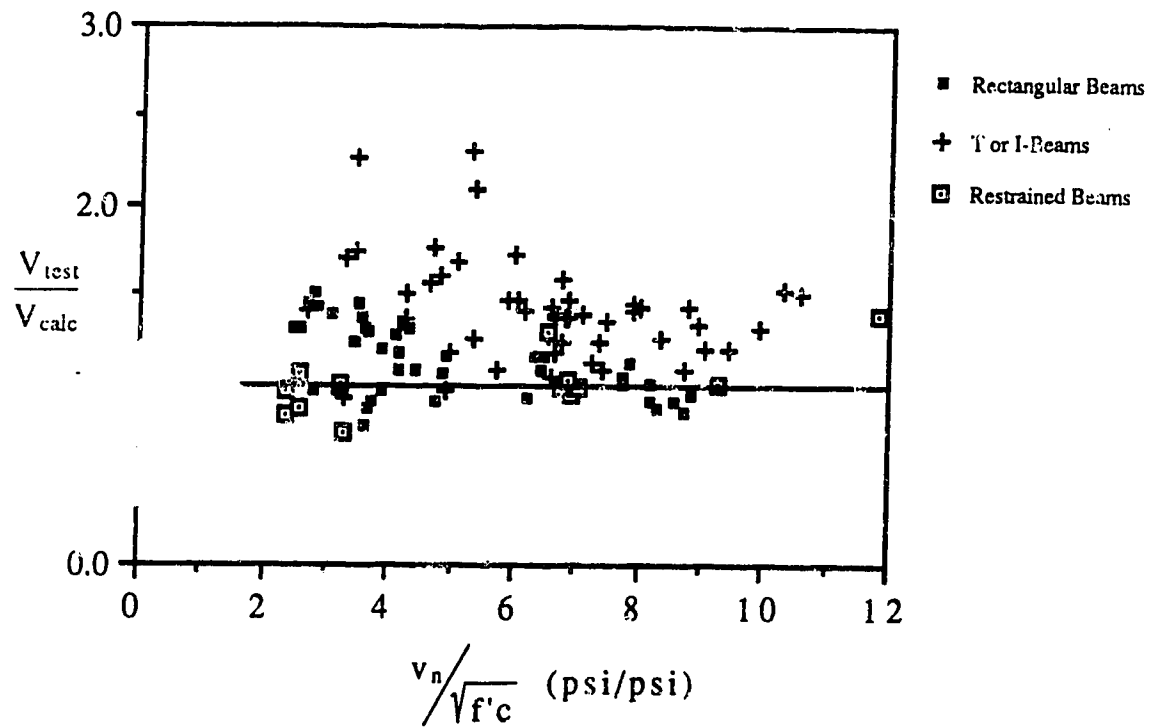


a) Proposed design procedure



b) ACI shear design procedure

**Figure 5.10** Influence of concrete strength on shear strength predictions, reinforced concrete beams.



**Figure 5.11** Influence of nominal shear stress on the proposed design equations, reinforced concrete beams.

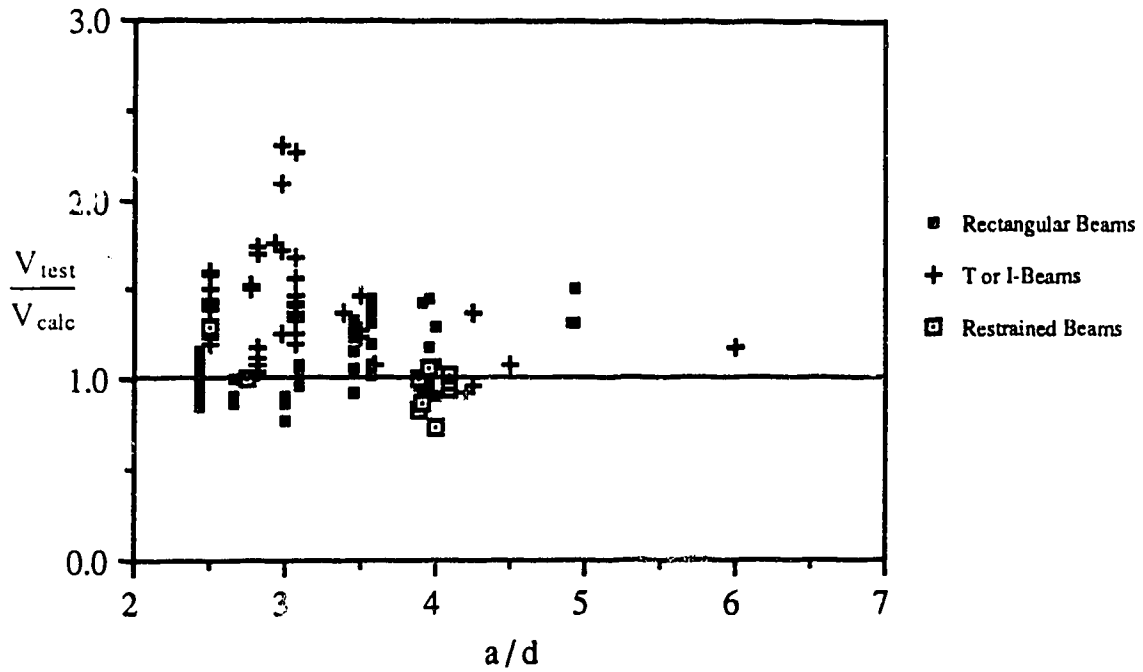


Figure 5.12 Effect of shear span to depth ratio on the proposed design equations, reinforced concrete beams.

## 5.3 Prestressed Concrete

### 5.3.1 Selection of Test Beams

Ramirez<sup>29</sup> reports the experimental data from a few different prestressed concrete beam tests in which yielding of stirrup reinforcement was reported at or before failure in shear. In addition to the test results summarized by Ramirez, additional shear tests available in the literature were also examined in order to evaluate the proposed concrete contribution expressions. The majority of the specimens are simply supported and subject to a third point loading. Ramirez summarizes the results of three uniformly loaded composite T-beams tested by Castrodale<sup>47</sup>. All of the other prestressed members examined are T or I-shaped, and all beams have straight strands. Consequently, the effects of draping strands are not included in this investigation. In total 77 beams are examined, three of which are composite beams. A general summary of the test specimens is provided in Tables 5.5 and 5.6. Concrete strengths ranged from 2430 psi to 10700 psi (16.7 - 73.8 MPa), and stirrup spacings varied between 2.4 and 12 inches (61 - 300 mm).








### 5.3.2 Comparison to ACI Code Procedure

The concrete contribution for prestressed beams was calculated from Eqns. 2.12 and 2.28 (ACI 11-11 and 11-13), neglecting the effect of beam dead load. The stirrup contribution was calculated from Eqn. 2.16, and the total shear resistance was determined using

TEST SERIES	$f_c$ (ksi)	s (in)	a/d	SECTION
Castrodale <sup>47</sup>	5.12 - 6.15	10.0 - 12.0	Uniform load	T*
Elzanaty, Nilson & Slate <sup>48</sup>	5.80 - 10.7	5.0 - 10.0	3.8 - 5.8	T&I
Olesen, Sozen & Seiss <sup>44</sup>	2.43 - 6.55	2.5 - 10.5	2.8 - 3.6	I
Lyngberg <sup>45</sup>	3.99 - 4.92	6.2	2.8	I
Bennett & Mlingwa <sup>49</sup>	5.93 - 6.42	3.2 - 7.9	3.4	I
Bennett & Debaiky <sup>50</sup>	5.22 - 8.35	3.2 - 9.5	3.0	I
Walraven & Krop <sup>51</sup>	5.89 - 6.21	2.4 - 3.4	3.1	I

\* Composite beams

**Table 5.5** Summary of prestressed concrete test beam properties.

TEST SERIES	TYPE	COMMENTS
Castrodale		Composite beams
Elzanaty, Nilson & Slate		Prestressing applied 5 days after casting
Olesen, Sozen & Seiss 1)		Yielding of stirrups inferred from measurements of crack openings
Lyngberg		Prestressed 14 days after casting
Bennett & Mlingwa 2)		Only the beams with nonprestressed web reinforcement
Bennett & Debaiky 2)		_____
Walraven & Krop 2)		Prestressing applied 5 days after casting

1) Average of two batches used in each beam

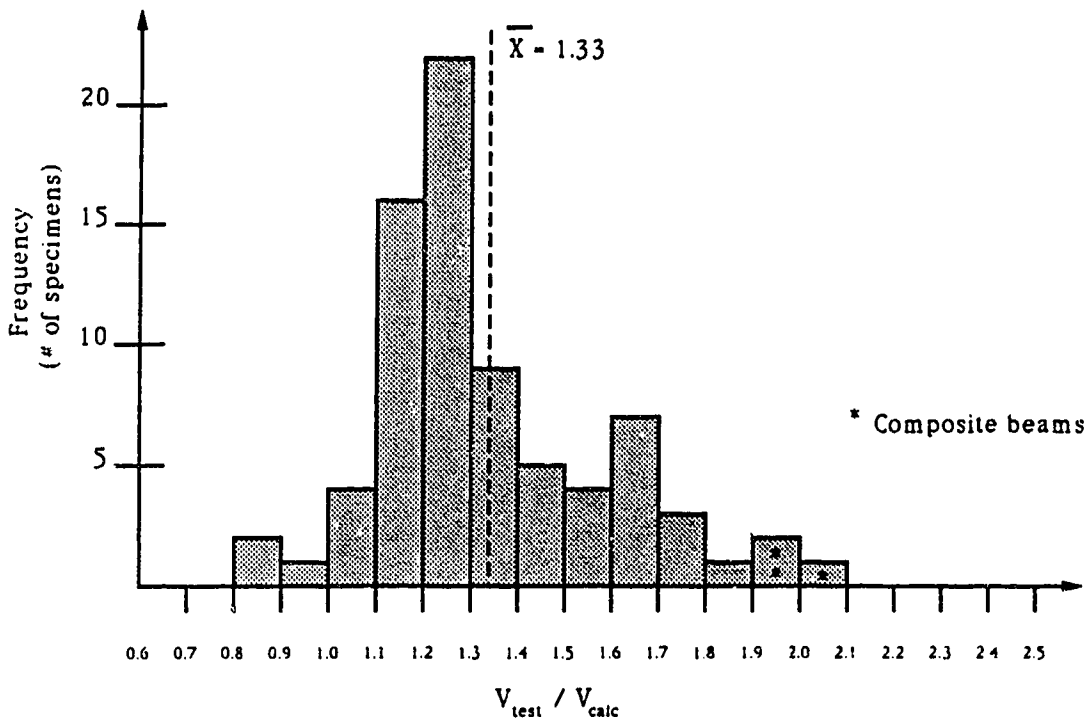
2)  $f_c$  taken as  $0.8 \times f_{cube}$

**Table 5.6** Details of prestressed concrete test beams.

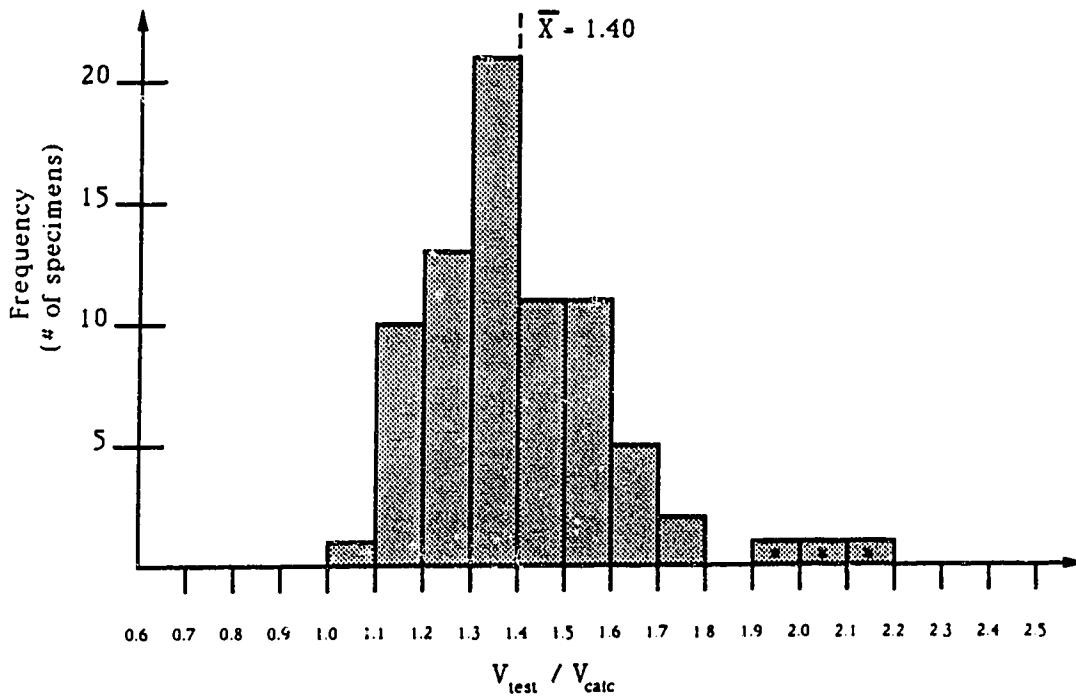
$\phi=1.0$ . A comparison of the actual failure shears to the predicted capacities is shown in Figure 5.13a. The mean  $V_{\text{test}}/V_{\text{calc}}$  ratio using the ACI Code is 1.33 with a standard deviation of 0.25 (coefficient of variation equal to 0.19), and extreme values of 0.82 and 2.06. The results are shown schematically in Figure 5.13a. The three composite beams have the largest test to predicted ratios of 1.97, 1.99 and 2.06. Three beams had ratios less than 1.0, and the lowest  $V_{\text{test}}/V_{\text{calc}}$  ratio of 0.82 was obtained from Bennett and Mlingwa's<sup>49</sup> specimen H99. Detailed results for each beam examined are provided in Appendix B.

### 5.3.3 Comparison to Concrete Contribution Equations

The concrete contribution for prestressed members was calculated according to Eqn. 4.39b, with  $\kappa_v$  determined from Eqn. 4.30 and  $\kappa_{vp}$  from Eqns. 4.37 and 4.38. Similar to the procedure used for nonprestressed beams,  $\theta$  was varied between  $15^\circ$  and  $45^\circ$  in one degree increments, and the allowable lower limit was determined in each case from Eqn. 4.41. For prestressed concrete beams,  $f_{s1}$  in Eqn. 4.41 is taken as  $f_y$  of the longitudinal reinforcing bars,  $(f_{ps} - f_{se})$  for members with prestressing tendons, or the larger of these two quantities for members with both types of longitudinal reinforcement. The effective stress in the prestressing tendons after all losses,  $f_{se}$ , is available in the test data, and the stress in the prestressed reinforcement at nominal strength,  $f_{ps}$ , was calculated from ACI Eqn. 18-3 neglecting any nonprestressed reinforcement such that



a) ACI shear design procedure



b) Proposed concrete contribution equations

Figure 5.13 Comparison of measured and computed failure shears for 77 prestressed concrete beams.



$$f_{ps} = f_{pu} \left( 1 - \frac{\gamma_p}{\beta_1} \left[ \rho_p \frac{f_{pu}}{f'_c} \right] \right) \quad (5.4)$$

where  $f_{pu}$  is the specified tensile strength of the prestressing tendons,  $\gamma_p$  and  $\beta_1$  are factors to include the type of tendon and concrete respectively, and  $\rho_p$  is the ratio of prestressed reinforcement. Although the ACI Code suggests the value of  $f_{ps}$  determined from ACI Eqn. 18-3 only be applied to beams with  $f_{se}$  greater than  $0.5f_{pu}$ , to be consistent in the analysis Eqn. 5.4 was used for all beams. The effect of  $f_{se}/f_{pu}$  will be discussed in a later section.

The stirrup contribution from Eqn. 4.33 was added to the proposed concrete contribution, and the optimum or largest shear capacity was determined for each beam. Using the proposed concrete contribution expressions, the mean test to predicted ratio for all beams examined is 1.40 with a standard deviation of 0.21 (coefficient of variation of 0.15). The lowest  $V_{test}/V_{calc}$  ratio using the proposed method is 1.0, and the results are shown in Figure 5.13b. Similar to the ACI procedure, the three composite beams provide the most conservative estimates of shear strength. From Figure 5.13 it is apparent the proposed concrete contribution has a smaller range of test to predicted ratios as compared to the ACI method, and results obtained from the proposed equations are safe for all beams examined.

In order to simplify the proposed design procedure further, it is

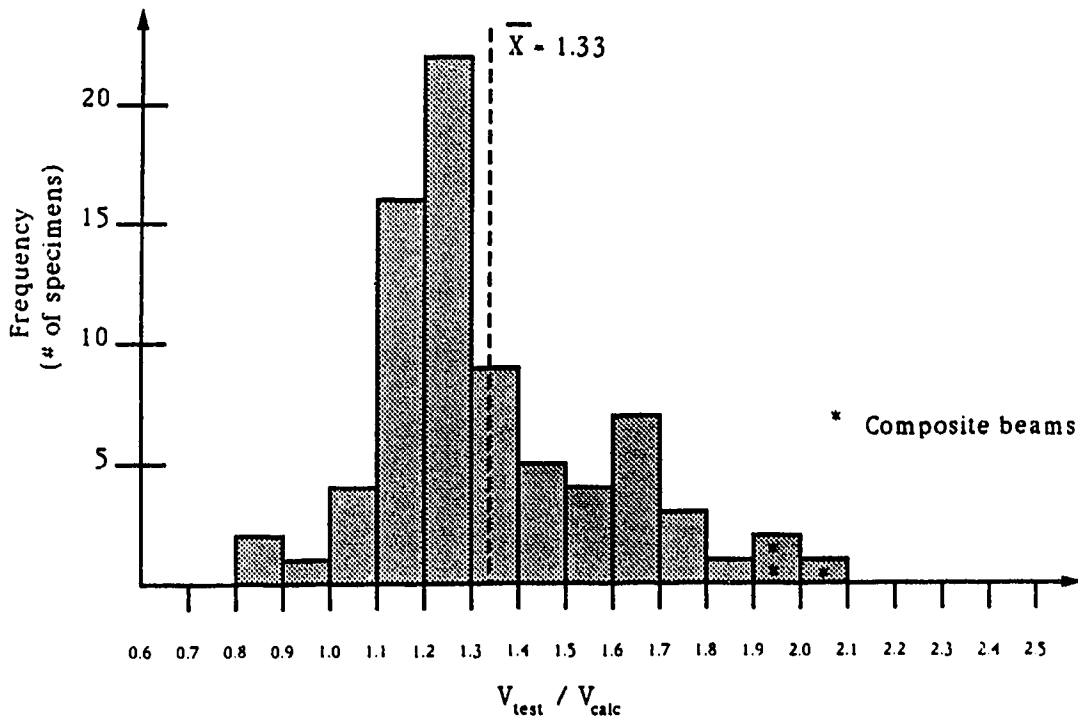
suggested the value of  $f_{ps}$  can be replaced by  $f_{py}$ . From the Modified Compression Field Theory, equating the inclined compressive stress  $f_2$  to the maximum allowable compressive stress  $f_{2 \max}$  results in an expression in terms of the principal tensile strain  $\epsilon_1$  such that

$$\left( \tan\theta + \frac{1}{\tan\theta} \right) \frac{V}{b_w d} - f_1 = \frac{f_c}{(0.8 + 170 \epsilon_1)} \quad (5.5)$$

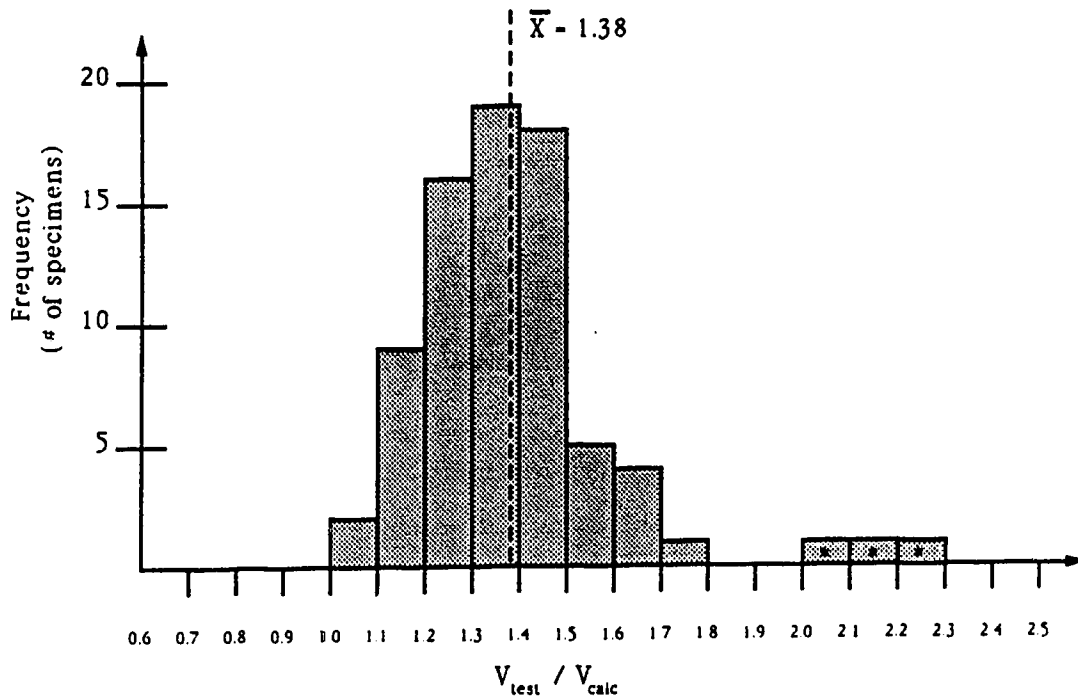
From Eqn. 4.9, the principal tensile strain can be related to the longitudinal strain  $\epsilon_x$ . Eqn. 4.41 approximates Eqn. 5.5, neglecting the concrete tension  $f_1$  and expressing the longitudinal strain in terms of the longitudinal reinforcement stress. Provided  $f_{ps}$  is equal to or less than  $f_y$ , the minimum permissible angle calculated from Eqn. 4.41 will be overestimated and safe. Figure 5.14 compares the ACI shear design procedure to the proposed concrete contribution equations using  $f_{ps}$  equal to  $f_y$  in Eqn. 4.41. For the test beams in which the yield strength was not reported,  $f_y$  was taken as  $0.85f_{pu}$ . This simplified procedure for determining the web crushing limits for prestressed beams has a mean test to predicted ratio of 1.38 with a standard deviation of 0.22 (coefficient of variation equal to 0.16).  $V_{\text{test}}/V_{\text{calc}}$  ratios ranged from 1.0 to 2.28, with the largest ratios obtained for the composite beams. A summary of results for all procedures is shown in Table 5.7.

#### 5.3.4 Influence of Amount of Shear Reinforcement on Shear Strength

The effect of the amount of shear reinforcement on the proposed



a) ACI shear design procedure



b) Proposed concrete contribution assuming  $f_{ps}$  equals  $f_y$

Figure 5.14 Comparison of measured and computed failure shears for 77 prestressed concrete beams.

TEST SERIES	# TESTS	ACI METHOD		PROPOSED EQNS.		** SIMPLIFIED PROCEDURE	
		$\bar{X}$	S	$\bar{X}$	S	$\bar{X}$	S
Castrodale *	3	2.00	0.047	2.08	0.105	2.18	0.102
Elzanaty, Nilson & Slate	16	1.20	0.067	1.30	0.138	1.31	0.145
Olesen, Sozen & Seiss	19	1.24	0.128	1.46	0.166	1.47	0.184
Lynberg	6	1.28	0.067	1.56	0.044	1.40	0.040
Bennett & Mlingwa	8	1.03	0.131	1.26	0.113	1.26	0.113
Bennett & Debaiky	18	1.51	0.186	1.37	0.104	1.34	0.103
Walraven & Krop	7	1.54	0.111	1.23	0.064	1.23	0.061
	77	1.33	0.247	1.40	0.208	1.38	0.221

\* Composite beams

$\bar{X}$  = mean  $V_{test} / V_{calc}$

\*\* Based on  $f_{ps} = f_y$  in determining  $\theta$  limits

S = sample standard deviation

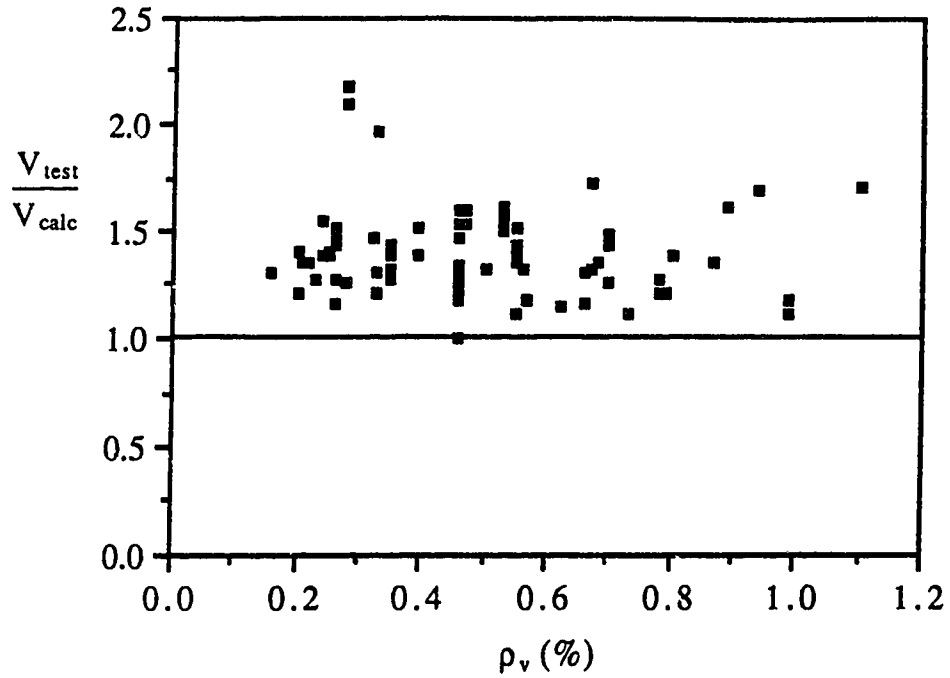
**Table 5.7** Summary of predicted shear capacity results for the prestressed concrete beams examined.

design equations and on the ACI procedure is shown in Figures 5.15 and 5.16. In contrast to the results for reinforced concrete beams, less conservative predictions of shear strength are not obtained as the amount of web reinforcement decreases. For the ACI shear design procedure the shear capacity predictions become more conservative as the amount of web reinforcement decreases. This trend is not pronounced in the proposed design equations.

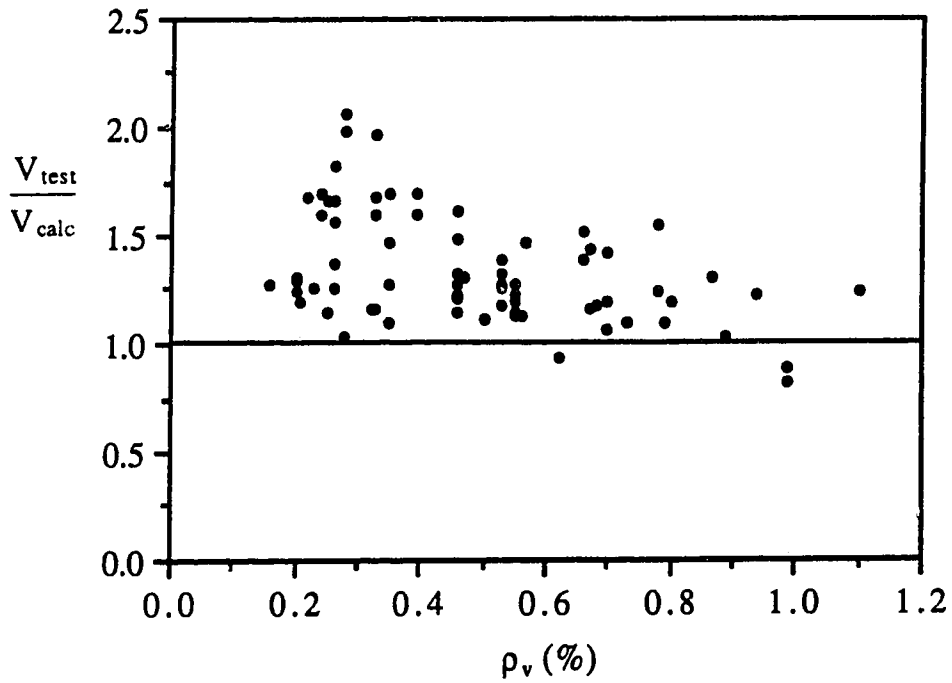
As shown in Figure 5.17, although several beams exceed stirrup spacings of  $d/2$  and  $d/3 \tan\theta$ , conservative predictions of shear strength using the proposed concrete contribution and stirrup capacity are obtained for all of the 77 beams examined.

The influence of the amount of prestressed reinforcement, expressed as  $\rho_p$ , is shown in Figure 5.18. As the amount of longitudinal prestressed reinforcement increases, the shear strength predictions of the ACI Code become less conservative. The prestressed reinforcement ratio generally appears to have no effect on the predictions of the proposed design method.

For the prestressed concrete beams examined, 24 members had deformed stirrups, 43 had smooth stirrups, and for the remaining 10 beams the type of stirrup was not reported. In contrast to the results for reinforced concrete members, beams with smooth stirrups had a higher  $V_{test}/V_{calc}$  ratio than beams with deformed stirrups for both the ACI procedure and the proposed design equations. For beams with smooth stirrups the ACI predictions have a mean

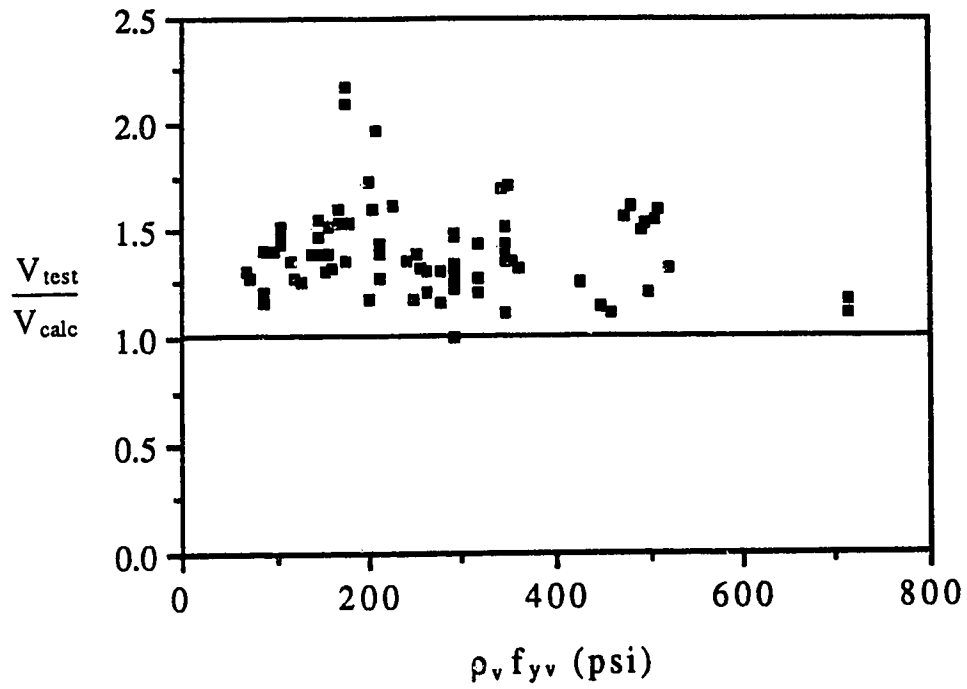


a) Proposed design equations

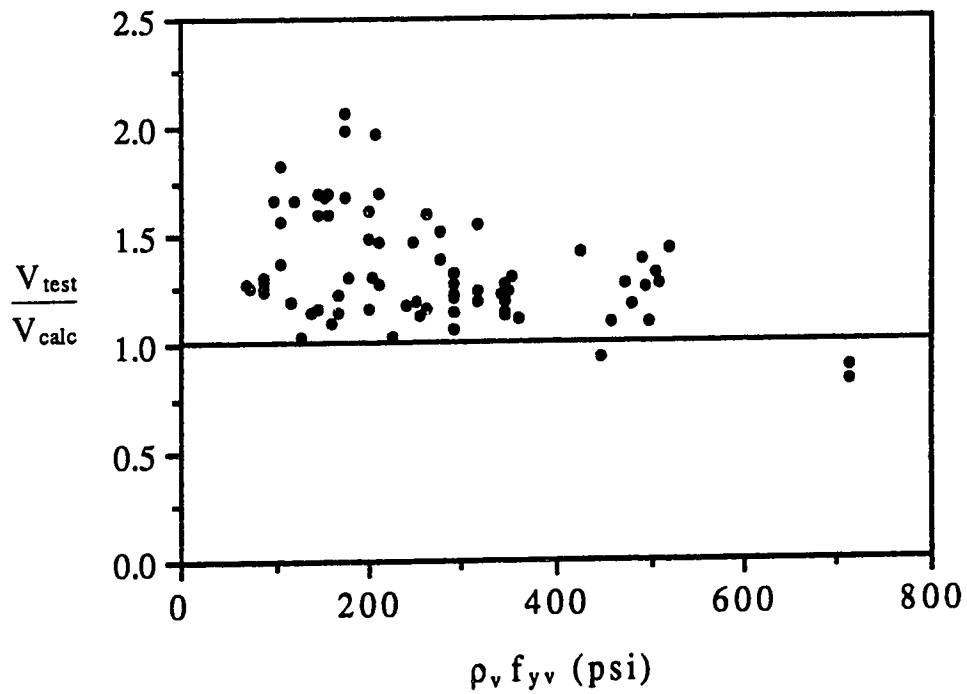


b) ACI shear design procedure

**Figure 5.15** Effect of amount of shear reinforcement on the predicted shear capacities, prestressed concrete beams.

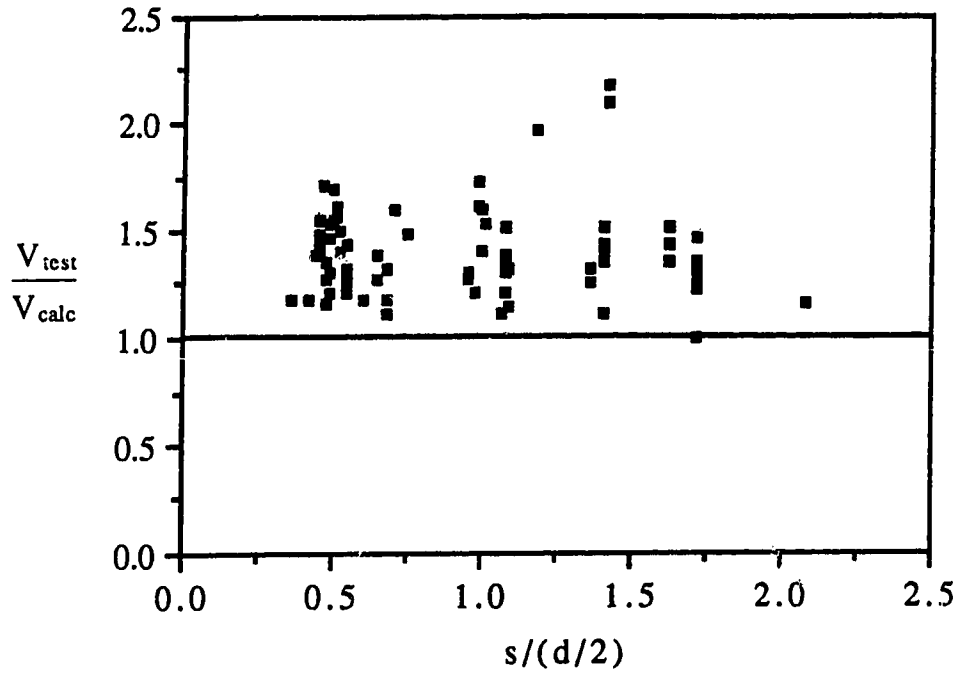


a) Proposed design equations

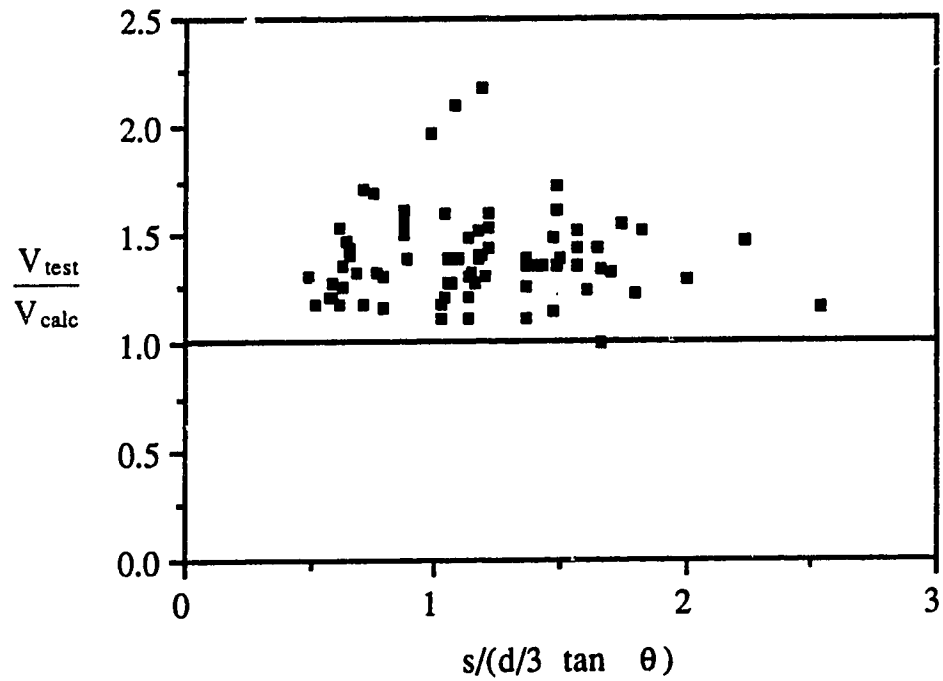


b) ACI shear design procedure

**Figure 5.16** Effect of shear reinforcement on the predicted shear capacities, prestressed concrete beams.



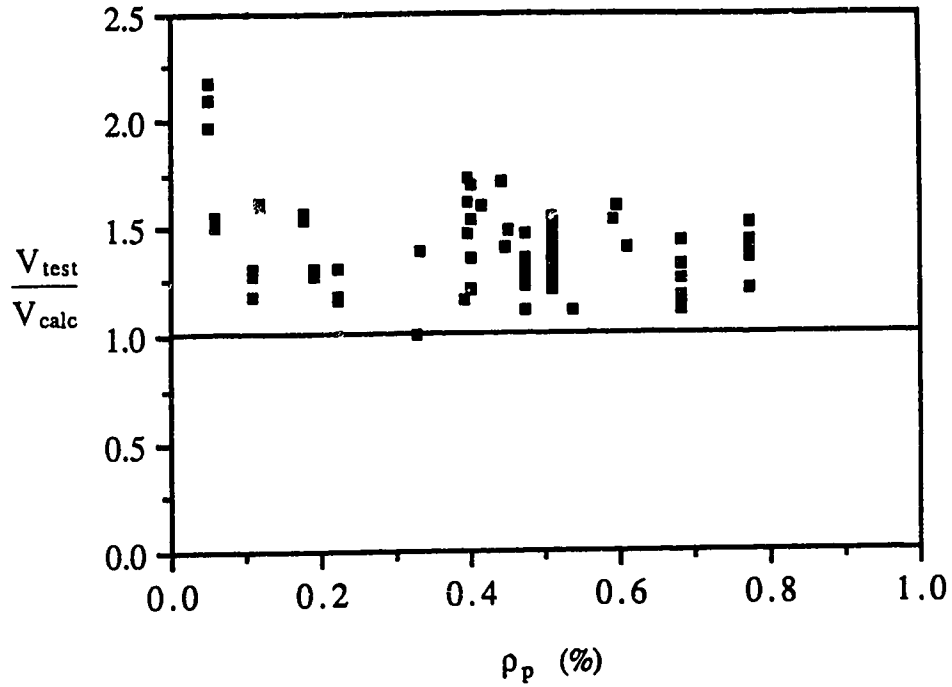
a) Effect of stirrup spacing



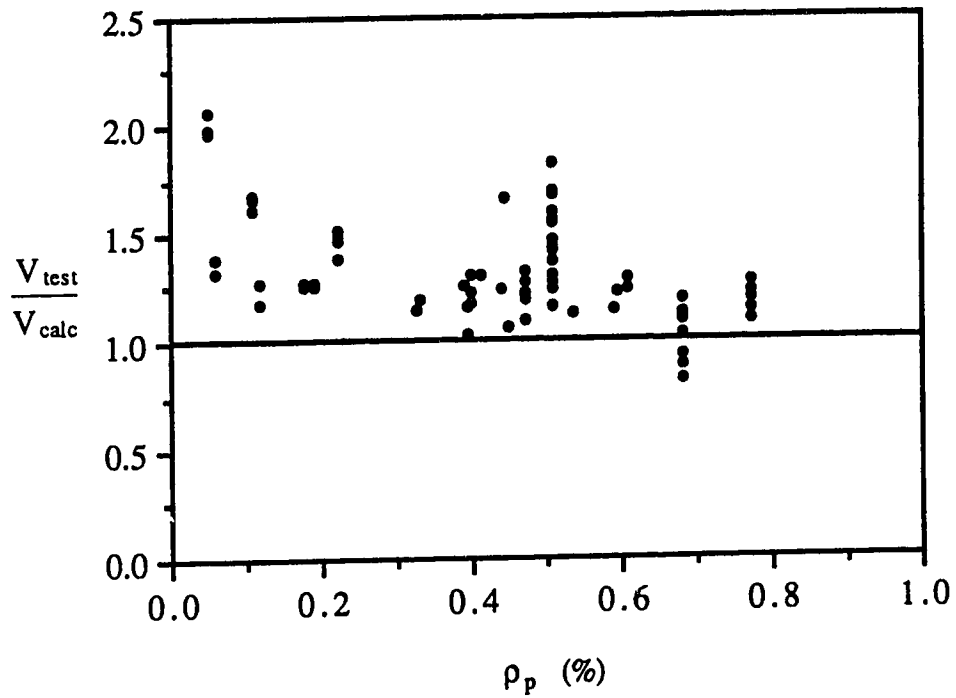
b) Effect of stirrup spacing

**Figure 5.17** Effect of stirrup spacing on predicted capacity using the proposed design method, prestressed concrete beams.





a) Proposed design equations



b) ACI shear design procedure

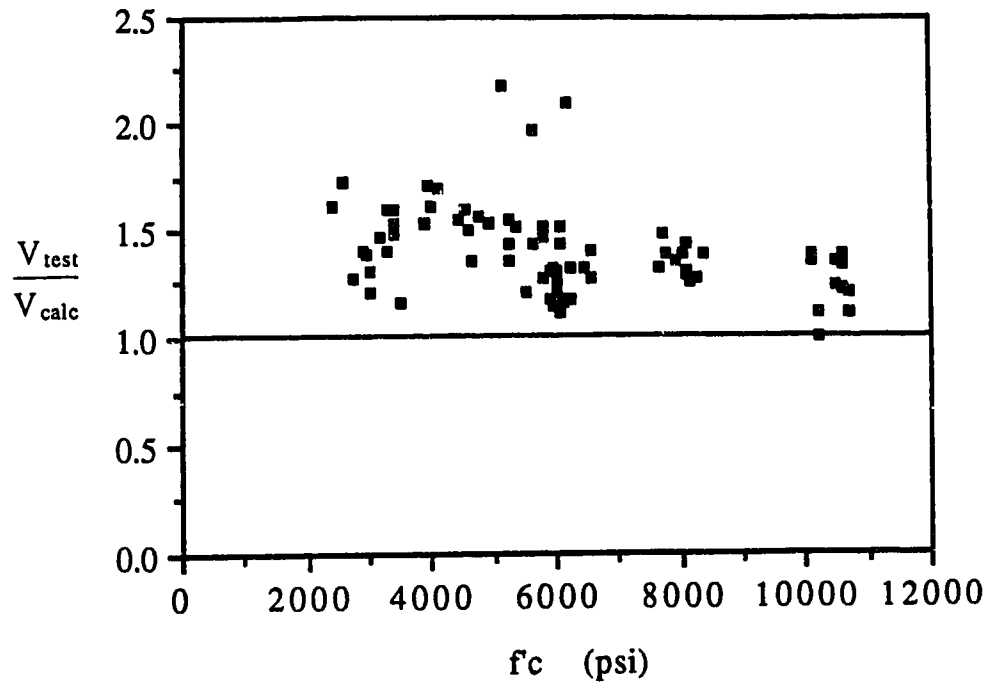
**Figure 5.18** Effect of amount of prestressed reinforcement on predicted shear capacities, prestressed concrete beams.

$V_{test}/V_{calc}$  ratio of 1.34 (standard deviation of 0.21) while the proposed design equations assuming  $f_{ps}$  equals  $f_{py}$  have a mean ratio of 1.40 (standard deviation of 0.15). Prestressed concrete beams with deformed stirrups have a mean  $V_{test}/V_{calc}$  ratio of 1.18 (standard deviation of 0.14) and 1.30 (standard deviation of 0.14) for predictions using the ACI Code and proposed design equations respectively.

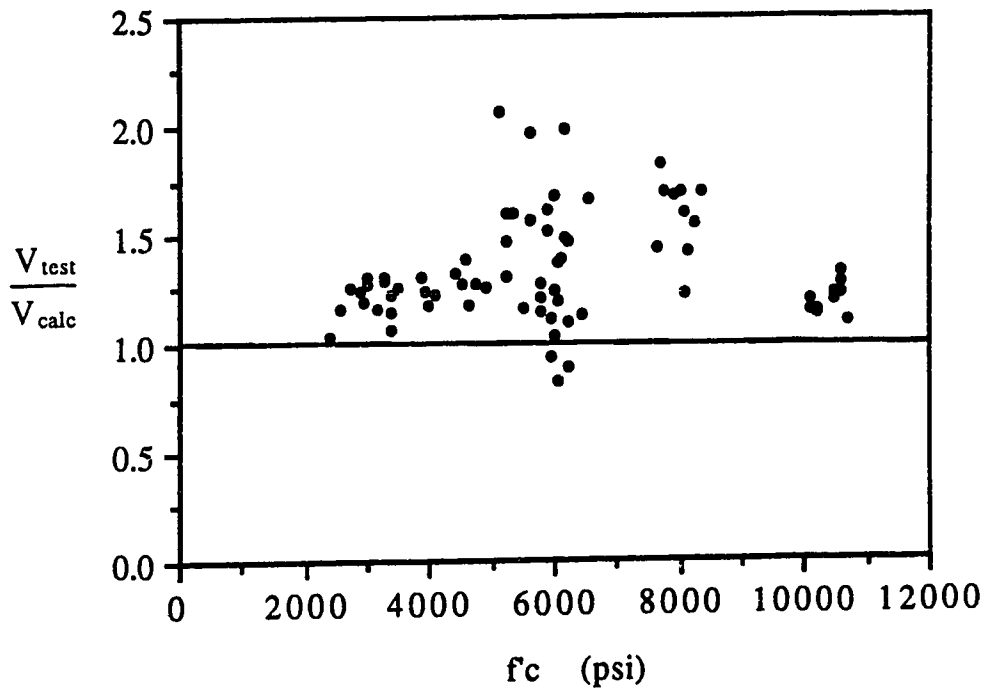
### 5.3.5 Other Factors Influencing Predicted Shear Strength

Figure 5.19 shows the effect of concrete strength on the calculated capacities for prestressed concrete beams using the proposed design procedure and the ACI Code . For the proposed method, the  $V_{test}/V_{calc}$  ratio decreases as the concrete strength increases. This may be attributed to the decrease in aggregate interlock due to the smooth crack surfaces of high strength concretes. However, even for the high strength concrete beams examined, the  $V_{test}/V_{calc}$  ratio remained greater than or equal to 1.0. From Figure 5.19b the influence of concrete strength on the ACI predictions indicates no significant trends.

The effect of the amount of prestress on the beams examined is shown in Figure 5.20. As the prestress force increases, the predicted capacities from the ACI procedure appear to become less conservative. The amount of prestress has no significant effect on the proposed design equations. In the determination of the minimum strut inclination  $\theta$  using  $f_{ps}$  from ACI Eqn. 18-3, the ACI

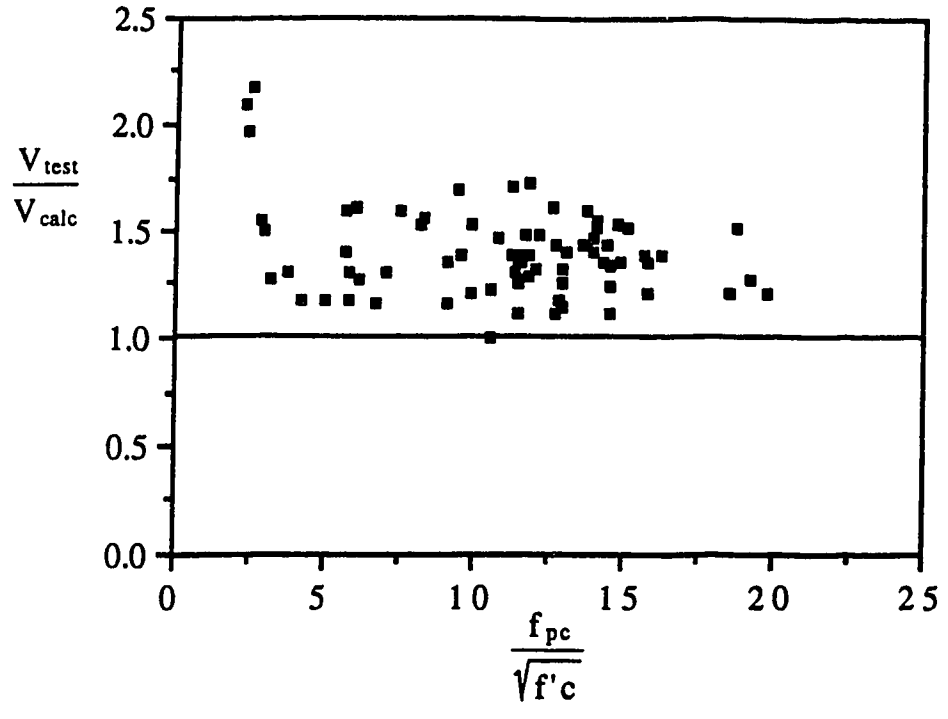


a) Proposed design equations

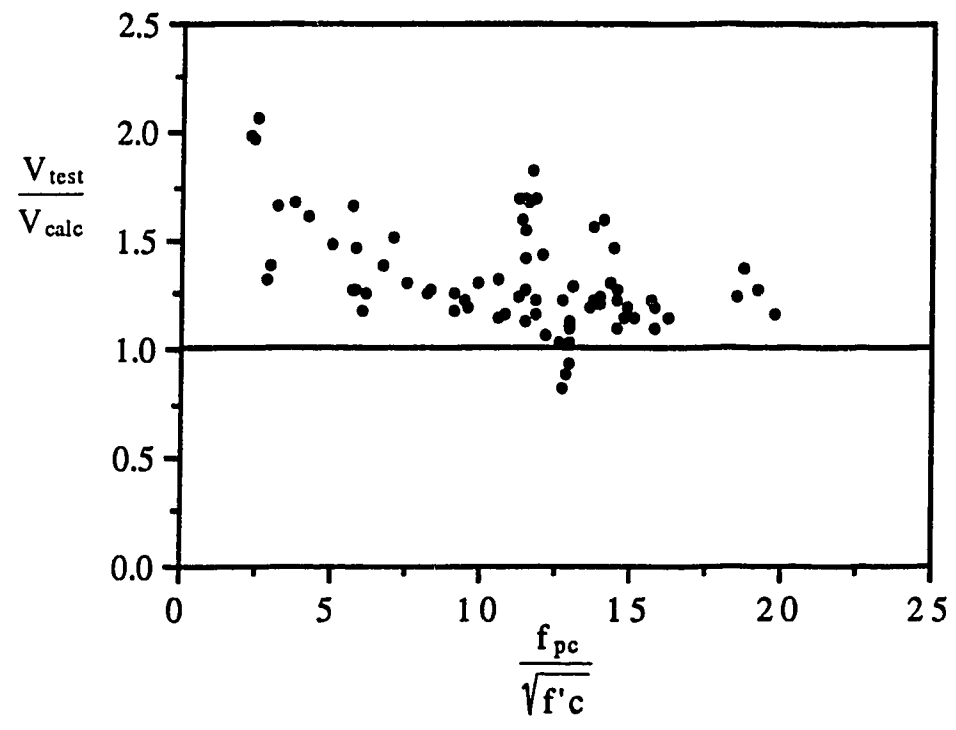


b) ACI shear design procedure

**Figure 5.19** Effect of concrete strength on predicted shear capacities, prestressed concrete beams.



a) Proposed design procedure

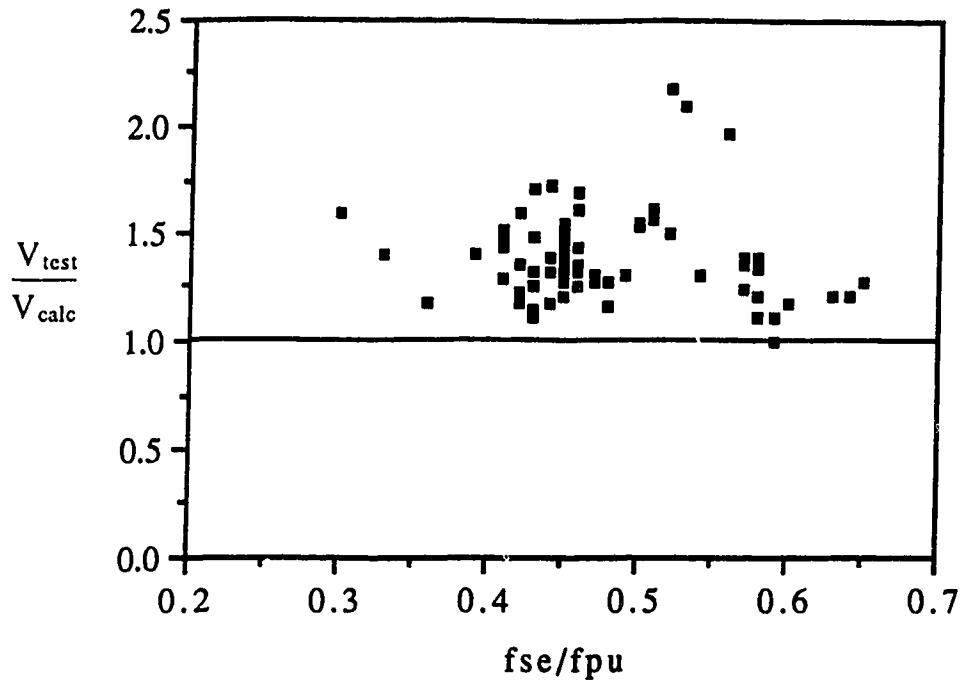


b) ACI shear design procedure

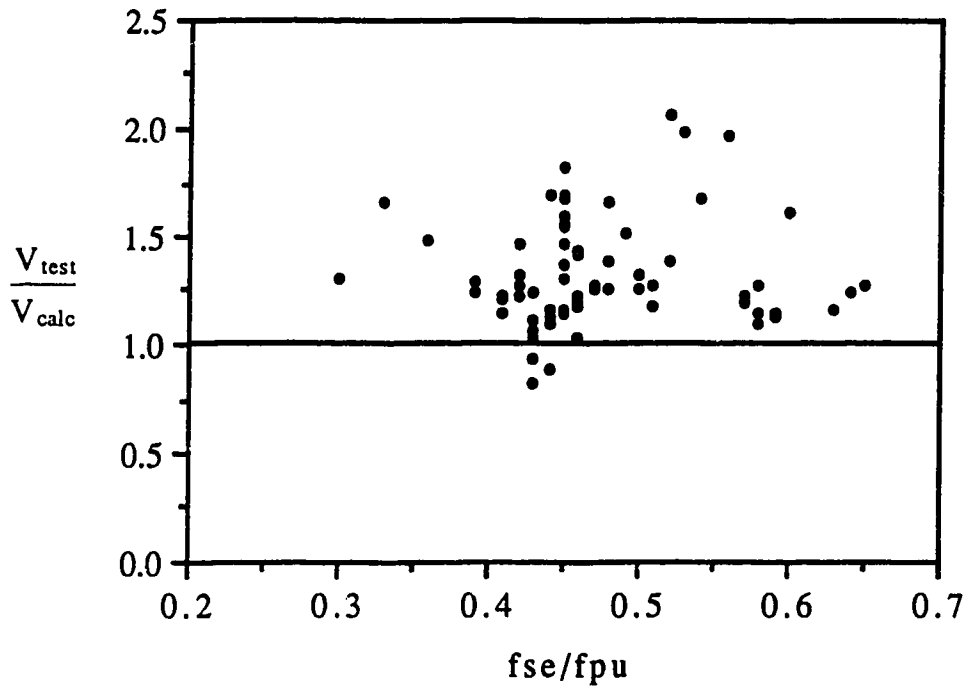
Figure 5.20 Effect of amount of prestress on predicted shear capacities, prestressed concrete beams.

Code suggests that  $f_{se}/f_{pu}$  should be greater than or equal to 0.5. For consistency, Eqn. 5.4 which is obtained from ACI Eqn. 18-3 was used for all test beams regardless of the  $f_{se}/f_{pu}$  ratio. Generally, most beams had a ratio greater than about 0.45, and the influence on Eqn. 5.4 is not believed to be critical. Figure 5.21 indicates there is no substantial effect of the  $f_{se}/f_{pu}$  ratio on the predicted shear capacities using either the proposed equation or the ACI procedure.

All of the beams examined have shear span to depth ratios greater than 2.5. The influence of  $a/d$  on the shear strength results is shown in Figure 5.22. Generally, as  $a/d$  increases the ACI predictions becomes less conservative, while the  $a/d$  ratio appears to have no effect on the proposed design equations.

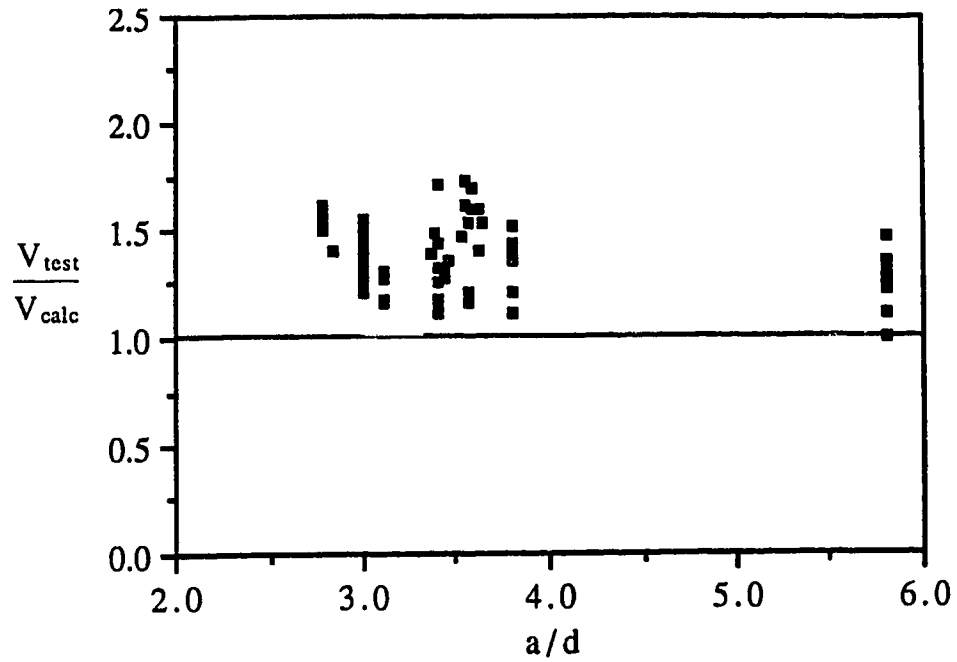


a) Proposed design equations

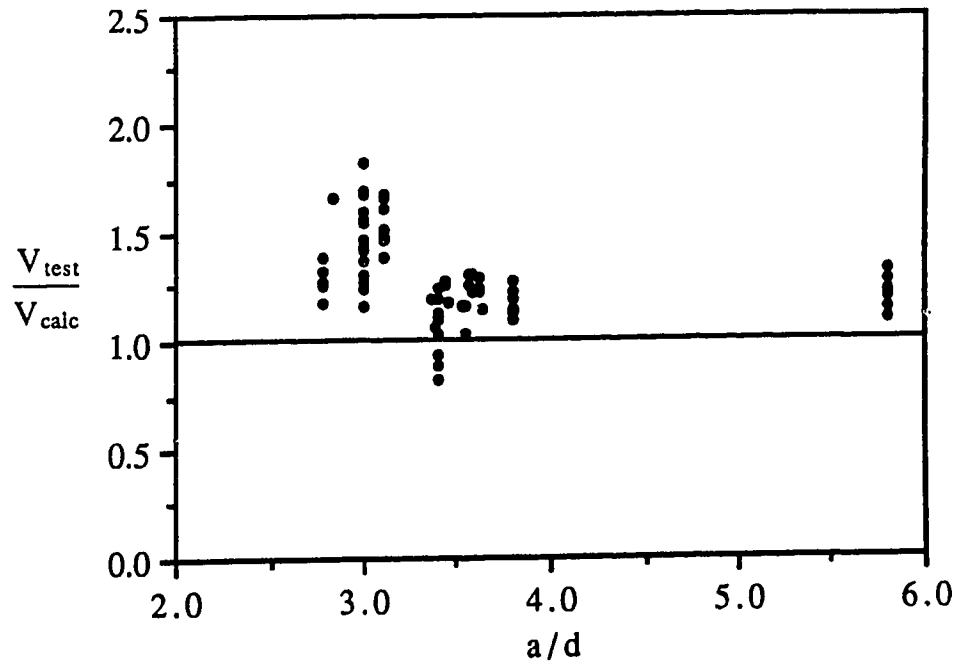


b) ACI shear design procedure

**Figure 5.21** Influence of prestress stresses on predicted shear capacities, prestressed concrete beams.



a) Proposed design equations



b) ACI shear design procedure

**Figure 5.22** Effect of shear span to depth ratio on predicted shear capacities, prestressed concrete beams.

## 6. Design and Analysis Examples



**Example 1.** Determine the web reinforcement required in the region adjacent to the supports for the simply supported beam shown in Figure 6.1 (adapted from Ref. 52).

The beam spans 30 feet with a factored load of 4.5 kips/ft, and is subjected to shear and flexure only. The beam is to be reinforced with vertical U-stirrups and has following member parameters:

$$b_w = 13 \text{ in.} \quad d = 20 \text{ in.} \quad f'_c = 3,000 \text{ psi} \quad f_{yv} = 40 \text{ ksi} \quad f_y = 60 \text{ ksi}$$

Calculations:

### ACI 318-83

1. Determine factored shear force diagram:

$$V_u @ \text{ support:} \\ = 4.5(15) = 67.5 \text{ kips}$$

$$V_u @ d: \\ = 67.5 - 4.5(20/12) = 60 \text{ kips}$$

2. Determine  $V_c$

$$\phi V_c = \phi 2 \sqrt{f'_c} b_w d \\ = .85(2) \sqrt{3000} (13) 20 = 24.2 \text{ kips}$$

Since  $V_u \geq \phi V_c / 2$  stirrups are required.

3. Determine the required spacing of stirrups within a distance  $d$  from the support (Assuming #4 stirrups with  $A_v = 0.4 \text{ in.}^2$ )

$$s_{\text{req'd}} = \phi A_v f_y d / (V_u - \phi V_c)$$

$$s = 0.85 (0.4) 40 (20) / (60 - 24.2) \\ = 7.6 \text{ in.}$$

### Proposed Design Procedure

1. Determine factored shear force diagram:

$$V_u @ \text{ support} = 67.5 \text{ kips}$$

2. Select a diagonal strut inclination  $\theta$

$$\text{Try } \theta = 26^\circ$$

$$V_u @ d/\tan\theta: \\ = 67.5 - 4.5 (20/\tan 26) / 12 \\ = 52.1 \text{ kips}$$

3. Check diagonal crushing limit:

$$\theta > 15^\circ + (75,000 + f_y) v_n / 1000 f'_c$$

$$v_n = 52.1(1000) / 13(20) 0.85 = 236 \text{ psi}$$

$$\theta > 15^\circ + (75 + 60) \times 10^3 236 / 1000(3000) \\ > 25^\circ \quad \text{Therefore } 26^\circ \text{ is satisfactory.}$$

Since the factored shear force exceeds the permissible limit of a beam without web reinforcement, given by

$$\phi V_c = \phi 1.0 \sqrt{f'_c} b_w d = 12.1 \text{ kips}$$

stirrups are required.

## Example 1. Continued.

Calculations:

### ACI 318-83

4. Check the maximum permissible spacing of stirrups:

$$s_{\max} \leq d/2 = 10 \text{ in.}$$

$$\text{or } \leq 24 \text{ in.}$$

$s_{\max}$  of the #4 stirrups corresponding to minimum reinforcement area requirements:

$$\begin{aligned} s_{\max} &= A_v f_y / 50 b_w \\ &= 0.40 (40,000) / 50 (13) \\ &= 24.6 \text{ in} \end{aligned}$$

Therefore,  $s^{\max} = 10 \text{ in.}$  governs.

5. Extend longitudinal steel  $d$  past where no longer needed for flexure.

Summary:

Within a distance  $d$  from the support use #4 stirrups @ 7.5 in. o.c.

### Proposed Design Procedure

4. Determine the concrete contribution to shear

$$\begin{aligned} \kappa_v &= 0.05 \theta - 0.25 \\ &= 0.05 (26) - 0.25 = 1.05 \end{aligned}$$

$$\begin{aligned} \phi V_c &= \phi \kappa_v \sqrt{f'_c} b_w d \\ &= 0.85 (1.05) \sqrt{3000} (13) 20 / 1000 \\ &= 12.7 \text{ kips} \end{aligned}$$

5. Determine the required spacing of #4 U-stirrups within  $d/\tan\theta$  from the support

$$s_{\text{req'd}} = \phi A_v f_y d / (V_u - \phi V_c) \tan \theta$$

$$\begin{aligned} s &= 0.85 (0.4) 40 (20) / (52.1 - 12.7) \tan 26 \\ &= 14.2 \text{ in.} \end{aligned}$$

6. Check the maximum permissible spacing of stirrups:

$$s_{\max} \text{ is the larger of } d/2 = 10 \text{ in.}$$

$$\text{or } d/3 \tan \theta = 13.7 \text{ in.}$$

$s_{\max}$  of the #4 stirrups corresponding to minimum reinforcement area requirements:

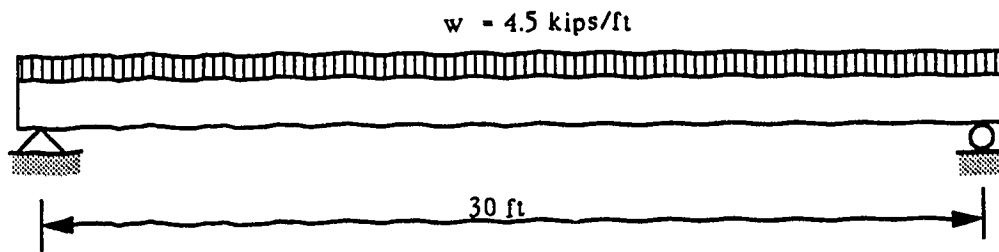
$$s_{\max} = A_v f_y / 50 b_w = 24.6 \text{ in}$$

Therefore,  $s_{\max} = 13.7 \text{ in.}$  governs.

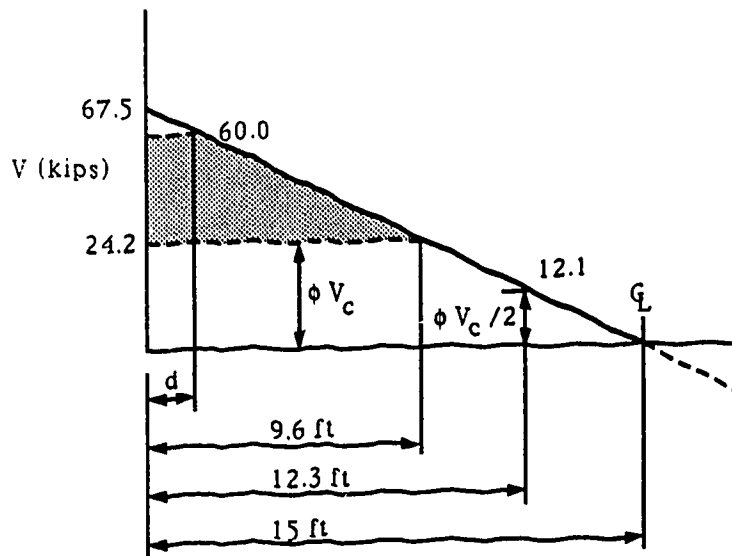
7. Extend longitudinal bars  $d/\tan\theta$  past where no longer needed for flexure.

Summary:

Within a distance  $d/\tan\theta$  from the support use #4 stirrups @ 13.7 in. o.c.



a) loading



b) shear force diagram

Figure 6.1 Simply supported beam - Example 1.

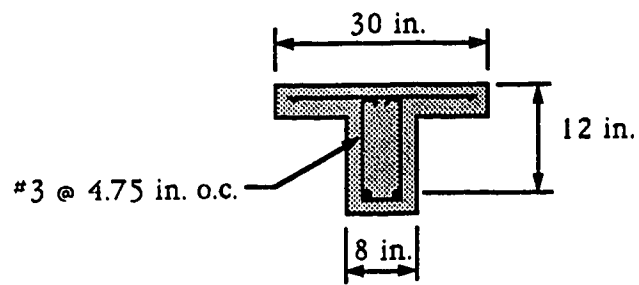
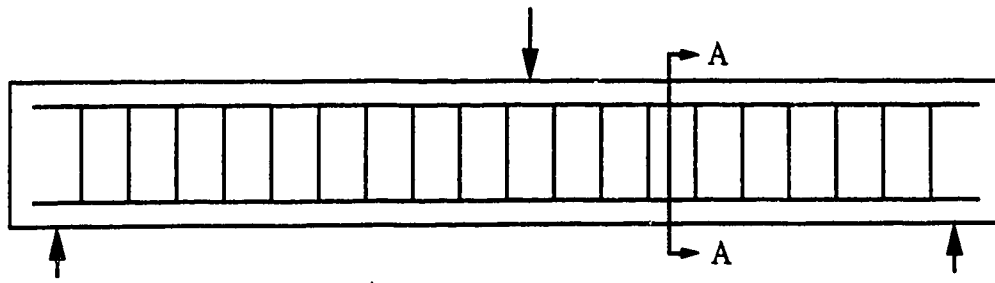
**Example 2.** Determine the nominal shear strength of the reinforced concrete T-beam shown in Figure 6.2. This beam section is similar to specimen 'A' tested by Mailhot<sup>19</sup> having an actual failure shear of 89.4 kips.

The specified 28 day strength of the concrete is 5700 psi, and the other beam parameters are:

$$b_w = 8 \text{ in. } d = 12 \text{ in. } A_v = 0.22 \text{ in}^2 \quad s = 4.75 \text{ in. } f_{yv} = 60 \text{ ksi } f_y = 60 \text{ ksi}$$

Calculations:

ACI 318-83	Proposed Analysis Procedure
1. Determine $V_s$	1. Select a diagonal strut inclination $\theta$
$V_s = A_v f_y d / s$	Try $\theta = 32^\circ$
$= 0.22 (60) 12 / 4.75 = 33.3 \text{ kips}$	2. Determine $V_s$
2. Check $V_s$ max	$V_s = A_v f_y d / s \tan \theta$
$V_{s \text{ max}} = 8 \sqrt{f'_c} b_w d$	$= 0.22(60) 12 / (4.75 \tan 32^\circ)$
$V_s \leq 8 \sqrt{5700} (8) 12 / 1000 = 58 \text{ kips}$	$= 53.4 \text{ kips}$
Therefore $V_s = 33.3 \text{ kips}$ is o.k.	3. Determine the concrete contribution to shear
3. Determine $V_c$	$\kappa_v = 0.05 \theta - 0.25$
$V_c = 2 \sqrt{f'_c} b_w d$	$= 0.05 (32) - 0.25 = 1.35$
$= 2 \sqrt{5700} (8) 12 / 1000 = 14.5 \text{ kips}$	$V_c = \kappa_v \sqrt{f'_c} b_w d$
4. Determine the nominal shear strength	$= 1.35 \sqrt{5700} (8) 12 / 1000$
$V_n = V_c + V_s$	$= 9.8 \text{ kips}$
$V_n = 14.5 + 33.3 = 47.8 \text{ kips}$	4. Check limit to avoid diagonal crushing.
	$\theta > 15^\circ + (75,000 + f_y) v_n / 1000 f'_c$
	$v_n = (9.8 + 53.4) 1000 / 8 (12) = 658 \text{ psi}$
	$\theta \geq 15^\circ + (75 + 60) \times 10^3 658 / 1000 (5700)$
	$\geq 31^\circ$ Therefore $32^\circ$ is satisfactory.
	5. Determine the nominal shear strength
	$V_n = 9.8 + 53.4 = 63.2 \text{ kips}$



Section A - A

Figure 6.2 Details of T-Beam for Example 2.

**Example 3.** Determine the shear strength of the prestressed concrete beam shown in Figure 6.3. The beam is prestressed using tendons with  $f_{py}=250$  ksi,  $f_{pu}=270$  ksi and an effective force  $P_e=97$  kips. The beam has vertical #3 single legged stirrups at 8 in. o.c. with a yield stress of 60 ksi. At the section under consideration the self weight moment and shear are 1.7 ft-kips and 0.17 kips respectively. The applied forces at the section give a  $V/M$  ratio of 0.22 and an extreme fiber tensile stress less than  $6\sqrt{f'_c}$ . The beam has the following section properties:

$$I = 1952 \text{ in}^4 \quad A = 91 \text{ in}^2 \quad y_t = 8.5 \text{ in} \quad e = 3.8 \text{ in} \quad f'_c = 5800 \text{ psi (40 MPa)}$$

$$b_w = 3 \text{ in} \quad d_p = 9.3 \text{ in} \quad h = 14 \text{ in} \quad A_v = 0.11 \text{ in}^2 \quad A_{ps} = 0.88 \text{ in}^2$$

Calculations:

### ACI 318-83

1. Determine the shear strength provided by the concrete using Eqn 11-13

$$V_{cw} = (3.5\sqrt{f'_c} + 0.3f_{pc}) b_w d$$

$$f_{pc} = P_e / A = 97000 / 91 = 1066 \text{ psi}$$

The effective shear depth can be taken as  $0.8h$  ( $0.8 \times 14$ ) = 11.2 in.

$$V_{cw} = (3.5\sqrt{5800} + 0.3(1066)) 3(11.2) / 1000 = 19.7 \text{ kips}$$

2. Determine the shear strength provided by the concrete using Eqn 11-11

$$V_{ci} = 0.6\sqrt{f'_c} b_w d + V_d + V_l M_{cr} / M_{max}$$

$$M_{cr} = (I / y_t) (6\sqrt{f'_c} + f_{pe} - f_d)$$

$$f_{pe} = P_e / A + P_e (e) y_t / I = 1066 + 97,000 (3.8) 8.5 / 1952 = 2670 \text{ psi}$$

$$f_d = M_d y_t / I = 1710 (12) 8.5 / 1952 = 89 \text{ psi}$$

$$M_{cr} = 1952 (6\sqrt{5800} + 2670 - 89) / 1000 (8.5) = 698 \text{ kip-in} = 58.2 \text{ kip-ft}$$

$$V_{ci} = 0.6\sqrt{5800} 3(11.2) / 1000 + 0.17 + 0.22(58.2) = 14.6 \text{ kips}$$

### Proposed Analysis Procedure

1. Select a diagonal strut inclination  $\theta$

$$\text{Try } \theta = 39^\circ$$

2. Determine  $V_s$

$$V_s = A_v f_y d / s \tan \theta$$

$$= 0.11(60) 11.2 / (8 \tan 39^\circ) = 11.4 \text{ kips}$$

3. Determine the concrete contribution to shear

$$V_c = (\kappa_v + \kappa_{vp}) \sqrt{f'_c} b_w d$$

$$\kappa_{vp} = (0.01\theta + 0.06) f_{pc} / \sqrt{f'_c} = 0.45 (1066 / \sqrt{5800}) = 6.3$$

$$\text{but } \leq 0.2\theta - 1.0 = .2(39) - 1.0 = 6.8$$

$$\leq 8.75 - 0.15\theta = 8.75 - .15(39) = 2.9$$

Therefore  $\kappa_{vp} = 2.9$  governs

$$\kappa_v = 0.05\theta - 0.25 = 0.05(39) - 0.25 = 1.7$$

$$V_c = (1.7 + 2.9) \sqrt{5800} (3) 11.2 / 1000 = 11.8 \text{ kips}$$

### Example 3. Continued

Calculations:

#### ACI 318-83

3. Check minimum limit on  $V_{ci}$

$$V_{ci \text{ min}} = 1.7 \sqrt{f'c} b_w d$$
$$= 1.7 \sqrt{5800} (3) 11.2 / 1000 = 4.4 \text{ kips}$$

Since  $V_{ci} = 14.6$  kips, o.k.

4. Determine  $V_s$

$$V_s = A_v f_y d / s$$
$$= 0.11 (60) 11.2 / 8 = 9.2 \text{ kips}$$

5. Check  $V_s$  max

$$V_s \text{ max} = 8 \sqrt{f'c} b_w d$$
$$V_s \leq 8 \sqrt{5800} (3) 11.2 / 1000 = 20.5 \text{ kips}$$

Therefore  $V_s = 9.2$  kips is o.k.

6. Determine the total shear strength

$$\phi(V_c + V_s) = 0.85(14.6 + 9.2) = 20.2 \text{ kips}$$

#### Proposed Analysis Procedure

4. Check limit to avoid diagonal crushing.

$$\theta > 15^\circ + (75,000 + f_{sl}) v_n / 1000 f'c$$
$$v_n = (11.8 + 9.5) 1000 / 3 (11.2) = 634 \text{ psi}$$

$$f_{sl} = f_{py} - f_{se} = 250,000 - 97,200 / 0.88$$
$$= 132,500 \text{ psi}$$

$$\theta \geq 15^\circ + (75 + 139.5) \times 10^3 \times 634 / 1000 \times 5800$$
$$\geq 38^\circ \quad \text{Therefore } 39^\circ \text{ is satisfactory.}$$

5. Determine the total shear strength

$$\phi(V_c + V_s) = 0.85(11.8 + 11.4) = 19.7 \text{ kips}$$

The beam in this example is similar to specimen CI12 tested by Elzanaty, Nilson and Slate<sup>48</sup>, with an actual failure shear of 27.5 kips.

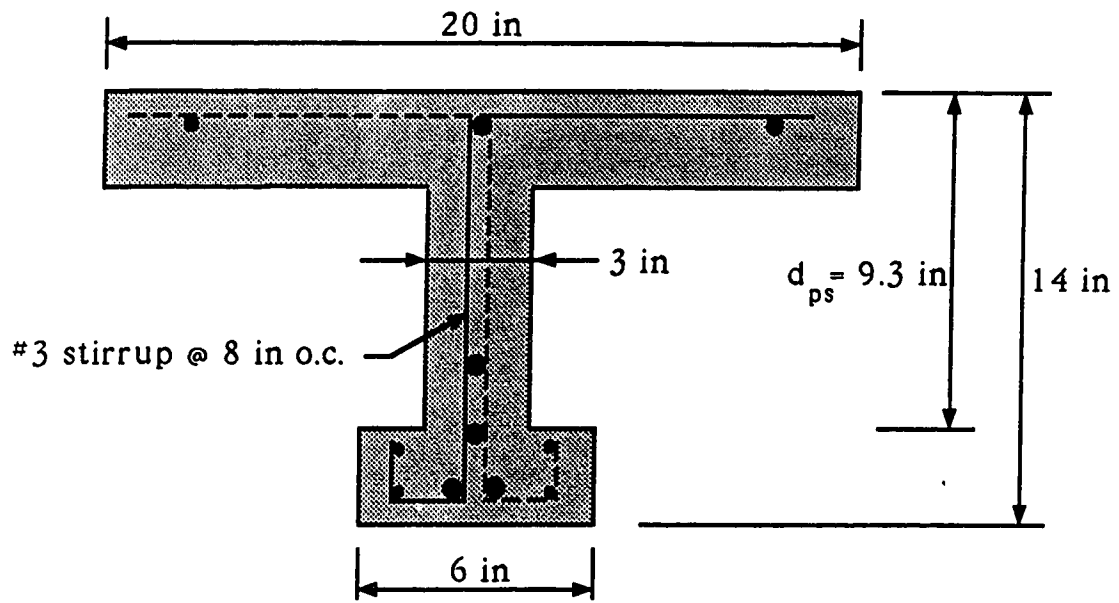


Figure 6.3 Prestressed concrete beam - Example 3.



## 7. Summary, Conclusions and Recommendations

### 7.1 Summary and Conclusions

A new concrete contribution term,  $V_c$ , was derived for both reinforced and prestressed concrete beams subjected to shear. The concrete contribution terms developed are based on a variable angle truss model using the Modified Compression Field Theory and are applicable to slender beams with  $a/d$  ratios greater than 2.5. The concrete contribution expressions were developed to supplement the truss model approach proposed in the General Method of Clause 11.4 in the 1987 draft of Chapter 11 of the ACI Code. A deliberate attempt was made to reduce the complexity of the Modified Compression Field Theory procedure and parallel the traditional format of the ACI Code expressions.

In Chapter 5, shear strength predictions using the proposed concrete contribution equations and the variable angle truss model approach proposed in the ACI 1987 draft were compared to test results reported in the literature. The test beam results were also used to verify the applicability of the current ACI Code provisions. For reinforced concrete beams, this study showed that within the range of variables considered, the scatter of predictions using the proposed design procedure is similar to the existing ACI Code equations, but the predicted capacities are closer to the actual strengths than the ACI Code. For a limited number of test beams

examined having small amounts of longitudinal and shear reinforcement in negative moment regions, both the current ACI Code procedure and the proposed design equations overestimate the actual shear strength.

For prestressed concrete beams, the proposed design procedure reduces the scatter of predicted strengths as compared to the current ACI procedure, and is slightly more conservative. Since the proposed concrete contribution expressions for prestressed beams are much simpler to use than the existing ACI equations, they are appealing as design equations.

A truss model approach is well suited to determining the shear strength of beams since it provides a simple rational examination of the internal force paths and failure mechanisms of concrete beams. The proposed design procedure is simple and easy to use, and departs from the empirical nature and unnecessary complexity of current ACI Code provisions, particularly for prestressed concrete beams. Although the proposed concrete contribution expressions were developed from a variable angle truss model, they are presented in the traditional section by section design approach, and are therefore suitable for codification in the ACI Code.

## 7.2 Recommendations

The following procedure is recommended to account for the concrete contribution to shear in the General Method proposed for the ACI Code Clause 11.4, in the 1987 draft:

### 1. Calculation of $V_c$ - Nonprestressed Members

1.1 - For members subject to shear and flexure only,

$$V_c = \kappa_v \lambda \sqrt{f'_c} b_w d \quad (A)$$

$$\kappa_v = 0.05\theta - 0.25 \quad (B)$$

where  $\theta$  is in degrees and shall not exceed 45.

1.2 - The angle  $\theta$  in Eqn. (B) shall not be less than

$$\theta > 15^\circ + (75,000 + f_{sl}) \frac{v_n}{1000 f'_c} \quad (C)$$

where the stress in the longitudinal reinforcement,  $f_{sl}$ , may be taken as the yield strength,  $f_y$ , of the longitudinal reinforcing bars.

1.3 - For members without web reinforcement,  $\kappa_v = 2.0$ .

## 2. Calculation of $V_c$ - Prestressed Members

2.1 - For the case of shear in prestressed concrete members

$$V_c = (\kappa_v + \kappa_{vp})\sqrt{f'_c} b_w d$$

where  $\kappa_v$  is calculated according to Section 1.1 and

$\kappa_{vp}$  is given by

$$\kappa_{vp} = (0.01\theta + 0.06) \frac{f_{pc}}{\sqrt{f'_c}}$$

but shall not be taken greater than 0.20 - 1.0 nor 8.75 - 0.15 $\theta$ .

In members where the stress in the extreme tension fiber due to the ultimate load and the applied effective prestress force exceeds  $6\sqrt{f'_c}$ ,  $\kappa_{vp}$  shall be taken equal to zero.

2.2 - The angle  $\theta$  shall not be less than given by Eqn. (C), where the stress in the longitudinal reinforcement,  $f_{sl}$ , may be taken as the yield strength,  $f_y$ , of the longitudinal reinforcing bars, as  $(f_{ps} - f_{se})$  for members in which the longitudinal reinforcement consists of only prestressing tendons, or the larger of these two quantities for members with tensile reinforcement consisting of a combination of reinforcing bars and prestressing tendons. In lieu of a more accurate determination of  $f_{ps}$  based on strain compatibility or the values given in Section 18.7,  $f_{ps}$  may be taken as  $f_y$ .

In order to retain the traditional ACI format in the stirrup

contribution to shear, it is suggested the effective shear depth given as  $0.9d$  in the 1987 draft be replaced by  $d$  such that

### 3. Calculation of $V_s$

3.1 The nominal shear transferred by shear reinforcement perpendicular to the axis of a member is

$$V_s = \frac{A_v f_y d}{s \tan \theta}$$

3.2 A minimum area of shear reinforcement shall be provided where the factored shear force  $V_u$  exceeds  $\phi 1.0 \lambda \sqrt{f'_c} b_w d$ .

### 7.3 Future Research

Useful areas of future research on the proposed concrete contribution expressions include further experimental investigation of continuous beams, and the effects of lightweight concrete. In addition, since the conclusions and recommendations in this study are based on members subjected to static loads, further research is required to evaluate the effects of dynamic loads, load reversals, sustained loads and fatigue. It would be advantageous to extend the variable angle truss procedure with the proposed concrete contribution expressions to include the effects of axial loads and torsion. In addition, in order to avoid excessive crack widths at working loads, serviceability cracking limits should be examined.

## References

1. Canadian Standards Association, "Design of concrete structures for buildings, (CAN3-A23.3-M84)", Canadian Standards Association, Rexdale, Ontario, 1984, 281 pp.
2. Vecchio, F.J. and Collins, M.P., "The Modified Compression Field Theory for reinforced concrete elements subjected to shear", American Concrete Institute Journal, Vol. 83, No. 2, March-April 1986, pp 219-231.
3. ACI Committee 318, "Redraft of Chapter 11 of ACI Code", June 8, 1987.
4. ACI Committee 318, "Building code requirements for reinforced concrete, (ACI 318-83)", American Concrete Institute, Detroit, Michigan, 1983, 111 pp..
5. Schlaich, J., Schafer, K. and Jennewein, M., "Toward a consistent design of structural concrete", Journal of the Prestressed Concrete Institute, Vol. 32, No.3, May-June 1987, pp. 74-150.
6. Ritter, W., "Die Bauweise Hennebique", Schweizerische Bauzeitung, Februaruy 1899, pp. 59-61.
7. Morsch, E., "Concrete-steel construction", English Translation by E.P. Goodrich, McGraw-Hill Book Company, New York, 1909, 368 pp. (Translation from third edition of "Der Eisenbetanbau", first edition, 1902).
8. Elstner, R.C. and Hognestad, E., "Laboratory Investigation of rigid frame failure", American Concrete Institute Journal, Vol. 53, January 1957, pp. 637-668.
9. ACI-ASCE Committee 326, "Shear and diagonal tension", American Concrete Institute Journal, Vol. 59, Jan., Feb., and March, 1962, pp. 1-30, 277-334, and 353-396.
10. ACI-ASCE Committee 426, "Suggested revisions to shear provisions for building codes", American Concrete Institute, Detroit 1978, 82 pp., abstract published in American Concrete Institute Journal, Vol 75, No. 9, Sept. 1977, pp 458-469, Discussion, Vol 75,

No. 10, October 1978, pp. 563-569.

11. MacGregor, James G. and Hanson, J.M., "Proposed changes in shear provisions for reinforced and prestressed concrete beams", American Concrete Institute Journal, Vol 66, No. 4, April 1969, pp. 276-288.

12. Collins, M.P. and Mitchell, D., "Shear and Torsion design of prestressed and non-prestressed concrete beams", Journal of the Prestressed Concrete Institute, Vol. 25, No. 5, Sept.-Oct. 1980, pp. 32-100, Discussion and closure, Journal of the Prestressed Concrete Institute, Vol. 26, No. 6, Nov.-Dec. 1981, pp 96-118.

13. MacGregor, James G., "Reinforced concrete, mechanics and design", Prentice Hall, 1988, pp. 169-217, 679-717.

14. Hsu, Thomas T. C., "Is the staggering concept of shear design safe?", American Concrete Institute Journal, Vol. 79, No. 6, Nov.-Dec. 1982, pp. 435-443.

15. Marti, P., Discussion of "Is the staggering concept of shear design safe?", by T. T. C. Hsu, American Concrete Institute Journal, Vol. 80, No. 5, pp. 445-446.

16. Regan, P., Discussion of "Is the staggering concept of shear design safe?", by T. T. C. Hsu, American Concrete Institute Journal, Vol. 80, No. 5, pp. 446-447.

17. Rogowski, D., Discussion of "Is the staggering concept of shear design safe?", by T. T. C. Hsu, American Concrete Institute Journal, Vol. 80, No. 5, pp. 447-448.

18. Mueller, P., Discussion of "Is the staggering concept of shear design safe?", by T. T. C. Hsu, American Concrete Institute Journal, Vol. 80, No. 5, pp. 448-450.

19. Mailhot, G., "Experiments on the staggering concept for shear design", M. Eng Thesis, McGill University, Montreal, Quebec, March 1984, 96 pp.

20. Cerruti, L.M. and Marti, P., "Staggered shear design of concrete beams: large scale tests", Canadian Journal of Civil Engineering, Vol. 14, No. 2, April 1987, pp. 257-268.

21. SIA, "Supplement to Structural Design Code SIA 162 (1968)", Directive RL 34, Zurich, 1976.
22. CEB-FIP, "Model code for concrete structure", CEB-FIP International Recommendations, Third Edition, Comite Euro-International du Beton, Paris, 1978, 348 pp.
23. Walraven, J.C., "Shear in prestressed concrete members", Bulletin D'information No. 180, Comite Euro-International du Beton, April 1987, 144 pp.
24. Regan, P.E., "Proposal for a task group on shear in prestressed concrete beams", Note to CEB Commission IV, Weisbaden, 1979.
25. CEB-FIP, "Model Code 1990, 1st predraft 1988", CEB Bulletin #190b, July 1988, pp. 6.17-6.32.
26. Ramirez, J. A. and Breen, J. E., "Experimental verification of design procedures for shear and torsion in reinforced and prestressed concrete", Research Report 248-3, Center for Transportation Research, The University of Texas at Austin, May 1984.
27. Collins, M.P. and Mitchell, D., "Prestressed concrete basics", Canadian Prestressed Concrete Institute, 1987, pp. 287-352, 386-430.
28. Ontario Ministry of Transportation, "OHBDC - III, Sections 2 & 8, draft copy for public review", Downsview, Ontario, July 1988.
29. Ramirez, J. A., "Draft copy- Experimental verification of shear design procedures for beams and beam type regions", Purdue University, 1989, 82 pp.
30. Vecchio, F.J. and Collins, M.P., "Response of reinforced concrete to In-plane shear and normal stresses", Publication No. 82-03, Department of Civil Engineering, University of Toronto, March 1982, 332 pp.
31. Anderson, N.S. and Ramirez, J. A., "Detailing of stirrup reinforcement", American Concrete Institute Journal, Vol. 86, No. 5, Sept.-Oct. 1989, pp. 507-515.



32. Johnson, M.K. and Ramirez, J. A., "Minimum shear reinforcement in beams with higher strength concrete", American Concrete Institute Journal, Vol. 86, No. 4, July-August 1989, pp 376-382.
33. Elzanaty, A. H., Nilson, A. H. and Slate, F.O., "Shear capacity of reinforced concrete beams using high strength concrete", American Concrete Institute Journal, Vol. 83, No. 2, March-April 1986, pp 290-296.
34. Bresler, B. and Scordelis, A.C., "Shear strength of reinforced concrete beams", American Concrete Institute Journal, Vol. 60, No. 1, January 1963, pp 51-74.
35. Haddadin, M.J., Sheu-Tien Hong and Mattock, A.H., "Stirrup effectiveness in reinforced concrete beams with axial force", ASCE Journal of the Structural Division, Vol. 97(ST9), Sept. 1971, pp. 2277-2297.
36. Mphonde, A.G. and Frantz, G. C., "Shear strength of high strength reinforced concrete beams" Research Report CE84-157, University of Connecticut, June 1984, 260 pp.
37. Hsiung, W. and Frantz, G.C., "Transverse stirrup spacing in R/C beams", ASCE Journal of Structural Engineering, Vol. 111, No. 2, February 1985, pp. 353-362.
38. Taylor, R., "Some shear tests on reinforced concrete T-beams with stirrups", Magazine of Concrete Research, Vol. 18, No. 57, Dec. 1966, pp. 221-230.
39. Sorensen, H. C., "Shear tests on 12 reinforced concrete T-beams", Translation - Structural Research Laboratory Report R60, Technical University of Denmark, 1974, 51 pp.
40. Rodriguez, J. J., Bianchini, A. C., Viest, I. M. and Kesler, C.E., "Shear strength of two-span continuous reinforced concrete beams", American Concrete Institute Journal, April 1959, pp. 1089-1130.
41. Bach, F., Nielsen, M. P. and Braestrup, M. W., "Shear tests on reinforced concrete T-beams series V, U, X, B and S", Structural Research Laboratory Report R120, Technical University of Denmark, 1980, 86 pp.

42. Debaiky, S. Y. and E'niema, E. I. "Behavior and strength of reinforced concrete haunched beams in shear", American Concrete Institute Journal, May-June 1982, pp 184-194.
43. Clark, A. P., "Diagonal tension in reinforced concrete beams", American Concrete Institute Journal, Vol. 48, October 1951, pp 145-156.
44. Olesen, S. E., Sozen, M. A. and Siess, C. P., "Investigation of prestressed reinforced concrete for highway bridges - part IV: strength in shear of beams with web reinforcement", Structural Research Series No. 295, University of Illinois, August 1965.
45. Lyngberg, B. S., "Ultimate shear resistance of partially prestressed reinforced concrete I-beams", American Concrete Institute Journal, Vol. 75, No. 4, April 1976, pp. 214-222.
46. Rodrigues, C. P., and Darwin, D., "Shear strength of lightly reinforced T-beams in Negative Bending", American Concrete Institute Journal, Vol. 84, No. 1, Jan.-Feb. 1987, pp. 77-85.
47. Castrodale, R. W., "The shear design of prestressed concrete members using the truss model", MSE Thesis, Univeristy of Texas at Austin, Dec. 1983, 348 pp.
48. Elzanaty, A. H., Nilson, A. H. and Slate, F. O., "Shear capacity of prestressed concrete beams using high strength concrete", American Concrete Institute Journal, Vol. 83, No. 3, May-June 1986, pp 359-368.
49. Bennett, E.W. and Mlingwa, G., "Cracking and shear strength of beams with prestressed web reinforcement", The Structural Engineer, Vol. 58b, No. 2, June 1980, pp. 25-32.
50. Bennett, E. W. and Debaiky, S. Y., "High strength steel as shear reinforcement in prestressed concrete beams", Shear in Reinforced Concrete, ACI Publication SP-42, 1974, pp. 231-248.
51. Walraven, J. C. and Kopp, F., "Tests on partially prestressed T-beams subjected to shear and bending", Heron, Vol. 23, No. 1, 1978, pp. 18-35.

52. Portland Cement Association, "Notes on ACI 318-83 - building code requirements for reinforced concrete, with design applications", Portland Cement Association, 4th Edition, 1984, pp. 13.1 - 13.25.

## **APPENDIX A - REINFORCED CONCRETE RESULTS**

COMPLEX EQUATION RESULTS

Anderson & Ramirez

BEAM	Av (sq in)	Fy (ksi)	s (in)	fc (psi)	bw (in)	d (in)	fyl (ksi)	Vtest (kips)
NW1	0.440	78.9	7.00	4230.	16.00	13.56	72.0	103.00
NW2	0.440	78.9	7.00	4670.	16.00	13.56	72.0	123.00
NW3	0.220	78.9	3.50	4690.	16.00	13.56	73.0	113.00

BEAM	THETA	R-Min	R-ACI	f2/f2max	Vc/Vt	s/smax	K	Vn/fc**0.5
NW1	35.	0.85	1.08	0.90	0.21	1.03	1.76	8.564
NW2	34.	0.99	1.27	0.89	0.20	1.03	1.68	8.400
NW3	35.	0.87	1.17	0.86	0.26	0.52	2.27	8.737

R mean            0.90    1.17  
 Stnd. Dev        0.073   0.095

Johnson & Ramirez

BEAM	Av (sq in)	Fy (ksi)	s (in)	fc (psi)	bw (in)	d (in)	fyl (ksi)	Vtest (kips)
J2	0.100	69.5	10.50	5280.	12.00	21.21	76.1	50.00
J4	0.100	69.5	10.50	10490.	12.00	21.21	76.1	71.00
J5	0.100	69.5	5.25	8100.	12.00	21.21	76.1	86.00
J7	0.100	69.5	10.50	7440.	12.00	21.21	76.1	63.00

BEAM	THETA	R-Min	R-ACI	f2/f2max	Vc/Vt	s/smax	K	Vn/fc**0.5
J2	43.	0.93	0.98	0.14	0.72	0.99	2.09	2.908
J4	43.	1.02	1.07	0.10	0.78	0.99	2.09	2.672
J5	22.	0.98	1.16	0.88	0.21	0.50	0.82	3.850
J7	43.	1.03	1.09	0.12	0.75	0.99	2.09	2.780

R mean            0.99    1.08  
 Stnd. Dev        0.047   0.075

Elzanaty et al

BEAM	Av (sq in)	Fy (ksi)	s (in)	fc (psi)	bw (in)	d (in)	fyl (ksi)	Vtest (kips)
G4	0.100	55.0	7.50	9100.	7.00	10.50	63.0	33.10
G5	0.100	55.0	7.50	5800.	7.00	10.56	63.0	25.45
G6	0.100	55.0	7.50	3000.	7.00	10.56	63.0	17.45

BEAM	THETA	R-Min	R-ACI	f2/f2max	Vc/Vt	s/smax	K	Vn/fc**0.5
G4	21.	1.34	1.52	0.80	0.19	1.43	0.67	3.529
G5	23.	1.12	1.34	0.89	0.20	1.42	0.80	4.041

G6 28. 0.91 1.10 0.86 0.24 1.42 1.16 4.761

R mean 1.12 1.32  
 Stnd. Dev 0.216 0.212

Bresler and Scordelis

BEAM	Av (sq in)	Fy (ksi)	s (in)	fc (psi)	bw (in)	d (in)	fyl (ksi)	Vtest (kips)
A1	0.100	47.2	8.25	3490.	12.00	18.35	80.5	52.50
A2	0.100	47.2	8.25	3520.	12.00	18.27	80.5	55.00
B1	0.100	47.2	7.50	3590.	9.00	18.15	80.5	50.00
B2	0.100	47.2	7.50	3360.	9.00	18.33	80.5	45.00
C1	0.100	47.2	8.25	4290.	6.00	18.25	80.5	35.00
C2	0.100	47.2	8.25	3450.	6.00	18.28	80.5	36.50

BEAM	THETA	R-Min	R-ACI	f2/f2max	Vc/Vt	s/smax	K	Vn/fc**0.5
A1	41.	1.32	1.44	0.21	0.70	0.90	2.13	3.061
A2	41.	1.38	1.51	0.21	0.70	0.90	2.13	3.057
B1	41.	1.45	1.61	0.25	0.62	0.83	2.17	3.517
B2	41.	1.32	1.47	0.26	0.61	0.82	2.17	3.562
C1	25.	1.21	1.41	0.93	0.23	0.90	0.92	4.038
C2	27.	1.33	1.56	0.90	0.25	0.90	1.06	4.244

R mean 1.34 1.50  
 Stnd. Dev 0.081 0.077

Mattock et al

BEAM	Av (sq in)	Fy (ksi)	s (in)	fc (psi)	bw (in)	d (in)	fyl (ksi)	Vtest (kips)
A2	0.100	52.0	7.50	4240.	7.00	15.00	75.0	43.70
A3	0.220	50.0	7.50	4360.	7.00	15.00	75.0	65.50
A4	0.220	50.0	4.00	4150.	7.00	15.00	75.0	77.00
B3	0.220	50.0	7.50	4020.	7.00	15.00	75.0	61.00
C2	0.100	52.0	7.50	4030.	7.00	15.00	75.0	39.00
C3	0.220	50.0	7.50	3500.	7.00	15.00	75.0	58.50
D3	0.220	50.0	7.50	4250.	7.00	15.00	75.0	54.20
E2	0.100	52.0	7.50	2200.	7.00	15.00	75.0	38.00
E3	0.220	50.0	7.50	1980.	7.00	15.00	75.0	42.50
F3	0.220	50.0	7.50	6520.	7.00	15.00	75.0	74.10
G3	0.220	66.2	7.50	3800.	7.00	15.00	75.0	74.80
G4	0.220	66.2	5.00	3880.	7.00	15.00	75.0	86.20
H1	0.220	50.0	7.50	4240.	7.00	15.00	75.0	63.70
H2	0.220	50.0	7.50	4090.	7.00	15.00	75.0	71.60
J3	0.220	50.0	7.50	4410.	7.00	15.00	75.0	59.10

BEAM	THETA	R-Min	R-ACI	f2/f2max	Vc/Vt	s/smax	K	Vn/fc**0.5
A2	25.	1.52	1.82	0.94	0.22	1.00	0.94	4.202
A3	31.	1.41	1.83	0.90	0.21	1.00	1.40	6.679

A4	39.	1.16	1.41	0.85	0.23	0.53	2.25	9.785
B3	32.	1.35	1.73	0.88	0.22	1.00	1.48	6.766
C2	26.	1.39	1.64	0.88	0.24	1.00	1.01	4.212
C3	33.	1.34	1.70	0.92	0.22	1.00	1.56	7.012
D3	31.	1.17	1.52	0.92	0.21	1.00	1.40	6.747
E2	31.	1.57	1.88	0.88	0.28	1.00	1.40	4.912
E3	41.	1.20	1.36	0.80	0.29	1.00	2.17	7.591
F3	27.	1.41	1.90	0.95	0.18	1.00	1.09	6.180
G3	35.	1.42	1.78	0.91	0.21	1.00	1.72	8.146
G4	40.	1.30	1.52	0.88	0.22	0.67	2.21	10.176
H1	31.	1.38	1.79	0.93	0.21	1.00	1.40	6.753
H2	32.	1.59	2.02	0.87	0.22	1.00	1.48	6.721
J3	31.	1.27	1.64	0.89	0.21	1.00	1.40	6.649

R mean            1.37    1.70  
 Stnd. Dev        0.132   0.188

Mphonde & Frantz

BEAM	Av (sq in)	Fy (ksi)	s (in)	fc (psi)	bw (in)	d (in)	fyl (ksi)	Vttest (kips)
B50-3-3	0.025	43.9	3.50	3200.	6.00	11.75	65.0	17.10
B50-7-3	0.025	43.9	3.50	5800.	6.00	11.75	65.0	21.10
B50-11-3	0.025	43.9	3.50	8600.	6.00	11.75	65.0	22.20
B50-15-3	0.025	43.9	3.50	12000.	6.00	11.75	65.0	25.00
B100-3-3	0.055	38.6	3.50	4000.	6.00	11.75	65.0	21.40
B100-7-3	0.055	38.6	3.50	6800.	6.00	11.75	65.0	27.10
B10011-3	0.055	38.6	3.50	9900.	6.00	11.75	65.0	34.00
B10015-3	0.055	38.6	3.50	11900.	6.00	11.75	65.0	26.00

BEAM	THETA	R-Min	R-ACI	f2/f2max	Vc/Vt	s/smax	K	Vn/fc**0.5
B50-3-3	36.	1.18	1.47	0.33	0.65	0.60	2.37	3.646
B50-7-3	36.	1.18	1.46	0.24	0.72	0.60	2.37	3.319
B50-11-3	36.	1.08	1.32	0.19	0.75	0.60	2.37	3.150
B50-15-3	36.	1.07	1.31	0.16	0.78	0.60	2.37	3.031
B100-3-3	26.	1.04	1.33	0.91	0.29	0.60	1.33	4.603
B100-7-3	36.	1.15	1.45	0.28	0.58	0.60	2.37	4.060
B10011-3	36.	1.29	1.61	0.22	0.63	0.60	2.37	3.771
B10015-3	36.	0.93	1.16	0.20	0.65	0.60	2.37	3.648

R mean            1.11    1.39  
 Stnd. Dev        0.109   0.137

Cerruti & Marti

BEAM	Av (sq in)	Fy (ksi)	s (in)	fc (psi)	bw (in)	d (in)	fyl (ksi)	Vttest (kips)
CM2	0.220	66.3	4.10	6480.	5.90	32.50	63.1	257.00

BEAM	THETA	R-Min	R-ACI	f2/f2max	Vc/Vt	s/smax	K	Vn/fc**0.5
------	-------	-------	-------	----------	-------	--------	---	------------

CM2 37. 1.36 1.75 0.89 0.19 0.25 2.33 12.273

R mean 1.36 1.75  
 Stnd. Dev 0.000 0.000

Hsiung & Frantz

BEAM	Av (sq in)	Fy (ksi)	s (in)	fc (psi)	bw (in)	d (in)	fyl (ksi)	Vtest (kips)
A	0.055	41.0	4.20	6110.	6.00	16.50	65.0	24.80
B	0.110	44.0	4.50	6540.	12.00	16.50	65.0	45.00
C	0.166	41.0	4.20	6280.	18.00	16.50	65.0	76.20
D	0.166	41.0	4.20	6000.	18.00	16.50	65.0	78.20

BEAM	THETA	R-Min	R-ACI	f2/f2max	Vc/Vt	s/smax	K	Vn/fc**0.5
A	37.	0.84	1.02	0.24	0.60	0.51	2.31	3.830
B	37.	0.76	0.90	0.23	0.60	0.55	2.25	3.722
C	37.	0.85	1.03	0.24	0.61	0.51	2.31	3.818
D	37.	0.88	1.07	0.25	0.60	0.51	2.31	3.853

R mean 0.83 1.01  
 Stnd. Dev 0.054 0.073

Taylor

BEAM	Av (sq in)	Fy (ksi)	s (in)	fc (psi)	bw (in)	d (in)	fyl (ksi)	Vtest (kips)
ST1-B-1	0.100	42.0	4.50	3000.	4.50	10.10	40.3	20.10
ST2-c-#3	0.100	42.0	3.50	3140.	4.50	10.10	40.3	23.97

BEAM	THETA	R-Min	R-ACI	f2/f2max	Vc/Vt	s/smax	K	Vn/fc**0.5
ST1-B-1	32.	1.03	1.40	0.95	0.23	0.89	1.77	7.827
ST2-c-#3	34.	1.02	1.39	0.96	0.24	0.69	2.17	9.223

R mean 1.03 1.39  
 Stnd. Dev 0.008 0.002

Sorensen

BEAM	Av (sq in)	Fy (ksi)	s (in)	fc (psi)	bw (in)	d (in)	fyl (ksi)	Vtest (kips)
T21	0.156	39.0	6.88	4710.	4.33	11.73	60.9	29.11
T22	0.119	64.6	8.27	4510.	4.33	11.73	60.9	28.70
T23	0.088	50.2	5.91	4970.	4.33	11.73	60.9	31.30



BEAM	THETA	R-Min	R-ACI	f2/f2max	Vc/Vt	s/smax	K	Vn/fc**0.5
T21	29.	1.26	1.68	0.92	0.19	1.17	1.27	6.640
T22	30.	1.23	1.62	0.90	0.19	1.41	1.28	6.818
T23	27.	1.46	1.96	0.95	0.20	1.01	1.17	5.981

R mean	1.32	1.75
Std. Dev	0.125	0.184

#### Rodrigues

BEAM	Av (sq in)	Fy (ksi)	s (in)	fc (psi)	bw (in)	d (in)	fy1 (ksi)	Vtest (kips)
E2A1	0.222	50.2	10.00	3590.	6.03	12.50	45.6	30.00
E2A2	0.222	50.3	10.00	2720.	6.00	12.50	44.5	26.95
E2A3	0.222	50.9	10.00	2860.	6.13	12.44	47.4	28.95
C2A2	0.222	50.6	10.00	3090.	6.19	12.25	45.0	27.45
C3A2	0.222	50.5	6.00	3140.	6.13	12.38	45.2	39.65

BEAM	THETA	R-Min	R-ACI	f2/f2max	Vc/Vt	s/smax	K	Vn/fc**0.5
E2A1	29.	0.99	1.31	0.97	0.17	1.60	1.15	6.710
E2A2	32.	0.97	1.24	0.93	0.19	1.60	1.36	7.071
E2A3	32.	1.03	1.30	0.90	0.20	1.61	1.36	6.876
C2A2	30.	0.95	1.24	0.99	0.18	1.63	1.22	6.871
C3A2	36.	0.99	1.25	0.91	0.21	0.97	1.94	9.426

R mean	0.99	1.27
Std. Dev	0.031	0.035

#### M.P. Nielsen

BEAM	Av (sq in)	Fy (ksi)	s (in)	fc (psi)	bw (in)	d (in)	fy1 (ksi)	Vtest (kips)
V6002	0.176	46.3	8.27	5180.	7.87	13.50	94.9	55.00
V6004	0.176	46.3	5.16	5280.	7.87	13.50	94.9	68.80
U6002	0.088	46.3	8.27	2830.	7.87	13.50	94.9	43.60
U6004	0.176	46.3	8.27	3075.	7.87	13.50	94.9	50.40
U6007	0.176	46.3	5.16	2130.	7.87	13.50	94.9	45.90
U6010	0.176	46.3	3.78	2390.	7.87	13.50	94.9	58.50
U6017	0.486	40.6	6.89	2915.	7.87	13.50	94.9	68.80
U6007c	0.176	49.6	5.16	2650.	7.87	13.50	94.9	55.00
U6010c	0.176	49.6	3.78	2800.	7.87	13.50	94.9	64.30
U6013c	0.176	49.6	3.78	1800.	7.87	13.50	94.9	45.90
U6017c	0.486	56.3	6.89	2650.	7.87	13.50	94.9	59.60
U6007h	0.352	49.6	5.16	2250.	7.87	13.50	94.9	52.80
X6009	0.176	49.6	8.27	1060.	7.87	14.11	134.0	29.90
X6018	0.176	49.6	4.13	1360.	7.87	13.90	134.0	49.20
B9009	0.238	50.3	6.89	1550.	15.00	13.90	102.1	55.00
B9025a	0.486	53.6	4.13	1780.	15.00	13.90	134.6	91.70
B9029	0.486	48.2	3.50	1400.	15.00	13.90	134.6	87.20

BEAM	THETA	R-Min	R-ACI	f2/f2max	Vc/Vt	s/smax	K	Vn/fc**0.5
V6002	26.	1.58	1.92	0.94	0.22	1.23	0.99	4.552
V6004	30.	1.42	1.87	0.91	0.24	0.76	1.50	6.279
U6002	41.	2.21	2.43	0.27	0.61	1.23	2.13	3.485
U6004	31.	1.67	2.01	0.88	0.27	1.23	1.36	5.115
U6007	42.	1.34	1.47	0.73	0.31	0.76	2.13	6.963
U6010	44.	1.43	1.48	0.75	0.26	0.56	2.05	7.856
U6017	44.	1.33	1.37	0.82	0.23	1.02	2.05	9.033
U6007c	40.	1.40	1.63	0.76	0.31	0.76	2.21	7.191
U6010c	42.	1.38	1.52	0.81	0.26	0.56	2.13	8.293
U6013c	**45.	1.36		0.76	0.27	0.56	2.01	7.476
U6017c	**45.	1.20		0.83	0.22	1.02	2.01	9.072
U6007h	**45.	1.25		0.80	0.24	0.76	2.01	8.373
X6009	**45.	1.78		0.50	0.43	1.17	2.01	4.658
X6018	**45.	2.31		0.60	0.38	0.59	2.01	5.282
B9009	41.	1.21	1.36	0.64	0.39	0.99	2.17	5.559
B9025a	**45.	1.73		0.69	0.33	0.59	2.01	6.032
B9029	**45.	2.09		0.61	0.38	0.50	2.01	5.350

R mean            1.57  
Std. Dev          0.348

\*\* Reduced area to obtain solution

Debakky et al

BEAM	Av (sq in)	Fy (ksi)	s (in)	fc (psi)	bw (in)	d (in)	fyl (ksi)	Vtest (kips)
A1	0.074	46.2	7.87	3560.	4.72	10.24	65.6	16.21
C1	0.074	46.2	7.87	4070.	4.72	10.24	65.6	15.99
D1	0.074	46.2	3.94	4330.	4.72	10.24	65.6	18.41
E3	0.044	45.5	5.91	4550.	4.72	10.24	65.6	13.78
F5	0.088	45.5	7.87	2930.	4.72	10.24	65.6	14.89
F6	0.088	45.5	7.87	2975.	4.72	10.24	65.6	13.78

BEAM	THETA	R-Min	R-ACI	f2/f2max	Vc/Vt	s/smax	K	Vn/fc**0.5
A1	25.	1.33	1.59	0.98	0.22	1.54	0.93	4.235
C1	25.	1.29	1.51	0.87	0.23	1.54	0.93	4.021
D1	30.	0.89	1.21	0.89	0.26	0.77	1.66	6.499
E3	39.	1.20	1.38	0.24	0.63	1.15	2.21	3.525
F5	28.	1.16	1.43	0.95	0.23	1.54	1.15	4.892
F6	28.	1.07	1.31	0.93	0.24	1.54	1.15	4.864

R mean            1.16    1.40  
Std. Dev          0.159   0.135

Clark

BEAM	Av	Fy	s	fc	bw	d	fyl	Vtest
------	----	----	---	----	----	---	-----	-------

	(sq in)	(ksi)	(in)	(psi)	(in)	(in)	(ksi)	(kips)
D2-6	0.222	48.0	6.00	4280.	6.00	12.37	46.5	37.86
D2-7	0.222	48.0	6.00	4120.	6.00	12.37	46.5	35.36
D2-8	0.222	48.0	6.00	3790.	6.00	12.37	46.5	37.86
D4-1	0.222	48.0	7.50	3970.	6.00	12.37	46.5	37.86
D4-2	0.222	48.0	7.50	3720.	6.00	12.37	46.5	35.36
D4-3	0.222	48.0	7.50	3200.	6.00	12.37	46.5	37.11
D5-1	0.222	48.0	10.00	4020.	6.00	12.37	46.5	32.86
D5-2	0.222	48.0	10.00	4210.	6.00	12.37	46.5	35.36
D5-3	0.222	48.0	10.00	3930.	6.00	12.37	46.5	35.36

BEAM	THETA	R-Min	R-ACI	f2/f2max	Vc/Vt	s/smax	K	Vn/fc**0.5
D2-6	32.	0.88	1.19	0.95	0.18	0.97	1.59	8.834
D2-7	32.	0.83	1.12	0.98	0.18	0.97	1.59	8.973
D2-8	33.	0.91	1.22	0.97	0.18	0.97	1.68	9.084
D4-1	31.	1.06	1.41	0.91	0.18	1.21	1.40	7.655
D4-2	31.	0.99	1.33	0.97	0.18	1.21	1.40	7.862
D4-3	33.	1.10	1.43	0.92	0.19	1.21	1.56	8.007
D5-1	28.	1.10	1.45	0.94	0.17	1.62	1.08	6.345
D5-2	27.	1.15	1.55	1.01	0.16	1.62	1.01	6.380
D5-3	28.	1.19	1.57	0.96	0.17	1.62	1.08	6.405

R mean            1.02    1.36  
Std. Dev         0.126   0.159

Olesen, Sozen & Siess

BEAM	Av	Fy	s	fc	bw	d	fyl	Vtest
	(sq in)	(ksi)	(in)	(psi)	(in)	(in)	(ksi)	(kips)
BW.23.18	0.021	38.6	2.75	6200.	3.00	10.62	234.0	15.00
BW.23.19	0.021	38.6	2.75	6690.	3.12	10.62	234.0	15.10
BW.23.20	0.041	38.6	2.75	6150.	3.06	10.62	234.0	14.90
BW.23.21	0.041	38.6	2.00	6665.	3.06	10.62	234.0	16.60
BW.23.22	0.101	36.8	3.50	6880.	3.06	10.62	234.0	18.55
BW.23.23	0.101	36.8	3.00	6600.	3.06	10.62	234.0	21.50
BW.25.19	0.021	38.6	2.75	6850.	3.06	10.69	234.0	8.30
BW.25.20	0.041	38.6	2.75	6290.	3.06	10.62	234.0	12.30

BEAM	THETA	R-Min	R-ACI	f2/f2max	Vc/Vt	s/smax	K	Vn/fc**0.5
BW.23.18	34.	1.42	1.85	0.66	0.57	0.52	2.40	4.212
BW.23.19	34.	1.37	1.78	0.62	0.59	0.52	2.40	4.077
BW.23.20	37.	1.06	1.33	0.77	0.42	0.52	2.33	5.532
BW.23.21	39.	1.01	1.21	0.77	0.36	0.38	2.25	6.185
BW.23.22	42.	1.01	1.11	0.74	0.31	0.66	2.13	6.781
BW.23.23	44.	1.13	1.17	0.76	0.28	0.56	2.05	7.214
BW.25.19	34.	0.75	0.98	0.61	0.59	0.51	2.40	4.090
BW.25.20	37.	0.87	1.09	0.76	0.42	0.52	2.33	5.497

R mean            1.08    1.31  
Std. Dev         0.228   0.327

Lyngberg

BEAM	Av (sq in)	Fy (ksi)	s (in)	fc (psi)	bw (in)	d (in)	fy1 (ksi)	Vtest (kips)
5A-O	0.156	97.8	6.18	3730.	4.72	21.26	89.3	97.80
5B-O	0.156	93.8	6.18	3860.	4.72	21.26	90.4	97.80

BEAM	THETA	R-Min	R-ACI	f2/f2max	Vc/Vt	s/smax	K	Vn/fc**0.5
5A-O	45.	1.51	1.51	0.89	0.19	0.58	2.01	10.577
5B-O	44.	1.51	1.56	0.85	0.20	0.58	2.05	10.415

R mean	1.51	1.53
Stnd. Dev	0.002	0.033

Rodrigues & Darwin

BEAM	Av (sq in)	Fy (ksi)	s (in)	fc (psi)	bw (in)	d (in)	fy1 (ksi)	Vtest (kips)
D-80(1)	0.094	46.6	7.00	5380.	7.58	15.44	229.0	27.85
D-80(2)	0.094	40.7	7.00	4070.	7.51	15.32	229.0	23.01
D-40	0.050	38.7	7.00	4200.	7.52	15.39	229.0	16.90
D-20	0.023	48.5	7.00	4290.	7.51	15.21	229.0	16.91
E-80	0.094	40.9	7.00	4010.	7.51	15.04	213.0	17.17
E-40	0.050	38.4	7.00	4550.	7.50	15.14	213.0	20.55
E-20	0.023	49.8	7.00	4210.	7.50	15.42	213.0	14.69

BEAM	THETA	R-Min	R-ACI	f2/f2max	Vc/Vt	s/smax	K	Vn/fc**0.5
D-80(1)	40.	0.92	1.04	0.40	0.62	0.91	2.17	3.510
D-80(2)	40.	0.89	1.00	0.44	0.61	0.91	2.17	3.528
D-40	40.	0.79	0.88	0.31	0.76	0.91	2.17	2.844
D-20	40.	0.88	0.97	0.26	0.85	0.92	2.17	2.554
E-80	40.	0.68	0.76	0.42	0.61	0.93	2.17	3.545
E-40	40.	0.95	1.06	0.29	0.77	0.92	2.17	2.814
E-20	40.	0.76	0.84	0.25	0.84	0.91	2.17	2.569

R mean	0.84	0.93
Stnd. Dev	0.099	0.111

Mailhot

BEAM	Av (sq in)	Fy (ksi)	s (in)	fc (psi)	bw (in)	d (in)	fy1 (ksi)	Vtest (kips)
A	0.220	59.0	4.72	5670.	7.87	12.00	62.4	89.40
B	0.220	59.0	6.70	5670.	7.87	12.00	62.4	70.00
C	0.130	36.3	11.80	5670.	7.87	13.40	65.0	30.10

BEAM	THETA	R-Min	R-ACI	f2/f2max	Vc/Vt	s/smax	K	Vn/fc**0.5
A	32.	1.37	1.89	0.95	0.19	0.79	1.74	9.162

B	29.	1.37	1.87	0.92	0.18	1.12	1.28	7.183
C	43.	1.36	1.42	0.12	0.74	1.76	2.06	2.781
R mean		1.37	1.73					
Std. Dev		0.005	0.268					

PROPOSED DESIGN EQUATION RESULTS

Anderson & Ramirez

BEAM	Av (sq in)	Fy (ksi)	s (in)	fc (psi)	bw (in)	d (in)	fyl (ksi)	Vtest (kips)
NW1	0.440	78.9	7.00	4230.	16.00	13.56	72.0	103.00
NW2	0.440	78.9	7.00	4670.	16.00	13.56	72.0	123.00
NW3	0.220	78.9	3.50	4690.	16.00	13.56	73.0	113.00

BEAM	THETA	R-Min	R-ACI	f2/f2max	Vc/Vt	s/d3tq	K	Vn/fc**0.5
NW1	35.	0.88	1.08	0.88	0.18	1.08	1.50	8.306
NW2	34.	1.01	1.27	0.88	0.18	1.04	1.45	8.175
NW3	34.	0.93	1.17	0.88	0.18	0.52	1.45	8.160

R mean	0.94	1.17
Std. Dev	0.069	0.095

Johnson & Ramirez

BEAM	Av (sq in)	Fy (ksi)	s (in)	fc (psi)	bw (in)	d (in)	fyl (ksi)	Vtest (kips)
J2	0.100	69.5	10.50	5280.	12.00	21.21	76.1	50.00
J4	0.100	69.5	10.50	10490.	12.00	21.21	76.1	71.00
J5	0.100	69.5	5.25	8100.	12.00	21.21	76.1	86.00
J7	0.100	69.5	10.50	7440.	12.00	21.21	76.1	63.00

BEAM	THETA	R-Min	R-ACI	f2/f2max	Vc/Vt	s/d3tq	K	Vn/fc**0.5
J2	21.	0.97	0.98	0.88	0.29	0.57	0.80	2.778
J4	45.	1.07	1.07	0.09	0.79	1.49	2.00	2.539
J5	22.	0.97	1.16	0.89	0.22	0.30	0.85	3.884
J7	45.	1.09	1.09	0.10	0.76	1.49	2.00	2.639

R mean	1.03	1.08
Std. Dev	0.064	0.075

Elzanaty et al

BEAM	Av (sq in)	Fy (ksi)	s (in)	fc (psi)	bw (in)	d (in)	fyl (ksi)	Vtest (kips)
G4	0.100	55.0	7.50	9100.	7.00	10.50	63.0	33.10
G5	0.100	55.0	7.50	5800.	7.00	10.56	63.0	25.45
G6	0.100	55.0	7.50	3000.	7.00	10.56	63.0	17.45

BEAM	THETA	R-Min	R-ACI	f2/f2max	Vc/Vt	s/d3tq	K	Vn/fc**0.5
G4	21.	1.29	1.52	0.83	0.22	0.82	0.80	3.661
G5	23.	1.09	1.34	0.91	0.22	0.90	0.90	4.141

G6 28. 0.91 1.10 0.86 0.24 1.13 1.15 4.747

R mean 1.10 1.32  
 Stnd. Dev 0.191 0.212

Bresler and Scordelis

BEAM	Av (sq in)	Fy (ksi)	s (in)	fc (psi)	bw (in)	d (in)	fyl (ksi)	Vtest (kips)
A1	0.100	47.2	8.25	3490.	12.00	18.35	80.5	52.50
A2	0.100	47.2	8.25	3520.	12.00	18.27	80.5	55.00
B1	0.100	47.2	7.50	3590.	9.00	18.15	80.5	50.00
B2	0.100	47.2	7.50	3360.	9.00	18.33	80.5	45.00
C1	0.100	47.2	8.25	4290.	6.00	18.25	80.5	35.00
C2	0.100	47.2	8.25	3450.	6.00	18.28	80.5	36.50

BEAM	THETA	R-Min	R-ACI	f2/f2max	Vc/Vt	s/d3tq	K	Vn/fc**0.5
A1	45.	1.44	1.44	0.16	0.71	1.35	2.00	2.807
A2	45.	1.51	1.51	0.16	0.71	1.35	2.00	2.804
B1	25.	1.46	1.61	0.87	0.29	0.58	1.00	3.503
B2	25.	1.31	1.47	0.92	0.28	0.57	1.00	3.587
C1	25.	1.18	1.41	0.95	0.24	0.63	1.00	4.122
C2	27.	1.32	1.56	0.91	0.26	0.69	1.10	4.286

R mean 1.37 1.50  
 Stnd. Dev 0.120 0.077

Mattock et al

BEAM	Av (sq in)	Fy (ksi)	s (in)	fc (psi)	bw (in)	d (in)	fyl (ksi)	Vtest (kips)
A2	0.100	52.0	7.50	4240.	7.00	15.00	75.0	43.70
A3	0.220	50.0	7.50	4360.	7.00	15.00	75.0	65.50
A4	0.220	50.0	4.00	4150.	7.00	15.00	75.0	77.00
B3	0.220	50.0	7.50	4020.	7.00	15.00	75.0	61.00
C2	0.100	52.0	7.50	4030.	7.00	15.00	75.0	39.00
C3	0.220	50.0	7.50	3500.	7.00	15.00	75.0	58.50
D3	0.220	50.0	7.50	4250.	7.00	15.00	75.0	54.20
E2	0.100	52.0	7.50	2200.	7.00	15.00	75.0	38.00
E3	0.220	50.0	7.50	1980.	7.00	15.00	75.0	42.50
F3	0.220	50.0	7.50	6520.	7.00	15.00	75.0	74.10
G3	0.220	66.2	7.50	3800.	7.00	15.00	75.0	74.80
G4	0.220	66.2	5.00	3880.	7.00	15.00	75.0	86.20
H1	0.220	50.0	7.50	4240.	7.00	15.00	75.0	63.70
H2	0.220	50.0	7.50	4090.	7.00	15.00	75.0	71.60
J3	0.220	50.0	7.50	4410.	7.00	15.00	75.0	59.10

BEAM	THETA	R-Min	R-ACI	f2/f2max	Vc/Vt	s/d3tq	K	Vn/fc**0.5
A2	25.	1.50	1.82	0.96	0.23	0.70	1.00	4.262
A3	31.	1.44	1.83	0.89	0.20	0.90	1.30	6.581

A4	38.	1.20	1.41	0.88	0.17	0.63	1.65	9.456
B3	32.	1.38	1.73	0.87	0.20	0.94	1.35	6.638
C2	26.	1.38	1.64	0.88	0.25	0.73	1.05	4.249
C3	33.	1.37	1.70	0.90	0.20	0.97	1.40	6.854
D3	31.	1.19	1.52	0.91	0.20	0.90	1.30	6.649
E2	31.	1.60	1.88	0.87	0.27	0.90	1.30	4.814
E3	40.	1.24	1.36	0.84	0.24	1.26	1.75	7.362
F3	27.	1.41	1.90	0.95	0.18	0.76	1.10	6.193
G3	35.	1.46	1.78	0.89	0.19	1.05	1.50	7.927
G4	39.	1.32	1.52	0.92	0.17	0.81	1.70	9.949
H1	31.	1.40	1.79	0.91	0.20	0.90	1.30	6.655
H2	31.	1.58	2.02	0.94	0.19	0.90	1.30	6.753
J3	31.	1.29	1.64	0.88	0.20	0.90	1.30	6.551

R mean            1.38    1.70  
 Stnd. Dev        0.123   0.188

Mphonde & Frantz

BEAM	Av (sq in)	Fy (ksi)	s (in)	fc (psi)	bw (in)	d (in)	fyl (ksi)	Vtest (kips)
B50-3-3	0.025	43.9	3.50	3200.	6.00	11.75	65.0	17.10
B50-7-3	0.025	43.9	3.50	5800.	6.00	11.75	65.0	21.10
B50-11-3	0.025	43.9	3.50	8600.	6.00	11.75	65.0	22.20
B50-15-3	0.025	43.9	3.50	12000.	6.00	11.75	65.0	25.00
B100-3-3	0.055	38.6	3.50	4000.	6.00	11.75	65.0	21.40
B100-7-3	0.055	38.6	3.50	6800.	6.00	11.75	65.0	27.10
B10011-3	0.055	38.6	3.50	9900.	6.00	11.75	65.0	34.00
B10015-3	0.055	38.6	3.50	11900.	6.00	11.75	65.0	26.00

BEAM	THETA	R-Min	R-ACI	f2/f2max	Vc/Vt	s/d3tq	K	Vn/fc**0.5
B50-3-3	23.	1.39	1.47	0.92	0.29	0.38	0.90	3.076
B50-7-3	45.	1.46	1.46	0.12	0.74	0.89	2.00	2.686
B50-11-3	45.	1.32	1.32	0.10	0.78	0.89	2.00	2.564
B50-15-3	45.	1.31	1.31	0.08	0.81	0.89	2.00	2.477
B100-3-3	25.	1.09	1.33	0.97	0.23	0.42	1.00	4.423
B100-7-3	22.	1.20	1.45	0.91	0.22	0.36	0.85	3.880
B10011-3	20.	1.37	1.61	0.90	0.21	0.33	0.75	3.538
B10015-3	20.	1.03	1.16	0.76	0.23	0.33	0.75	3.293

R mean            1.27    1.39  
 Stnd. Dev        0.154   0.137

Cerruti & Marti

BEAM	Av (sq in)	Fy (ksi)	s (in)	fc (psi)	bw (in)	d (in)	fyl (ksi)	Vtest (kips)
CM2	0.220	66.3	4.10	6480.	5.90	32.50	63.1	257.00

BEAM	THETA	R-Min	R-ACI	f2/f2max	Vc/Vt	s/d3tq	K	Vn/fc**0.5
------	-------	-------	-------	----------	-------	--------	---	------------



CM2 36. 1.40 1.75 0.93 0.13 0.27 1.55 11.860

R mean 1.40 1.75  
 Stnd. Dev 0.000 0.000

Hsiung & Frantz

BEAM	Av (sq in)	Fy (ksi)	s (in)	fc (psi)	bw (in)	d (in)	fyl (ksi)	Vtest (kips)
A	0.055	41.0	4.20	6110.	6.00	16.50	65.0	24.80
B	0.110	44.0	4.50	6540.	12.00	16.50	65.0	45.00
C	0.166	41.0	4.20	6280.	18.00	16.50	65.0	76.20
D	0.166	41.0	4.20	6000.	18.00	16.50	65.0	78.20

BEAM	THETA	R-Min	R-ACI	f2/f2max	Vc/Vt	s/d3tq	K	Vn/fc**0.5
A	22.	0.87	1.02	0.90	0.23	0.31	0.85	3.683
B	22.	0.78	0.90	0.85	0.24	0.33	0.85	3.593
C	22.	0.88	1.03	0.89	0.23	0.31	0.85	3.662
D	22.	0.91	1.07	0.92	0.23	0.31	0.85	3.727

R mean 0.86 1.01  
 Stnd. Dev 0.056 0.073

Taylor

BEAM	Av (sq in)	Fy (ksi)	s (in)	fc (psi)	bw (in)	d (in)	fyl (ksi)	Vtest (kips)
ST1-B-1	0.100	42.0	4.50	3000.	4.50	10.10	40.3	20.10
ST2-c-#3	0.100	42.0	3.50	3140.	4.50	10.10	40.3	23.97

BEAM	THETA	R-Min	R-ACI	f2/f2max	Vc/Vt	s/d3tq	K	Vn/fc**0.5
ST1-B-1	32.	1.09	1.40	0.91	0.18	0.84	1.35	7.410
ST2-c-#3	33.	1.08	1.39	0.99	0.16	0.68	1.40	8.728

R mean 1.08 1.39  
 Stnd. Dev 0.008 0.002

Sorensen

BEAM	Av (sq in)	Fy (ksi)	s (in)	fc (psi)	bw (in)	d (in)	fyl (ksi)	Vtest (kips)
T21	0.156	39.0	6.88	4710.	4.33	11.73	60.9	29.11
T22	0.119	64.6	8.27	4510.	4.33	11.73	60.9	28.70
T23	0.088	50.2	5.91	4970.	4.33	11.73	60.9	31.30

BEAM	THETA	R-Min	R-ACI	f2/f2max	Vc/Vt	s/d3tq	K	Vn/fc**0.5
T21	29.	1.27	1.68	0.91	0.18	0.98	1.20	6.566
T22	30.	1.24	1.62	0.89	0.18	1.22	1.25	6.787
T23	27.	1.48	1.96	0.94	0.19	0.77	1.10	5.909
R mean		1.33	1.75					
Std. Dev		0.130	0.184					

Rodrigues

BEAM	Av (sq in)	Fy (ksi)	s (in)	fc (psi)	bw (in)	d (in)	fyl (ksi)	Vtest (kips)
E2A1	0.222	50.2	10.00	3590.	6.03	12.50	45.6	30.00
E2A2	0.222	50.3	10.00	2720.	6.00	12.50	44.5	26.95
E2A3	0.222	50.9	10.00	2860.	6.13	12.44	47.4	28.95
C2A2	0.222	50.6	10.00	3090.	6.19	12.25	45.0	27.45
C3A2	0.222	50.5	6.00	3140.	6.13	12.38	45.2	39.65

BEAM	THETA	R-Min	R-ACI	f2/f2max	Vc/Vt	s/d3tq	K	Vn/fc**0.5
E2A1	29.	0.98	1.31	0.98	0.18	1.33	1.20	6.765
E2A2	32.	0.98	1.24	0.93	0.19	1.50	1.35	7.061
E2A3	32.	1.03	1.30	0.90	0.20	1.51	1.35	6.866
C2A2	30.	0.94	1.24	0.99	0.18	1.41	1.25	6.904
C3A2	35.	1.01	1.25	0.96	0.16	1.02	1.50	9.269
R mean		0.99	1.27					
Std. Dev		0.034	0.035					

M.P. Nielsen

BEAM	Av (sq in)	Fy (ksi)	s (in)	fc (psi)	bw (in)	d (in)	fyl (ksi)	Vtest (kips)
V6002	0.176	46.3	8.27	5180.	7.87	13.50	94.9	55.00
V6004	0.176	46.3	5.16	5280.	7.87	13.50	94.9	68.80
U6002	0.088	46.3	8.27	2830.	7.87	13.50	94.9	43.60
U6004	0.176	46.3	8.27	3075.	7.87	13.50	94.9	50.40
U6007	0.176	46.3	5.16	2130.	7.87	13.50	94.9	45.90
U6010	0.176	46.3	3.78	2390.	7.87	13.50	94.9	58.50
U6017	0.486	40.6	6.89	2915.	7.87	13.50	94.9	68.80
U6007c	0.176	49.6	5.16	2650.	7.87	13.50	94.9	55.00
U6010c	0.176	49.6	3.78	2800.	7.87	13.50	94.9	64.30
U6013c	0.176	49.6	3.78	1800.	7.87	13.50	94.9	45.90
U6017c	0.486	56.3	6.89	2650.	7.87	13.50	94.9	59.60
U6007h	0.352	49.6	5.16	2250.	7.87	13.50	94.9	52.80
X6009	0.176	49.6	8.27	1060.	7.87	14.11	134.0	29.90
X6018	0.176	49.6	4.13	1360.	7.87	13.90	134.0	49.20
B9009	0.238	50.3	6.89	1550.	15.00	13.90	102.1	55.00
B9025a	0.486	53.6	4.13	1780.	15.00	13.90	134.6	91.70
B9029	0.486	48.2	3.50	1400.	15.00	13.90	134.6	87.20

BEAM	THETA	R-Min	R-ACI	f2/f2max	Vc/Vt	s/d3tq	K	Vn/fc**0.5
V6002	26.	1.56	1.92	0.95	0.23	0.90	1.05	4.617
V6004	30.	1.48	1.87	0.89	0.21	0.66	1.25	6.033
U6002	27.	2.26	2.43	0.83	0.32	0.94	1.10	3.410
U6004	31.	1.69	2.01	0.87	0.26	1.10	1.30	5.058
U6007	41.	1.38	1.47	0.77	0.26	1.00	1.80	6.802
U6010	43.	1.42	1.48	0.80	0.24	0.78	1.90	7.909
U6017	44.	1.34	1.37	0.82	0.22	1.48	1.95	8.929
U6007c	39.	1.47	1.63	0.79	0.25	0.93	1.70	6.857
U6010c	42.	1.43	1.52	0.80	0.23	0.76	1.85	8.009
U6013c	**45.	1.36		0.76	0.27	0.84	2.00	7.462
U6017c	**45.	1.20		0.83	0.22	1.53	2.00	9.079
U6007h	**45.	1.25		0.80	0.24	1.15	2.00	8.360
X6009	**45.	1.77		0.50	0.43	1.76	2.00	4.668
X6018	**45.	2.31		0.60	0.38	0.89	2.00	5.269
B9009	39.	1.26	1.36	0.74	0.32	1.20	1.70	5.333
B9025a	**45.	1.73		0.69	0.33	0.89	2.00	6.019
B9029	**45.	2.09		0.61	0.37	0.76	2.00	5.337

R mean            1.59  
Std. Dev         0.346

\*\* Reduced area to obtain solution

Debaiky et al

BEAM	Av (sq in)	Fy (ksi)	s (in)	fc (psi)	bw (in)	d (in)	fy1 (ksi)	Vtest (kips)
A1	0.074	46.2	7.87	3560.	4.72	10.24	65.6	16.21
C1	0.074	46.2	7.87	4070.	4.72	10.24	65.6	15.99
D1	0.074	46.2	3.94	4330.	4.72	10.24	65.6	18.41
E3	0.044	45.5	5.91	4550.	4.72	10.24	65.6	13.78
F5	0.088	45.5	7.87	2930.	4.72	10.24	65.6	14.89
F6	0.088	45.5	7.87	2975.	4.72	10.24	65.6	13.78

BEAM	THETA	R-Min	R-ACI	f2/f2max	Vc/Vt	s/d3tq	K	Vn/fc**0.5
A1	26.	1.33	1.59	0.88	0.25	1.12	1.05	4.213
C1	25.	1.27	1.51	0.89	0.24	1.08	1.00	4.094
D1	29.	0.93	1.21	0.93	0.19	0.64	1.20	6.240
E3	23.	1.24	1.38	0.86	0.26	0.73	0.90	3.407
F5	28.	1.16	1.43	0.95	0.23	1.23	1.15	4.895
F6	28.	1.07	1.31	0.93	0.24	1.23	1.15	4.867

R mean            1.17    1.40  
Std. Dev         0.148   0.135

Clark

BEAM	Av	Fy	s	fc	bw	d	fy1	Vtest
------	----	----	---	----	----	---	-----	-------

	(sq in)	(ksi)	(in)	(psi)	(in)	(in)	(ksi)	(kips)
D2-6	0.222	48.0	6.00	4280.	6.00	12.37	46.5	37.86
D2-7	0.222	48.0	6.00	4120.	6.00	12.37	46.5	35.36
D2-8	0.222	48.0	6.00	3790.	6.00	12.37	46.5	37.86
D4-1	0.222	48.0	7.50	3970.	6.00	12.37	46.5	37.86
D4-2	0.222	48.0	7.50	3720.	6.00	12.37	46.5	35.36
D4-3	0.222	48.0	7.50	3200.	6.00	12.37	46.5	37.11
D5-1	0.222	48.0	10.00	4020.	6.00	12.37	46.5	32.86
D5-2	0.222	48.0	10.00	4210.	6.00	12.37	46.5	35.36
D5-3	0.222	48.0	10.00	3930.	6.00	12.37	46.5	35.36

BEAM	THETA	R-Min	R-ACI	f2/f2max	Vc/Vt	s/d3tq	K	Vn/fc**0.5
D2-6	32.	0.91	1.19	0.93	0.16	0.91	1.35	8.594
D2-7	32.	0.85	1.12	0.96	0.15	0.91	1.35	8.733
D2-8	33.	0.94	1.22	0.95	0.16	0.94	1.40	8.807
D4-1	30.	1.04	1.41	1.00	0.16	1.05	1.25	7.762
D4-2	31.	1.01	1.33	0.96	0.17	1.09	1.30	7.764
D4-3	33.	1.13	1.43	0.91	0.18	1.18	1.40	7.849
D5-1	28.	1.09	1.45	0.95	0.18	1.29	1.15	6.420
D5-2	28.	1.17	1.55	0.91	0.18	1.29	1.15	6.300
D5-3	28.	1.17	1.57	0.97	0.18	1.29	1.15	6.480

R mean	1.03	1.36
Std. Dev	0.116	0.159

#### Olesen, Sozen & Sless

BEAM	Av	Fy	s	fc	bw	d	fyl	Vttest
	(sq in)	(ksi)	(in)	(psi)	(in)	(in)	(ksi)	(kips)
BW.23.18	0.021	38.6	2.75	6200.	3.00	10.62	234.0	15.00
BW.23.19	0.021	38.6	2.75	6690.	3.12	10.62	234.0	15.10
BW.23.20	0.041	38.6	2.75	6150.	3.06	10.62	234.0	14.90
BW.23.21	0.041	38.6	2.00	6665.	3.06	10.62	234.0	16.60
BW.23.22	0.101	36.8	3.50	6880.	3.06	10.62	234.0	18.55
BW.23.23	0.101	36.8	3.00	6600.	3.06	10.62	234.0	21.50
BW.25.19	0.021	38.6	2.75	6850.	3.06	10.69	234.0	8.30
BW.25.20	0.041	38.6	2.75	6290.	3.06	10.62	234.0	12.30

BEAM	THETA	R-Min	R-ACI	f2/f2max	Vc/Vt	s/d3tq	K	Vn/fc**0.5
BW.23.18	29.	1.75	1.85	0.82	0.35	0.43	1.20	3.408
BW.23.19	28.	1.70	1.78	0.83	0.35	0.41	1.15	3.281
BW.23.20	35.	1.18	1.33	0.81	0.30	0.54	1.50	4.942
BW.23.21	38.	1.09	1.21	0.77	0.29	0.44	1.65	5.724
BW.23.22	41.	1.04	1.11	0.77	0.27	0.86	1.80	6.613
BW.23.23	43.	1.12	1.17	0.80	0.26	0.79	1.90	7.244
BW.25.19	28.	0.93	0.98	0.83	0.35	0.41	1.15	3.297
BW.25.20	35.	0.97	1.09	0.79	0.31	0.54	1.50	4.903

R mean	1.22	1.31
Std. Dev	0.320	0.327

Lyngberg

BEAM	Av (sq in)	Fy (ksi)	s (in)	fc (psi)	bw (in)	d (in)	fyl (ksi)	Vtest (kips)
5A-0	0.156	97.8	6.18	3730.	4.72	21.26	89.3	97.80
5B-0	0.156	93.8	6.18	3860.	4.72	21.26	90.4	97.80

BEAM	THETA	R-Min	R-ACI	f2/f2max	Vc/Vt	s/d3tq	K	Vn/fc**0.5
5A-0	45.	1.51	1.51	0.89	0.19	0.87	2.00	10.564
5B-0	44.	1.52	1.56	0.85	0.19	0.84	1.95	10.311

R mean	1.52	1.53
Stnd. Dev	0.008	0.033

Rodrigues & Darwin

BEAM	Av (sq in)	Fy (ksi)	s (in)	fc (psi)	bw (in)	d (in)	fyl (ksi)	Vtest (kips)
D-80(1)	0.094	46.6	7.00	5380.	7.58	15.44	229.0	27.85
D-80(2)	0.094	40.7	7.00	4070.	7.51	15.32	229.0	23.01
Γ-40	0.050	38.7	7.00	4200.	7.52	15.39	229.0	16.90
D-20	0.023	48.5	7.00	4290.	7.51	15.21	229.0	16.91
E-80	0.094	40.9	7.00	4010.	7.51	15.04	213.0	17.17
E-40	0.050	38.4	7.00	4550.	7.50	15.14	213.0	20.55
E-20	0.023	49.8	7.00	4210.	7.50	15.42	213.0	14.69

BEAM	THETA	R-Min	R-ACI	f2/f2max	Vc/Vt	s/d3tq	K	Vn/fc**0.5
D-80(1)	29.	1.00	1.04	0.82	0.37	0.75	1.20	3.231
D-80(2)	31.	0.98	1.00	0.78	0.41	0.82	1.30	3.199
D-40	45.	0.88	0.88	0.21	0.78	1.36	2.00	2.567
D-20	45.	0.97	0.97	0.17	0.86	1.38	2.00	2.324
E-80	30.	0.74	0.76	0.82	0.38	0.81	1.25	3.250
E-40	45.	1.06	1.06	0.19	0.79	1.39	2.00	2.542
E-20	45.	0.84	0.84	0.17	0.86	1.36	2.00	2.336

R mean	0.92	0.93
Stnd. Dev	0.110	0.111

Maihot

BEAM	Av (sq in)	Fy (ksi)	s (in)	fc (psi)	bw (in)	d (in)	fyl (ksi)	Vtest (kips)
A	0.220	59.0	4.72	5670.	7.87	12.00	62.4	89.40
B	0.220	59.0	6.70	5670.	7.87	12.00	62.4	70.00
C	0.130	36.3	11.80	5670.	7.87	13.40	65.0	30.10

BEAM	THETA	R-Min	R-ACI	f2/f2max	Vc/Vt	s/d3tq	K	Vn/fc**0.5
A	32.	1.43	1.89	0.92	0.15	0.74	1.35	8.776

B	29.	1.39	1.87	0.91	0.17	0.93	1.20	7.098
C	45.	1.42	1.42	0.10	0.75	2.64	2.00	2.675
R mean		1.41	1.73					
Std. Dev		0.023	0.268					

## **APPENDIX B - PRESTRESSED CONCRETE RESULTS**

PRESTRESSED CONCRETE RESULTS-COMPLEX METHOD

Castrodale Composite Beams

BEAM	Av (sq in)	Fy (ksi)	s (in)	fc (psi)	bw (in)	d (in)	fyl (ksi)	Vtest (kips)
O.40A	0.100	62.6	12.00	6150.	3.00	16.92	70.0	51.60
O.40B	0.100	62.6	12.00	5120.	3.00	16.92	72.0	51.20
O.45	0.100	62.6	10.00	5630.	3.00	16.92	72.0	53.00

BEAM	fpc (ksi)	fse (ksi)	fpv (ksi)	fpu (ksi)	rho	B1	pxfpu (ksi)
O.40A	0.18	143.	261.	270.	.00052	0.743	0.140
O.40B	0.18	140.	261.	270.	.00052	0.794	0.140
O.45	0.18	150.	261.	270.	.00052	0.769	0.140

BEAM	THETA	R-Min	f2/f2max	fpc/fc*.5	s/3dtq	K	rho	v%
O.40A	27.	2.09	0.80	2.30	1.08	1.86	0.28	
O.40B	29.	2.18	0.75	2.52	1.18	2.08	0.28	
O.45	29.	1.97	0.81	2.40	0.98	2.04	0.33	

R mean            2.08  
 Stnd. Dev        0.105

Elzanaty, Nilson & Slate

BEAM	Av (sq in)	Fy (ksi)	s (in)	fc (psi)	bw (in)	d (in)	fyl (ksi)	Vtest (kips)
CW10	0.110	63.0	10.00	10600.	2.00	14.22	63.0	39.00
CW11	0.110	63.0	10.00	8100.	2.00	14.22	63.0	35.20
CW12	0.110	63.0	10.00	5800.	2.00	14.22	63.0	31.60
CW13	0.110	63.0	10.00	10500.	2.00	14.22	63.0	41.00
CW14	0.110	63.0	7.00	10700.	2.00	14.22	63.0	42.20
CW15	0.110	63.0	10.00	10200.	2.00	14.22	63.0	33.80
CW16	0.110	63.0	10.00	10600.	2.00	14.22	63.0	42.00
CW17	0.050	55.0	10.00	10100.	2.00	14.22	63.0	32.00
CI10	0.110	63.0	8.00	10600.	3.00	9.32	63.0	31.80
CI11	0.110	63.0	8.00	8100.	3.00	9.32	63.0	28.60
CI12	0.110	63.0	8.00	5800.	3.00	9.32	63.0	27.50
CI13	0.110	63.0	8.00	10500.	3.00	9.32	63.0	34.80
CI14	0.110	63.0	5.00	10700.	3.00	9.32	63.0	37.00
CI15	0.110	63.0	8.00	10200.	3.00	9.32	63.0	27.20
CI16	0.110	63.0	8.00	10600.	3.00	9.32	63.0	36.70
CI17	0.050	55.0	8.00	10100.	3.00	9.32	63.0	29.10

BEAM	fpc (ksi)	fse (ksi)	fpv (ksi)	fpu (ksi)	rho	B1	pxfpu (ksi)
CW10	1.18	112.	254.	270.	.00774	0.650	2.090
CW11	1.15	110.	254.	270.	.00774	0.650	2.090
CW12	1.15	110.	254.	270.	.00774	0.760	2.090
CW13	1.62	154.	254.	270.	.00774	0.650	2.090



CW14	1.63	156.	254.	270.	.00774	0.650	2.090
CW15	1.16	160.	261.	270.	.00536	0.650	1.447
CW16	1.62	155.	254.	270.	.00774	0.650	2.090
CW17	1.63	155.	254.	270.	.00774	0.650	2.090
CI10	1.09	112.	254.	270.	.00472	0.650	1.274
CI11	1.06	110.	254.	270.	.00472	0.650	1.274
CI12	1.07	111.	254.	270.	.00472	0.760	1.274
CI13	1.49	154.	254.	270.	.00472	0.650	1.274
CI14	1.51	157.	254.	270.	.00472	0.650	1.274
CI15	1.07	160.	261.	270.	.00327	0.650	0.883
CI16	1.50	156.	254.	270.	.00472	0.650	1.274
CI17	1.50	155.	254.	270.	.00472	0.650	1.274

BEAM	THETA	R-Min	f2/f2max	fpc/fc*.5	s/3dtq	K	rho	v%
CW10	35.	1.36	0.80	11.46	1.48	5.00	0.55	
CW11	38.	1.43	0.74	12.78	1.65	4.70	0.55	
CW12	41.	1.51	0.69	15.10	1.83	4.40	0.55	
CW13	33.	1.35	0.80	15.81	1.37	5.20	0.55	
CW14	35.	1.21	0.80	15.76	1.03	5.00	0.79	
CW15	33.	1.12	0.82	11.49	1.37	5.20	0.55	
CW16	33.	1.38	0.82	15.73	1.37	5.20	0.55	
CW17	29.	1.39	0.81	16.22	1.17	5.60	0.25	
CI10	35.	1.23	0.75	10.59	1.80	5.00	0.46	
CI11	38.	1.29	0.68	11.78	2.01	4.70	0.46	
CI12	41.	1.47	0.64	14.05	2.24	4.40	0.46	
CI13	32.	1.24	0.84	14.54	1.61	5.30	0.46	
CI14	35.	1.12	0.80	14.60	1.13	5.00	0.73	
CI15	33.	1.00	0.76	10.59	1.67	5.20	0.46	
CI16	33.	1.34	0.76	14.57	1.57	5.20	0.46	
CI17	29.	1.35	0.80	14.93	1.43	5.60	0.21	

R mean            1.30  
Std. Dev           0.138

Olesen, Sozen & Sless

BEAM	Av (sq in)	Fy (ksi)	s (in)	fc (psi)	bw (in)	d (in)	fyl (ksi)	Vtest (kips)
BW. 14.34	0.078	34.0	10.50	3505.	2.90	10.10	0.0	12.90
BW. 14.38	0.014	43.5	2.50	3000.	2.95	10.11	0.0	13.20
BW. 14.58	0.029	43.0	5.00	3278.	2.91	9.97	0.0	15.30
BW. 14.60	0.029	43.0	5.00	2878.	2.89	9.98	0.0	14.60
BW. 23.25	0.021	38.6	2.75	6545.	3.00	10.55	0.0	20.80
CW. 13.28	0.041	36.8	2.50	4095.	1.75	10.03	0.0	17.70
CW. 14.17	0.014	43.5	5.00	3005.	1.76	10.49	0.0	7.89
CW. 14.22	0.029	35.7	2.50	4660.	1.71	10.41	0.0	13.80
CW. 14.23	0.020	36.8	5.00	2745.	1.75	10.48	0.0	7.97
CW. 14.34	0.049	31.8	2.50	3940.	1.77	10.60	0.0	18.20
CW. 14.37	0.020	36.8	2.50	3850.	1.70	10.11	0.0	12.90
CW. 14.38	0.049	31.8	3.50	2950.	1.77	10.70	0.0	13.50
CW. 14.39	0.014	43.5	2.50	3185.	1.75	10.21	0.0	10.90
CW. 14.41	0.049	46.0	4.00	3400.	1.75	10.61	0.0	14.50
CW. 14.47	0.057	35.7	5.00	2585.	1.70	10.14	0.0	12.00
CW. 14.50	0.078	34.0	5.00	2425.	1.75	10.15	0.0	12.10
CW. 14.51	0.041	36.8	5.00	3383.	1.80	9.92	0.0	12.90

CW. 14.54	0.041	36.8	5.00	3400.	1.78	9.96	0.0	13.40
CW. 24.37	0.029	43.0	3.50	3290.	1.75	10.06	0.0	12.10
CU. 14.31	0.049	46.0	4.00	3135.	1.77	10.65	0.0	13.00
CU. 14.32	0.049	46.0	4.00	3420.	1.75	10.63	0.0	10.20
CU. 14.38	0.049	46.0	4.00	3605.	1.79	10.68	0.0	11.50

BEAM	fpc (ksi)	fse (ksi)	fpv (ksi)	fpu (ksi)	rho	B1	pxfpu (ksi)
BW. 14.34	0.54	123.	218.	258.	.00390	0.850	1.006
BW. 14.38	0.54	120.	222.	267.	.00398	0.850	1.062
BW. 14.58	0.75	109.	242.	280.	.00611	0.850	1.711
BW. 14.60	0.75	110.	242.	280.	.00608	0.850	1.702
BW. 23.25	0.46	86.	234.	265.	.00445	0.723	1.179
CW. 13.28	0.60	119.	219.	256.	.00402	0.845	1.029
CW. 14.17	0.32	126.	222.	267.	.00192	0.850	0.513
CW. 14.22	0.62	122.	222.	267.	.00400	0.817	1.068
CW. 14.23	0.32	126.	222.	267.	.00192	0.850	0.513
CW. 14.34	0.70	117.	244.	274.	.00443	0.850	1.214
CW. 14.37	0.61	121.	222.	267.	.00401	0.850	1.071
CW. 14.38	0.52	156.	244.	274.	.00333	0.850	0.912
CW. 14.39	0.61	120.	222.	267.	.00397	0.850	1.060
CW. 14.41	0.71	118.	244.	274.	.00451	0.850	1.236
CW. 14.47	0.60	119.	222.	267.	.00396	0.850	1.057
CW. 14.50	0.62	122.	222.	267.	.00397	0.850	1.060
CW. 14.51	0.86	116.	218.	258.	.00593	0.850	1.530
CW. 14.54	0.80	107.	218.	258.	.00595	0.850	1.535
CW. 24.37	0.43	85.	242.	280.	.00412	0.850	1.154
CU. 14.31	0.55	121.	244.	274.	.00336	0.850	0.921
CU. 14.32	0.54	120.	244.	274.	.00336	0.850	0.921
CU. 14.38	0.68	114.	244.	274.	.00447	0.850	1.225

BEAM	THETA	R-Min	f2/f2max	fpc/fc*.5	s/3dtq	K	rho	v%
BW. 14.34	39.	1.16	0.64	9.12	2.53	4.60	0.26	
BW. 14.38	38.	1.21	0.65	9.86	0.58	4.70	0.20	
BW. 14.58	38.	1.40	0.65	13.10	1.18	4.70	0.20	
BW. 14.60	38.	1.40	0.65	13.98	1.17	4.70	0.20	
BW. 23.25	40.	1.40	0.40	5.69	0.66	4.37	0.25	
CW. 13.28	45.	1.69	0.73	9.38	0.75	4.00	0.93	
CW. 14.17	40.	1.30	0.49	5.84	1.20	4.44	0.16	
CW. 14.22	41.	1.35	0.72	9.08	0.63	4.40	0.67	
CW. 14.23	39.	1.28	0.62	6.11	1.16	4.45	0.23	
CW. 14.34	**45.	1.71	0.73	11.15	0.71	4.00	1.00	
CW. 14.37	40.	1.53	0.71	9.83	0.62	4.50	0.48	
CW. 14.38	42.	1.39	0.75	9.57	0.88	4.30	0.79	
CW. 14.39	41.	1.47	0.66	10.81	0.64	4.40	0.33	
CW. 14.41	**45.	1.49	0.70	12.18	1.13	4.00	0.63	
CW. 14.47	**45.	1.73	0.65	11.80	1.48	4.00	0.56	
CW. 14.50	**45.	1.61	0.69	12.59	1.48	4.00	0.66	
CW. 14.51	39.	1.53	0.74	14.79	1.22	4.60	0.45	
CW. 14.54	39.	1.59	0.74	13.72	1.22	4.60	0.46	
CW. 24.37	45.	1.60	0.67	7.50	1.04	4.00	0.47	
CU. 14.31	**45.	1.44	0.70	9.82	1.13	4.00	0.55	
CU. 14.32	**45.	1.05	0.74	9.23	1.13	4.00	0.63	
CU. 14.38	**45.	1.15	0.72	11.33	1.12	4.00	0.62	

R mean            1.43  
 Stnd. Dev        0.188

\*\* Reduced area to obtain solution

Lyngberg

BEAM	Av (sq in)	Fy (ksi)	s (in)	fc (psi)	bw (in)	d (in)	fy1 (ksi)	Vtest (kips)
2A-3	0.156	89.3	6.18	4730.	4.72	21.26	81.7	113.80
2B-3	0.156	93.3	6.18	4920.	4.72	21.26	81.6	115.80
3A-2	0.156	96.2	6.18	4510.	4.72	21.26	82.4	109.90
3B-2	0.156	90.7	6.18	3990.	4.72	21.26	82.5	97.30
4A-1	0.156	92.7	6.18	4570.	4.72	21.26	89.0	105.40
4B-1	0.156	95.4	6.18	4410.	4.72	21.26	89.8	102.10

BEAM	fpc (ksi)	fse (ksi)	fpv (ksi)	fpu (ksi)	rho	B1	pxfpu (ksi)
2A-3	0.57	135.	227.	267.	.00179	0.813	0.478
2B-3	0.57	135.	227.	267.	.00179	0.804	0.478
3A-2	0.38	135.	227.	267.	.00120	0.824	0.320
3B-2	0.38	135.	227.	267.	.00120	0.850	0.320
4A-1	0.20	139.	227.	267.	.00060	0.821	0.160
4B-1	0.19	134.	227.	267.	.00060	0.829	0.160

BEAM	THETA	R-Min	f2/f2max	fpc/fc*.5	s/3dtq	K	rho	v%
2A-3	**45.	1.57	0.76	8.29	0.87	4.00	0.50	
2B-3	**45.	1.54	0.77	8.13	0.87	4.00	0.50	
3A-2	**45.	1.60	0.76	5.66	0.87	4.00	0.43	
3B-2	**45.	1.62	0.73	6.02	0.87	4.00	0.38	
4A-1	**45.	1.50	0.76	2.96	0.87	3.51	0.50	
4B-1	**45.	1.55	0.74	2.86	0.87	3.46	0.45	

R mean            1.56  
 Stnd. Dev        0.044

\*\* Reduced area to obtain solution

Bennett & Mlingwa

BEAM	Av (sq in)	Fy (ksi)	s (in)	fc (psi)	bw (in)	d (in)	fy1 (ksi)	Vtest (kips)
M77	0.044	45.3	3.15	6080.	2.00	11.66	66.7	25.20
M62	0.044	45.3	3.94	6420.	2.00	11.60	66.7	22.10
M39	0.044	45.3	6.30	6240.	2.00	11.60	66.7	19.10
M31	0.044	45.3	7.87	6000.	2.00	11.60	66.7	17.00
H99	0.078	72.1	3.94	6030.	2.00	11.60	66.7	24.00
H99R	0.078	72.1	3.94	6200.	2.00	11.60	66.7	26.80
H62	0.078	72.1	6.30	5950.	2.00	11.60	66.7	22.00

H49 0.078 72.1 7.87 5930. 2.00 11.60 66.7 23.80

BEAM	fpc (ksi)	fse (ksi)	fpv (ksi)	fpu (ksi)	rho	B1	pxfpu (ksi)
M77	1.06	112.	221.	245.	.00682	0.746	1.671
M62	1.03	109.	221.	245.	.00682	0.729	1.671
M39	1.03	109.	221.	245.	.00682	0.738	1.671
M31	1.01	106.	221.	245.	.00682	0.750	1.671
H99	0.99	105.	221.	245.	.00682	0.748	1.671
H99R	1.01	107.	221.	245.	.00682	0.740	1.671
H62	1.00	105.	221.	245.	.00682	0.752	1.671
H49	0.99	105.	221.	245.	.00682	0.754	1.671

BEAM	THETA	R-Min	f2/f2max	fpc/fc*.5	s/3dtq	K	rho	v%
M77	41.	1.53	0.73	13.59	0.70	4.40	0.70	
M62	37.	1.32	0.74	12.85	0.77	4.80	0.56	
M39	35.	1.33	0.72	13.04	1.14	5.00	0.35	
M31	34.	1.26	0.74	13.04	1.37	5.10	0.28	
H99	**45.	1.11	0.78	12.75	1.02	4.00	0.86	
H99R	**45.	1.18	0.80	12.83	1.02	4.00	0.93	
H62	42.	1.15	0.76	12.96	1.47	4.30	0.62	
H49	40.	1.33	0.76	12.86	1.71	4.50	0.50	

R mean 1.27  
 Stnd. Dev 0.134

Bennett & Debaiky

BEAM	Av (sq in)	Fy (ksi)	s (in)	fc (psi)	bw (in)	d (in)	fyI (ksi)	Vtest (kips)
NL-6-240	0.049	40.6	9.45	5630.	2.00	11.70	59.5	18.52
NL-6-160	0.049	40.6	6.30	5340.	2.00	11.70	59.5	20.35
NL10-160	0.110	40.6	6.30	5260.	2.00	11.70	59.5	23.04
PL-6-240	0.049	40.6	9.45	6030.	2.00	11.70	59.5	20.01
PH-6-160	0.042	79.0	6.30	5500.	2.00	11.70	59.5	21.02
PL-6-80	0.049	40.6	3.15	5980.	2.00	11.70	59.5	23.80
CH-6-240	0.042	79.0	9.45	7890.	2.00	11.70	59.5	23.04
CL-6-160	0.049	40.6	6.30	8000.	2.00	11.70	59.5	23.04
CH-6-160	0.042	79.0	6.30	8100.	2.00	11.70	59.5	25.18
CL-6-80	0.049	40.6	3.15	8240.	2.00	11.70	59.5	26.08
CM-6-80	0.044	60.6	3.15	8120.	2.00	11.70	59.5	28.33
CH-6-80	0.042	79.0	3.15	7630.	2.00	11.70	59.5	31.47
NM6-240	0.044	60.6	9.36	5250.	2.00	11.70	59.5	20.00
NM6-160	0.044	60.6	6.30	5220.	2.00	11.70	59.5	21.00
PM6-160	0.044	60.6	6.30	5760.	2.00	11.70	59.5	21.50
CL6-240	0.049	40.6	9.57	7710.	2.00	11.70	59.5	22.50
CM6-240	0.044	60.6	9.36	7710.	2.00	11.70	59.5	22.50
CM6-160	0.044	60.6	6.30	8350.	2.00	11.70	59.5	25.10

BEAM	fpc (ksi)	fse (ksi)	fpv (ksi)	fpu (ksi)	rho	B1	pxfpu (ksi)
NL-6-240	1.03	113.	212.	250.	.00510	0.769	1.275
NL-6-160	1.03	112.	212.	250.	.00510	0.783	1.275

NL 10-160	1.04	113.	212.	250.	.00510	0.787	1.275
PL-6-240	1.46	112.	212.	250.	.00510	0.748	1.275
PH-6-160	1.47	159.	212.	250.	.00510	0.775	1.275
PL-6-80	1.43	161.	212.	250.	.00510	0.751	1.275
CH-6-240	1.03	112.	212.	250.	.00510	0.656	1.275
CL-6-160	1.03	113.	212.	250.	.00510	0.650	1.275
CH-6-160	1.03	112.	212.	250.	.00510	0.650	1.275
CL-6-80	1.04	113.	212.	250.	.00510	0.650	1.275
CM-6-80	1.04	114.	212.	250.	.00510	0.650	1.275
CH-6-80	1.05	114.	212.	250.	.00510	0.669	1.275
NM6-240	1.02	111.	212.	250.	.00510	0.787	1.275
NM6-160	1.04	113.	212.	250.	.00510	0.789	1.275
PM6-160	1.46	161.	212.	250.	.00510	0.762	1.275
CL6-240	1.03	113.	212.	250.	.00510	0.665	1.275
CM6-240	1.04	114.	212.	250.	.00510	0.665	1.275
CM6-160	1.02	111.	212.	250.	.00510	0.650	1.275

BEAM	THETA	R-Min	f2/f2max	fpc/fc*.5	s/3dtq	K	rho	v%
NL-6-240	33.	1.43	0.78	13.73	1.57	5.20	0.26	
NL-6-160	36.	1.51	0.71	14.10	1.17	4.90	0.39	
NL 10-160	41.	1.35	0.74	14.34	1.40	4.40	0.87	
PL-6-240	33.	1.51	0.75	18.80	1.57	5.20	0.26	
PH-6-160	35.	1.21	0.77	19.82	1.13	5.00	0.33	
PL-6-80	35.	1.21	0.80	18.49	0.57	5.00	0.78	
CH-6-240	33.	1.35	0.80	11.60	1.57	5.20	0.22	
CL-6-160	33.	1.39	0.76	11.52	1.05	5.20	0.39	
CH-6-160	35.	1.31	0.79	11.44	1.13	5.00	0.33	
CL-6-80	36.	1.27	0.79	11.46	0.59	4.90	0.78	
CM-6-80	38.	1.25	0.80	11.54	0.63	4.70	0.70	
CH-6-80	40.	1.32	0.82	12.02	0.68	4.50	0.66	
NM6-240	36.	1.55	0.70	14.08	1.74	4.90	0.24	
NM6-160	37.	1.43	0.75	14.39	1.22	4.80	0.35	
PM6-160	33.	1.28	0.78	19.24	1.05	5.20	0.35	
CL6-240	31.	1.49	0.82	11.73	1.47	5.40	0.26	
CM6-240	32.	1.39	0.82	11.84	1.50	5.30	0.24	
CM6-160	34.	1.38	0.77	11.16	1.09	5.10	0.35	

R mean 1.37  
 Stnd. Dev 0.104

Walraven & Krop

BEAM	Av (sq in)	Fy (ksi)	s (in)	fc (psi)	bw (in)	d (in)	fyl (ksi)	Vtest (kips)
3	0.061	43.7	2.95	5890.	4.53	9.45	64.4	28.55
4	0.039	46.1	2.57	6000.	4.53	9.45	59.0	26.10
5	0.039	46.1	3.35	6550.	4.53	9.45	59.5	22.50
6	0.088	42.1	2.95	5890.	4.53	9.45	61.4	37.50
7	0.088	42.1	2.95	6100.	4.53	9.45	58.7	33.95
8	0.061	43.7	2.36	6210.	4.53	9.45	64.4	32.60
9	0.061	43.7	2.95	6170.	4.53	9.45	64.1	28.30

BEAM	fpc (ksi)	fse (ksi)	fpv (ksi)	fpu (ksi)	rho	B1	pxfpu (ksi)
------	--------------	--------------	--------------	--------------	-----	----	----------------

3	0.32	166.	267.	278.	.00111	0.756	0.309
4	0.29	149.	267.	278.	.00111	0.750	0.309
5	0.26	132.	267.	278.	.00111	0.723	0.309
6	0.54	138.	267.	278.	.00221	0.756	0.614
7	0.52	133.	267.	278.	.00221	0.745	0.614
8	0.46	117.	267.	278.	.00221	0.740	0.614
9	0.39	101.	267.	278.	.00221	0.742	0.614

BEAM	THETA	R-Min	f2/f2max	fpc/fc*.5	s/3dtq	K	rho v%
3	29.	1.18	0.80	4.17	0.52	2.66	0.46
4	31.	1.31	0.73	3.74	0.49	2.69	0.33
5	45.	1.27	0.27	3.21	1.06	3.64	0.26
6	40.	1.30	0.72	7.04	0.79	4.50	0.66
7	40.	1.16	0.70	6.66	0.79	4.50	0.66
8	39.	1.17	0.73	5.84	0.61	4.33	0.57
9	37.	1.18	0.72	4.97	0.71	3.73	0.46

R mean            1.23  
Std. Dev         0.064

PRESTRESSED CONCRETE RESULTS-PROPOSED METHOD

Castrodale Composite Beams

BEAM	Av (sq in)	Fy (ksi)	s (in)	fc (psi)	bw (in)	d (in)	fyl (ksi)	Vtest (kips)
0.40A	0.100	62.6	12.00	6150.	3.00	16.92	70.0	51.60
0.40B	0.100	62.6	12.00	5120.	3.00	16.92	72.0	51.20
0.45	0.100	62.6	10.00	5630.	3.00	16.92	72.0	53.00

BEAM	fpc (ksi)	fse (ksi)	fpv (ksi)
0.40A	0.18	143.	261.
0.40B	0.18	140.	261.
0.45	0.18	150.	261.

BEAM	THETA	R-Min	f2/f2max	Vc/Vt	s/smax	K	Vn (psi)
0.40A	30.	2.19	0.75	0.35	1.42	1.25	464.0
0.40B	32.	2.28	0.73	0.37	1.42	1.35	443.3
0.45	32.	2.07	0.75	0.34	1.18	1.35	503.6

R mean            2.18  
 Stnd. Dev        0.102

Elzanaty, Nilson & Slate

BEAM	Av (sq in)	Fy (ksi)	s (in)	fc (psi)	bw (in)	d (in)	fyl (ksi)	Vtest (kips)
CW10	0.110	63.0	10.00	10600.	2.00	14.22	63.0	39.00
CW11	0.110	63.0	10.00	8100.	2.00	14.22	63.0	35.20
CW12	0.110	63.0	10.00	5800.	2.00	14.22	63.0	31.60
CW13	0.110	63.0	10.00	10500.	2.00	14.22	63.0	41.00
CW14	0.110	63.0	7.00	10700.	2.00	14.22	63.0	42.20
CW15	0.110	63.0	10.00	10200.	2.00	14.22	63.0	33.80
CW16	0.110	63.0	10.00	10600.	2.00	14.22	63.0	42.00
CW17	0.050	55.0	10.00	10100.	2.00	14.22	63.0	32.00
CI10	0.110	63.0	8.00	10600.	3.00	9.32	63.0	31.80
CI11	0.110	63.0	8.00	8100.	3.00	9.32	63.0	28.60
CI12	0.110	63.0	8.00	5800.	3.00	9.32	63.0	27.50
CI13	0.110	63.0	8.00	10500.	3.00	9.32	63.0	34.80
CI14	0.110	63.0	5.00	10700.	3.00	9.32	63.0	37.00
CI15	0.110	63.0	8.00	10200.	3.00	9.32	63.0	27.20
CI16	0.110	63.0	8.00	10600.	3.00	9.32	63.0	36.70
CI17	0.050	55.0	8.00	10100.	3.00	9.32	63.0	29.10

BEAM	fpc (ksi)	fse (ksi)	fpv (ksi)
CW10	1.18	112.	254.
CW11	1.15	110.	254.
CW12	1.15	110.	254.
CW13	1.62	154.	254.

CW14	1.63	156.	254.
CW15	1.16	160.	261.
CW16	1.62	155.	254.
CW17	1.63	155.	254.
CI10	1.09	112.	254.
CI11	1.06	110.	254.
CI12	1.07	111.	254.
CI13	1.49	154.	254.
CI14	1.51	157.	254.
CI15	1.07	160.	261.
CI16	1.50	156.	254.
CI17	1.50	155.	254.

BEAM	THETA	R-Min	f2/f2max	Vc/Vt	s/smax	K	Vn (psi)
CW10	36.	1.40	0.75	0.51	1.41	1.55	981.4
CW11	39.	1.47	0.70	0.49	1.41	1.70	841.9
CW12	42.	1.56	0.67	0.46	1.41	1.85	712.3
CW13	33.	1.35	0.83	0.50	1.41	1.40	1066.4
CW14	35.	1.21	0.83	0.42	0.98	1.50	1224.1
CW15	34.	1.16	0.77	0.50	1.41	1.45	1028.8
CW16	33.	1.38	0.82	0.50	1.41	1.40	1068.9
CW17	29.	1.39	0.84	0.69	1.41	1.20	810.8
CI10	35.	1.23	0.75	0.56	1.72	1.50	927.2
CI11	37.	1.25	0.74	0.53	1.72	1.60	815.2
CI12	41.	1.47	0.64	0.50	1.72	1.80	667.3
CI13	32.	1.24	0.83	0.54	1.72	1.35	1005.2
CI14	35.	1.12	0.79	0.44	1.07	1.50	1177.0
CI15	33.	1.00	0.77	0.54	1.72	1.40	969.8
CI16	32.	1.30	0.82	0.54	1.72	1.35	1007.8
CI17	29.	1.35	0.79	0.73	1.72	1.20	769.5

R mean            1.31  
 Stnd. Dev        0.145

#### Olesen, Sozen & Siess

BEAM	Av (sq in)	Fy (ksi)	s (in)	fc (psi)	bw (in)	d (in)	fyl (ksi)	Vtest (kips)
BW. 14.34	0.078	34.0	10.50	3505.	2.90	10.10	0.0	12.90
BW. 14.38	0.014	43.5	2.50	3000.	2.95	10.11	0.0	13.20
BW. 14.58	0.029	43.0	5.00	3278.	2.91	9.97	0.0	15.30
BW. 14.60	0.029	43.0	5.00	2878.	2.89	9.98	0.0	14.60
BW. 23.25	0.021	38.6	2.75	6545.	3.00	10.55	0.0	20.80
CW. 13.28	0.041	36.8	2.50	4095.	1.75	10.03	0.0	17.70
CW. 14.17	0.014	43.5	5.00	3005.	1.76	10.49	0.0	7.89
CW. 14.22	0.029	35.7	2.50	4660.	1.71	10.41	0.0	13.80
CW. 14.23	0.020	36.8	5.00	2745.	1.75	10.48	0.0	7.97
CW. 14.34	0.049	31.8	2.50	3940.	1.77	10.60	0.0	18.20
CW. 14.37	0.020	36.8	2.50	3850.	1.70	10.11	0.0	12.90
CW. 14.38	0.049	31.8	3.50	2950.	1.77	10.70	0.0	13.50
CW. 14.39	0.014	43.5	2.50	3185.	1.75	10.21	0.0	10.90
CW. 14.41	0.049	46.0	4.00	3400.	1.75	10.61	0.0	14.50
CW. 14.47	0.057	35.7	5.00	2585.	1.70	10.14	0.0	12.00
CW. 14.50	0.078	34.0	5.00	2425.	1.75	10.15	0.0	12.10
CW. 14.51	0.041	36.8	5.00	3383.	1.80	9.92	0.0	12.90



CW. 14.54	0.041	36.8	5.00	3400.	1.78	9.96	0.0	13.40
CW. 24.37	0.029	43.0	3.50	3290.	1.75	10.06	0.0	12.10
CU. 14.31	0.049	46.0	4.00	3135.	1.77	10.65	0.0	13.00
CU. 14.32	0.049	46.0	4.00	3420.	1.75	10.63	0.0	10.20
CU. 14.38	0.049	46.0	4.00	3605.	1.79	10.68	0.0	11.50

BEAM	fpc (ksi)	fse (ksi)	fpv (ksi)
BW. 14.34	0.54	123.	218.
BW. 14.38	0.54	120.	222.
BW. 14.58	0.75	109.	242.
BW. 14.60	0.75	110.	242.
BW. 23.25	0.46	86.	234.
CW. 13.28	0.60	119.	219.
CW. 14.17	0.32	126.	222.
CW. 14.22	0.62	122.	222.
CW. 14.23	0.32	126.	222.
CW. 14.34	0.70	117.	244.
CW. 14.37	0.61	121.	222.
CW. 14.38	0.52	156.	244.
CW. 14.39	0.61	120.	222.
CW. 14.41	0.71	118.	244.
CW. 14.47	0.60	119.	222.
CW. 14.50	0.62	122.	222.
CW. 14.51	0.86	116.	218.
CW. 14.54	0.80	107.	218.
CW. 24.37	0.43	85.	242.
CU. 14.31	0.55	121.	244.
CU. 14.32	0.54	120.	244.
CU. 14.38	0.68	114.	244.

BEAM	THETA	R-Min	f2/f2max	Vc/Vt	s/smax	K	Vn (psi)
BW. 14.34	36.	1.07	0.70	0.71	2.08	1.55	410.1
BW. 14.38	38.	1.21	0.64	0.70	0.49	1.65	366.9
BW. 14.58	39.	1.43	0.65	0.72	1.00	1.70	367.7
BW. 14.60	40.	1.48	0.63	0.70	1.00	1.75	342.8
BW. 23.25	40.	1.40	0.46	0.75	0.52	1.75	468.0
CW. 13.28	43.	1.59	0.76	0.42	0.50	1.90	635.9
CW. 14.17	40.	1.30	0.48	0.74	0.95	1.75	328.6
CW. 14.22	39.	1.27	0.76	0.51	0.48	1.70	610.0
CW. 14.23	39.	1.28	0.58	0.69	0.95	1.70	339.0
CW. 14.34	**45.	1.71	0.73	0.44	0.47	2.00	568.7
CW. 14.37	39.	1.49	0.72	0.57	0.49	1.70	503.6
CW. 14.38	43.	1.43	0.73	0.46	0.65	1.90	498.9
CW. 14.39	40.	1.43	0.67	0.60	0.49	1.75	425.8
CW. 14.41	**45.	1.59	0.70	0.48	0.75	2.00	490.2
CW. 14.47	**45.	1.65	0.68	0.48	0.99	2.00	423.0
CW. 14.50	**45.	1.69	0.66	0.49	0.99	2.00	403.3
CW. 14.51	40.	1.57	0.70	0.57	1.01	1.75	460.1
CW. 14.54	41.	1.68	0.68	0.57	1.00	1.80	450.2
CW. 24.37	**44.	1.69	0.66	0.58	0.70	1.95	406.7
CU. 14.31	**44.	1.50	0.71	0.50	0.75	1.95	459.0
CU. 14.32	**45.	1.12	0.69	0.48	0.75	2.00	490.9
CU. 14.38	**45.	1.15	0.73	0.46	0.75	2.00	523.5

R mean            1.44  
 Stnd. Dev        0.197

\*\* Reduced area to obtain solution

Lyngberg

BEAM	Av (sq in)	Fy (ksi)	s (in)	fc (psi)	bw (in)	d (in)	fy1 (ksi)	Vtest (kips)
2A-3	0.156	89.3	6.18	4730.	4.72	21.26	81.7	113.80
2B-3	0.156	93.3	6.18	4920.	4.72	21.26	81.6	115.80
3A-2	0.156	96.2	6.18	4510.	4.72	21.26	82.4	109.90
3B-2	0.156	90.7	6.18	3990.	4.72	21.26	82.5	97.30
4A-1	0.156	92.7	6.18	4570.	4.72	21.26	89.0	105.40
4B-1	0.156	95.4	6.18	4410.	4.72	21.26	89.8	102.10

BEAM	fpc (ksi)	fse (ksi)	fpv (ksi)
2A-3	0.57	135.	227.
2B-3	0.57	135.	227.
3A-2	0.38	135.	227.
3B-2	0.38	135.	227.
4A-1	0.20	139.	227.
4B-1	0.19	134.	227.

BEAM	THETA	R-Min	f2/f2max	Vc/Vt	s/smax	K	Vn (psi)
2A-3	44.	1.46	0.75	0.36	0.58	1.95	776.5
2B-3	44.	1.43	0.76	0.36	0.58	1.95	804.3
3A-2	45.	1.40	0.79	0.34	0.58	2.00	783.1
3B-2	**45.	1.37	0.77	0.36	0.58	2.00	706.6
4A-1	43.	1.39	0.77	0.30	0.58	1.90	758.1
4B-1	44.	1.35	0.78	0.30	0.58	1.95	752.8

R mean 1.40  
Std. Dev 0.040

Bennett & Mlingwa

BEAM	Av (sq in)	Fy (ksi)	s (in)	fc (psi)	bw (in)	d (in)	fy1 (ksi)	Vtest (kips)
M77	0.044	45.3	3.15	6080.	2.00	11.66	66.7	25.20
M62	0.044	45.3	3.94	6420.	2.00	11.60	66.7	22.10
M39	0.044	45.3	6.30	6240.	2.00	11.60	66.7	19.10
M31	0.044	45.3	7.87	6000.	2.00	11.60	66.7	17.00
H99	0.078	72.1	3.94	6030.	2.00	11.60	66.7	24.00
H99R	0.078	72.1	3.94	6200.	2.00	11.60	66.7	26.80
H62	0.078	72.1	6.30	5950.	2.00	11.60	66.7	22.00
H49	0.078	72.1	7.87	5930.	2.00	11.60	66.7	23.80

BEAM	fpc	fse	fpv
------	-----	-----	-----

	(ksi)	(ksi)	(ksi)
M77	1.06	112.	221.
M62	1.03	109.	221.
M39	1.03	109.	221.
M31	1.01	106.	221.
H99	0.99	105.	221.
H99R	1.01	107.	221.
H62	1.00	105.	221.
H49	0.99	105.	221.

BEAM	THETA	R-Min	f2/f2max	Vc/Vt	s/smax	K	Vn (psi)
M77	39.	1.44	0.73	0.48	0.54	1.70	749.4
M62	37.	1.32	0.75	0.53	0.68	1.60	720.3
M39	35.	1.33	0.72	0.64	1.09	1.50	620.9
M31	34.	1.26	0.75	0.68	1.36	1.45	582.8
H99	**45.	1.11	0.79	0.33	0.68	2.00	932.8
H99R	**45.	1.18	0.81	0.32	0.68	2.00	982.9
H62	42.	1.15	0.77	0.40	1.09	1.85	827.4
H49	40.	1.33	0.77	0.45	1.36	1.75	772.3

R mean            1.26  
 Std. Dev         0.113

Bennett & Debaiky

BEAM	Av (sq in)	Fy (ksi)	s (in)	fc (psi)	bw (in)	d (in)	fyl (ksi)	Vtest (kips)
NL-6-240	0.049	40.6	9.45	5630.	2.00	11.70	59.5	18.52
NL-6-160	0.049	40.6	6.30	5340.	2.00	11.70	59.5	20.35
NL10-160	0.110	40.6	6.30	5260.	2.00	11.70	59.5	23.04
PL-6-240	0.049	40.6	9.45	6030.	2.00	11.70	59.5	20.01
PH-6-160	0.042	79.0	6.30	5500.	2.00	11.70	59.5	21.02
PL-6-80	0.049	40.6	3.15	5980.	2.00	11.70	59.5	23.80
CH-6-240	0.042	79.0	9.45	7890.	2.00	11.70	59.5	23.04
CL-6-160	0.049	40.6	6.30	8000.	2.00	11.70	59.5	23.04
CH-6-160	0.042	79.0	6.30	8100.	2.00	11.70	59.5	25.18
CL-6-80	0.049	40.6	3.15	8240.	2.00	11.70	59.5	26.08
CM-6-80	0.044	60.6	3.15	8120.	2.00	11.70	59.5	28.33
CH-6-80	0.042	79.0	3.15	7630.	2.00	11.70	59.5	31.47
NM6-240	0.044	60.6	9.36	5250.	2.00	11.70	59.5	20.00
NM6-160	0.044	60.6	6.30	5220.	2.00	11.70	59.5	21.00
PM6-160	0.044	60.6	6.30	5760.	2.00	11.70	59.5	21.50
CL6-240	0.049	40.6	9.57	7710.	2.00	11.70	59.5	22.50
CM6-240	0.044	60.6	9.36	7710.	2.00	11.70	59.5	22.50
CM6-160	0.044	60.6	6.30	8350.	2.00	11.70	59.5	25.10

BEAM	fpc (ksi)	fse (ksi)	fpv (ksi)
NL-6-240	1.03	113.	212.
NL-6-160	1.03	112.	212.
NL10-160	1.04	113.	212.
PL-6-240	1.46	112.	212.
PH-6-160	1.47	159.	212.
PL-6-80	1.43	161.	212.

CH-6-240	1.03	112.	212.
CL-6-160	1.03	113.	212.
CH-6-160	1.03	112.	212.
CL-6-80	1.04	113.	212.
CM-6-80	1.04	114.	212.
CH-6-80	1.05	114.	212.
NM6-240	1.02	111.	212.
NM6-160	1.04	113.	212.
PM6-160	1.46	161.	212.
CL6-240	1.03	113.	212.
CM6-240	1.04	114.	212.
CM6-160	1.02	111.	212.

BEAM	THETA	R-Min	f2/f2max	Vc/Vt	s/smax	K	Vn (psi)
NL-6-240	33.	1.43	0.74	0.71	1.62	1.40	552.3
NL-6-160	33.	1.43	0.75	0.62	1.08	1.50	590.9
NL10-160	33.	1.43	0.77	0.44	1.08	1.75	748.8
PL-6-240	33.	1.43	0.80	0.71	1.62	1.35	580.0
PH-6-160	33.	1.43	0.83	0.49	1.08	1.45	765.8
PL-6-80	33.	1.43	0.80	0.46	0.54	1.50	837.6
CH-6-240	33.	1.43	0.83	0.63	1.62	1.35	749.7
CL-6-160	33.	1.43	0.79	0.65	1.08	1.35	726.7
CH-6-160	34.	1.27	0.83	0.54	1.08	1.45	846.6
CL-6-80	35.	1.23	0.80	0.50	0.54	1.50	904.8
CM-6-80	37.	1.22	0.81	0.44	0.54	1.60	994.2
CH-6-80	39.	1.28	0.83	0.38	0.54	1.70	1047.5
NM6-240	35.	1.51	0.72	0.64	1.60	1.50	565.7
NM6-160	37.	1.43	0.73	0.55	1.08	1.60	627.6
PM6-160	33.	1.28	0.78	0.55	1.08	1.40	720.5
CL6-240	30.	1.46	0.85	0.73	1.64	1.25	660.6
CM6-240	31.	1.35	0.85	0.67	1.60	1.30	711.2
CM6-160	33.	1.34	0.79	0.59	1.08	1.40	801.0

R mean            1.34  
 Std. Dev         0.103

Walraven & Krop

BEAM	Av (sq in)	Fy (ksi)	s (in)	fc (psi)	bw (in)	d (in)	fy1 (ksi)	Vtest (kips)
3	0.061	43.7	2.95	5890.	4.53	9.45	64.4	28.55
4	0.039	46.1	2.57	6000.	4.53	9.45	59.0	26.10
5	0.039	46.1	3.35	6550.	4.53	9.45	59.5	22.50
6	0.088	42.1	2.95	5890.	4.53	9.45	61.4	37.50
7	0.088	42.1	2.95	6100.	4.53	9.45	58.7	33.95
8	0.061	43.7	2.36	6210.	4.53	9.45	64.4	32.60
9	0.061	43.7	2.95	6170.	4.53	9.45	64.1	28.30

BEAM	fpc (ksi)	fse (ksi)	fpv (ksi)
3	0.32	166.	267.
4	0.29	149.	267.
5	0.26	132.	267.
6	0.54	138.	267.

7	0.52	133.	267.
8	0.46	117.	267.
9	0.39	101.	267.

BEAM	THETA	R-Min	f2/f2max	Vc/Vt	s/smax	K	Vn (psi)
3	32.	1.22	0.75	0.41	0.62	1.35	544.4
4	31.	1.31	0.71	0.45	0.54	1.30	465.0
5	45.	1.27	0.26	0.71	0.71	2.00	412.9
6	40.	1.30	0.70	0.51	0.62	1.75	675.8
7	40.	1.16	0.70	0.52	0.62	1.75	681.9
8	39.	1.17	0.73	0.53	0.50	1.70	648.9
9	37.	1.18	0.72	0.53	0.62	1.60	558.1

R mean	1.23
Std. Dev	0.061